

**Molecular Basis of Recognition of Rust Effectors
by the M Flax Resistance Protein**

Md Motiur Rahman

2091054

A thesis submitted for the Degree of Doctor of Philosophy

at

**The School of Biological Sciences
Flinders University South Australia**



April 2016

Contents

Abstract.....	v
Declaration.....	vii
Acknowledgements	viii
Chapter One: Introduction	1
1. Introduction.....	2
1.1 Plant pathogen - a constraint on agriculture.....	2
1.2 Flax and flax rust disease	2
1.3. Plant defending system.....	4
1.3.1 Physical barriers	6
1.3.2 Plant innate immunity.....	6
1.3.2.1 MAMP- or PAMP-triggered immunity - perception of microbes through PRRs	7
1.3.2.2 Effector proteins - weapons to facilitate pathogenicity	7
1.3.2.3 Effector-triggered immunity (ETI)	8
1.3.2.4 Resistance modes of pathogen recognition	9
1.4 Flax rust resistance and M resistance gene	10
1.5 Plant pathogens.....	11
1.5.1 Haustorium.....	11
1.5.2 Oomycete pathogens	12
1.5.2.1 <i>Phytophthora</i> species.....	12
1.5.2.2 <i>Hyaloperonospora arabidopsidis</i> - an oomycete pathogen model species	14
1.5.3. Bacterial pathogens.....	15
1.5.3.1 <i>Pseudomonas syringae</i>	16
1.5.3.2 <i>Xanthomonas</i> species.....	17
1.5.4 Fungal pathogens.....	18
1.5.5 Rust fungi	20
1.5.5.1 Rust fungus as a pathogen	21
1.5.5.2 Rust effectors	21
1.5.5.3 Flax rust effectors.....	23
1.5.5.4 Biochemistry of flax rust disease	25
1.5.5.5 The AvrM: multiple homologs.....	25
1.5.5.6 AvrM and avrM - two contrasting effectors	27
1.5.5.7 AvrM-A and avrM - two representatives	30
1.5.5.8 Determining AvrM regions responsible for M recognition	32
1.6 Plant-pathogen interaction	33
1.6.1 Gene-for-gene hypothesis.....	33

1.6.2 Flax and flax rust: a model system	34
1.7 Plant Agrobacterium transformation.....	35
1.8 Aims and experimental approaches	36
Chapter Two: Materials and Methods	38
2.1 Materials.....	39
2.1.1 General chemicals	39
2.1.2 Culture media, solutions and buffers	39
2.1.3 Effector genes, AvrM-A and avrM.....	39
2.1.4 Plasmids	39
2.1.5 Oligonucleotides/primers	40
2.1.6 Plant materials	40
2.1.7 Bacterial stains	40
2.1.8 Cultures and antibiotics	41
2.2 Methods	41
2.2.1 Preparation of electrocompetent bacterial cells.	41
2.2.2 Transformation of electrocompetent cells by electroporation	41
2.2.3 Preparation of chemically competent <i>E. coli</i> cells	42
2.2.4 Heat-shock transformation	42
2.2.5 Long term storage of bacterial constructs	42
2.2.6 Colony PCR	43
2.2.7. Growing transgenic tobacco plants.....	43
2.3 DNA Methods	44
2.3.1 Gene constructs preparation	44
2.3.2 Site-directed mutagenesis to generate point mutation	46
2.3.3 Mutant genes preparation and transformation.....	46
2.3.4 Plasmid DNA purification	46
2.3.5 DNA sequencing and analysis.....	47
2.4 <i>In planta</i> methods.....	47
2.4.1 Transient <i>in planta</i> expression assays.....	47
2.4.2 Quantification of HR.....	48
2.4.3 Protein extraction from tobacco leaves.....	50
2.4.4 Sodium Dodecyl Sulphate Polyacrylamide Gel Electrophoresis (SDS-PAGE)	50
2.4.5 Ponceau staining of the nitrocellulose membrane	50
2.4.6 Immunoblot analysis	51
2.4.7 Coomassie staining of SDS-PAGE gel.....	52
2.5 Methods for protein production.....	52
2.5.1 AvrM-A/avrM construction for expression	52
2.5.2 Transformation of effector genes in BL21 cells	52

2.5.3. Growth and test expression	52
2.5.4. Large-scale expression	53
2.5.5 Extraction of effector proteins	53
2.5.6 Purification of the extracted proteins	53
2.5.7 Protein quantification	54
2.6 Methods for biophysical analysis	54
2.6.1 Yeast Two-Hybrid assay	54
2.6.2 Size-exclusion chromatography (SEC)-coupled multi-angle light scattering (MALS)	54
2.6.3 Size-exclusion chromatography (SEC)-coupled small-angle X-ray scattering (SAXS)	55
Chapter 3: Single residue mutation	56
3.1 Introduction.....	57
3.2 Results.....	59
3.2.1 Mutation of polymorphic residues.....	59
3.2.1.1 AvrM-A ^{K226Q} and avrM ^{Q164K}	59
3.2.1.2 AvrM-A ^{K232R} and avrM ^{R170K}	63
3.2.1.3 AvrM-A ^{L241S} and avrM ^{S179L}	63
3.2.1.4 AvrM-A ^{I248T} and avrM ^{T179I}	63
3.2.1.5 AvrM-A ^{T259N} and avrM ^{N197T}	64
3.2.1.6 AvrM-A ^{PI280/ΔL218} and avrM ^{ΔL218/PI280}	64
3.2.1.7 AvrM-A ^{I310} and avrM ^{T247}	65
3.2.2 Mutation of non-polymorphic residues in AvrM-A.....	66
3.2.2.1 AvrM-A ^{E237A}	66
3.2.2.2 AvrM-A ^{E309A}	66
3.2.2.3 AvrM-A ^{R313A}	67
3.3 Discussion.....	70
3.3.1 Structural differences in AvrM-A and avrM proteins.....	70
3.3.2 AvrM-A and avrM dimer interfaces comprise two different central patches.....	71
3.3.3 Selection of critical residue/s involved in M detection.....	74
3.3.4 Mutagenesis <i>and in planta</i> assay	74
3.3.4.1 Reciprocal mutation in polymorphisms	74
3.3.4.2 Alanine substitution of non-polymorphic charged residues.....	75
3.4 Conclusion	77
Chapter Four: Combined residue mutation	78
4.1 Summary	79
4.2 Significance.....	80
4.3 Introduction.....	80
4.4 Results.....	83
4.4.1 AvrM construct.....	83

4.4.2 Structures comparison of the coiled-coil regions in AvrM-A and avrM.....	83
4.4.3. Mutations in avrM that restore M recognition.....	91
4.4.4. Mutations that neutralize the non-polymorphic charged residues of AvrM-A abolish recognition	96
4.4.5. Solution properties of AvrM-A, avrM and mutants therein	101
4.4.6 Yeast Two-hybrid Assay.....	106
4.5 Discussion.....	108
4.5.1 AvrM polymorphic residues provide physical support for recognition specificity	109
4.5.2 AvrM charged residues contribute chemical support for recognition specificity.....	111
4.5.3 Surface properties also influence recognition	112
4.6 Conclusion	113
4.7 Experimental procedures	114
4.7.1 AvrM constructs preparation.....	114
4.7.2 Site-directed mutagenesis and transformation of the recombinant genes	114
4.7.3 Transient <i>in planta</i> expression assays.....	114
4.7.4 Protein extraction and purification.....	114
4.7.6 Immunoblot analysis.....	115
4.7.7 AvrM-A/avrM construction for expression	115
4.7.8 Size-exclusion chromatography (SEC)-coupled multi-angle light scattering (MALS).....	115
4.7.9 Size-exclusion chromatography (SEC)-coupled small-angle X-ray scattering (SAXS).....	116
4.7.10 Yeast Two-Hybrid assay.....	116
4.8 References.....	117
4.9 Supplementary Materials.....	118
Chapter Five: Final Discussion	122
5.1 Discussion.....	123
5.1.1 Dimerization of AvrM favours M recognition	126
5.1.2 Central charged pocket of AvrM dimer favours M recognition.....	128
5.1.3 AvrM is a highly evolved complex effector	129
5.1.4 Multiple contacts provide dynamic rather than cumulative support.....	131
5.1.5 Polymorphism K253/E316 has extra support to overcome effector targets.....	133
5.1.6 AvrM quaternary structure has an important role in M recognition.....	134
5.2 Future direction	135
5.2.1 A proposed model for the AvrM-M interaction.....	135
5.2.2 AvrM/M complex structure - a future direction	138
5.3 Conclusion	140
Appendices.....	141
Bibliography	150

Abstract

Food supply and security are urgent issues in a world of increasing population. Plants, which provide almost all of the world food supply, are under constant attack by various types of microbial invaders, thus posing tremendous threats to global food security. Of these microbes, rust fungi, a diverse group of obligate biotrophic phytopathogens having over 7,000 species, are causal agents of some devastating plant diseases, responsible for significant yield losses of several important crop species. Among the rust fungi, flax rust (*Melampsora lini*), the cause of rust disease to flax cultivars (*Linum usitatissimum*), is of great research curiosity more so from a scientific perspective and to a lesser extent economic. As an obligate biotroph, the flax rust fungus requires a living host, and hence it has to contend with the host's defence machinery to establish a successful infection and absorb nutrients from the infected host before sporulation. To protect themselves, plants devote a large proportion of their genome to the recognition of effector molecules secreted into the plant cells by the invading pathogen. This recognition and defence activation is orchestrated by disease resistance or R proteins. But the pathogen effector molecules show low sequence homology to other known proteins, making it difficult to predict their role in the infection process. For many years, flax and flax rust have been used as a model system for studying rust infection and disease resistance. The experiments described in this thesis aim to identify the crucial residues involved in recognition specificity of the flax rust effector AvrM and elucidate the roles of these residues in the interaction with the M flax resistance protein.

The *AvrM* effector locus of the flax rust fungus encodes six variants, designated *AvrM A-E* and *avrM*. Published structural and biophysical analysis of the AvrM-A protein predicts that it exists as a stable homodimer, forming a unique negatively charged pocket at the dimer interface, but not found in the similar region of *avrM* (Ve, 2011; Ve et al., 2011). Previous research has demonstrated that AvrM-A is recognised by, and interacts with, the M flax rust resistance protein, but that *avrM*'s lack of recognition and interaction is limited to a region containing 13 polymorphic residues between AvrM-A and *avrM* (Catanzariti et al., 2010). Chapter 3 of this thesis describes a mutation analysis, coupled with an *in planta* hypersensitive response (HR) assay, showing that no single polymorphic residue controls this recognition event. Results presented in Chapter 4 demonstrate that a combined mutant of

three polymorphic residues in *avrM*, when changed to their *AvrM-A* counterparts, enable partial M recognition, and the addition of another mutation enables full recognition. On the contrary, the same polymorphic substitutions, as in *avrM*, were also tested in the avirulence protein, *AvrM-A*, which is recognized by M, and found that multiple reciprocal substitutions (up to a quadruple mutant) did not prevent recognition by M. This suggests that other residues in *AvrM-A* still provide enough support to induce M-activated HR.

Furthermore, three non-polymorphic charged residues, which collectively form a negatively charged pocket at the interface of the *AvrM-A* dimer, when substituted for alanine, neutralize the charged pocket and thus prevent M interaction and recognition. Yeast-Two Hybrid (Y2H) assay confirmed that *avrM* does not, but the *AvrM-A* interacts with the M flax resistance protein. Size-exclusion chromatography (SEC) coupled with Multi-angle Light Scattering (MALS) and Small-angle X-ray Scattering (SAXS) show that *AvrM-A* is a stable dimer in solution, but *avrM* is a monomer. By the comparison of these results, the *AvrM-A* mutants that abolished HR, showed no interaction in the Y2H assay, but they are still dimeric as determined by SEC-SAXS analysis. On the other hand, the gain-of-recognition mutants of *avrM* could not be shown to interact with the M protein in the Y2H assay, but were still dimers as revealed by the SEC-MALS and SEC-SAXS analyses.

Collectively, these data suggest that for *AvrM* effector molecules to be recognisable by M, they must form homo-dimers. Also, the negatively charged pocket at the dimer interface of *AvrM-A* protein facilitates interaction with, and activation of, the M protein. Alteration of the quaternary structure of an effector protein represents another way in which a pathogen can avoid recognition by the plant innate immune system. This research has unravelled how the *AvrM* protein escapes M detection and will help guide further research aimed to understand how the effector molecules function to aid the pathogen, and how host R proteins detect them and protect the plant.

Declaration

I hereby declare that this thesis does not contain any material previously submitted for a degree or diploma in any university or institute, and does not incorporate with any material previously published or written by another person except where due references have been made in the text.

Signature
Md Motiur Rahman
April 2016

Acknowledgements

I would like to thank my supervisor, Dr Peter Anderson, for his day to day support and guidance. A special thanks for all of your times and efforts during my research and thesis preparation. I would like to thank my co-supervisor, Associate Professor Kathleen Soole: thank you for your ideas and introducing me to the world of molecular plant pathology.

I am very much grateful to Dr Simon Williams, Lachlan Casey and Alan Zhang (University of Queensland, Brisbane) for your continuous suggestion as well as assistance in doing the SEC-MALS and SEC-SAXS analyses. I am also very much thankful to Dr Maud Bernoux (CSIRO Plant Industry, Canberra) for your kind efforts in doing Yeast Two-Hybrid analysis. A special thanks to Michael Roach for responding to my endless emails with queries of protein purification, structural analysis (Chimera and PDB Viewer programs) and for the friendship we have developed through research. A huge thanks go to the people who made coming to University each day fun because, I knew I was going to see some of my best friends. Nick (x105), Emma (x100), Hayden (x100), Chris, Vajira, Crystal, Jajon, Crystal, Alex, Lettee, Badr - there are so many reasons to thank you all! Firstly, for all of the fun times at work, in the lab, the tearoom and in everyone office. Secondly, for always being happy to help and offer science advices. . Thanks to Dr Imran House and Dr Ahmad H. Kabir for your kind efforts in guiding me to settle in laboratory at the beginning of my candidature. Many thanks to Mr Afzal and Mr Lotus for giving me times in the school and in the tea room for the whole period of my PhD candidature and always giving me company.

Special thanks to my beloved wife, Mst Farzana Mehonaz for all of your supports and encouragement. Thanks also to my son, Sajid F Rahman and my daughter, Nooha Mooni: you both helped release my stress- you were my stress releasers during my PhD candidature.

My parents (Maa and Abba), thanks for your endless patient and inspiration during my staying in Adelaide for the completion of this PhD thesis. To my relatives, neighbours and friends: thank you for always showing an interest in my PhD and asking when it's done. Well, it is done now (April 2016)!

Alhamdulillah!

Chapter One: Introduction

(Pages 2 - 37)

1. Introduction

1.1 Plant pathogen - a constraint on agriculture

With the increasing demands of the world population, the food deficit is increasing day by day and food supply and food security are currently the most urgent issues in the world. Plants, which provide almost all of the world food supply for the human being and are the primary source of nutrients for many organisms from bacteria to vertebrates, are under constant attack by various types of microbial invaders, posing a tremendous threat to food security. Of the microbial invaders, fungi (Dean et al., 2012), oomycetes (Kamoun et al., 2015), viruses (Scholthof et al., 2011), bacteria (Mansfield et al., 2012), nematodes (Jones et al., 2013), viroids, virus-like organisms, phytoplasmas, etc. are the most destructive agents for huge economic losses and threatening food security globally. Hence, plant diseases are being considered as an environmental, social and economic threat that affects crop production worldwide. To the plant breeder, plant diseases are a major stimulus for improvement of economically important crops to balance the demand for world food supply. Despite the continued release of many new resistant cultivars, pathogen-associated global yield losses are still substantial (Baker et al., 2010; Oerke and Dehne, 2004). For maintaining an abundant and steady supply of food and fibre crops, there is no better alternative to controlling diseases in crop plants, for which we require an in-depth understanding of pathogenicity and disease resistance in plants.

1.2 Flax and flax rust disease

The flax or linseed (*Linum usitatissimum*) is a member of the genus *Linum* that belongs to the family, Linaceae. It is an economically important food and fibre crop cultivated in cooler regions of the world. Among the rust fungi, flax rust (*Melampsora lini*), the causal agent of rust disease in flax cultivars, is of great research interest from a scientific perspective and to a lesser extent economic (Dean et al., 2012). Flax rust fungus is a biotroph capable of causing severe losses in crop yield and of decreasing the fibre quality in flax plants cultivated for linen production. Indeed, this pathogen is an economically and environmentally damaging agent on many plant species of the Linaceae family.

In agriculture, flax rust disease is a leading constraint on flax and linseed production. Because of its economic and social significance as well as genetic tractability, this disease has been extensively studied and emerged as a model system for studying plant-microbe interaction. Flax rust is closely related to cereal rusts that are aggressive and potentially devastating diseases of important crop plants such as wheat and barley. Accordingly, before releasing any new variety to the farmers, plant breeders have to ensure the variety is genetically resistant to any of the rust strains of the geographical area. Then the farmers should only embrace such resistant varieties to cultivate in their field.

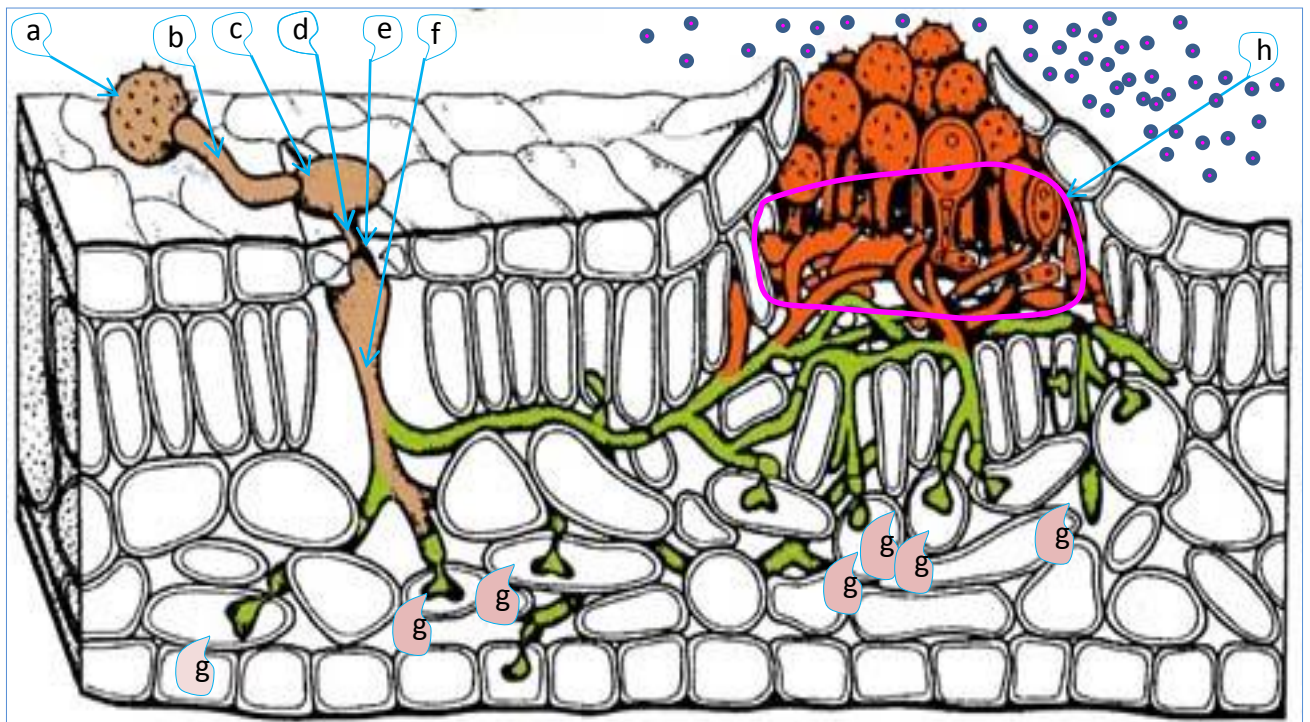


Figure 1.1: A diagrammatic view of a process of flax rust infection.

A rust uredospore (a) lands on a leaf surface and produces a germ tube (b), generating an appressorium (c) that enters the leaf by using its infection peg (d), penetrating through a stomata (e). A thread-like haustorium (f) invaginates the internal cells (g) to obtain nutrients. Eventually, the fungus produces blisters (h) that press against the host epidermis and breakthrough, releasing new spores (●) to the environment

(<http://web.ncf.ca/ah748/diagram.html>).

The flax rust infection proceeds by spores that germinate on the surface of the softer parts (mainly leaves) and enter through the gas exchange pores (stomata). Once inside

the leaf, hyphae grow between the cells and push feeding structures into the photosynthetically active cells. It is at this point that a cocktail of molecules, collectively known as effectors, is secreted and coerces the physiology of the invaded cells to redirect nutrients out of the host and into the fungus. After 10-12 days, the fungal fruiting bodies erupt through the leaf surface, producing a multitude of spores that complete the lifecycle and spread to healthy plants (Figure 1.1). Infection by flax rust fungus drastically reduces plant crop yields and in some cases heavily infected plants do not set seed at all and may eventually die. This pathogen has been adopted as a model system of great research significance, as it is easily tractable and provides vital insights into the molecular mechanism of host infection and plant immunity (Dean et al., 2012).

1.3. Plant defending system

Plants, like all other organisms, are continuously confronted by pathogen attack. As a result of evolution, almost all pathogens have adapted to subvert general plant defence mechanisms. Research has unravelled an ancient, yet ongoing, the conflict between pathogens and plants consisting of sophisticated and specialized molecular weapons of defence and confrontation (Dodds and Rathjen, 2010). Such weapons constitute a natural defence resistance mechanism for the plants to defend themselves against various types of abiotic stresses and biotic agents (de las Mercedes Dana et al., 2006). As a consequence of host plant innate immunity, successful pathogens evolved strategies for evading host plant immune responses (Dodds and Rathjen, 2010), while host plants evolved a complex multi-layered defence system to prevent pathogenic infection (Nurnberger et al., 2004; Chisholm et al., 2006). One much-studied plant-pathogen interaction is Effector-Triggered Immunity (ETI), in which the plant resistance machinery detects and interacts with the effector proteins secreted by the pathogen (Boller and He, 2009). ETI has been thoroughly investigated via the interaction between the biotrophic flax rust fungus and flax plant. Key components of host plant immunity are resistance genes (*R*) that encode receptor-like proteins capable of recognizing specific pathogenic effector molecules. Upon recognition of Avr effectors, the R protein switches on a defence response characterized by rapid induced necrotic cell death at the infection site (Luderer and Joosten, 2001; Martin et al., 2003; Dodds et al., 2004; Catanzariti et al., 2010a; Ve, 2011), which restricts the further growth and spread of the pathogens (Morel and Dangl, 1997; Catanzariti et al. 2007). The

interactions between the effector proteins and the cognate R proteins underlie gene-for-gene specificity and coevolution of pathogenic avirulence genes and plant resistance genes (Dodds et al., 2006).

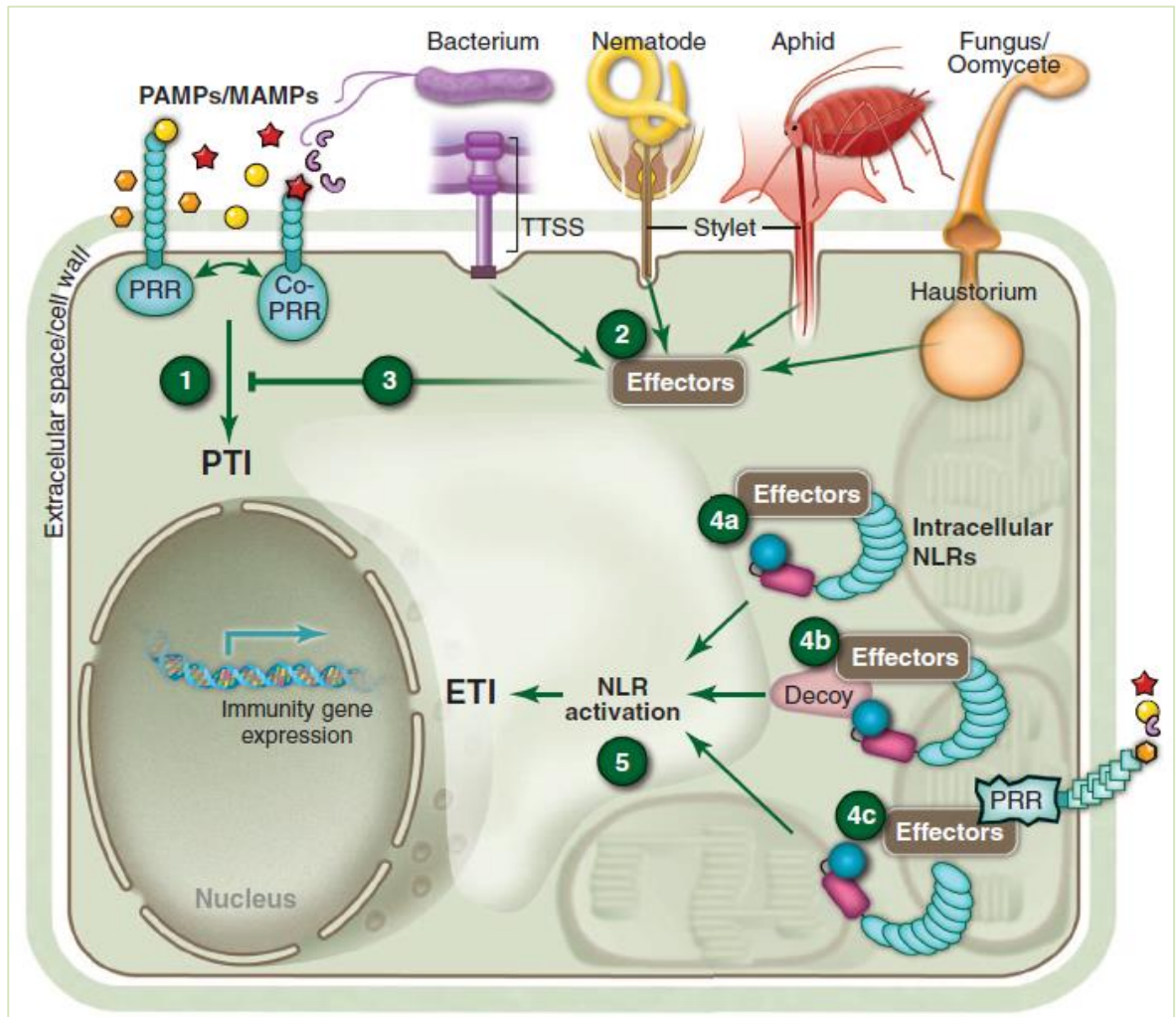


Figure 1.2: Schematic view of the plant immune system interacting with biotic invaders. Different pathogens, as colour coded and labelled, express PAMPs (Pathogen-associated molecular patterns) and MAMPs (Microbe-associated molecular patterns) so as to infect the hosts. **Step 1:** Plants sense these MAMPs and PAMPs through extracellular PRRs (Pattern Recognition Receptors) eliciting PTI (Pathogen Triggered Immunity). **Step 2:** Pathogens secrete virulence effectors to (i) the host cell apoplast to inhibit MAMP/PAMP detection (not shown) and (ii) the host cell interior. **Step 3:** The secreted effectors locate in specific subcellular sites where they can block PTI and favour virulence. **Step 4:** Intracellular nucleotide-binding leucine rich repeat (NB-LRR) receptors can perceive effectors mainly in three tactics: firstly (**4a**), by direct interaction of ligand; secondly (**4b**),

by perceiving effector modification in a decoy protein that physically imitates an effector target, and thirdly **(4c)**, by spying effector-mediated modification of a host virulence target, such as the cytosolic domain of the PRR (adapted from Dangl et al., 2013 followed by Dodds and Rathjen, 2010).

1.3.1 Physical barriers

Plants use physical barriers as a borderline of defence strategy. Unlike animals, plants have developed a ravishing array of physical, chemical and protein-based defences for detection of assaulting organisms and protection against severe damage. The simplest mechanisms are pre-existing passive resistance barriers like waxy cuticular surfaces, rigid cell walls and a variety of antimicrobial compounds (Gururani et al., 2012; Freeman and Beattie, 2008; Huckelhoven, 2007). Pathogens have to subvert these barriers as the first tier of defence installed by the plants (Göhre and Robatzek, 2008). The cuticular surface consists of a waxy layer on top of epidermal cells covering the plant tissue, safeguarding the host from many pathogens (Göhre and Robatzek, 2008). However, some physiological entry sites like stomata, hydathodes or wound points are unavoidably present in plants, which allow pathogens easy access. Once inside, the invading pathogens confront an adverse environment such as unfavourable pH, antimicrobial compounds and even thick cell walls before reaching host cellular contents (Göhre and Robatzek, 2008). Even after overcoming such obstacles, an invading pathogen faces the molecular weapons of plant innate immunity. Most pathogens have evolved the capacity to penetrate the passive barriers and enter the intracellular space of the plants but in turn, plants have evolved more sophisticated and specialized defensive strategies to perceive and prevent such assaults (Dangl and Jones, 2001).

1.3.2 Plant innate immunity

Plants are not defenceless against pathogenic attack, and host genotypes possess resistance (*R*) genes, the products of which have evolved the capacity to recognize specific effector molecules and activate a disease resistance response (Figure 1.2). *R* proteins of the nucleotide-binding leucine-rich repeat (NB-LRR) class recognise and interact with effector proteins, activating ETI as described above (Dodds and Rathjen, 2010). This response culminates in the death of the infected cell, which effectively starves the pathogen of nutrients, preventing colonization and disease symptoms. The

host is thus forfeiting a few cells to maintain a competitive advantage for the whole plant to ensure flowering and fruit setting. Plant *R* genes have been mobilized by cross-breeding into crop genotypes of cereals for over 100 years and are the basis of many of the elite varieties that are grown (this equates to a national benefit of \$1,500M/year to Australian cereal crops; Murray and Brennan, 2009). Also, host plants deploy a two-layered innate immune system incorporating both plasma membrane-associated and cytoplasmic immune responses (Dodds and Rathjen, 2010; Dangl et al., 2013).

1.3.2.1 MAMP- or PAMP-triggered immunity - perception of microbes through PRRs

The primary immune strategy is referred to as microbe or pathogen associated molecular pattern (MAMP/PAMP)-triggered immunity (PTI) (Jones and Dangl, 2006), by which the common features (MAMP or PAMP) of microbial invaders are detected, and a basal resistance response is triggered. This immune strategy is coined as MAMP/PAMP-triggered immunity (PTI). In this case, PAMP recognition receptors (PRRs) detect the macromolecules (MAMP/PAMP) usually within the extracellular spaces of the host plants (Jones and Dangl, 2006; Chisholm et al., 2006). Apparently, a threshold level of PAMP (e.g., flagellin) needs to come in contact with host surfaces for activation of a PTI response. This pathway involves the recognition of conserved pathogen molecules (PAMPs), by receptors positioned at plant cell surfaces named as transmembrane PRRs (Zipfel and Felix, 2005). A well characterised feature of PTI is the recognition of bacterial flagellin by the PRRs in both plant and animal systems (Gómez-Gómez and Boller, 2000). Recognition of a PAMP by the PRRs stimulates a signalling cascade involving Mitogen-Activated Protein Kinases (MAPK) and Ca^{2+} fluxes. This leads to a set of defensive maneuvers such as induction of reactive oxygen species (ROS), cell alkalinisation and accumulation of callose in the cell walls, for restricting pathogen permeation (Göhre and Robatzek, 2008). However, most pathogens have evolved competence to evade such maneuvers by deploying effector molecules in the cells (Cui et al., 2009). Furthermore, the secreted effectors can in some cases coerce the physiology of the host cell into service of the invading pathogen (Sohn et al., 2007).

1.3.2.2 Effector proteins - weapons to facilitate pathogenicity

Effectors are small protein molecules secreted by pathogens into host plant to promote infection through manipulating host metabolism and other physiological

processes to favour pathogenic survival (Win et al., 2012; van der Hoorn and Kamoun, 2008). The pathogen delivers effectors whose collective function is to blockade the detection mechanism of the host defence system and to boost pathogenicity by facilitating nutrient flow from the host plant cells (Staskawicz et al., 2001; Chisholm et al., 2006). Though the host plants have resistance proteins (R) as part of innate immunity, it renders race-specific resistance through recognition of pathogenic effectors (Catanzariti et al., 2015). However, there are many effectors secreted by a diverse range of pathogens. A better knowledge of pathogen effectors can assist biotechnologists in understanding the functions of the R proteins and facilitate the development of resistant plants that can ensure food security. When a particular R protein recognizes an individual effector molecule, is termed an avirulence (Avr) effector with respect to that R protein, whereas those that are not recognised are known as virulence effectors (*avr*) (Lo Presti et al., 2015; Ellis et al., 2006; Dodds et al., 2007; Bent and Mackey, 2007; Panstruga and Dodds, 2009; Staskawicz et al., 1995; Luderer and Joosten, 2001). Much research has been carried out on the general aspects of pathogen effectors (Petre and Kamoun 2014; Petre et al., 2014; Bonas and Ackerveken, 1997; Collmer, 1998; Laugé and Wit, 1998; White et al., 2000), showing that for successful biotrophic infection in a plant, fungal pathogens must first bypass plant basal defence and then overcome plant innate immunity either by modifying host cell structure and/or function. It has been advocated that avoidance of host resistance has become possible by the deployment of effector proteins secreted by the pathogen (Rafiqi et al., 2012).

Effectors are an important aspect of plant disease resistance research, and breeders are embracing such research for accelerating and improving resistance genes intending to identify, characterize and deploy in their breeding programs (Vleeshouwers and Oliver, 2014).

1.3.2.3 Effector-triggered immunity (ETI)

In the co-evolution of host-microbe interactions, pathogens evolved effector proteins secreted into the plant cells, the role of some being to deceive PTI and thus favour pathogen growth and disease. To confront such pathogenic manoeuvres, host plants advanced a second layer of immune strategy by recognising the effectors with proteins

known as R proteins, which leads defence responses towards microbial invaders that have acclimatized to elude PTI. In this case, the pathogens are identified by the plants through detection of specialized effector molecules delivered by the pathogens at the onset of infection process (Bent and Mackey, 2007; Panstruga and Dodds, 2009). The genetic basis of ETI has been designated as the “Gene-for-Gene” concept (Flor, 1971), where every *R* gene has a corresponding pathogenic gene capable of conferring pathogenicity for the pathogen, which is in most cases an effector. Recognition of the effector proteins appears to occur in the cytoplasm, either by the direct or indirect interaction between the individual effector and its cognate R protein (Jones and Dangl, 2006; Dodds et al., 2006; Krasileva et al., 2010). In contrast to PTI, ETI culminates in a hypersensitive response (HR) leading to programmed cell death (PCD) at the sites of infection (Greenberg, 1997).

This project intends to investigate the molecular basis of the interaction of flax and flax rust to determine how flax rust effectors are detected by the cognate R protein. The effector proteins investigated here are the flax rust effector, AvrM, derived from the flax rust strain CH5, and the cognate resistance protein is the M flax resistance protein, M. By agroinfiltration, when the genes that encode the effector proteins AvrM are injected into cells of tobacco leaves having M gene (W38::M), a resistance response (HR) is induced as a result of ETI.

1.3.2.4 Resistance modes of pathogen recognition

Six decades ago, Flor (1955, 1956) deduced the genetics of the alleles in flax and flax rust loci that have recently been cloned and utilized by scientists (Dodds et al., 2004). Such breakthroughs indicated that the products of the host *R* genes function either as receptors that interact directly with the corresponding Avr protein (the ligand-receptor model) or as monitors (“guards”) of the host proteins that are targets of the effectors and thus indirectly detect the Avr proteins (the guard hypothesis; van der Biezen and Jones, 1998; Dangl and Jones, 2001). The latter case relies on the perception of effector--induced modifications in the host proteins termed as ‘decoys’, ‘guardees’, or more commonly co-factors by the R proteins (Dangl and Jones, 2001; van der Hoorn and Kamoun, 2008; Collier and Moffett, 2009). The host proteins can also evolve to resemble and “decoy” those targets (decoy model; van der Hoorn and Kamoun, 2008). As per the ‘gene-for-gene theory’ (Flor, 1971), host R proteins trigger a successful disease resistance by detecting a

particular Avr protein secreted by the pathogen. The viewpoint of this theory indicates that evolutionary force works in the pathogens to evolve a diverse range of effector proteins that are no longer genetically detectable by the cognate R proteins, but retain the core function for the advancement of pathogenicity. Conversely, host immunity is favoured by natural selection to evolve allelic diversity at the R loci, enabling the hosts to develop a broad spectrum of recognition specificity. This standpoint is supported by the direct interaction between flax rust effectors (*AvrL567*) and the cognate variants of the flax plant R protein (Dodds et al., 2006).

It has been reported that an activation of ETI by an R protein can follow the “ligand-receptor model” (Jia et al., 2000; Dodds et al., 2006; Catanzariti et al., 2010a; Krasileva et al., 2010; Ravensdale et al., 2012). Alternatively, the R proteins can trigger ETI following either by preferably the “guard” model or the decoy model.

1.4 Flax rust resistance and M resistance gene

The basis of plant-pathogen relationship is the interaction of the host R protein and pathogen effector protein, which is an important aspect of studying plant pathogenesis. One of the plant known R genes is the *M* flax resistance gene that was isolated and cloned from flax plant (Anderson et al., 1997). A yeast expression system was developed ten years later to express and purify recombinantly expressed M protein (Schmidt et al., 2007a).

The M protein, belonging to the TIR-NB-LRR (Toll Interleukin 1 Receptor-Nucleotide-Binding-Lucine-Rich Repeat) class, is one of the R proteins of flax located in the tonoplast membrane (Takemoto et al., 2012). Several flax rust effector genes and their cognate flax R-genes have been identified and cloned. Of the flax rust effectors, *AvrM* and *AvrL567* are two model rust effector genes that have been demonstrated to interact directly with the R proteins M and L6, respectively. The crystal structures of these two model effectors have also been resolved (Wang et al., 2007; Ve et al., 2013). Using the Yeast Two-Hybrid (Y2H) system, the M protein has been found to interact directly with its flax rust cognate effector *AvrM-A* protein, but not with the virulence variant, *avrM* (Catanzariti et al., 2010a). In flax cultivars, the 31 genes that confer resistance to different strains of flax rust have been mapped to five separate loci, namely *K*, *L*, *M*, *N* and *P*, each of which having several allelic variants (Islam and Mayo, 1990). Of these, 19 R genes have been cloned from flax cultivars

and characterized as TIR-NBS-LRR class proteins (Anderson et al., 1997; Dodds et al., 2001a, Dodds et al., 2001b; Ellis et al., 1999; Lawrence et al., 1995; Lawrence et al., 2010b).

1.5 Plant pathogens

Plants are continually under attack by various types of microbial invaders in different ways; some settle on the plant surface, others colonize the plant tissue, and others move through vascular bundles into specific areas such as the leaves, stems and roots. Most plant pathogens are very diverse and evolve to infect a particular plant species or the whole genus of the host plants. Plant pathogens receive the benefits of host metabolic processes, or use the host plants as a source of valuable nutrient resources. In this way, they commonly cause damage like brown spots, tissue death, problems with flower setting, decrease in fruit setting and so forth. The acute stage of infection can severely reduce the growth and yield of the crop plants or the host plants can be devastated or eventually die.

1.5.1 Haustorium

As obligate biotrophs, rust fungi solely depend on a living host, obtaining nutrients from the host plants through a haustorium (Voegelé and Mendgen, 2003; Hahn and Mendgen, 2001; Catanzariti et al., 2006; Weßling et al., 2012). As a part of the fungal lifestyle, the haustorium is a specialized feeding structure originating from a fungal hypha, which invaginates the plasma membrane of the host cell tissues and intracellular spaces of the host plants for absorbing nutrients and other fluids (Figure 1.3) (Catanzariti et al., 2006).

Haustoria form a bridge to facilitate the molecular translocation between the fungal parasite and the host, most remarkably the translocation of effector molecules into the host cytoplasm (Rafiqi et al., 2012). It is also reported that fungal pathogens have structures such as infection hyphae, which may also mediate such molecular trafficking (Rafiqi et al., 2010). The rust haustorium has a neckband that makes the haustorium a discrete compartment, surrounded by the extrahaustorial membrane and the extrahaustorial matrix (Voegelé and Mendgen, 2003). By use of haustoria, rust fungi establish a successful biotrophic relationship with the host plant and manipulate the host plant metabolism in favour of their pathogenic growth and propagation (Voegelé and Mendgen, 2003). During host colonization, fungal pathogens release effector proteins into the host cells to defend against the host resistance mechanisms (Kobayashi et al., 1994; Heath, 1997; Voegelé and Mendgen, 2003).

1.5.2 Oomycete pathogens

Evolution of the parasitic and pathogenic lifestyle in eukaryotes has occurred many times, and fungi and oomycetes (sometimes known as water molds) form two distinct groups with separate evolutionary origins (Sogin and Silberman, 1998). Nevertheless, both use similar strategies for infection and host colonization (Latijnhouwers et al., 2003). Oomycetes constitute a distinct group of plant pathogens previously placed in the kingdom of fungi due to their filamentous morphology, similar feeding habits and reproduction strategies. However, oomycetes are eukaryotic microbes superficially resembling filamentous fungi. The modern science categorizes them in the kingdom of Heterokonts or Stramenopiles, which is phylogenetically linked to a diverse group of protists including brown algae and diatoms (Gunderson et al., 1987; Sogin and Silberman, 1998; Baldauf, et al., 2000; Thines and Kamoun, 2010; Thines, 2014). Of the oomycetes, some are saprophytic and hence contribute to soil fertility by decomposing organic materials and recycling nutrients. Conversely, most of the Oomycetes form a profound lineage of plant pathogens affecting both agriculture and natural ecosystems. On the basis of scientific and economic importance, there is a survey carried out with the oomycete pathologists (with an association with the Journal of *Molecular Plant Pathology*) and a published report on the introduction of current research of the 'Top 10' oomycete pathogens as a point of reference for future research in oomycetes (Kamoun et al., 2015). Among the pathogenic oomycetes, *Phytophthora* and *Pythium* species are necrotrophic and hemibiotrophic, while downy mildews (e.g., *Hyaloperonospora* species) are obligate biotrophs (Stassen and Van den Ackerveken, 2011). Identification of a large repertoire of effectors and thereby a greatly improved understanding of oomycete pathogens became possible by genome sequencing of *P. infestans* (Haas et al., 2009), *Hyaloperonospora arabidopsidis* (Coates and Beynon, 2010), *P. ramorum* and *P. sojae* (Tyler et al., 2006), and *Pythium ultimum* (Levesque et al., 2010). *P. infestans* is one of the most studied oomycete pathogens, as it is the causative agent of late blight in tomatoes and potatoes (Kamoun, 2003).

1.5.2.1 *Phytophthora* species

Phytophthora infestans is a hemibiotrophic oomycete responsible for the Irish potato famine (Yoshida et al., 2013; Goss et al., 2014), and a vast amount of chemicals are required to protect the potato harvests from this pathogen (Judelson et al., 2005). To date, late blight remains a significant barrier to producing consistent yields of potato,

which is one of the staple crops in the world (Smith, 2012). Thus, *P. infestans* is a perpetual threat to food security (Haverkort et al., 2008; Fisher et al., 2012). Other members of this taxon include *P. ramorum* and *P. sojae*, responsible for causing sudden oak death and soybean stem/root rot agent, respectively. At the onset of infection, the pathogen confronts the plant-produced anti-microbial enzymes in the apoplast and hence needs to bypass detection by the pattern recognition receptors (PRRs). There are two broad classes of *Phytophthora* effectors, apoplastic and cytosolic effectors (Hardham and Cahill, 2010). Apoplastic effectors comprise the secreted hydrolytic enzymes (e.g., proteases and glycosylases) that degrade the host cell walls, frustrate the host defence enzymes and acts as toxins to induce host cell death in facilitating infection. The soybean pathogen *P. sojae* secretes glucanase inhibitor proteins (GIPs) that block endo-glucanase-mediated resistance of the host plants (Rose et al., 2002; York et al., 2004). *P. infestans* secretes EPIC1 and EPIC2B, effectors that interact with and inhibit multiple apoplastic proteases in tomato (Tian et al., 2007; Song et al., 2009) and *N. benthamiana* (Kaschani et al., 2010). Another unrelated biotrophic fungus, *Cladosporium fulvum*, secretes the Avr2 effector that interacts with and inhibits the tomato cysteine protease, Rcr3 (Song et al., 2009).

In contrast, the cytoplasmic effectors of the oomycetes translocate into and function inside the host cells. Two major types of oomycete-secreted cytoplasmic effectors have been reported (Kamoun et al., 2006), RXLR-effectors and crinkler (CRN)-effectors (Stassen and Van den Ackerveken, 2011; Wawra et al., 2012a). The former type contains a conserved N-terminal amino acid (aa) sequence, RxLR (arginine-any amino acid-leucine-arginine) that is assembled at the N-terminal signal peptide involved in host translocation (Whisson et al., 2007). Oomycete RXLR-effectors that have been studied in detail include AvrM3a and Avrblb2 from *P. infestans* (Bos et al., 2006; Bozkurt et al., 2011) and Avr1b from *P. sojae* (Duo et al., 2008). *P. infestans* has the *Avr3a* effector gene that has two alleles encoding AVR3a^{K80, I103} and AVR3a^{E80, M103}, differing by two aa polymorphisms (as shown therein) in the C-terminal regions. The former (Avr3a^{KI}) is recognized by the potato resistance protein R3a, while the latter (Avr3a^{EM}), avoids detection (Armstrong et al., 2005). The Avrblb2 effector specifically targets and interacts with plant cysteine protease, C14, preventing it from a secretion in the apoplast. This significantly enhances

susceptibility to *P. infestans* (Bozkurt et al., 2011), indicating an active role of C14 in plant resistance and for Avrblb2 as a virulence factor.

The second class of oomycete effector, the CRN-effector, is often cysteine-rich (Kamoun, 2006), including the CRN1 and CRN2 effectors that are secreted by *P. infestans* and cause leaf-crianking in *Nicotiana* spp and tomato plants (Torto et al., 2003). Similar to the RXLR effectors, the CRN effectors consist of modular domains with a predicted signal peptide sequence motif at the N-terminal followed by a translocation domain LFLAK (leucine-phenylalanine-leucine-alanine-lysine) and a C-terminal domain (Schornack et al., 2010). Genome analysis confirms that there are 196 CRN genes in *P. infestans*, 100 in *P. sojae* and 19 in *P. ramorum* (Haas et al., 2009). Subcellular localization of the diverse CRNs secreted by *P. infestans* confirmed their presence and accumulation in the plant nuclei. It has been found that accumulation of CRN8 in the host nuclei is required to trigger PCD, supporting the hypothesis that CRN molecules target and perturb the nuclear processes of the host plants to facilitate infection (Schornack et al., 2010).

1.5.2.2 *Hyaloperonospora arabidopsidis* - an oomycete pathogen model species

Hyaloperonospora arabidopsidis (*Hpa*), formerly known as *H. parasitica* and *Peronospora parasitica*, is one of 700 downy mildew species belonging to the family of Peronosporaceae (Thines, 2014). The *Phytophthora* genus includes several plant pathogens that are causative agents of some of the most devastating diseases in not only ornamental and forestry plants but also in agricultural plants, and thereby impact severely on global crop production (Tyler et al., 2006; Haas et al., 2009). This genus is one of the several pathogens that cause downy mildew on *A. thaliana* (Coates and Beynon, 2010). Moreover, other taxa of downy mildew pathogens cause destructive diseases on important crop plants, particularly *Plasmopara viticola* on grape, *Pseudoperonospora cubensis* on cucurbits, *Hyaloperonospora* and *Peronospora* spp. on brassica crops, *Bremia lactucae* on lettuce and *Peronosclerospora* spp. on sorghum and maize (Lucas et al., 1995).

Like the flax rust fungus, *Hpa* is an obligate biotrophic microbe and considered to be a model pathogen in oomycete research (Holub, 2008). Research in *Hpa* has made a significant contribution to our understanding of plant-pathogen interactions, notably for the identification and isolation of *Arabidopsis RPP* genes (resistance to *P. parasitica*),

several of which have been identified (Parker et al., 1996, 1997; Holub and Beynon, 1997; McDowell et al., 1998; Bittner-Eddy et al., 2000). In addition to the *RPP* genes, their cognate effectors *ATR* (*Arabidopsis thaliana* recognised) genes have also been identified and cloned from the pathogen (Allen et al., 2004; Rehmany et al., 2005; Bailey et al., 2011). *ATR1* and *ART13*, both RXLR-type effector genes from *Hpa*, have been studied in detail (Rehmany et al., 2005; Krasileva et al., 2010; Chou et al., 2011; Allen et al., 2004; Sohn et al., 2007; Mishra et al., 2015). On the basis of avirulence specificity, several RxLR-effectors, additional to *ATR1* and *ART13*, have been identified, including *AVR3a*, *AVR4*, *AVRblb1* and *AVRblb2* from *P. infestans* (Schornack et al., 2009). The *ATR5^{Emoy2}* and *ATR5L* effector genes from *Hpa* have been cloned and characterized, and the former has been shown to trigger a defence response in *Arabidopsis* lines expressing the *RPP5* resistance protein, while the latter does not (Bailey et al., 2011).

Downy mildew (*H. parasitica*) is an *Arabidopsis* pathogen that secretes *ATR1* and *ATR13*, effector proteins that are recognised by resistance proteins, *RPP1-Nd/WsB* and *RPP13-Nd*, respectively (Sohn et al., 2007). *AVR3a*, secreted by *P. infestans*, was identified as a cognate effector protein that confers avirulence on potato plants expressing the *R3a* resistance protein (Armstrong et al., 2005). Use of gene-silencing has confirmed that *P. infestans* produces elicitor protein *INF1* that functions as an avirulence factor, inducing an HR in plants (Kamoun et al., 1998). *AVR3a* has two alleles, *Avr3a* and *avr3a* that contribute recognition specificity by the *R3a* and suppression of *INF1* HR (Bos et al., 2006). *PexRD2* and *AVR3a11* (a homologue of *P. infestans* *AVR3a*) are RXLR-effectors secreted by *P. infestans* and *P. capsici*, respectively (Vleeshouwers et al., 2008; Oh et al., 2009; Armstrong et al., 2005; Bos et al., 2006, 2009). Knowledge of oomycete pathogens can support research on fungal pathogens as their infection processes are very similar.

1.5.3. Bacterial pathogens

Though many bacteria are beneficial for plants, there are about 200 species that are devastating plant pathogens, mostly belonging to the *Pseudomonas* and *Xanthomonas* genera of the family of Pseudomonadaceae. Bacteria form a major group of plant pathogens. Given their scientific and economic importance, a survey with bacterial pathologists (with an association with the Journal of Molecular Plant Pathology) ranked the 'top ten' bacterial plant pathogens (Mansfield et al., 2012), listing as (1) *Pseudomonas*

syringae pathovars; (2) *Ralstonia solanacearum*; (3) *Agrobacterium tumefaciens*; (4) *Xanthomonas oryzae* pv. *oryzae* (Xoo); (5) *X. campestris* pathovars; (6) *X. axonopodis* pathovars; (7) *Erwinia amylovora*; (8) *Xylella fastidiosa*; (9) *Dickeya* (*dadantii* and *solani*); (10) *Pectobacterium carotovorum* (and *P. atrosepticum*). Of the pathogenic bacteria, *P. syringae* and *X. oryzae* are the most-studied, offering insight into the infection process.

1.5.3.1 *Pseudomonas syringae*

Pseudomonas syringae, a rod-shaped, Gram-negative bacterium with polar flagellae, infects a broad range of host species. It is a hemibiotrophic plant pathogen living on the leaf surface as well as in the apoplastic space. This microbe exists as over 50 pathovars, making the strongest advent on the scientific and economic arenas. A recent survey suggested this pathogen has had an enormous impact on the scientific interpretation of microbial pathogenicity and is a continuous causative agent of economically important plant diseases (Mansfield et al., 2012). Of the bacterial plant pathogens, *P. syringae* is considered as a model for cytoplasmic effector proteins and their pathogenicity in biotrophic infection (Lindeberg et al., 2012). Plant and animal pathogenic bacteria such as *P. syringae* employ the Type III secretion system (T3SS) to translocate effector molecules directly into the cytosol of the host cells (Hueck, 1998; Gálan and Collmer, 1999), using a needle-like structure (Gálan and Collmer, 1999; Schraidt et al., 2011). In turn, plants have evolved resistance proteins (R) to detect and counteract the bacterial effectors and thus reinstate resistance to the host against pathogens. For detection of bacterial pathogens, plants use pattern recognition receptors (PRRs) to initiate innate immunity, either by FLS2 (a PRR), or EFR (another PRR) (Göhre et al., 2008). A recent review reported host plant evolved a plethora of sensors for perceiving the type III secreted effectors (T3Es) and thereby triggered ETI (Khan et al., 2016).

Many effector proteins have been identified from different pathovars of *P. syringae* (Joardar et al., 2005; Studholme et al., 2009). For example, *P. syringae* pv. *pisi* secretes the AvrRPS4 effector protein that is recognised by the RPS4 resistance protein (Sohn et al., 2009). Most of the effector proteins secreted by the other pathovars of *P. syringae* employ T3SS for their secretion (Lindeberg et al., 2008; Buell et al., 2003). AvrPto and AvrPtoB, two effectors secreted by *P. syringae*, each suppresses several PAMP responses after elicitation (Block et al., 2008). AvrPto is one of the type III effectors (T3Es) that promote disease in susceptible

plants and trigger immunity in plants having the Pto kinase and another related resistance protein, Prf. Moreover, AvrPto has been shown to bind receptor kinases to inhibit host immune responses in infected cells, including tomato LeFLS2, and *Arabidopsis* FLS2 and EFR (Xiang et al., 2008). AvrPtoB, which activates HR in tomato cultivars having the Pto kinase, is composed of two functional domains, an N-terminus that interacts with Pto and a C-terminus with E3 ligase capacity. Both domains of the AvrPtoB effector function together for virulence specificity of PtoDC3000 in *Arabidopsis* by eliminating FLS2 from the cell periphery and other PAMP sensors of the host plants (Göhre et al., 2008). AvrPtoB also targets the Chitin Elicitor Receptor Kinase 1 CERK1 (Gimenez-Ibanez et al., 2009), a PRR capable of detecting chitin. Another study suggested that AvrPtoB uses its different domains to interact with the receptor kinases, and that the principal target is BAK1, a signalling cofactor for several other plant PRRs (Cheng et al., 2011).

1.5.3.2 *Xanthomonas* species

Xanthomonas is a group of 27 species of Gram-negative bacteria that collectively cause severe disease in about 400 plant species, many of which are economically important crops (Ryan et al., 2011). Individual *Xanthomonas* species often comprise numerous pathovars that exhibit a broad range of host specificity. Some even show tissue specificity, infecting either the mesophyll tissues or the vascular systems of the host plants (Parkinson et al., 2007). For example, *X. oryzae* has host-specific pathovars that infect rice and some of its wild relatives, whereas *X. campestris* sp. assault different Solanaceous, brassicaceous and related species. Both bacterial species include pathovars that infect through the vascular tissue and others that colonize the apoplastic spaces of parenchyma tissue. *Xoo* makes multiple virulence elements including iron-chelating siderophores, extracellular enzymes, type III-secretion dependent effectors and exopolysaccharides (EPS), which are collectively critical for virulence specificity (Mole et al., 2007; He et al., 2010).

To tackle host immunity, *Xoo* utilizes two types of quorum-sensing (QS) elements, DSF (Diffusible Signal Factor) and Ax21 (Activator of XA21-mediated immunity) protein, a type I secreted protein (He et al., 2010; Han et al., 2011). Among the *Xanthomonas* spp and related genera, Ax21 is highly conserved, and some of the orthologues are capable of activating XA21-regulated immunity (Lee et al., 2009), indicating that Ax21 plays an important role in the sabotage of host resistance. Ax21 was demonstrated to serve as a

key biological factor, showing a dual role in QS and the activation of host innate immunity (Han et al., 2011). Ax21-facilitated QS regulates biofilm formation, motility and virulence. However, *rpf* (regulation of pathogenicity factors) is a gene cluster involved in DSF-mediated QS (Jeong et al., 2008), while *rax* (required for AvrXa21) genes regulate Ax21-mediated QS (Lee et al., 2006). Given the genetic and genomic evidence, *Xoo* has been suggested to deplete the DSF-type QS system to control virulence factor synthesis (He et al., 2010). Like other plant pathogenic bacteria, *Xanthomonas* spp secrete effectors through the T3SS into the host cytosol. *X. campestris* pv. *vesicatoria* (*Xcv*), the causative factor of spot disease in tomato and pepper plants, secretes AvrBs3, a TAL effector. This effector localizes to the host nucleus and stimulates hypertrophy of the mesophyll cells in the host plant (Marois et al., 2002; Kay et al., 2007), thus facilitating the spread of *Xcv* to other crops (Wichmann and Bergelson, 2004).

The resistance proteins of rice and pepper, Xa27 and BS3 respectively, contain UTP (upregulated by TAL effectors) domains to which the AvrXa27 and AvrBs3 effectors respectively bind, thereby activating the R proteins and inducing defence signalling (Gu et al., 2005; Romer et al., 2007). Exceptionally, the *Bs4* resistance gene of tomato plant encodes an NB-LRR receptor, which recognises the AVRbs4 effector molecule in the cytosol (Schornack et al., 2004). Research advancement of bacterial pathogens can be supportive for fungal pathogen research.

1.5.4 Fungal pathogens

Fungi are heterotrophic microbes exhibiting diversity in habitat and morphology. Their cell walls are mostly composed of carbohydrate chitin, while that in plants is formulated by cellulose. Most of the fungal microbes being investigated scientifically are pathogens of agricultural plants. Of those fungal pathogens and the effectors that they secrete, more is known about effector translocation to the host plant cell than of their recognition specificity and pathogenicity.

Fungi acquire nutrients by absorption from the organic source they live on or in, as they are incapable of producing their own food. Of those fungi that interact with plants, some are beneficial, but most of them are pathogenic to plants. Most fungal plant pathogens

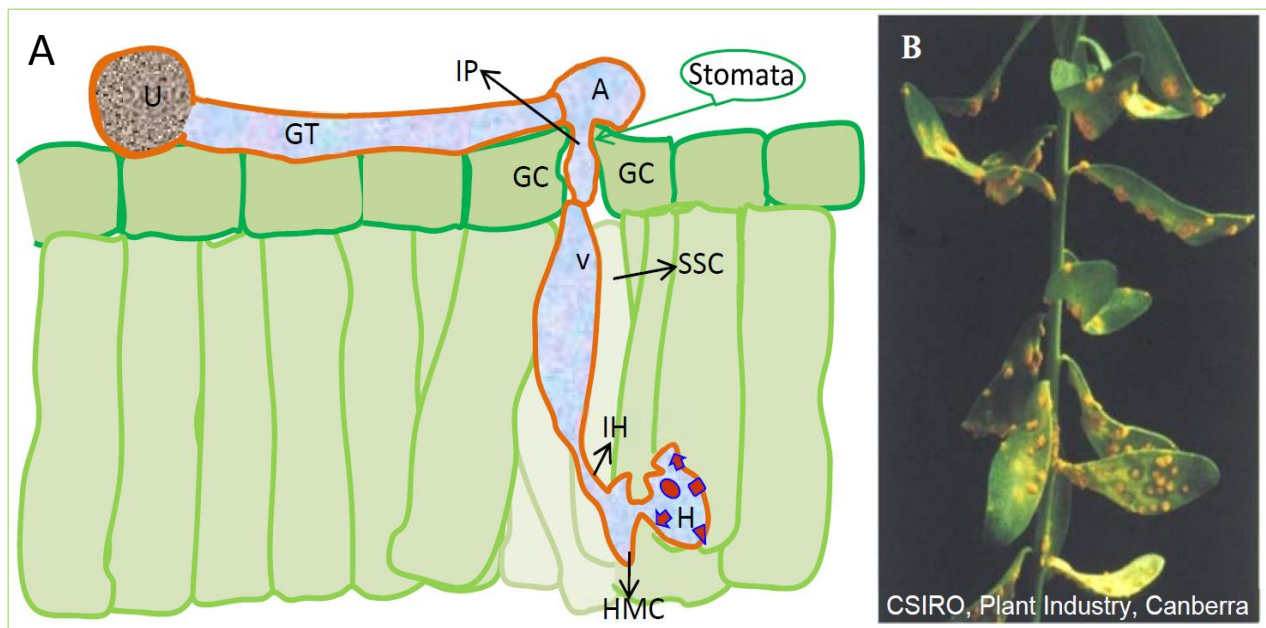


Figure 1.3: A diagrammatic illustration of fungal infection. (A) A uredospore germinates producing a haustorium that invaginates plasma membrane and secretes effectors (red). (Here, **U** = uredospore; **GT** = germ tube; **A** = appressorium; **GC** = stomatal guard cells; **IP** = infection peg; **V** = sub-stomatal vesicle; **SSC** = sub-stomatal cavity; **IH** = infection hypha; **HMC** = haustorial mother cell; **H** = haustorium, plural Haustoria (Adapted from Hoch et al., 1987). (B) A flax plant having flax rust disease (CSIRO Plant Industry, Canberra).

belong to the Ascomycete and Basidiomycete families and have a substantially deleterious effect on yield and quality of many different crop plants. Fungal pathogens manipulate host metabolism and alter host physiology in favour of their life cycle, thereby inducing disease in the host plants. Over the last 60 years, genetic studies of virulence in fungal microbes with different pathogenic lifestyles have advanced by use of comparative interaction studies of plant pathogens. Such advancements have indicated the importance of a range of molecules in the armoury of plant pathogens, such as carbohydrate active enzymes (CAZys) and secondary metabolites, and effector proteins (Stergiopoulos et al., 2013; McDowell, 2013; Ohm et al., 2012; O’Connell et al., 2012).

Hundreds of small secreted proteins, considered as Candidate Secreted Effector Proteins (CSEPs), have been reported in a broad array of rust fungi (Petre et al., 2014). Among other

fungal effectors, four *Avr* genes, denoted as *Avr2*, *Avr4*, *Avr4E* and *Avr9*, have been cloned from *Cladosporium fulvum*, which are recognized by the cognate tomato *R* genes (De Wit et al., 1997; Joosten and De Wit, 1999; Thomma et al., 2005). *Rhynchosporium secalis* secretes three low-molecular-weight peptides, named as Nip1-Nip3, which trigger defense responses (non-HR) in barley cultivars carrying cognate *Rrs* resistance genes (Hahn et al., 1993). *Fusarium oxysporum* f. sp. *Lycopersici* is reported to secrete the *Avr3* effector protein that triggers ETI in the presence of the tomato *I-3* resistance gene (Huang and Lindhout, 1997; Rep et al., 2004). Nine avirulence genes, designated *AvrLm1-AvrLm9*, have been mapped in the genome of *Leptosphaeria maculans* (Balesdent et al., 2002). *Magnaporthe oryzae* is a devastating rice pathogen that secretes several *Avr* genes including *Avr-Pita* (Orbach et al., 2000; Valent et al., 1991), *Avr1-CO39* (Farman and Leong, 1998), *Ace1* (Bohnert et al., 2004; Collemare et al., 2008) and the *Pwl* effectors (Kang et al., 1995; Sweigard et al., 1995). So, effector proteins are ubiquitous amongst plant fungal pathogens, however, this project and subsequent sections will concentrate on effector proteins found in the rust fungi and specifically flax rust, *Melampsora lini*.

Understanding the interactions between plants and these molecules (enzymes, secondary metabolites and effector proteins) has allowed identification and deployment of host plants of increased resistance to pathogens (Vleeshouwers and Oliver, 2014; Dangl et al., 2013). Indeed, this novel discovery has facilitated the involvement of effectoromics as well as pathogen owned maneuverings in a wider range of host plants (Dangl et al., 2013). Understanding the mode of fungal infection and the mode of host plant immunity is a great challenge to food security and success in breeding resistant crops may hopefully bring the green revolution to crop plants that will balance the food demand and supply in the world. This project aims to contribute knowledge to research in fungal resistance breeding program.

1.5.5 Rust fungi

Rust fungi belong to the order of Pucciniales (previously known as Uredinales) and are examples of haustorial-producing fungal pathogens that secrete effector proteins into host cells. There are many pathogen species capable of causing rust diseases, which are devastating to many valuable crop cultivars. Therefore, production of plants that tolerate such microbes is now a significant global challenge. Research aimed to understand the

pathogenic pattern of the microbial invaders, and the mode of resistance of the host plants is of great importance to food security, making it an urgent issue to unravel the molecular mechanism of rust disease pathogenicity and host resistance. In contrast to many other pathogens, rust fungi are of both scientific and economic importance. In fact, as a haustoria-producing pathogen, rust fungus is one of the most destructive plant parasites. They cause enormous economic losses in the world agricultural industry as well as having a devastating effect on natural ecosystems (Catanzariti et al., 2007). Rust fungi, as obligate biotrophs, produce haustoria to draw nutrient from the living cells of host plants, and depend fully on the host for completing their life cycle (Catanzariti et al., 2006; Hahn and Mendgen, 2001). During infection, these pathogens manipulate the host metabolism and defence mechanisms in support of biotrophic growth and propagation, by secreting effector proteins into host cells (Kobayashi et al., 1994; Heath, 1997; Voegelé and Mendgen, 2003).

1.5.5.1 Rust fungus as a pathogen

Rust fungi are filamentous eukaryotic plant pathogens, many of which are devastating to economically important crop plants (Hahn and Mendgen, 2001; Yin et al., 2011), causing disease in agricultural crop plants such as corn, wheat and other cereals, sugarcane, grasses, potato, soybean, junipers (red cedar), apple, Japanese quince, hawthorn, currant, species of gooseberry, asparagus, bean, coffee, rose, chrysanthemum, hollyhock, snapdragon, pines and poplars (Encyclopedia Britannica: <http://www.britannica.com/science/rust>)

Typically, rust fungi secrete effector molecules at the onset of infection, so that they can establish and colonise the host prior to sporulation (McDowell, 2013; Vleeshouwers and Oliver, 2014). The host-pathogen interaction is controlled by the gene-for-gene specificity (Flor, 1971) of the host R proteins with the pathogen avirulence effectors. Immune activation by a host R protein induces HR at the infected sites of the host.

1.5.5.2 Rust effectors

Of the 30 *Avr* genes have been identified in *Melampsora lini* (Ellis et al., 1997), genes have been cloned from four loci and shown to encode Haustorially Expressed Secreted Proteins (HESPs) that elicit HR in flax plants carrying the cognate *R* genes (Catanzariti et al., 2006). From all rusts, only six effector genes have been identified and described (Table 1.1) by mapping the candidate genes (Catanzariti et al., 2006; Dodds et al., 2006; Dodds et al.,

2006; Kemen et al., 2005; Upadhyaya et al., 2014). These effectors are all secreted from haustoria and translocated into host cells. Of the four flax rust effectors (Table 1.1), AvrM and AvrL567 have been verified as recognized directly by cytosolic plant immune receptors, indirectly authenticating their internalization in the plant cell (Ellis et al., 2007). Furthermore, AvrM and RTP1 (Rust Transferred Protein 1) have been demonstrated to be smuggled directly from haustoria to plant cells during infection (Kemen et al., 2005, 2013; Rafiqi et al., 2010). PGTAUSPE-10-1 has been identified as the successfully recovered top candidate among 42 CSEPs in *P. graminis* f. sp. *tritici* (Upadhyaya et al., 2014). Recent research has suggested that AvrP4, AvrM and AvrL567 effector molecules are capable of migrating into host cells independently (Catanzariti et al., 2006; Kale et al., 2010; Rafiqi et al., 2010). Host cell entry of AvrL567 and AvrM has been shown to be governed by the divergent N-terminal uptake domains (Rafiqi et al., 2010), which further have been proven to carry hydrophobic residues that are critical for host cell entry of AvrM (Ve et al., 2013). Almost all the rust fungal effector proteins studied to date are avirulence factors, such as AvrM, AvrL567, AvrP123 and AvrP4 of the flax rust fungus, *M. lini* (Ravensdale et al., 2011), and PGTAUSPE-10-1 of wheat stem rust *P. graminis* f. sp. *tritici* (Upadhyaya et al., 2014). However, their specific role in pathogenicity remains mysterious.

Another fungal pathogen, *Leptosphaeria maculans*, causes stem canker or blackleg disease in Brassica crops. This fungus secretes the AvrLm4-7 effector protein that shows a dual recognition specificity by two R proteins, Rlm4 and Rlm7 of oilseed rape (Parlange et al., 2009). The effector gene *AvrPiz-t* from *M. oryzae* and the cognate R gene *Piz-t* from rice were isolated and cloned (Zhou et al. 2006; Li et al., 2009). *AvrPiz-t* is recognized by the *Piz-t* protein mounting an immune response in rice (Li et al., 2009). The AVR1-CO39 effector, also secreted by *M. oryzae*, is independent of host translocation and is recognised by the Pi-CO39 rice R protein (Ribot et al., 2013). Another effector protein *Avr2*, secreted by *Fusarium oxysporum*, interacts with the tomato R protein I-2, culminating in a resistance response in the host plants (Ma et al., 2013).

Table 1.1: Cloned rust avirulence genes (Catanzariti et al., 2010b; Petre et al., 2014).

Avr locus	Mature protein size*	No. of cloned genes and rust strains identified	Protein features	References
<i>AvrL567</i>	127	12 (C, H, I, J, Bs1, Fi)	Directly interacts with L5/L6 in yeast	Dodds et al. (2004); Dodds et al. (2006)
<i>AvrM</i>	184–349	6 (CH5)	Directly interacts with M in yeast	Catanzariti et al. (2006, 2010)
<i>AvrP/P123</i>	88–94	6 (CH5, H, I, J, Bs1, Fi)	10 Cys; Kazal consensus sequence	Catanzariti et al. (2006); Dodds & Thrall (2009)
<i>AvrP4</i>	67	3 (CH5, WA)	6 Cys; potential Cys-knot structure	Catanzariti et al. (2006)
RTP1	201	bean rust fungus <i>Uromyces fabae</i>	protease inhibitor function	Kemen et al., 2005; Pretsch et al., 2013
PGTAUSPE-10-1	not published	Wheat stem rust fungus <i>Puccinia graminis</i> f. sp. <i>tritici</i>	candidate for AvrRs22, interact with Sr22	Upadhyaya et al., 2014

Note: *Predicted amino acid size excluding signal peptide.

1.5.5.3 Flax rust effectors

Like other plant pathogens, there is also a report on ‘top 10’ fungal pathogens, and flax rust fungus is one of them, that is considered as more famous than infamous (Dean et al., 2012). Four effector gene loci have so far been identified in flax rust fungi (Dodds et al., 2004, 2006; Catanzariti et al., 2006; Eckardt, 2006). As an indication of avirulence activity, expression of these genes leads to a resistance gene-mediated cell death response (in this case HR) when recognised by the product of the cognate resistance gene of the flax host plant. This HR is the determinant for flax-flax rust resistance.

Flax rust effector, *AvrL567*, is a haustorially expressed avirulence gene cluster encoding 12 effector variants (*AvrL567* A-L) from six rust strains (Dodds et al., 2004, 2006). These effector proteins show differential recognition specificities by the cognate L flax R protein (Wang et al., 2007; Ravensdale et al., 2012). Seven of the variants isolated from Avr loci provoke necrotic responses when expressed in flax plants having corresponding resistance genes (L5, L6, L7), the remaining five options from avr loci do not. The *AvrM* effector protein interacts directly with the cognate M flax resistance protein (Catanzariti et al., 2010a, Rafiqi et al., 2010; Ve et al., 2013). *AvrM* is expressed in germinated spores

and is detected on Northern blots four days after infection of flax plants (Catanzariti et al., 2006). There are six naturally occurring allelic variants of AvrM so far identified (Table 1.1), among which M can detect AvrM-A to D and induce HR, while the remaining two, AvrM-E and avrM, bypass recognition by the M (Catanzariti et al., 2006). The C-terminal region of AvrM (residues 108-343 of AvrM-A) forms a protease-resistant domain that is reported to dimerize both in yeast and *in vitro* (Catanzariti et al., 2010a; Ve et al., 2011). Moreover, deletion studies have revealed that the N-terminal part of this domain (residues 123-153) is necessary and sufficient for host cell translocation (Rafiqi et al., 2010), while the C-terminal portion (residues 225-343) is required for M-dependent ETI (Catanzariti et al., 2010a). AvrM-A can also bind to negatively charged phospholipids including phosphatidylinositol 3-phosphate (PI3P) but the role of PIP binding in host cell translocation is not clear (Gan et al., 2010).

Flax rust AvrM and AvrL567 are used as model effectors for the study of immune receptor function in effector recognition (Petre et al., 2014), as the specific immune receptors of the hosts can recognize these effector proteins inside the host cells following a direct physical interaction (Dodds et al., 2004, 2006; Ellis et al., 2007; Catanzariti et al., 2006, 2010). On the basis of 3D structures, mutational analysis of these two effectors revealed that multiple contact points control the interaction with their cognate receptors (Wang et al., 2007; Ravensdale et al., 2011; Ve et al., 2013).

The four flax rust effector proteins have been demonstrated to have avirulence properties (Ellis et al., 2007). The flax rust fungal effector genes are deployed to manipulate the host physiology in favour of pathogenic growth. Despite the use of these effector proteins as models to investigate the mechanisms of immune receptor activation and host cell entry, the mechanism by which they function inside plant tissues to facilitate pathogenic growth remains a mystery (Petre et al., 2014). The rust research community requires a high-throughput approach to increase knowledge of characterization and pathogenicity in the host plants, but due to the obligatory pathogen lifestyle within the host and subsequent difficulty with laboratory culture, rust pathosystems are very challenging to conventional genetic approaches (Petre et al., 2014).

1.5.5.4 Biochemistry of flax rust disease

During the life cycle, flax rust fungi secrete an array of effector molecules from the haustoria, that via an unknown mechanism, enter the cytoplasm of the infected plant cells to establish a biotrophic relationship whilst avoiding the host resistance mechanism (Heath, 1997; Voegelé and Mendgen, 2003; Dodds et al., 2007; Birch et al., 2008; Ellis et al., 2009; Panstruga and Dodds, 2009; Tyler, 2009; Yi and Valent, 2013). It is suggested that once inside the host cytoplasm, rust effectors are likely to alter host metabolism and defense pathways (Voegelé & Mendgen, 2003; Dodds et al., 2007; Yi and Valent, 2013). One such effector molecule in *M. lini* is AvrM that interacts with the host M protein (a member of the NBS-LRR class of R proteins), which upon recognition induces localised cell death as a resistance response (Ellis et al., 1999; Catanzariti et al., 2006; Dodds et al., 2006; Ellis et al., 2007; Lawrence et al., 2007; Rafiqi et al., 2010). However, the nature of this interaction and the mechanism by which the M protein activates the HR remains unresolved.

1.5.5.5 The AvrM: multiple homologs

The AvrM effector is a small protein that is secreted by the flax rust fungus to manipulate the host plant and thereby facilitate infection of the host plants. Catanzariti et al. (2006) identified the *AvrM* effector gene in rust fungus (strain CH5), and determined that the *AvrM* locus contains multiple homologs. There are six different variants of the *AvrM* gene, constituting a small effector gene family of five avirulence alleles (*AvrM-A*, *AvrM-B*, *AvrM-C*, *AvrM-D*, and *AvrM-E*) and a single virulence allele (*avrM*) (Figure 1.4; Catanzariti et al., 2006). *AvrM-A* effector protein has been demonstrated to trigger the strongest M-mediated cell death response, followed by *AvrM-D*, but *AvrM-B* and *AvrM-C* give a significantly weaker cell death response. The remaining two variants (*AvrM-E* and *avrM*) do not show any HR (Catanzariti et al., 2006). The N-terminal domain (residues 123-153) of flax rust effector protein plays an important role in host cell entry (Rafiqi et al., 2010; Ve et al., 2013).

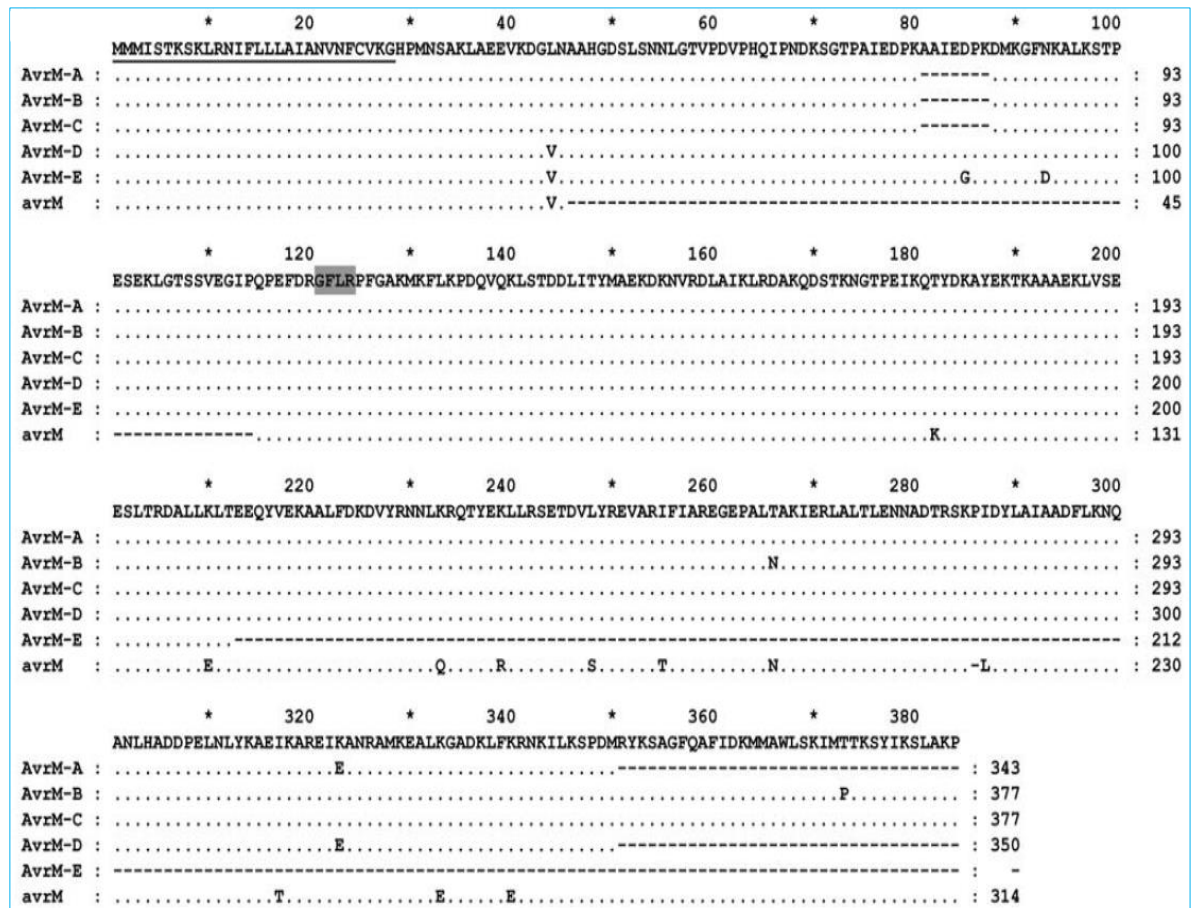


Figure 1.4: Sequence alignment of flax rust effector proteins.

The polymorphic aa residues differing from the consensus sequence (top line) are shown, remaining residues and gaps are indicated by dots and dashes, respective. The signal peptide and the GFLR motif are shown by underlined and grey shaded, respectively (Catanzariti et al., 2006).

The AvrM proteins translated from the six variants (Figure 1.4) include not only amino acid substitutions but also internal gaps, and hence vary in size. AvrM-A encodes a 343-residues protein having a C-terminal truncation of 34aa. AvrM-B and -C share the greatest sequence similarity, both carrying the C-terminal extension of 34-aa and constitute proteins of 377-aa residues. AvrM-D is similar to AvrM-A except for a polymorphic residue (L44V) and a 7aa insertion, encoding a total of 350 aa protein. Due to having a premature stop codon in the coding sequence, AvrM-E is the smallest variant (212aa), containing the same insertion as in AvrM-D and two polymorphic residues (D85G and N93D) with respect to AvrM-D. The virulent allele, *avrM*, encodes a protein of 314-aa residues, with an

internal deletion of 69aa at the N-terminal and a deletion of 1aa at the middle of the C-terminal domain, and also has the C-terminal extension of 34-aa as seen in AvrM-B and AvrM-C. On top of these sequence variations, the *avrM* protein also has 13 polymorphic residues within the protein sequence. It has been demonstrated that the 34 aa C-terminal extension interferes with detection and interaction by M flax resistance protein (Catanzariti et al., 2010a). There are no polymorphic residues in the first 28 residues in any of the AvrM variants, and this section is predicted to be a signal peptide.

Catanzariti et al. (2006) also suggested that AvrM induces necrotic cell death when expressed intracellularly, indicating its self-translocation into host cells during infection. This concept has recently been confirmed and reported that the secreted AvrM protein can internalize into host cells in the absence of the pathogen and be recognized directly by the M flax R protein (Catanzariti et al., 2010a; Ve et al., 2013). It has also been clearly demonstrated by interaction in the Y2H system (Catanzariti et al., 2010a) that the M flax resistance protein can physically interact with AvrM-A, and that it also induces a strong HR in *in planta* assays. Furthermore, AvrM-A has been shown by Gel Filtration (GF) to form a dimer. Conversely, the M flax R protein can neither recognize *avrM* *in planta* nor interact with it in the Y2H system (Catanzariti et al., 2010a). The differences between AvrM-A and *avrM* responsible for M recognition have been determined by the 13 polymorphic residues and the 34-aa C-terminal extension. Therefore, these two variants, AvrM-A and *avrM*, are ideal candidates of avirulent and virulent effectors of the AvrM gene family for further study.

1.5.5.6 AvrM and *avrM* - two contrasting effectors

The flax rust AvrM-A and *avrM* effectors have been demonstrated to remain as homodimers achieving a negative charge (acidic) in the central patch of AvrM-A dimer and positive charge (basic) in that of the *avrM* dimer (Figure 1.6). And the M resistance protein was predicted to require the negative surface patch for its recognition as a resistance response of the host plants (Ve, 2011). These effectors are structurally bipartite, comprising a variable N-terminus and a conserved C-terminal structure. Only the C-terminal domain (residues 106-343) of the AvrM is required for recognition by M flax R protein and a physical association of the C-terminal region is a prerequisite for its recognition in yeast (Catanzariti et al., 2010a). This C-terminal domain plays a significant role in the interaction with M flax

resistant protein, and the extension of 34-aa residues at the C-terminal end hinders the interaction with the M protein. AvrM-A protein directly associates and interacts with M flax R protein in the Y2H assay (Catanzariti et al., 2010a).

It has been shown that *avrM* varies by an internal gap of 69 residues in the N-terminal region as well as 13 individual polymorphic residues in different locations (as illustrated in figure 1.5), which may be a result of diversifying selection (Catanzariti et al., 2006). Catanzariti et al. (2010) also demonstrated that AvrM-A and M interact directly *in vivo* using a yeast-based assay for protein-protein interaction. AvrM-A and *avrM* proteins have been expressed, purified, crystallized, and the molecular structures have been solved (Figures 1.6, 1.7) (Ve et al., 2011; Ve et al., 2013). Furthermore, each of these proteins has been demonstrated to exist as a stable homodimer in solution (Ve et al., 2011) and thus should be homodimers in host plants. Recently the surface of the AvrM-A protein dimer has been mapped to a unique negatively charged pocket (Figure 1.6) that is predicted to be involved in the physical interaction with the cognate M protein (Ve et al., 2013).

1	MMMI	STKSKLRNIFLLLAIANVNF	CVK	GHPMNSAKLAE	EVKDGLNAAHGD	50
1	MMMI	STKSKLRNIFLLLAIANVNF	CVK	GHPMNSAKLAE	EVKDGVN-----	45
51	SLSNNL	GTVPDVPHQI	PNDKSGT	PAIEDPKDMKGF	NKALKSTPESEKLG	100
46	-----	-----	-----	-----	-----	45
101	SSVEGIPQPEFDR	GFLR	PFGAKMKFLK	PDQVQKLSTDDL	LITYMAEKDKNV	150
46	-----	QPEFDR	GFLR	PFGAKMKFLK	PDQVQKLSTDDL	88
151	RDLAIKLRDAKQD	STKNGTPEIKQ	TYDKAYEKT	KAAA	EKL	200
89	RDLAIKLRDAKQD	STKNGTPEIKQ	KYDKAYEKT	KAAA	EKL	138
201	LLKL	TEEQYVEKAAL	FDKDVYRNNL	KRQTYEK	LLRSETD	250
139	LL	ELTEEQYVEKAAL	FDKDVYRNNL	QRQTYER	LLRSETD	188
251	AREGEPAL	TAKIERLALT	LENNADTRSKP	IDYLAIAAD	FLKNQANLHADD	300
189	AREGEPAL	NAKIERLALT	LENNADTRSK	LDYLAIAAD	FLKNQANLHADD	237
301	PELNLYKA	EIKAREIEAN	RAMKEALK	GADKLF	KRNKILKSPDM	343
238	PELNLYKA	ETKAREIKAN	RAMKEALE	GADKLF	ERNKILKSPDM	287
344	-----	-----	-----	-----	-----	343 = AvrM 1029 bps
288	QAFIDKMMAWLSKIM	TTKSYIKSLAKP	-----	-----	-----	314 = avrM 942 bps

Figure 1.5: Alignment of AvrM-A and avrM protein sequences.

The blue colour represents the sequence of AvrM-A protein (upper line), and the black indicates avrM protein (lower line). The red colour shows polymorphic residues, and the pink are three conserved residues predicted to be critical for creating charge patches in the central pockets of the effector dimers, as shown in Figure 1.6.

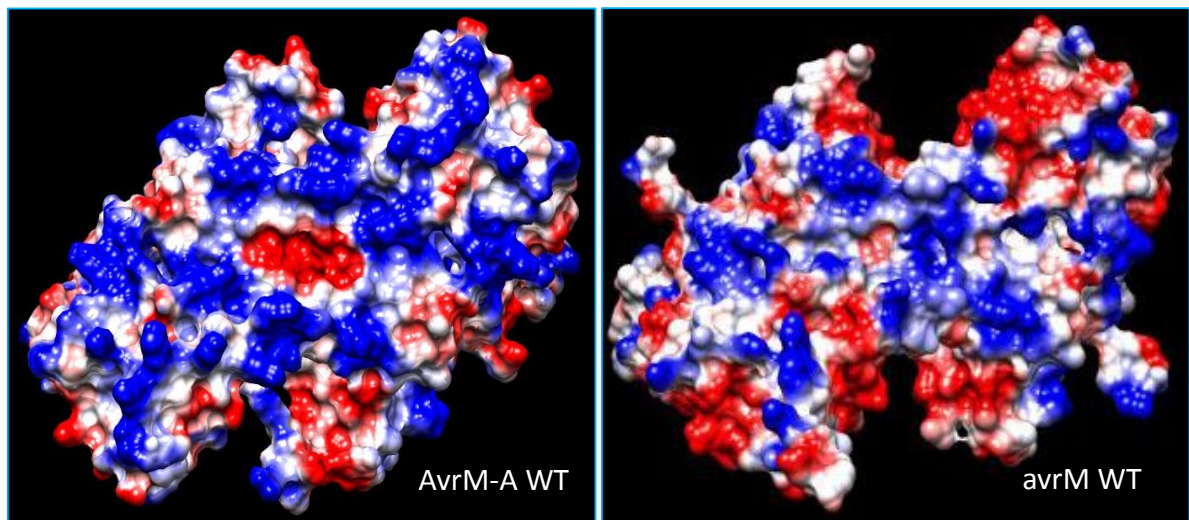


Figure 1.6: Crystal Structures of AvrM-A and avrM showing the central pockets of charge surface predicted as critical for M protein interaction. AvrM-A has a central acidic surface, which is shown in red (left), and avrM possesses a basic surface that is shown in blue (right).

1.5.5.7 AvrM-A and avrM - two representatives

This project focuses on the molecular interactions between flax and flax rust fungus, more specifically on the flax rust AvrM effector, which has six naturally occurring variants (AvrM A-D and avrM) so far identified (Catanzariti et al., 2006). AvrM-A and avrM effectors are very similar, having 96% sequence identity with only 13 polymorphic amino acids (Figure 1.5), that slightly alter the structures of the effectors (Figure 1.6) and hence influence the function. This project aims to change these polymorphic residues individually by site-directed mutagenesis (SDM) to try to understand which changes are required for the ability to bypass detection by M flax R protein and thus to induce disease in the host plants. The AvrM-A and M proteins directly associate and interact in the Y2H system, and there is a correlation between the interaction and recognition specificity for each of the AvrM variants when expressed in the plant (Catanzariti et al., 2010a).

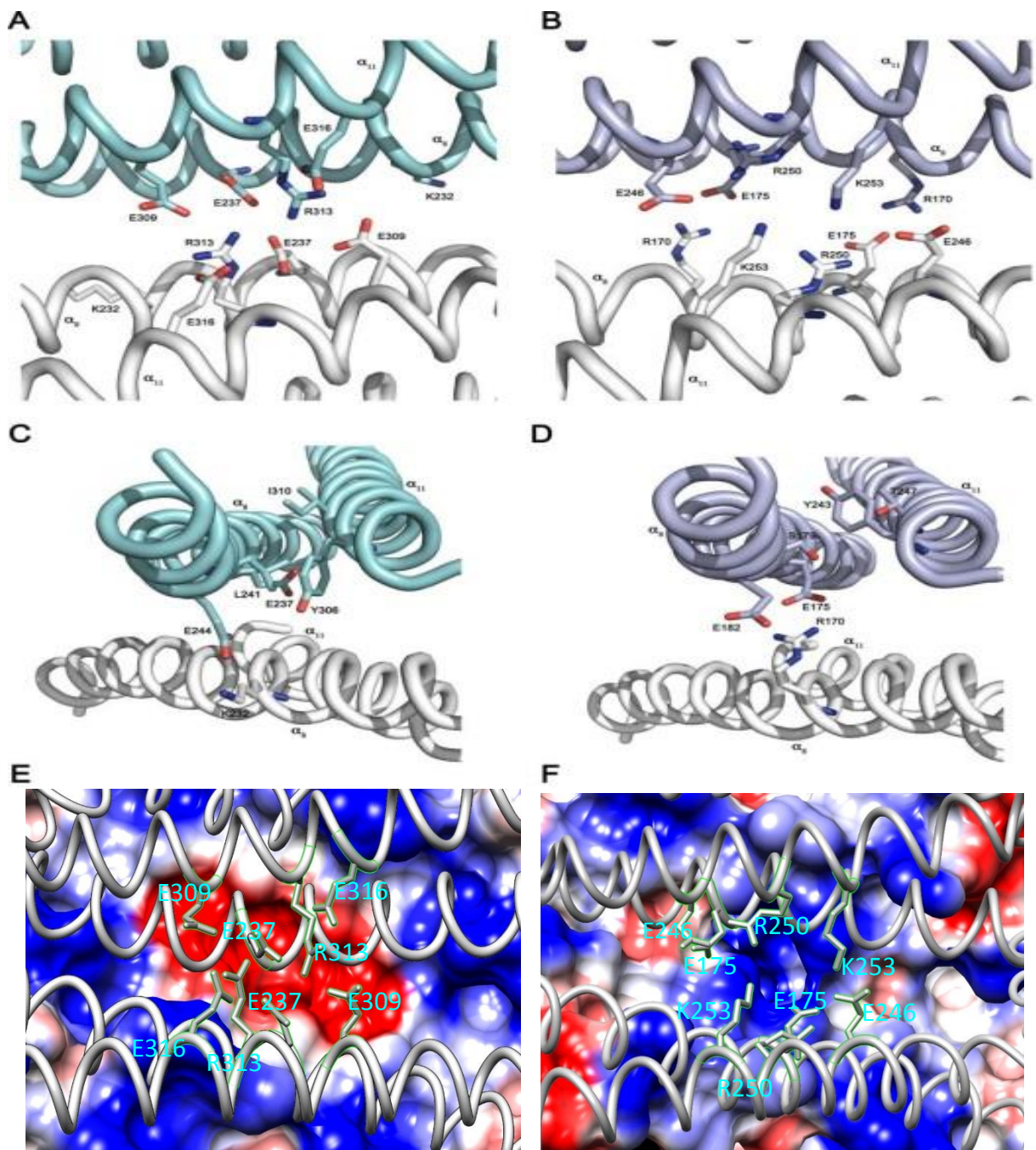


Figure 1.7: Conformational variations of AvrM-A and avrM proteins. (A-D) Interactive (ribbon) displays of the α_8 and α_{11} helices in AvrM-A (A & C) and avrM (B & D) showing the structural variations due to the K232/R170, L241/S179 and I310/T247 polymorphisms in AvrM-A/avrM. (E-F) Transparent surface presentations of AvrM-A (E) and avrM (F) with electrostatic potential (calculated using APBS; Baker et al., 2001) mapped to the surface. They are identically orientated to the molecules in (A) and (B). The coulombic surface is continuous from blue (potential +5 kT/e) through white to red (potential -5 kT/e) (Ve, 2011).

The M resistance protein is the immune component of the flax plant and can recognise only the first four variants (AvrM A-D) and interact to resist disease invasion, while AvrM-E and avrM evade M recognition (Catanzariti et al., 2006). In this project, AvrM-A and avrM have been selected as two representatives of the six variants to investigate the molecular basis of their recognition by the M flax resistant proteins. More specifically, this project addresses the question, 'Why is the AvrM-A detected by the M flax resistance protein, but the avrM is not?'

1.5.5.8 Determining AvrM regions responsible for M recognition

Previous analysis has narrowed the region responsible for M recognition to the C-terminus of AvrM-A, in particular, residues 108-343 (Catanzariti et al., 2010a). This region is also sufficient for interaction with the M protein as measured by the Y2H assay (Catanzariti et al., 2010a). Although avrM also varies from AvrM-A by an internal 69-aa deletion and by an additional single aa gap, the deletion does not cover residues 108-343 of AvrM-A. Closer inspection of AvrM-A and avrM reveals that there are 13 polymorphic residues between AvrM-A and the corresponding region of avrM (Catanzariti et al., 2006; Catanzariti et al., 2010a). However, three of these polymorphic residues, E316/K253, K326/E263 and K333/E270 do not alter M recognition either as single mutations or in combination (Catanzariti et al., 2010a). So this project targeted the remaining polymorphisms to demonstrate their roles in M detection. There are three non-polymorphic charged residues (E237/E175, E309/E246 and R313/R250) in the C-terminus, which may be involved in creating charge differences in the central patches of the effector proteins.

Recent structural characterization of AvrM-A and avrM reveals that these effectors possess a C-terminal globular domain that forms a stable homodimer in solution (Ve et al., 2011). Furthermore, inspection of the structures reveals a highly negatively charged pocket (acidic) at the exterior surface of the AvrM-A dimer that is not found in the equivalent region of the avrM dimer (Ve, 2011). So it is predicted that the acidic pocket is formed indirectly by the singular or cumulative effects of the polymorphic side-chains found, such as K232/R170, L241/S179 and I310/T247 in AvrM-A and avrM, respectively. Based this prediction, and to further investigate the molecular basis of M/AvrM specificity, SDM will be used to change these residues one after another and the effect on M recognition tested using an in planta transgenic assay. To confirm the likely stable expression of these proteins in plant tissue, a

hemagglutinin (HA) epitope tag has been engineered onto the N-terminal of the effector protein with a view to detect protein expression by immunoblot analysis.

1.6 Plant-pathogen interaction

Plant innate immunity is based on the interaction between the plant R proteins and pathogen effector proteins. This interaction is a unique feature to study at a molecular level the very moment of host/pathogen interaction and understand how plant disease resistance becomes activated, which is a far reaching application to agricultural productivity and, therefore, food security. All biological processes are controlled by such interactions, none more so than the innate immune response of plants and animals. When mounting an infection, most pathogenic micro-organisms must contend with the immune system of their host and, therefore, find a way to suppress it, or bypass it undetected. It is therefore not surprising that for an infection to succeed, or for a host to resist infection, crucial proteins from the pathogen and the host must interact, which is the basis for focusing on the interaction between flax and the flax rust fungal pathogen. This project addresses the plant-pathogen interaction using flax and flax rust as a model system that has for been used for several decades to investigate the genetics of the avirulence/virulence mechanism.

1.6.1 Gene-for-gene hypothesis

The ability to explore the biochemical roles of the flax/flax rust interaction has been advanced considerably by the isolation of the genes that encode the flax resistance proteins and the flax rust effector proteins (Catanzariti et al., 2006). The interactions between these proteins are thought to be a result of long-term co-evolutionary selection and counter selection between the plants and pathogens (Dodds and Thrall, 2009). In the absence of the paired interactions between host and pathogen proteins, the pathogen avoids detection by the host plants, facilitating pathogenic growth within the host cells and leading the outbreak of disease. Consequently, host plants evolved systematic defence mechanisms against a multitude of pathogens. The key components of such defence mechanisms are the *R* genes, and many of such components have been identified and cloned from a broad spectrum of plant species. Side by side, many cognate effector genes have been identified and cloned, which has accelerated research on the basis of gene-for-gene resistance in molecular plant pathology (Collins et al., 1999; Martin, 1999). More than six decades ago, J. B. S. Haldane

(1949) predicted that microorganisms are very rapidly evolving polymorphisms in proteins that interact with the host R proteins. H. H. Flor (1955) delineated the genetic basis of resistance in flax to the flax rust fungus and documented polymorphism and recognition specificity of R proteins (Flor, 1955). Soon after that, H. H. Flor (1956) proposed the gene-for-gene hypothesis of disease resistance, illustrated by the relationship of the flax rust and flax host cultivars, which was widely accepted.

The gene-for-gene hypothesis has been shown to be applicable to many other host-pathogen interactions, for instance, rice blast fungus *M. oryzae* and its host *Oryza sativa* (Leung et al., 1988; Valent et al., 1991; Ellingboe, 1992; Smith and Leong, 1994). Subsequently, this elementary relationship has gained practical interest as the pathogens are seen to be rapidly evolving to overcome new disease resistances in the host soon after their deployment (Bonman et al., 1992). Indeed, this assumption has been supported by genetic analysis of the flax-flax rust interaction, enabling the researchers to identify many R genes in the host plant as well as many pathogenicity genes in plant pathogens. This hypothesis affirms that for each R gene of the host plant there exists a cognate Avr gene product in a pathogen, by which the host can detect the pathogenic attack and thereby resist the infection. According to the hypothesis, the cognate R gene product in a host plant interacts with the dominant Avr gene product of the pathogen, leading to activation of host defence responses like HR, which prevents the further growth of the pathogen (Stergiopoulos and Wit, 2009). Thus, the consequence of host plant infection by a pathogenic organism is controlled by a complex series of interactions between the host plant and pathogen.

1.6.2 Flax and flax rust: a model system

The flax and flax rust fungus have been established as an excellent model system for studying rust infection (Dodds and Thrall, 2009), a broad range of flax rust strains and the corresponding cultivars of the Linaceae family. The same system has been used to investigate the molecular fundamentals of M/AvrM protein interaction and recognition. The basic principle of this model system is the gene-for-gene concept (Flor 1971; Lawrence et al. 2007). Ellis et al. (2007) reported that the gene-for-gene specificity of flax-flax rust model system has been formulated on the basis of the interaction between R and Avr proteins in the flax-flax rust system, and there is a co-evolutionary arms race between

the obligate rust pathogen and the infected host plants. The knowledge of the interaction between pathogen effectors and host receptors is of immense importance for improving plant immune receptors capable of recognizing the broad-spectrum of effector proteins (Harris et al., 2013; Segretin et al., 2014), which can be supportive for breeding a widespread resistance crop plants (Dangl et al., 2013). In fact, this model has been considered as a novel paradigm for studying the host-microbe interactions, effector function and genome evolution. In flax-flax rust system, two interacting models, M/AvrM (Ve, 2011) and L/AvrML567 (Wang et al., 2007) were built that really strengthened the ideas about host-pathogen interactions.

1.7 Plant *Agrobacterium* transformation

Agrobacterium-mediated transformation is a popularly used approach for transferring a desired gene into the genome of a target plant cell. *A. tumefaciens* is a soil bacterium responsible for crown gall disease in a wide variety of plant species. As an apparatus for disease transmission, *Agrobacterium* carries a Tumor-inducing (Ti) plasmid hosting virulence genes (*vir*), which translate the protein machinery needed to transfer and integrate disease-causing genes into the genome of host plants. In addition, the Ti plasmid contains a transferable segment, termed T-DNA, having two inverted flanking repeats, Right Border (RB) and Left Border (LB) sequences. The pathogenic *Agrobacterium* utilizes the flanked sequences to induce tumor in the infected plants. Interestingly, the T-DNA can transfer any DNA sequence introduced within the RB and LB into the plant genome. After integrating into the host genome, the *Agrobacterium* genes behave as oncogenes to induce the host plant protein machinery to produce phytohormones that lead to uncontrolled cell proliferation, causing a gall or tumor. As a technique of plant transformation and genetic engineering, this naturally occurring *Agrobacterium* ability to insert foreign DNA into plant chromosomes has been manipulated in order to develop highly efficient vectors. In this system, the oncogenes were replaced by a plant gene expression cassette (a gene with a promoter and a transcriptional terminator sequence). Thus, integration of a particular gene of interest into the host genome became possible without causing disease. This system is called a binary transformation system, as two plant gene expression cassettes have been placed between the LB and RB sequences of the T-DNA. One of the cassettes is used to translate the inserted gene of interest, and the

second for expressing an antibiotic resistance gene to select the successful transformants. This technique has been employed in this project in order to elucidate the function of the AvrM effector proteins from flax rust fungi in pathogenesis and interaction with the host.

1.8 Aims and experimental approaches

The flax rust M resistance protein is a plant R protein that recognizes the flax rust effector protein, AvrM and interacts to protect the plant from rust invasion. As reported by Catanzariti et al. (2010), three variants of the *M* gene (Anderson *et al.*, 1997; Lawrence *et al.*, 2010a) and six variants of the AvrM gene (Catanzariti et al., 2006) have been identified, but the details of the recognition event between these cognate proteins remains unknown. Furthermore, the M resistance protein can detect AvrM, but not avrM. To further investigate the molecular basis of rust pathogenicity, this study aimed to identify the polymorphic residues required for the structural configuration of the AvrM-A effector protein that makes it recognisable to M, as well as three non-polymorphic residues (as mentioned before) that are likely to be involved in creation of the charge in the central patch of the effector dimers.

It is of immense importance to determine effector function in fungal disease of plants. With an attempt to contribute to the molecular basis of fungal effector function, this research focused on determining the responsible features of such an effector, flax rust AvrM effector protein, involved in activation of, and detection by the resistance protein, M. Though many effector genes and their cognate resistance genes have been identified and cloned, the pathogenicity and recognition specificity of the effector proteins by the analogous R proteins remain poorly understood and the mechanisms controversial. This study aimed to investigate the recognition specificity of AvrM-A and avrM effector proteins by SDM coupled with an *in planta* assay using transgenic tobacco plant stably transformed with the *M* flax rust resistance gene. It was anticipated to alter the specificity by single residue mutation/s (Chapter 3), but the effector proteins appeared to be highly evolved, encountering some unforeseen experimental roadblocks, which were solved by setting new experimental approaches. The modified goal was to determine the crucial multiple residues that facilitate AvrM-A to establish interaction with M, and avrM to be undetectable by M. This has been addressed and confirmed by combined mutational study followed by Y2H assay, Size Exclusion Chromatography coupled with Multi-Angle

Light Scattering (SEC-MALS) as well as Small-Angle X-ray Scattering (SEC-SAXS) analyses (Chapter 4). Prediction of the pathogenic function of fungal effectors is difficult due to the high level of diversity and low sequence homology to other known proteins. That is why a better understanding of the structure and function of a diverse array of effector molecules of plant pathogens is an urgent issue to improve resistance by breeding or biotechnology in agriculturally important plant species. It is hoped that the knowledge gained from this project will assist engineering of resistant crop varieties with expanded effector recognition and thereby develop broad-spectrum pathogen resistance in plants.

The data from this project will be helpful in showing how effectors of flax rust fungi are conserved across species and how they promote infectious disease in the host plant. Therefore, the broad aim of this project, as presented in this thesis, is to provide knowledge to molecular plant pathologists on one of the diverse range of mechanisms utilised by rust fungi to avoid the host immune response. Overall, this study generated a wealth of information on flax rust pathogenesis and the results presented in this thesis have advanced the understanding of flax rust effectors and are hoped to contribute to the success of rust resistance breeding in other crop species. We would like to think that these data will open new research avenues in molecular plant pathology and contribute to restriction of the impact of plant disease on food production, which will ultimately assist in the production of food for those in hungry communities in the world.

Chapter Two: Materials and Methods

(Pages 39 - 55)

2.1 Materials

2.1.1 General chemicals

All chemicals used in this project were molecular grade and most of them were purchased from Sigma-Aldrich (Castle Hill, New South Wales, Australia) unless otherwise mentioned. Other general chemicals used in reagents, buffers, LB media, and other broth for culturing bacteria, were obtained from Oxoid, England. The restriction enzymes with reaction components, ligases, phosphatases and protein molecular markers were purchased from New England Bio-labs (NEB) (USA), while high fidelity DNA polymerase (Phusion Taq) (Finnzymes, Finland) was used for polymerase chain reaction (PCR). For PCR and DNA sequencing reactions, oligonucleotides (primers) were sourced from Life Technologies Pty Ltd, Australia, while Promega was the supplier for DNA purification and clean up kits. For making all the media and buffers, de-ionized water (MilliQ Millipore) was used. All chromatography columns and other equipment were purchased from GE Life Sciences. Merc Millipore (Billerica, MA, USA) was the provider for Amicon Ultra-15 Centrifugal Filter Units for concentrating the purified proteins.

2.1.2 Culture media, solutions and buffers

Autoclaved Milli-Q water was used for preparing all of the culture media, solutions and buffers, for which summary tables of the chemical components are detailed in Appendix 1a.

2.1.3 Effector genes, AvrM-A and avrM

DNA constructs containing the flax rust effector genes, AvrM-A and avrM, were provided by Peter N. Dodds, CSIRO, Canberra.

2.1.4 Plasmids

Two plasmids were used to facilitate the AvrM-A (NT Δ 107), avrM (NT Δ 45+CT Δ 34) and thereof mutant genes, from this point on, and for the purposes of brevity and simplicity, these truncated versions of AvrM-A and avrM will be referred to as AvrM-A and avrM, respectively. The plasmids facilitating the effector gene manipulation in this project are enumerated in the following Table 2.1.

Table 2.1: Plasmids and its usage in this project (detail map of each plasmid is shown in Appendices 4-6)

Name	Usage	Origin and Resistant to
pDONR207	Cloning the truncated AvrM-A and avrM genes	Gentamycin 50mg/ml
pEG201	Regular cloning and transformation of the genes inserted in.	Earley et al., 2006; Kanamycin 50mg/ml
pMCSG7	Protein expression of the inserted genes	Stols et al., 2002; Spectinomycin 100mg/ml

2.1.5 Oligonucleotides/primers

In this study, forward primers and their analogous reverse complementary primers were designed to engineer point mutations in the effector genes. The oligonucleotide primers used for PCR-driven site-directed mutagenesis (SDM) are listed in Appendix 2b.

2.1.6 Plant materials

The transgenic tobacco plants (*Nicotiana tabacum*, variety W38) used in this study contained a genomic version of the M flax resistant gene under the control of its native promoter (W38::M), the same construct as that reported by Anderson et al. (1997). M-containing transgenic tobacco seeds were supplied by Jeff Ellis (CSIRO Canberra). For protein expression studies of infiltrated tissue, *N. benthamiana* was used, for which seeds were sourced from Dr. Ian Dry (CSIRO, Adelaide).

2.1.7 Bacterial stains

The bacterial strains used for the mutated gene cloning, genetic transformation and protein expression are enumerated in the following Table 2.2.

Table 2.2: Bacterial strains

Bacteria (Strain)	Resistant	Usage
<i>E. coli</i> (DH10B)	--	Regular gene cloning
<i>E. coli</i> {BL21 (DE3)}	--	Protein expression
<i>Agrobacterium</i> (GV3101)	Gnt50, Rf25	Genetic transformation in plants

Note: Gnt50: resistant at 50µg/ml and Rf25: resistant at 25µg/ml rifampicin

2.1.8 Cultures and antibiotics

E. coli {DH10B, BL21 (DE3)}:

- pEG201 vector hosted by DH10B: LB with 50 µg/ml kanamycin (kn)
- pMCSG7 vector hosted by BL21 (DE3): LB with 100 µg/mL ampicillin (Amp)

Agrobacterium tumefaciens (GV3101):

- pEG201 vectors hosted by GV3101: LB with 50 µg/ml kanamycin, 25 µg/ml rifampicin and 50 µg/ml gentamycin.

2.2 Methods

2.2.1 Preparation of electrocompetent bacterial cells.

Electrocompetent *E. coli* (Strain DH10B and BL21 (DE3)) and *Agrobacterium tumefaciens* (Strain GV3101) cells were prepared mostly following a protocol stated by Sambrook et al., (1989). For this purpose, 10ml of an overnight LB culture inoculated from a single colony on an agar plate was used to inoculate a final culture of 250ml LB broth with the appropriate antibiotic/s. The culture was grown for maximum four hours so that its OD₆₀₀ should not exceed more than 0.8. Cultures exceeding this density will produce low competence cells. Afterwards, the cells were harvested at 5000rpm on a BECKMAN COULTER™ Centrifuge (USA) for 15 minutes at 4°C. Then the pellet was re-suspended with 50ml ice-cold sterile water and centrifuged to make cell pellet again. This step was repeated three times with a view to wash the cells' surfaces followed by a final wash with ice-chilled 10% glycerol and centrifuged for pelleting the cells. Finally, the supernatant was discarded carefully, and the cell pellet was re-suspended in as small volume of ice-chilled 10% glycerol as possible. Then the electrocompetent cells were stored at –80°C by making aliquots of 20 µl following quick frozen in liquid nitrogen.

2.2.2 Transformation of electrocompetent cells by electroporation

Site-directed mutagenesis (SDM) PCR products or plasmid DNAs (1 µl of 100 ng/µl) hosting effector genes with or without mutation/s were mixed with a 20 µl aliquot of electrocompetent cells (*E. coli* with respect to SDM PCR, or *A. tumefaciens*, strain GV3101) followed by an incubation on ice for 5 minutes. Then electroporation was performed with a Cell Porator (Cell Porator®, BRL, Life Technologies, Inc.) in accordance with the manufacturer's protocol. Following electroporation, cells were immediately transferred into 200µl non-selective LB medium and incubated at 37°C for 30 minutes (45 minutes at

30°C for GV3101). With a view to get single individual colonies, different volumes of the LB containing the electroporated cells were plated onto selective LB plates and incubated overnight at 37°C (48 hours at 28°C for GV3101).

2.2.3 Preparation of chemically competent *E. coli* cells

Protocol stated by Sambrook et al., (1989) was mostly followed for preparing chemically-competent *E. coli* cells (DH10B and BL21 (DE3)). The bacterial cells were cultured and harvested as pellet as stated in the section 2.2.1. The cell pellet was re-suspended in 20 ml of ice-cold 0.1 M CaCl₂ followed by incubation on ice for approximately 30 minutes. Then the cells were harvested again by centrifugation at 4500 × *g* for 10 minutes and re-suspended in 2 ml of ice-cold 0.1 M CaCl₂ containing 12% glycerol. Following this, the competent cells were stored at 4 °C for up to one week use, or at -80°C following snap-freezing in liquid nitrogen for long term use with heat-shock transformation. Prior to storing at -80°C, single aliquots of 50µl were prepared.

2.2.4 Heat-shock transformation

Following Sambrook et al., (1989), heat-shock transformations were performed with chemically competent *E. coli* cells of the relevant strain (DH10B and BL21 (DE3)). Prior to use, a single aliquot having 50µl competent cells was thawed and approximately 100 ng of plasmid DNAs or PCR products were gently mixed in an Eppendorf (or similar) tube following incubation on ice for 30 minutes. Then the cells were heat-shocked by incubating on a water bath or heat-block at 42°C for 45-60 seconds following immediately placing back on ice for 2 minutes. Following heat shock, 50µl of non-selective LB medium was added to the reaction and then incubated at 37°C for at least 60 minutes without shaking. Finally, the transformed cells were plated on selective LB-agar plates and grown overnight at 37°C and single colonies were selected to purify the plasmid DNA for further analysis.

2.2.5 Long term storage of bacterial constructs

The bacterial constructs hosting effector genes are stored at -80°C for any time use in this project. For storing the bacterial cells, the constructs were cultured overnight and stored in LB medium with appropriate cryoprotectant (7.5% DMSO for DH10B & BL21(DE3); 12% Glycerol for GV3101) followed by snap freezing in liquid nitrogen and storage at -80 °C.

2.2.6 Colony PCR

Colony PCR was used as a confirmation test of the electroporation of effector genes in DH10B cell mostly following a previous method (Williams, 2009). For this purpose, single colonies were selected and resuspended in 20µl of sterile 1X TE buffer (Appendix 1c) following heating at 100°C for 5 minutes. For the polymerase chain reaction (PCR), 2µl of the heated cell suspension was used as template DNA to a total volume of 20 µl with 0.2µl of standard *Taq* Polymerase (New England Bio-Lab), 1µl dNTP mix (10 mM of each), 50ng of forward and reverse primers, buffer, and remaining H₂O. The PCR conditions were maintained as 98°C for 30 seconds, then 30 cycles of 98°C for 10 seconds, 55°C for 20 seconds, 72°C for 1 minutes and finally 72°C for 4 minutes in a Gene Amplification DNA system (PerkinElmer) PCR machine. Then the whole reactions (20µl) were loaded and electrophoresed at 90 volts for 1 hour followed by visualizing and image capture with a Bio-Rad gel doc imager.

2.2.7. Growing transgenic tobacco plants

The transgenic tobacco plants (W38::M) were germinated on MS (Murashige and Skoog, 1962) selection medium containing 50µgL⁻¹ spectinomycin. Two weeks after seed sowing, the non-transgenic plants bleached and the resistant plants were green (Figure 2.1) which were selected for the *in planta* assay for studying interaction of the effector proteins with M flax resistant proteins. The resistant plants were grown in single individual pots up to 4 weeks and then the plants became suitable for infiltration. The non-transgenic plants (*N. benthamiana*) were germinated on soil. In both cases, the temperature was maintained at 26°C with 12 hours light and 12 hours dark.

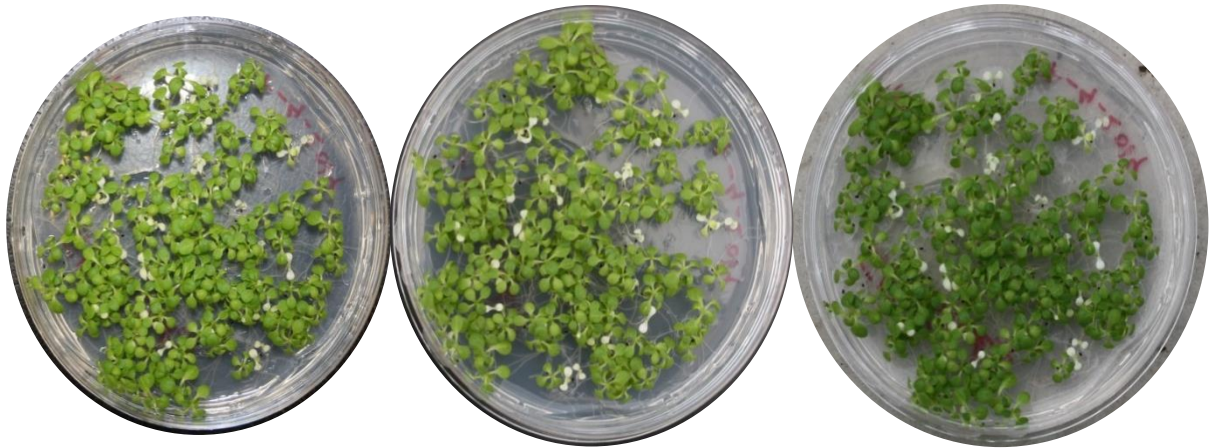


Figure 2.1: Selection of transgenic tobacco (W38::M) plantlets on MS media supplemented with $50\mu\text{gL}^{-1}$ spectinomycin. The non-transgenic plants bleaches and the seedlings having M genes are green.

2.3 DNA Methods

2.3.1 Gene constructs preparation

DNA constructs containing the flax rust effector genes, *AvrM-A* and *avrM*, were provided by Dr. Peter Dodds, CSIRO, Canberra. On the basis of a deletion study (Catanzariti et al., 2010a), and the crystal structures of *AvrM-A* and *avrM* (Ve et al., 2013), the N-terminal regions of *AvrM-A* and *avrM* as well as the C-terminal extension of *avrM* were truncated for studying their interaction with the flax rust resistant protein, M. After truncation, the encoded *AvrM-A* protein contains amino acids 108-343 (can be defined as *AvrM-A* Δ 107) and *avrM* contains 46-280 amino acids (can be defined *avrM* Δ 45/*CT* Δ 34). For such truncations, the effector genes, *AvrM-A* and *avrM* were amplified by PCR using Phusion Taq Polymerase with a forward primer, *AvrMattBF* and a reverse primer, *AvrMattBR* (Appendix 2a). The successful PCR products were checked by agarose gel electrophoresis. Following Gateway® Cloning Protocols, the amplified PCR products were then inserted into the entry vector pDONR207 via BP recombination reaction. Following the BP reaction, the resulting gene constructs of the *AvrM-A/avrM* were cloned in *E. coli* and purified as a stock designated as *AvrM*+pDONR207. After this, the *AvrM*+pDONR207 was sub-cloned into the destination vector, pEG201 by an LR recombination reaction, so that the target effector gene sequence is placed downstream of the Cauliflower mosaic virus (CaMV) 35S promoter (Earley et al., 2006) (Figure 2.2).

This is how the DNA constructs encoding AvrM-A Δ 107 and avrM Δ 45/CT Δ 34 proteins governed by the CaMV 35S promoter were engineered in the binary vector, pEG201 (Figure 2.1) with a view to study the AvrM/M interaction, gene knock-out/knock-in by mutating specific amino acid side-chains and expression *in planta* by *Agrobacterium*-mediated transient expression (AMTE).

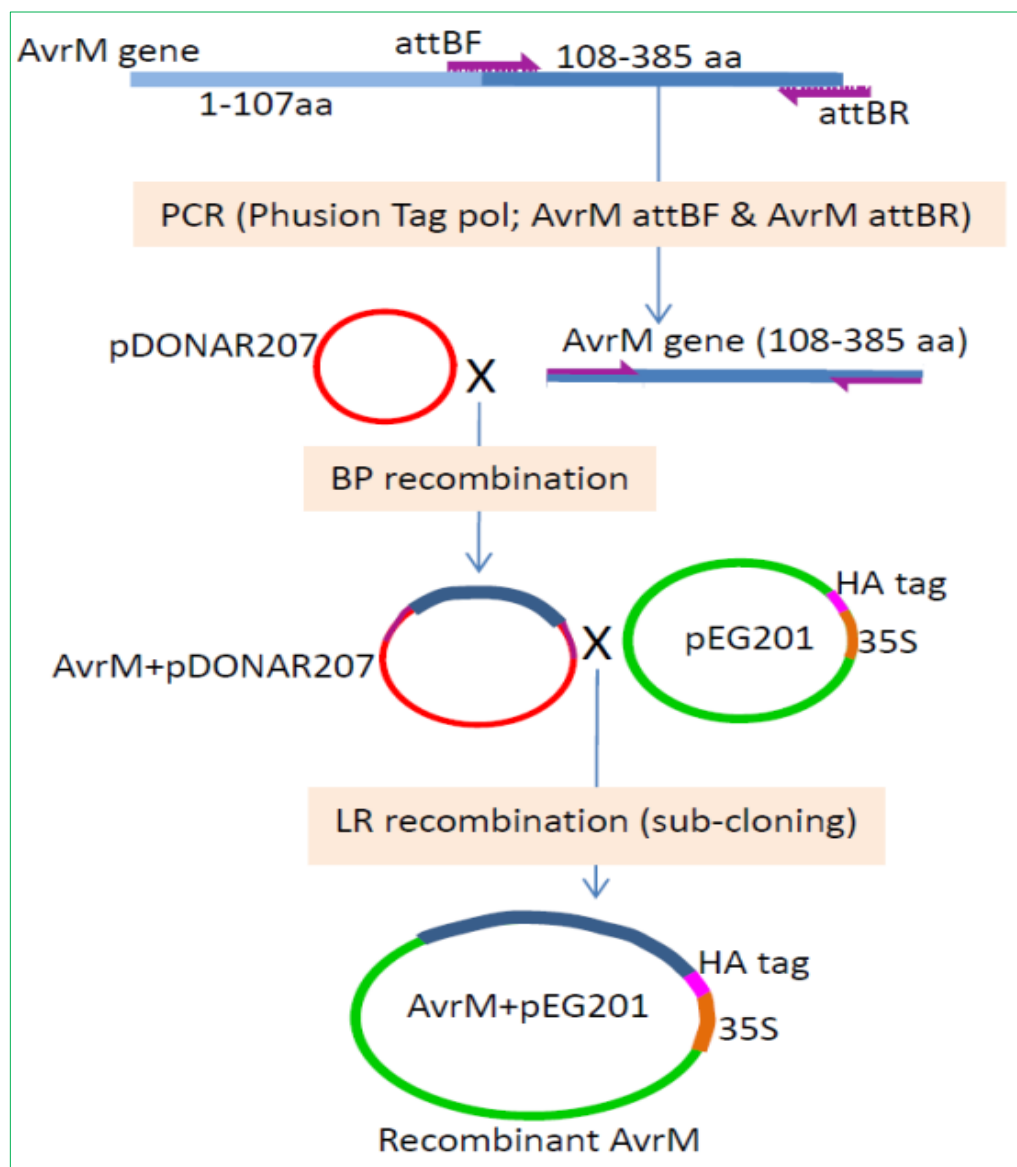


Figure 2.2: Different steps in engineering recombinant AvrM construct (AvrM-A and avrM).

2.3.2 Site-directed mutagenesis to generate point mutation

PCR-driven site-directed mutagenesis (SDM) was performed to engineer the individual point/combined mutation/s in AvrM-A and avrM genes harboured by the pEG201 vector following some previous methods (Catanzariti et al., 2006, 2010, Williams et al., 2011). Miss-match primers were designed (Appendix 2b) to introduce the desired mutations with a view to study molecular effects of the specific residues for being recognized by M flax resistance protein. High-fidelity DNA polymerase (Phusion DNA Taq Polymerase, Finnzymes) was used for the PCR-driven SDM with a long extension time (5-6 minutes) for the amplification of the entire pEG201 plasmid hosting the effector genes in accordance with the manufacturer's recommendations. Typically 100 ng of templates and 50ng of each primer (forward and reverse) were used in the PCR reaction and conditions were maintained as 98°C for 30 seconds, then 30 cycles of 98°C for 10 seconds, 55°C for 20 seconds, 72°C for 6 minutes and finally 72°C for 5 minutes.

2.3.3 Mutant genes preparation and transformation

Following the PCR, the template DNAs were digested with *DpnI* endonuclease (New England Bio-Lab Kit) to ensure the template DNA is removed remaining the newly amplified daughter DNAs only. This was followed by PCR clean up using Sigma kits (GenElute™ PCR Clean-Up Kit), and subsequently, the DNAs were concentrated by ethanol precipitation (Sambrook et al., 1989). Then the PCR products were transformed (by either electroporation or heat shock) into the appropriate competent *E. coli* cells (strain DH10B) for cloning the mutant effector genes. The transformed DH10B cells were cultured for cloning the genes, and subsequently purifying the plasmid DNA (Section 2.5.4).

2.3.4 Plasmid DNA purification

The PCR products (effector genes in pEG201) were transformed into *E. coli* (DH10B) cells for cloning the genes. Either newly electroporated cells or pre-stored at -80°C were cultured in liquid Luria-Bertani (LB_{liq}) media at 37°C for overnight and harvested by centrifugation at 4500rpm for 7 minutes. The harvested cells were used to purify the plasmid DNA using the commercially ready-made kit (Wizard® Plus SV Minipreps DNA Purification System, Promega, Australia) following the instructions provided by the manufacturer. Then the purified DNAs were checked by electrophoresing with 1% (w/v) agarose following Sambrook et al. (1989).

2.3.5 DNA sequencing and analysis

Following purification, the successful integration of the desired mutations in the effector genes was confirmed by DNA Sanger sequencing (Sanger and Coulson, 1975). The sequencing reactions were carried out by the Australian Genome Research Facility Ltd (AGRF). As per the instruction of AGRF, the sequencing reactions were prepared with about 500ng of plasmid DNA and about 50ng of primer chosen on the basis of mutation location on the effector genes. The Sequencer software (Gene Codes Corporation; Michigan, USA) was used for analysing the raw sequencing data, and a non-mutant effector gene sequence was used as a template to compare the correct integrity of the desired mutation. For all mutations, the entire sequence of the effector genes was determined to ensure that only the desired codon was mutated and no other PCR or cloning-induced mutations were generated.

2.4 *In planta* methods

2.4.1 Transient *in planta* expression assays

Agrobacterium tumefaciens (Strain GV3101) containing the binary vector, pEG201, harbouring either of AvrM-A or avrM gene were cultured in LB_{liq} media supplemented with kanamycin (50µg/ml), gentamycin (50µg/ml) and rifampicin (25µg/ml). Then the *Agrobacterium* cultures were harvested by centrifugation and prepared to an OD₆₀₀ of 1.0 in 10mM MES buffer (pH 5.6), 10mM MgCl₂ and 200µM acetosyringone for infiltration in tobacco leaves expressing M genes (W38::M) according to some methods previously described (Catanzariti et al., 2010a, Williams et al., 2011; Krasileva et al., 2010). Prior to infiltration, the bacterial suspension was incubated minimally for 4 hours at room temperature. Tobacco plants, W38::M (4-5 weeks old) were used for the infiltration experiments and the third and fourth leaves were found to give the most consistent hypersensitive response (HR). For infiltration, a small nick was made by a scalpel blade at the upper side of each leaf sector and a 1ml needleless syringe with the *Agrobacterium* suspension was used to infiltrate *Agrobacterium* suspension into the leaf with a slight counter-pressure to the lower side of the leaf with a gloved finger (Ma et. al., 2012). In this experiment, wild type AvrM-A and avrM genes were also used for the observation/analysis of HR as a positive and a negative control, respectively. After infiltration, the plants were maintained at 26°C with an equal period of light and dark. At

two days post infiltration (dpi), HR was visualized at the infiltrated leaf sectors and the images were documented as the experimental data.

Prior to commencing infiltration experiments reported here, non-transgenic tobacco leaves were infiltrated many times with *AvrM-A* and *avrM* genes, but no HR was observed. Similarly, *Agrobacterium* (strain GV3101) with no effector gene was also infiltrated into *M*-containing tobacco leaves on many occasions with no resulting HR (data not shown).

2.4.2 Quantification of HR

To quantify the *M*-dependent HR intensity for *AvrM-A*, *M* expressing tobacco leaves (W38::*M*) were infiltrated with *AvrM-A* and *avrM* (Figure 2.3a), and collected after 2 days post infiltration (dpi).

The collected tobacco leaves were scanned with UV Transillumination by BioRad gel doc machine (Gel Doc™ EZ System). Then the leaf sectors showing good HR were captured, and the HR intensity was quantified using ImageLab program (Bio-Rad). To standardize the HR intensity of *AvrM-A*, *avrM* was used in the infiltration assay as a negative control of the HR. In this case, the exposure time was set 0.388 sec with stain free option and the leaf sector treated with *AvrM-A* was used as a reference of control. Afterwards, the individual leaf sectors were selected and labelled after the name of effector genes, and the HR data was converted to average values per 500mm². Then the calculated HR intensities (for *AvrM-A* and *avrM*) were plotted to obtain bar diagram (Figure 2.3b) which shows that HR intensity of *AvrM-A* is 100%, but *avrM* induces no HR. The same effector genes were expressed in non-transgenic tobacco leaves (*N. benthamiana*) and shown by immuno-detection using an anti-HA antibody (clone 16B12) (Figure 2.3c). However, at the end, this method was not used to quantify the HR in the subsequent Chapters 3 and 4, but rather a visual quantification assay of the HR was used as described by Bernoux et al., 2016.

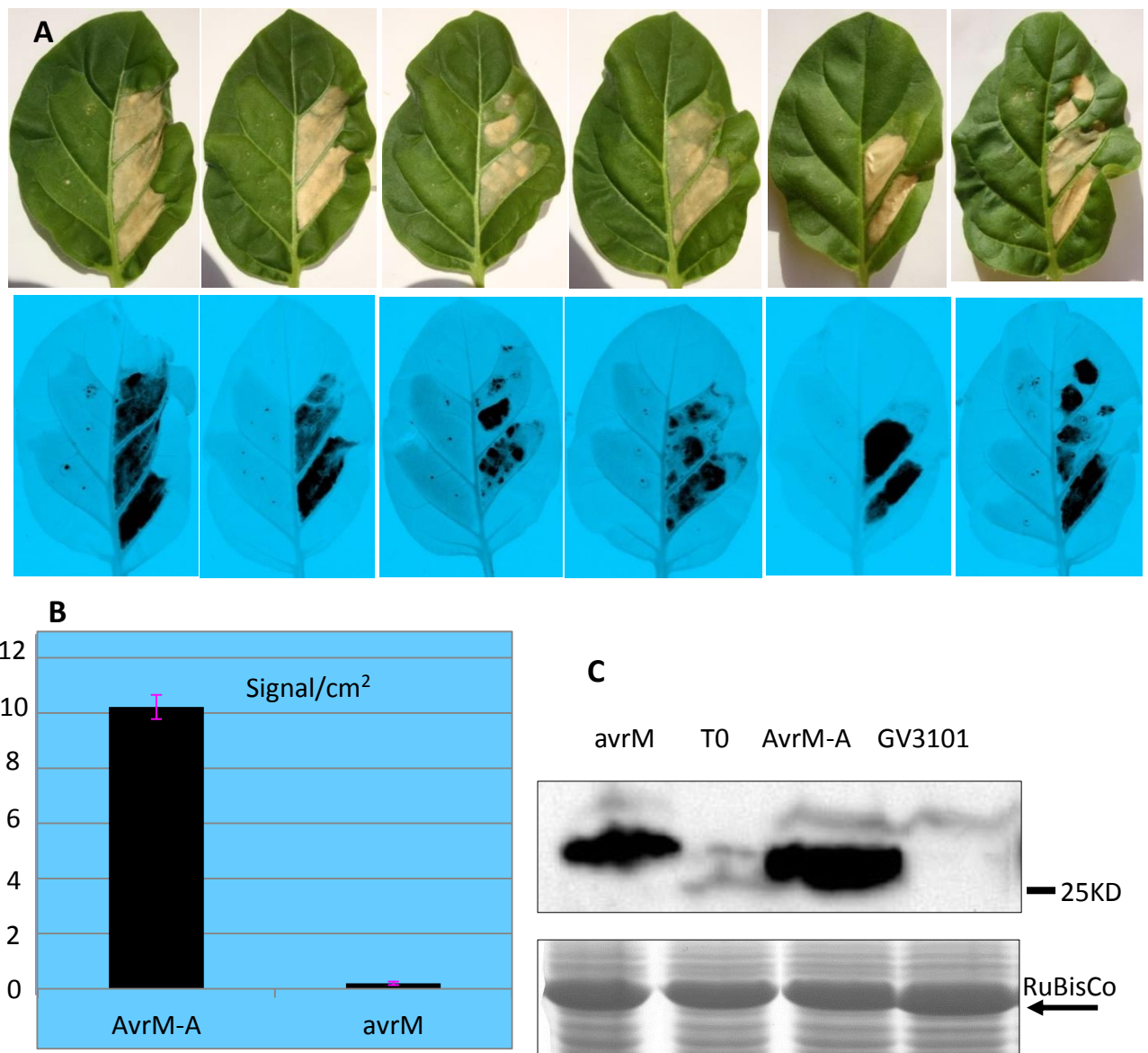


Figure 2.3: Measurement of HR intensities by BioRad GelDoc machine and ImageLab program. (A) HR assay for AvrM-A and avrM in six different leaves of *N. Tabacum* expressing M protein (upper panel) and same leaves were scanned in BioRad GelDoc machine (lower panel). (B) The HR intensities of the scanned tobacco leaves (A) were calculated using ImageLab program, and their average data were presented by a bar diagram. (C) Expression of AvrM-A and avrM showing by immunoblot analysis (upper panel) and coomassie stained gel (lower panel) used for assessing equal protein loading.

2.4.3 Protein extraction from tobacco leaves

For confirming the expression of avrM/AvrM-A proteins and mutants thereof in tobacco plants, 3-4 week old non-transgenic tobacco leaves (*N. benthamiana*) were infiltrated following the method stated above (Section 2.4.1). After one day post infiltration (dpi), equal quantities (~7cm²) of the infiltrated tobacco leaf tissues were collected by a cork borer and stored at -80°C in a 1.5ml Eppendorf tube following snap freezing with liquid nitrogen. For extracting the proteins, the stored leaf samples were manually pulverized into fine powder maintaining in liquid nitrogen to avoid thawing of the tissue samples. After grinding, 110µl of 3X Laemmli buffer (Appendix 1b) was added in the fine tissue powder following homogenization by drilling with a Ryobi LSD-120 12 V drill fitted with a modified drill bit for 60 seconds. Then the 3X Laemmli buffer dissolved tissue samples were incubated at 100°C for 5 minutes followed by centrifugation at 14,000 rpm for 10 minutes in a Benchtop Centrifuge at room temperature for pelleting leaf or cell debris. Finally, the supernatant was collected and stored at -80°C or directly loaded for further analysis by SDS-PAGE.

2.4.4 Sodium Dodecyl Sulphate Polyacrylamide Gel Electrophoresis (SDS-PAGE)

Polyacrylamide gels (15%) were prepared (Appendix 3) for separation by SDS-PAGE following the procedure previously stated by Laemmli, 1970. For *E. coli* produced protein samples, each protein sample was mixed with 3x SDS-PAGE sample buffer (Appendix 1b) in a ratio of 2:1 and boiled/denatured at 98°C for 5 minutes before loading. Following loading the samples, the gels were electrophoresed in 1X running buffer (Appendix 1b) by running at 170V for 60min or until the dye had run off the gel in a Mini-Protean® Tetra Cell gel electrophoresis unit (Bio-Rad, NSW, Australia). For each gel, a pre-stained Protein Marker (Broad Range, 7-175kDa, NEB) was used for enabling the molecular weights of the desired protein. Then the gels were used for either Coomassie staining (Section 2.4.7), or immunoblot analysis by transferring the proteins onto a nitrocellulose membrane (Section 2.4.6).

2.4.5 Ponceau staining of the nitrocellulose membrane

Following transfer of the proteins from gel to the membrane (Hybond ECL nitrocellulose membrane, GE Healthcare Life Sciences), the membrane was washed with TBS-T buffer for 2-3 minutes. Then the membrane was stained with Ponceau S (Sigma) solution for up to an hour following destaining in water or TBS-T until the protein bands were visible plus

a clean background was obtained. Afterward, an image was captured by the Bio-Rad ChemiDoc™ MP system and the visualized images were documented by the ImageLab program of the same system as per the instruction of the manufacturer. Ponceau staining was performed prior to blocking the membrane and immunoblot steps as a measure of equal or equivalent protein loadings.

2.4.6 Immunoblot analysis

The immunoblotting technique was adapted from the methods previously described (Towbin et al., 1979; Gallagher and Chakavarti, 2008; Williams, 2009; Sornaraj, 2013) for the confirmation of expression of the recombinant effector proteins. For this analysis, collected protein samples in Section 2.4.3 were separated by 15% SDS-PAGE (Section 2.4.4). When immunoblotting was necessary, two gels were run in duplicate, one for blotting, and another for Coomassie staining (Section 2.4.7). The protein samples were loaded at the rate of 30µl for western and 5µl for coomassie staining. Following separation by SDS-PAGE, the proteins were transferred from gel to a nitrocellulose membrane (Hybond-ECL, GE Biosciences). The post-transfer membrane was washed with blocking buffer (Appendix 1b) for 1 hour at room temperature followed by overnight incubation in 5ml blocking buffer containing appropriate dilution of primary antibody. Then the membrane was washed twice for 15 minutes in fresh blocking buffer followed by a further incubation in 5ml blocking buffer supplemented with the appropriate secondary antibody for 45 minutes. The leaf extracted protein samples were probed by immunoblotting with mouse anti-HA (clone 16B12; Covance, Emeryville, CA, USA) as the primary antibody (1:5,000 dilution) and the *E. coli* produced protein with Pierce 6×-His Epitope Tag Antibody (21HCLC), ABfinity Rabbit Oligoclonal (1:5,000 dilution). As the secondary antibody, the horseradish peroxidase-conjugated goat anti-mouse (Rockland, Gilbertsville, PA) was used in a dilution ration of 1:10,000. Afterwards, the membrane was washed twice with TBS-T buffer (Appendix 1b) for 15 minutes at room temperature. This was followed by 5 minutes incubation with 500ml chemiluminescence reagents (250 µl of each, Bio-Rad Clarity™ Western ECL Substrate). Finally, the immunoblots were visualized with the Bio-Rad ChemiDoc™ MP system and the visualized images were documented by the ImageLab program of the same system as per the instruction of the manufacturer.

2.4.7 Coomassie staining of SDS-PAGE gel

All the solutions required for this experiment are recorded in Appendix 1b. Prior to the staining, the electrophoresed gel was treated with a fixer solution for 20 minutes. Then the gel was stained with coomassie blue as previously described (Sornaraj 2013). After staining, the gels were scanned with a Bio-Rad Gel Doc™ EZ Imaging System and photos were analyzed by ImageLab Software 4.0 (Bio-Rad Laboratories, California, USA).

2.5 Methods for protein production

2.5.1 AvrM-A/avrM construction for expression

For production and purification of the recombinant effector proteins, the *AvrM-A/avrM* genes were cloned into pMCSG7 vector (Stols et al., 2002) encoding a 6× histidine tag at the beginning of the effector protein. These constructs were provided by Dr. Simon Williams (The University of Queensland, Australia). In these recombinant genes, only those mutations that changed M recognition in transgenic tobacco leaves (W38::M), were engineered for protein production in *E. coli* (strain BL21) (Section 2.3.2). Methods used for effector protein extraction is outlined by Ve et al. (2011) but are also briefly described here.

2.5.2 Transformation of effector genes in BL21 cells

AvrM-A, *avrM* genes and mutants thereof were transformed into electrocompetent BL21 (DE3) cells by electroporation as stated in Section 2.2.2. The transformed cells were plated onto LB-agar medium supplemented with 100µg/ml ampicillin. Following this, six well-separated single colonies were randomly selected, pooled, and used to seed cultures for expressing the effector proteins.

2.5.3. Growth and test expression

In this experiment, all of the procedures followed were previously described (Williams 2009; Ve et al., 2011) and in some cases, the processes were optimized when required. For the expression, typically six individual well-separated colonies were selected to inoculate a starter culture of 5 ml of LB broth containing 100 µg/ml ampicillin followed by incubation at 37°C for 5-6 hours with shaking at 200rpm. Subsequently, 50µl of the starter culture was used to inoculate 10ml of fresh LB medium with 100 µg/ml ampicillin. This culture was incubated under the same conditions for 4 hours at which point its OD₆₀₀ should be 0.6-0.8. Thereupon, the temperature was reduced at 20°C and isopropyl β-D-1-thio-galactopyranoside (IPTG) was added to a final concentration of 1.0mM to induce

protein expression, followed by continuation of the culture for a further 16 hours. Then the proteins were extracted and purified after harvesting the cells, and the proteins were analysed by SDS-PAGE, coomassie and western blotting.

2.5.4. Large-scale expression

Initially, a starter culture of 10ml LB supplemented with 100µg/ml ampicillin was prepared with six independent single colonies of effector gene-transformed BL21 (DE3) cells selected from LB plates. This starter culture was grown at 37°C for 4-5 hours. Afterward, this culture was used (1µl/ml) to inoculate two cultures of 2.5L fresh LB medium supplemented with 100 µg/ml ampicillin. For this culture, 5L Erlenmeyer flasks having 2.5L fresh LB medium (pre-warmed at 37°C) were used and incubated under the same conditions for 4 hours at which point the cultures' OD₆₀₀ was within 0.6-0.8. Thereupon the temperature was reduced at 20°C and IPTG was supplemented to a final concentration of 1.0mM followed by a further incubation at 20°C for 16 hours. Finally, the expressed cells were harvested by centrifugation at 5000g at 4°C for 20min in a Beckman Centrifuge Machine. The harvested cells were then washed with washing buffer (Appendix 1b) and centrifuged again to a cell pellet in a 50ml falcon tube, noting its weight, and snap frozen in liquid nitrogen and stored at -80°C until required for extraction.

2.5.5 Extraction of effector proteins

The cell pellet was resuspended in a pre-chilled lysis buffer (Appendix 1b) @ 7ml/gm cell pellet and the cells were then lysed at 30kpsi in a Cell Disruptor TS Series 0.75kw (Constant Systems Ltd., UK), as per the manufacturers' instructions. Afterwards, the cell debris was removed by ultracentrifugation at 45000g for 60 min in a 70,000 RPM rotor (Type: 70 TI, Serial: 484) at 4°C by Beckman Coulter Optima™ L-100 X_P Ultracentrifuge Machine and the resulting supernatant was collected as a ready crude extract for purification.

2.5.6 Purification of the extracted proteins

Following extraction, the supernatant was applied to a 5 ml HisTrap FF column (GE Healthcare) on an AKTA FPLC machine (GE Healthcare Life Sciences). Prior to loading, the lysate sample was filtered through a 0.22 µm filter (Millex® syringe filter units, Sigma-Aldrich, Australia), and the column was washed with 20 column volumes of the same lysis buffer, but with imidazole added to 30 mM. Afterwards, the protein was eluted using a linear gradient of imidazole from 30 to 250 mM over 20 column volumes. The fractions

containing the target proteins were detected by SDS-PAGE and subsequent coomassie stain analysis. Finally, the fractions containing the target proteins were pooled and concentrated using Amicon Ultracentrifugal devices (10 kDa molecular-weight cutoff; Millipore) according to the manufacturer's specifications. During concentration, the buffer was exchanged with the same lysis buffer to avoid imidazole that was used to elute the proteins from the nickel column and the protein was concentrated to a final volume of 2ml.

2.5.7 Protein quantification

Following the methods of Ve et al., 2011, the concentrations for all of the proteins were calculated using an extinction coefficient of $13.41 \text{ mM}^{-1} \text{ cm}^{-1}$ followed by measuring the absorbance at 280 nm by a Spectrophotometer (NanoDrop 1000, Thermo Scientific). In some cases, the Bradford reagent (Bio-Rad) was used and assayed as stated by Bradford (1976). Finally, the protein samples were *aliquoted into Eppendorf tubes, snap frozen in liquid nitrogen and stored at -80°C*.

2.6 Methods for biophysical analysis

2.6.1 Yeast Two-Hybrid assay

For confirming the interaction of the mutated effector proteins with the cognate M resistance protein, Yeast two-hybrid (Y2H) assay was conducted following some previous protocols (Dodds et al, 2006, Catanzariti et al 2010). For this assay, M (21-1305) was cloned into pGBT9 and pGADT7 vectors (Clontech) as previously described (Catanzariti et al., 2010a). AvrM-A (108-344), avrM (46-281) and corresponding mutants were cloned into pGBT9 and pGADT7 vectors (Clontech) as *EcoRI-BglII* fragments. All constructs were verified by sequencing. Yeast (strain HF7c) transformation and growth assays were performed as described in the Yeast Protocols Handbook (Clontech, 2009). Yeast protein extraction for immunoblot analysis was performed following a post-alkaline extraction method as described by Kushnirov, 2000. Protein fusion detection was performed using anti HA-hrp (Roche, clone 3F10), and anti GAL4 DNA BD (SIGMA, G3042) antibodies. This was done by Maud Bernoux at CSIRO, Plant Industry, Canberra.

2.6.2 Size-exclusion chromatography (SEC)-coupled multi-angle light scattering (MALS)

SEC-MALS was performed using an inline Superdex 200 100/300 GL SEC column (GE Healthcare) combined with a Dawn Heleos II 18-angle light-scattering detector coupled with an Optilab TrEX refractive index detector (Wyatt Technology, Santa Barbara, CA, USA). Purified effector proteins (1-0.5mg) were separated at 0.5 ml/min in 10 mM HEPES pH 7.5,

150 mM NaCl at room temperature. Molecular mass calculation was performed using Astra6.1 software (Wyatt Technology). To estimate the molecular mass, the input of the refractive increment (dn/dc values) was fixed at 0.186 ml/g, with an assumption that dn/dc is invariable for unmodified proteins (Wen et al., 1996). The peak of the eluted protein was used to determine the molecular mass. This was done by Simon Williams, Lachlan Casey and Alan Zhang at the University of Queensland, Brisbane.

2.6.3 Size-exclusion chromatography (SEC)-coupled small-angle X-ray scattering (SAXS)

SEC-SAXS was performed at the SAXS/WAXS beamline of the Australian Synchrotron using a Pilatus 1M detector. For each protein, 50 μ L of sample was injected into an inline 3ml Superdex S200 Increase column (GE Healthcare) at 16°C and flow rate of 0.1 ml/min, in 10 mM HEPES (pH 7.5), 150 mM NaCl buffer with 1.0 mM DTT. Data were collected through a 1mm quartz capillary mounted post-column, in 1 s exposures. The sample-to-detector distance was 2.6 m, and a wavelength of 1.033 Å at 12 keV yielded a range of momentum transfer $0.007 < q < 0.361 \text{ \AA}^{-1}$, where $q = 4\pi \cdot \sin(\theta)/\lambda$. Data reduction and subtraction were performed using scatterBrain from the link below:

<http://www.synchrotron.org.au/index.php/aussyncbeamlines/saxswaxs/software-saxswaxs>).

Unless noted otherwise, subsequent analysis was performed using the tools in version 2.6 of the ATSAS program suite. 100 frames immediately preceding each peak were summed and normalised for exposure time to obtain buffer blanks. These buffers were subtracted from each image individual to generate a series of subtracted frames across the elution peak, from which I and R_g were calculated for each frame using the Guinier approximation as implemented in batch-mode AUTORG. Molecular weights were calculated using the volume of correlation (V_c) method in the range $0 < q < 0.3$.

Frames corresponding to the peak centres were summed and averaged to produce high signal-to-noise datasets for shape analysis. Invariant parameters were calculated in PRIMUS. Distance distributions, $P(r)$, were obtained by indirect transformation in GNOM, informed by AUTOGNOM. Theoretical scattering was derived from atomic models using FoXS. Normalised Kratky plots were calculated manually, incorporating R_g values obtained using PRIMUS. This was done by Simon Williams, Lachlan Casey and Alan Zhang at the University of Queensland, Brisbane.

Chapter 3: Single residue mutation

(Pages 56 - 77)

Parts of the data presented in this chapter have been published in the following journal article.

Journal: *Proceedings of the National Academy of Sciences*, 110(43), 17594-17599, 2013.

Title: Structures of the flax-rust effector AvrM reveal insights into the molecular basis of plant-cell entry and effector-triggered immunity.

Authors: Thomas Ve^a, Simon J. Williams^a, Ann-Maree Catanzariti^b, Maryam Rafiqib^c,
Motiur Rahman^d, Jeffrey G. Ellis^e, Adrienne R. Hardham^b, David A. Jones^b,
Peter A. Anderson^d, Peter N. Dodds^e, and Bostjan Kobe^{a,1}

Address: ^aSchool of Chemistry and Molecular Biosciences, Australian Infectious Diseases Research Centre and Institute for Molecular Bioscience, University of Queensland, Brisbane, QLD 4072, Australia; ^bPlant Science Division, Research School of Biology, Australian National University, Canberra, ACT 0200, Australia; ^cInstitute of Phytopathology and Applied Zoology, Research Centre for BioSystems, Land Use, and Nutrition, Justus Liebig University, 35390 Giessen, Germany; ^dSchool of Biological Sciences, Flinders University, Adelaide, SA 5001, Australia; and ^eCommonwealth Scientific and Industrial Research Organization Plant Industry, Canberra, ACT 2601, Australia.

¹To whom correspondence should be addressed. E-mail: b.kobe@uq.edu.au.

Edited by Brian J. Staskawicz, University of California, Berkeley, CA, and approved September 14, 2013 (received for review April 23, 2013)

As a part of this publication, following data were contributed:

The mutational analysis in polymorphic residues of avrM and AvrM-A effector proteins coupled with *in planta* transgenic assay confirming that single residue contacts cannot alter the recognition specificity by the M flax resistance protein.

3.1 Introduction

Agrobacterium-mediated transient expression (AMTE) of AvrM-A has been demonstrated to trigger a very strong HR in *N. tabacum* expressing the M gene (Catanzariti et al., 2006, 2010). Therefore, this HR response has been utilized as a robust tool to further explore the residue/s of structural and functional importance to the AvrM effector family. To determine the key residue/s needed for detection by M protein, the polymorphic residues of AvrM-A and avrM have been exchanged one by one, and AMTE has been employed for an *in planta* assay to induce an M-dependent HR in transgenic *tobacco* leaves. Three polymorphic residues, K253/E316, E263/K326 and E270/K333 in avrM/AvrM-A have previously been demonstrated to have no role in AvrM/M recognition (Catanzariti et al., 2010a). For further investigation, AvrM-A and avrM genes were cloned into pEG201 with an N-terminal hemagglutinin (HA) epitope tag and the 35S CaMV promoter and expressed in the leaves of tobacco plants (W38::M) carrying the M transgene. As described in Catanzariti et al., 2010a, site-directed mutagenesis was employed to generate mutations of the remaining polymorphic residues in the same effector alleles, which were assayed by *in planta* HR induction to ascertain the residue/s responsible for detection by M. In this chapter, the polymorphic side-chains Q164/K226, R170/K232, S179/L241, T186/I248, N197/T259, Δ L218/P1280 and T247/I310 of avrM/AvrM-A (Figure 3.1) were mutated one by one to the corresponding allelic residue to identify which residue/s enable the effector proteins to change the level of detection by M protein. In addition, three conserved charged residues, E175/E237, E246/E309 and R250/R313, are exposed in the central surface of the effector dimer interface (Figures 3.2A, C and 3.3A, C). These charged residues in AvrM-A were also subjected to mutational analysis, as they are likely to transmute negative and positive patches in the central interfaces of the avrM (hypothesised) and AvrM-A dimers, respectively (Ve, 2011).

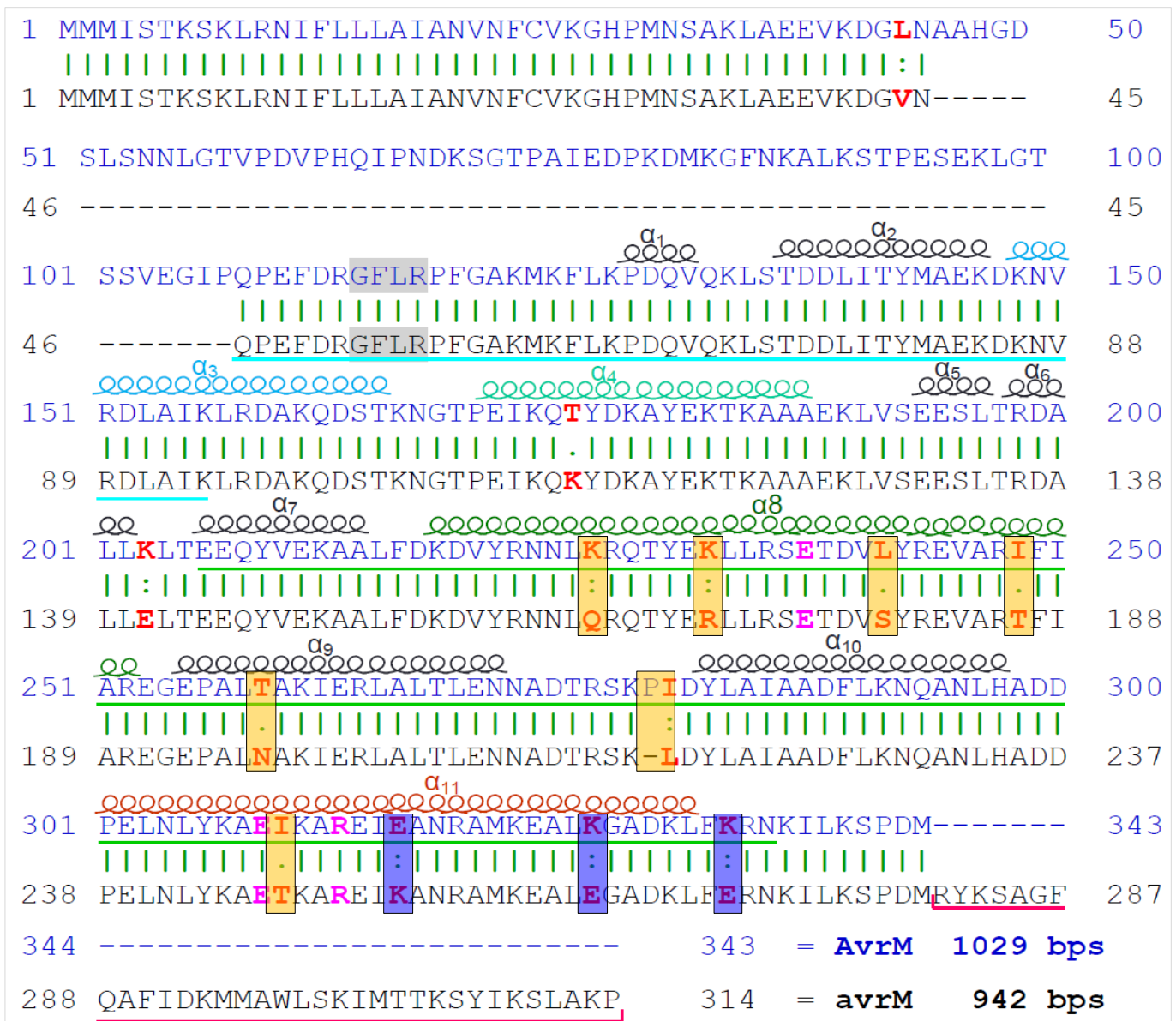


Figure 3.1: Sequence alignment of AvrM-A and avrM effector proteins showing the targeted polymorphic residues (yellow shaded boxes) for SDM. Three polymorphic residues reported to have roles in M resistance protein recognition are indicated by purple boxes (Catanzariti et al., 2010a). Three non-polymorphic residues located in the central charged pockets are shown in pink. Each effector protein encompasses eleven α -helices, which are indicated above the corresponding residues. Sequences responsible for host trafficking are underlined in cyan. The minimum sequence necessary for interaction with M protein are underlined in green. The 34-amino acid sequence that interferes with M-interaction is underlined in red (adapted from Catanzariti et al., 2006; Ve, 2011).

3.2 Results

Crystal structures of avrM and AvrM-A have been developed, including atomic coordinates and structural factors (Ve 2011; Ve et al., 2013), and deposited in the Protein Data Bank (www.pdb.org). All the structural analyses in this project have been modelled using avrM and AvrM-A template structures for which the PDB ID codes are [4BJM](#) and [4BJN](#), respectively. Insights from the molecular structures available in the Protein Data Bank (Ve et al., 2013) form the basis of the mutation analysis in this project. The residue locations in avrM and AvrM-A effector proteins are indicated in Figure 3.1. The exact positions and exposure of the targeted residues of avrM and AvrM-A in each protein structure are indicated in Figures 3.2 - 3.3.

3.2.1 Mutation of polymorphic residues

3.2.1.1 AvrM-A^{K226Q} and avrM^{Q164K}

K226 in AvrM-A and Q164 in avrM are polymorphic residues located in the α_8 helices and exposed at the exterior surface of the effector dimers, making them accessible to mediate a direct interaction with the cognate M protein. In avrM, Q164 is a hydrophobic residue that has no direct role in the charged pocket of the protein but contributes to the structural configuration. However, the counterpart in AvrM-A, K226, is a positively charged residue and so contributes to the basic nature of the dimer surface. Mutational exchange of either with the counterpart residue did not change the HR intensity (Figure 3.5), indicating that these two distal polymorphisms (K226 and Q164) do not directly affect the interaction with M. As AvrM-A^{K226Q} induced a necrotic cell death response to a similar degree to the wild type AvrM, there is no doubt that the protein is expressed in the plant, and it is clear that these mutations do not significantly affect the protein structure or stability.

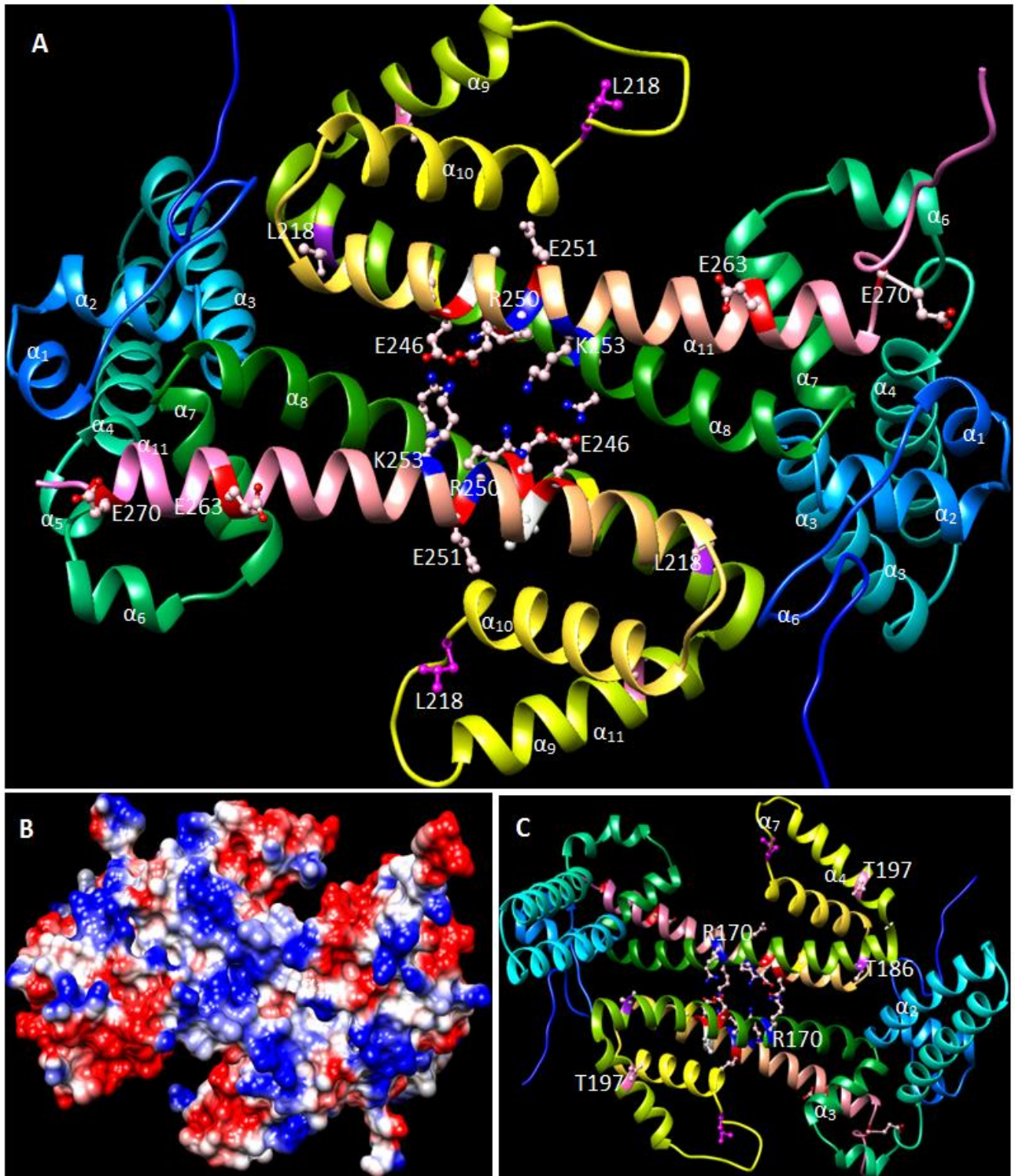


Figure 3.2: Structure of avrM (predicted dimer) showing the residues thought to be important for interaction with M protein. (A) Exterior view of the secondary structure showing the residues in the α -helices. (B) Surface representation of the effector protein with same orientation as in A. (C) Interior view of the secondary structure with opposite orientation of A.

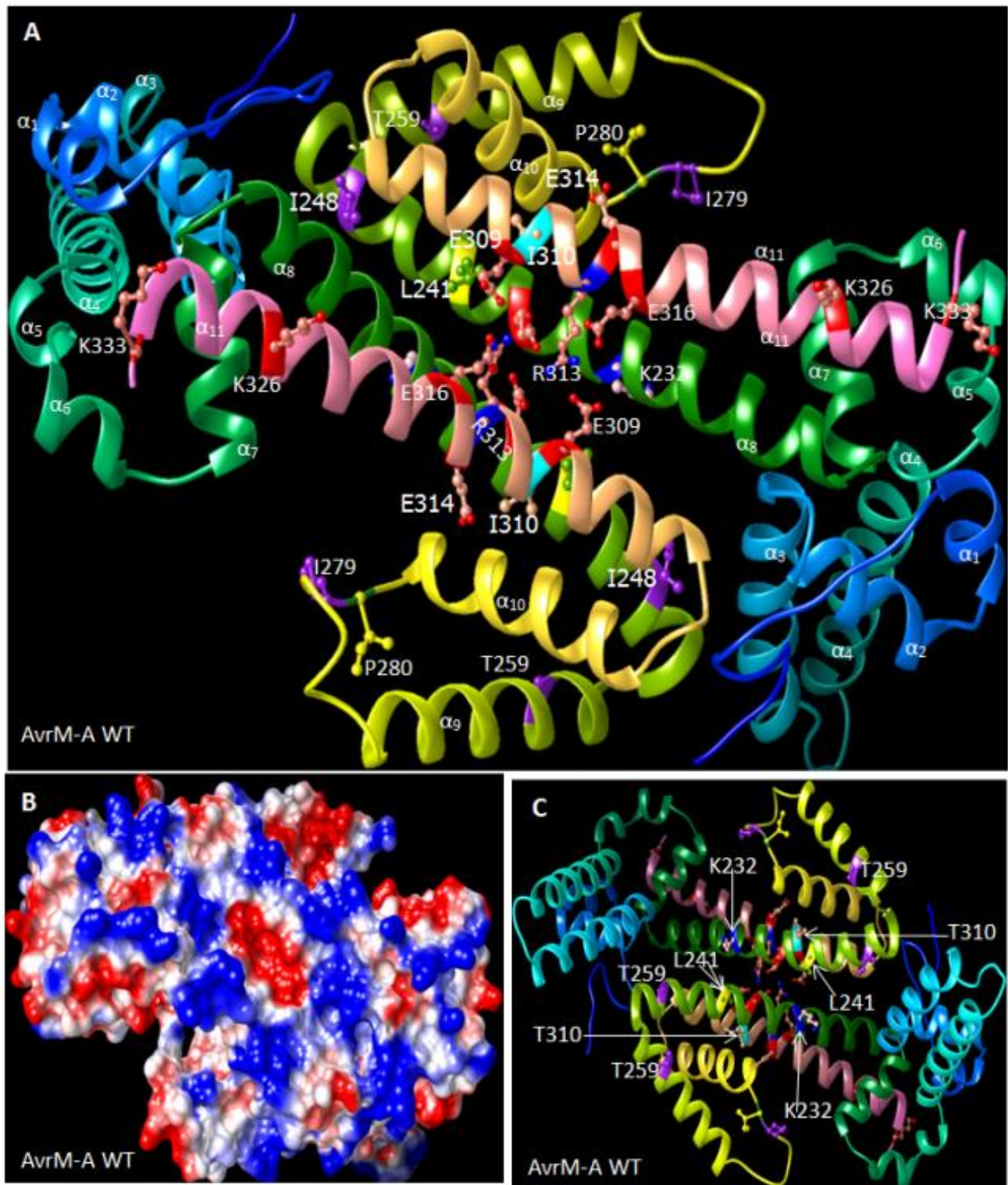


Figure 3.3: Structure of AvrM-A showing the different residues thought to be important for the interaction with M protein. (A) Exterior view of the secondary structure showing the residues in the α -helices. (B) Surface representation of the effector protein with same orientation as in A. (C) Interior view of the secondary structure with opposite orientation of A.

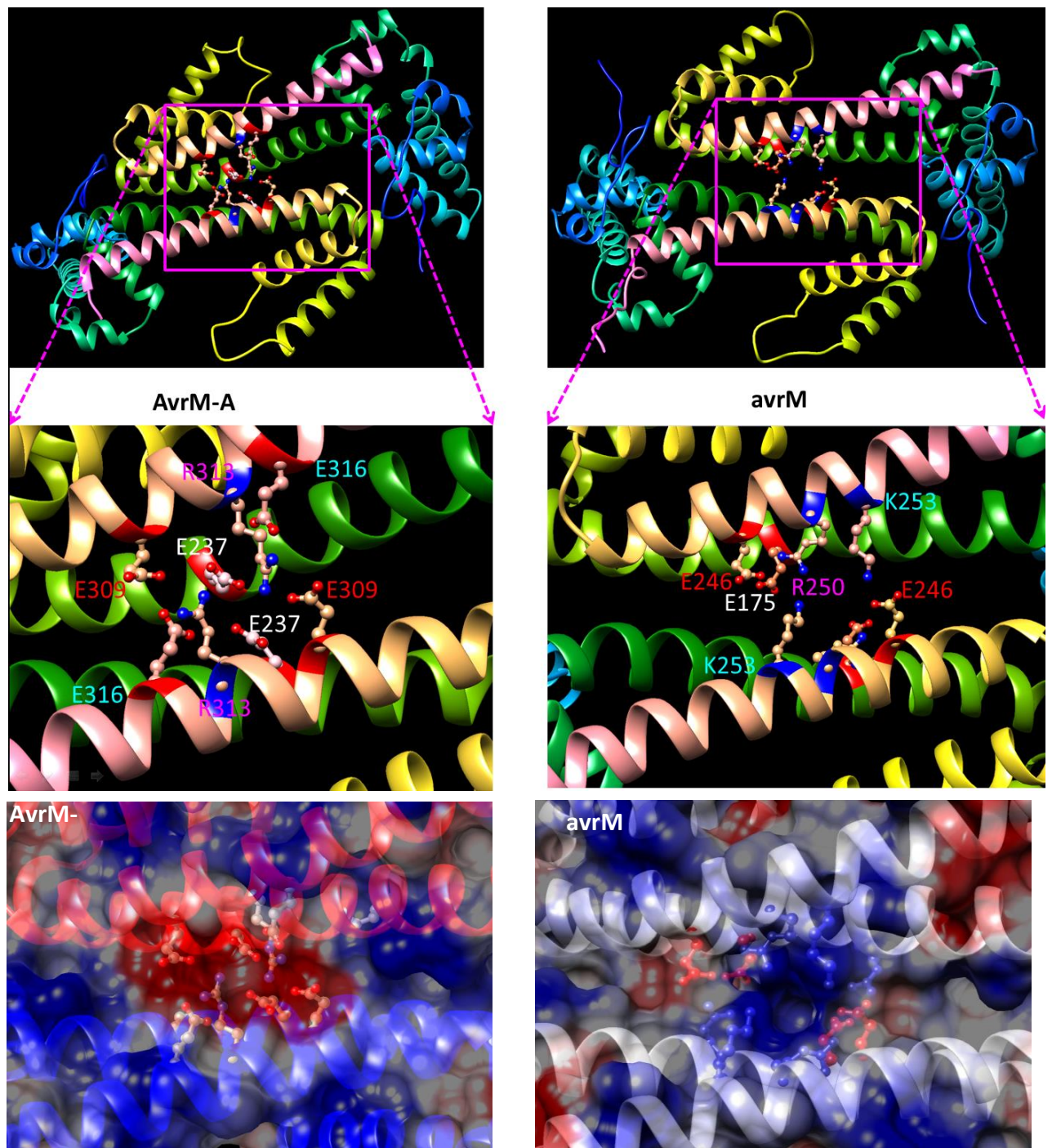


Figure 3.4: Secondary Structures of AvrM-A and avrM showing the residues supposed to transmute the central charge surfaces that control the interaction with M.

3.2.1.2 AvrM-A^{K232R} and avrM^{R170K}

Similar to K226 and Q164, K232 in AvrM-A and R170 in avrM are two polymorphic residues located in the α_8 helices of the anti-parallel coiled coil (APCC) region of the protein dimers (AvrM-A and avrM). In this case, both residues are positively charged and capable of providing basic surface patches in the mature proteins. These two residues have direct input to the charged pockets in the effector proteins and are likely to support interaction with the M protein. But mutation of either to the counterpart, AvrM-A^{K232R} and avrM^{R170K}, induced HR at a similar intensity to the wild type progenitor (Figure 3.5), indicating that K232 and R170 alone have no effect on interaction with the M protein. Moreover, AvrM-A^{K232R} triggers a necrotic cell death response similar to the wild type AvrM, indicating that these mutants are expressed in plant at a threshold level for interaction with M protein and that these mutants do not have a significant effect on the protein structure or stability.

3.2.1.3 AvrM-A^{L241S} and avrM^{S179L}

L241 in AvrM-A and S179 in avrM are hydrophobic residues located in the α_8 helices, one of the backbones of the charged pocket in the effector dimer interface. In the α_8 helices, these residues are entombed inside the surfaces of the protein dimers. Hence these residues have no direct contribution to the central charged pockets, but are likely to have an important role in generating a conformation of the α_8 and α_{11} helices in AvrM-A appropriate for achieving the acidic surface patch required for M detection. These residues have been reported to give significant differences in the orientation of the α_8 and α_{11} helices, possibly affecting interaction with the M protein (Ve, 2011). However, substitution of either of the residues, AvrM-A^{L241S} and avrM^{S179L}, demonstrated that these mutations alone cannot affect interaction with M (Figure 3.5). In addition, the AvrM-A^{L241S} mutant induced a strong HR, which indicates that the substitution is expressed and detected by the M protein in plant and has no notable effect on the structure and stability of the effector dimers.

3.2.1.4 AvrM-A^{I248T} and avrM^{T179I}

Like L241/S179, AvrM-A^{I248T} and avrM^{T179I} are hydrophobic residues positioned at the end of the α_8 helices and submerged in the protein surface. As both are distant from the central pocket, they have no direct input to the charged pockets of the effector dimers. Consequently, the exchange of either with the counterpart, AvrM-A^{I248T} and avrM^{T179I}, induces HR at the same intensity as the corresponding wild type protein, indicating that the

recombinant proteins are expressed and interact (only AvrM-A) in the plant. So they also do not directly affect the protein structure and stability or the central charged pockets.

3.2.1.5 AvrM-A^{T259N} and avrM^{N197T}

T259/T179 is the only polymorphism distinguishing the α_9 helices of the AvrM-A and avrM proteins. Both are hydrophobic residues exposed at the interior sides of the effector protein dimer. The residue position on the protein surface indicates a location distal from the central pocket, which may render an antiparallel orientation of the α_8 and α_{11} helices. Thus there is no direct effect on the central charged pocket and the role of these residues is more likely to support structural configuration of the proteins. The *in planta* assays of the reciprocal mutations, AvrM-A^{T259N} and avrM^{N197T}, produced HR intensities similar to their wild type progenitor suggesting that neither T259 nor N197 is able to re-orientate the α_8 and α_{11} helices and alter the interaction with the cognate M protein. In addition, protein structure and stability are not markedly affected by either mutant, as AvrM-A^{T259N} induced a necrotic cell death response similar to the wild type AvrM-A, also indicating that the residue exchanges did not hamper protein expression in the plant.

3.2.1.6 AvrM-A^{PI280/ Δ L218} and avrM ^{Δ L218/PI280}

In AvrM-A, there is a proline (P) at position 280 and an isoleucine (I) at 280 on a wire loop connecting the α_9 and α_{10} helices of the effector proteins. Conversely, in avrM there is a gap at the equivalent position to the counterpart of PI280, followed by leucine (Δ L218) as the counterpart of PI280 (Figure 3.1). Moreover, of these three residues, proline (P279) and isoleucine (I280) are unique residues, but Δ L218 is hydrophobic (Figure 3.5A). So although they have no direct role in the central charged pockets, they are likely to expose the α_9 and α_{10} helices and thus assist in presenting the most critical helices of the proteins, the α_8 and α_{11} helices. As a result, they are likely to contribute indirectly to the central pocket conformation as well to the interaction with M. But frustratingly, reciprocal mutations of these residues with their counterparts (AvrM-A^{PI280/ Δ L280} and avrM ^{Δ L218/PI280}) did not change the intensity of each induced HR with respect to each non-mutant effector. As AvrM-A ^{Δ L280PI} induced a similar HR to AvrM-A, it seems likely that these residues are unlikely to alter the stability and configuration of the protein or hamper protein expression in the plant.

3.2.1.7 AvrM-A^{I310} and avrM^{T247}

The side-chains I310 in AvrM-A and the counterpart T247 in avrM are hydrophobic residues located in the α_{11} helices and entombed in the protein surfaces (Figures 3.2 -3.3) and are thus unlikely to contribute directly to the central charged pockets of the dimer interface. This assumption is supported by the *in planta* assays of the reciprocal mutations of AvrM-A^{I310T} and avrM^{T247I}, that indicated no change in HR intensity compared to the respective wild type proteins. This confirms that the mutant protein is expressed in the plant and that replacement of either residue with the allelic counterpart does not alter the configuration of each effector protein, suggesting that alone these residues are very unlikely to alter protein stability or expression in plants.

AvrM-A	44	175	203	226	232	241	248	259	278	279	310	316	326	333
	L	T	K	K	K	L	I	T	P	I	I	E	K	K
	V	K	E	Q	R	S	T	N	-	L	T	K	E	E
avrM	44	113	141	164	170	179	186	197	217	218	247	253	263	270
A	Hydrophobic							(-)ve charged		(+)ve charged		Unic aa		
	A, I, L, V, F, W, Y, N, M, C, S, Q, T							D, E		R, H, K		G, P		

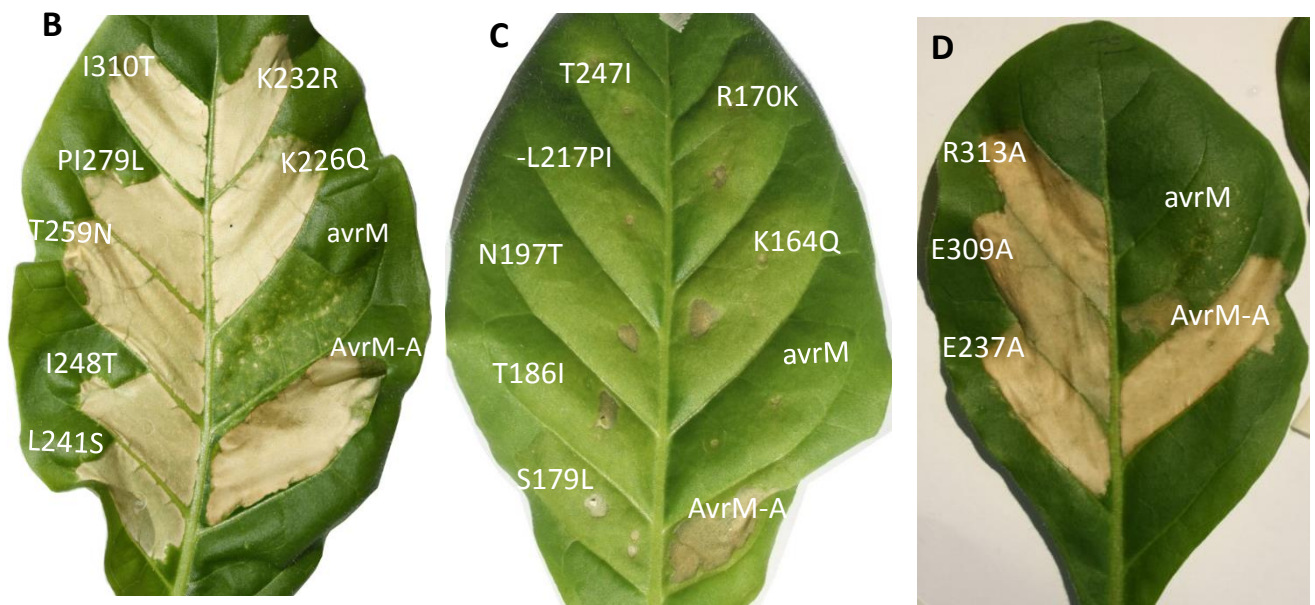


Figure 3.5: (A) Polymorphic residues with the corresponding locations in AvrM-A and avrM proteins. The negatively charged residues are shaded in red; positively charged residues are indicated by white letters shaded in blue, and hydrophobic residues are shaded in yellow. Green lines indicate the minimal region sufficient to induce M-dependent HR and to interact directly with the cognate M protein in the Y2H assay (Catanzariti et al., 2010a). (B & C) *In planta* assay of the reciprocal single residue mutants in polymorphic residues of AvrM-A (B)

and avrM (C). Each residue has been exchanged with the allelic counterpart and tested in transgenic tobacco leaves expressing M protein (W38::M). (D) *In planta* results of alanine substitutions in three non-polymorphic charged residues in AvrM-A.

3.2.2 Mutation of non-polymorphic residues in AvrM-A

3.2.2.1 AvrM-A^{E237A}

In the AvrM-A dimer, E237 is a negatively charged residue located in the α_8 helices and exposed inside the central cleft (not visible on either exterior or interior surface of AvrM-A dimer, Figure 3.4), which makes it likely to contribute directly to the negative charge of the central pocket in the AvrM-A dimer. Exchange of this residue with an alanine residue (A, a neutral amino acid) was expected to reduce the negative charge at the central pocket, but the *in planta* assay of the mutant construct, AvrM-A^{E237A} in transgenic tobacco leaves (W38::M) showed no change in HR intensity compared to AvrM-A (Figure 3.5 D). The *in planta* assay reveals that the M resistance protein recognises this recombinant protein (AvrM-A^{E237A}), which also demonstrates that it is expressed in the plant and the protein structure and stability are not disturbed. Structural analysis showed that this alanine substitution led to a mild reduction in the negative charge at the interface of the central cleft (Figure 3.6), but this reduction is below the threshold level for destabilization of interaction with the M protein.

3.2.2.2 AvrM-A^{E309A}

In the AvrM-A dimer structure, the α_{11} helices exposes the negatively charged side-chain E309 to the surface exactly at the central cleft of the dimer interface. So this residue is predicted to make a strong contribution to the negative charge of the central pocket in the dimer interface. However, following exchange of E309 with an alanine (A) residue, AvrM-A^{E309A} did not knockdown the HR intensity in M-containing tobacco leaves compared to the wild type effector protein, AvrM-A (Figure 3.5 D). Therefore, the alanine substitution of E309 alone does not affect protein structure, stability or expression in the plant and only moderately neutralizes the negative charge in the central pocket, not to a sufficient degree to make the AvrM-A protein undetectable by the M protein.

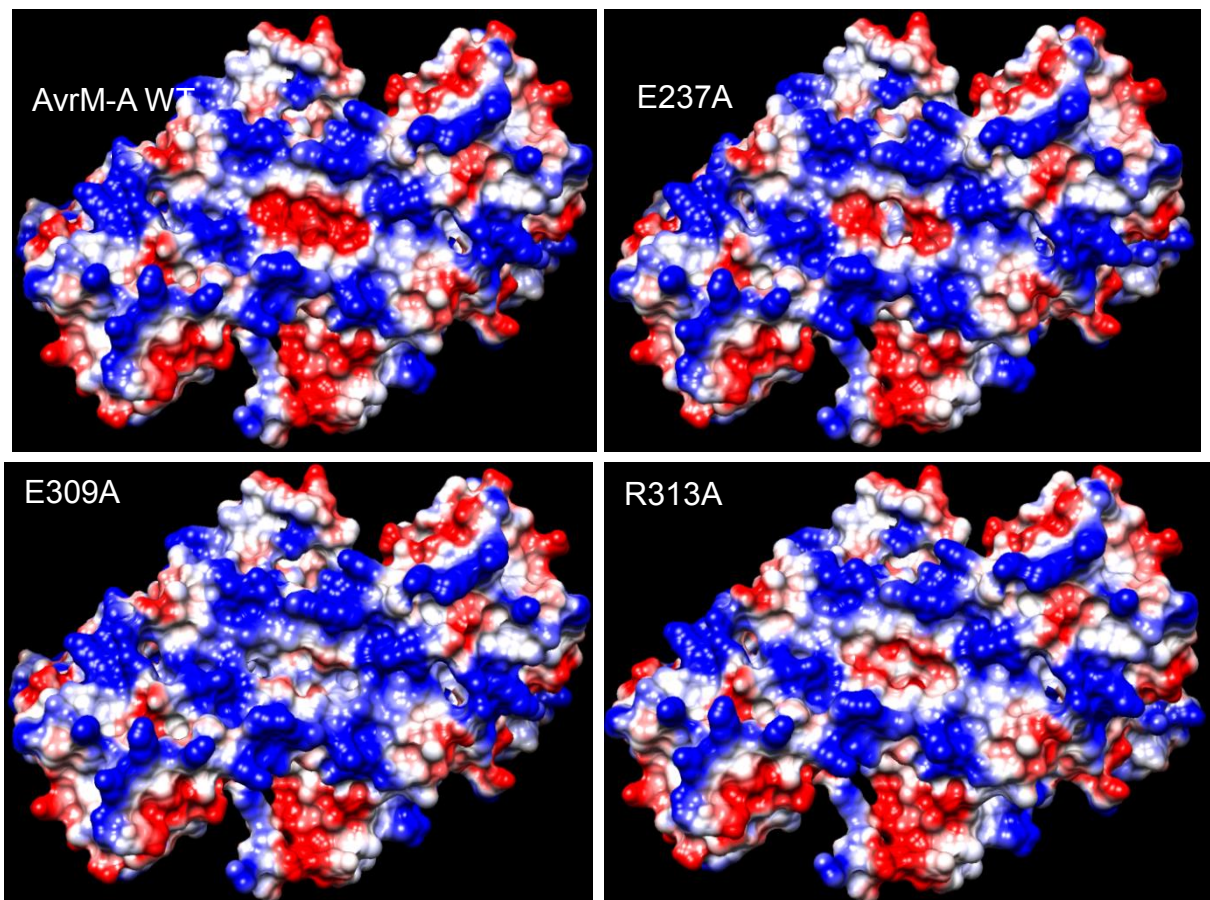


Figure 3.6: Comparative views of the central charged clefts in AvrM-A with the same of the three alanine substitutions in the side chains of E237, E309 and R313.

3.2.2.3 AvrM-A^{R313A}

The side-chain R313 is a positively charged residue located in the α_{11} helix of the AvrM-A dimer, and is surface exposed in the central cleft of the highly negatively charged central pocket. The positive charge of the R313 residue is neutralized by transmuting H-bonds with either of the surrounding side chains E237, E309 and E316 (Ve, 2011), which maintains the central cleft in an overall negatively charged condition (Figure 3.4 and 3.6). Substitution of the arginine residue with alanine to give AvrM-A^{R313A} did not alter the HR intensity in an *in planta* assay with tobacco leaves containing M resistance proteins (Figure 3.5 D). This *in planta* test clearly demonstrates that the alanine mutation, AvrM-A^{R313A} is insufficient to knock down the negatively charged cleft that appears to control recognition of the AvrM-A effector protein by M. The surface representation shows that although replacement of R313

with alanine decreased the negative charge of the central pocket (Figure 3.6), the charge reduction is not enough to knock down the interaction with M protein. This also indicates that the alanine mutation (R313A) neither hampers the protein expression in plant nor impedes the protein stability and structure.

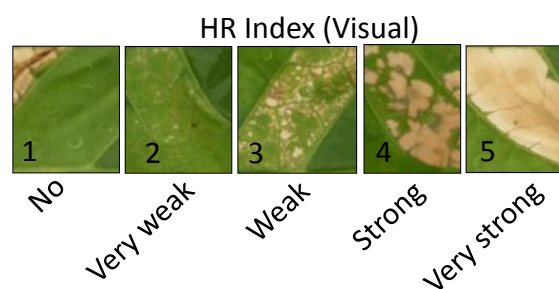
In the mutational analyses, all the AvrM-A mutants are recognized by the M protein, inducing a strong HR in tobacco leaves (W38::M). These *in planta* assays clearly demonstrate that the reciprocal mutations and alanine substitution in AvrM-A neither hamper protein expression in plant nor impair protein stability and structure. In the following chapter, immuno-blot analyses confirm that double, triple and quadruple mutants of some combinations of the single mutants from this chapter have not affected expression *in planta*.

The results of *in planta* assays for the single residue mutants in AvrM-A and avrM are summarized in Table 3.1.

Table 3.1: Single residue mutations in AvrM-A and avrM with their cognate R-recognition in tobacco leaves expressing M protein. Red colour codes the mutated residues while magenta indicates the non-polymorphic residues between the two effector proteins.

Variants	Mutation	226	232	237	241	248	259	280	309	310	313	316	HR induction
AvrM-A	Wt :	K	K	E	L	I	T	PI	E	I	R	E	VS
	K226Q :	Q	K	E	L	I	T	PI	E	I	R	E	VS
	K232R :	K	R	E	L	I	T	PI	E	I	R	E	VS
	E237A :	K	K	A	L	I	T	PI	E	I	R	E	VS
	L241S :	K	K	E	S	I	T	PI	E	I	R	E	VS
	I248T/A :	K	K	E	L	T	T	PI	E	I	R	E	VS
	T259N :	K	K	E	L	I	N	PI	E	I	R	E	VS
	PI280L :	K	K	E	L	I	T	ΔL	E	I	R	E	VS
	E309A :	K	K	E	L	I	T	PI	A	I	R	E	VS
	I310T :	K	K	E	L	I	T	PI	E	T	R	E	VS
	R313A :	K	K	E	L	I	T	PI	E	I	A	E	VS
	E316A :	Q	K	E	L	I	T	PI	E	I	R	A*	VS
avrM^P	WT :	Q	R	E	S	T	N	ΔL	E	T	R	K	No
	Q164K :	K	R	E	S	T	N	ΔL	E	T	R	K	No
	R170K :	Q	K	E	S	T	N	ΔL	E	T	R	K	No
	S179L :	Q	R	E	L	T	N	ΔL	E	T	R	K	No
	T186I :	Q	R	E	S	I	N	ΔL	E	T	R	K	No
	N197T :	Q	R	E	S	T	T	ΔL	E	T	R	K	No
	ΔL218PI :	Q	R	E	S	T	N	PI	E	T	R	K	No
	T247I :	Q	R	E	S	T	N	ΔL	E	I	R	K	No
		164	170	175	179	186	197	218	246	247	250	253	HR induction

*Catanzariti et al., 2010a tested E316K (conserved substitution). ^Ppositions are shown in the bottom lane. M-recognition specificity is indicated as very strong (VS) and no HR (no) following a cell death scoring scale (Bernoux et al., 2016) as follows:



3.3 Discussion

3.3.1 Structural differences in AvrM-A and avrM proteins

Structural analysis of any protein can provide data important to the success of a functional mutational analysis. Superimposition of AvrM-A with avrM revealed considerable differences in the conformation of the α_8 and α_{11} helices (Ve, 2011). The structural analysis suggested that these configuration differences are a result of the side chain exposures of I310/T247 in the α_{11} helix and of L241/S280 in the α_8 helix (Figure 3.7).

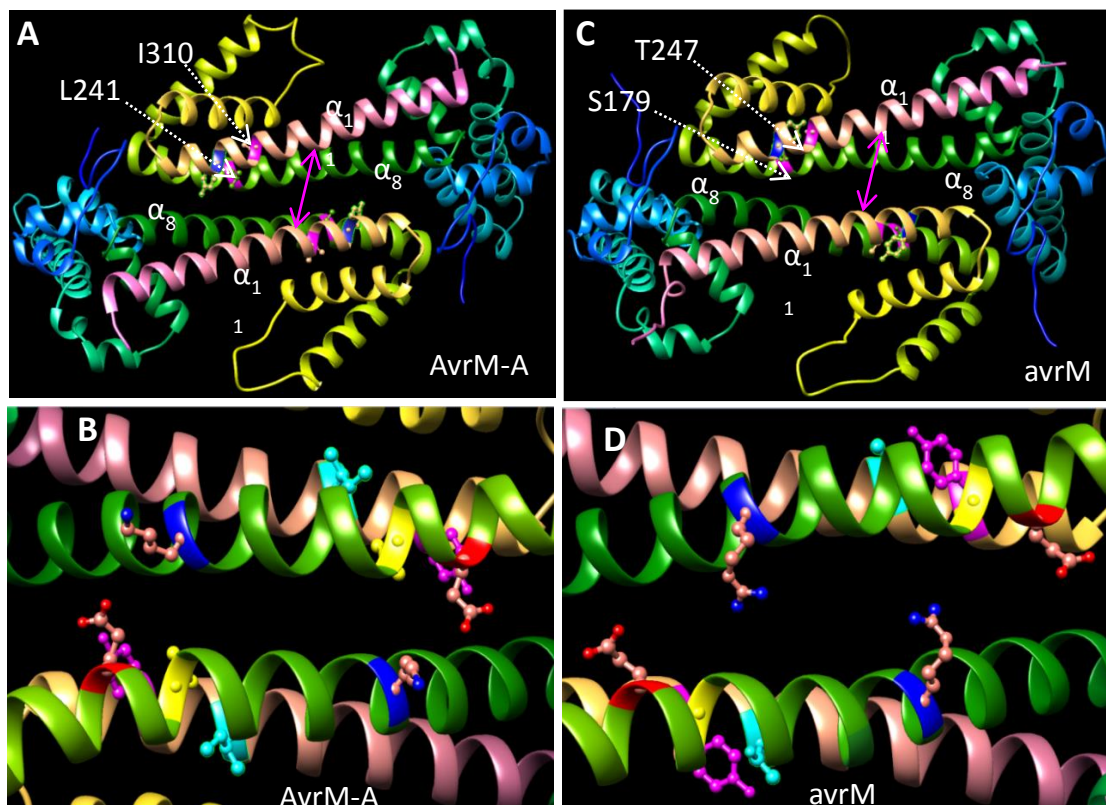


Figure 3.7: Differences in configuration at the α_8 and α_{11} helices of AvrM-A and avrM dimers due to exposure of their respective side chains of L241S, I310 and S179L, T247. The exterior views of AvrM-A and avrM are shown respectively in A & C and their respective interior magnified views in B & C. Colour codes for the residues indicated here: K232/R170- blue, L241/S179- yellow, E244/E182-red, Y306/Y243-magenta and I310/T247-cyan.

Interestingly, the polymorphisms L241/S179 at α_8 and I310/T247 at α_{11} helices induce an almost 180° rotation of the Y306 side-chain in AvrM-A compared to the corresponding side-chain (Y247) in avrM. As a result, the Y306 side-chain juts out from the plane of its coiled-coil domain towards the α_8 and α_{11} helices of the other monomer, which is likely to remodel the configuration of the CC domains compared to avrM (Figure 3.7B shown by magenta colour). But in avrM, the side chain Y247 has a changed orientation and is exposed in the outer direction from the central patch of the dimer interface. In AvrM-A, Y306 hides just underneath the E244 side chain, while the counterpart residue E182 in avrM is distant from the Y243 side chain (Figure 3.7 D, shown by magenta colour). More accurately, the Y247 side-chain is entombed in within the CC domain and likely to stabilize the interaction between the α_8 and α_{11} helices of the monomer. As a consequence, the Y306 orientates E244 side-chain in AvrM-A allowing it to transmute a hydrogen bond with K232 (Ve, 2011). Furthermore, the K232 side-chains are interiorly exposed with an outward trend from the central pocket (Figure 3.7A- B), while its polymorphic counterpart R170, although also interiorly exposed, has an inward trend towards the central pocket (Figure 3.7 C - D), which is likely to contribute a positive charge to the central surface of the avrM dimer.

The structural analysis, which clearly revealed that the flax rust AvrM effector protein exists as a homo-dimer in solution, is also supported by gel filtration (Ve et al., 2011). In contrast, the oomycete effector ATR1 has been found to be a monomer with a repeat structure comprising repeat-1 and repeat-2 (Krasileva et al., 2010; Chou et al., 2011), and the AvrL567 effector protein is also a monomer of a β -sandwich dominated with two antiparallel β -sheets A and B that arrange into an incompletely closed β -barrel (Wang et al., 2007). Indeed, it can be predicted that some effector proteins require duplication either by homo-dimerization or self-repetition to deploy the proper function, either for pathogenicity or to defend against resistance detection by the host plant.

3.3.2 AvrM-A and avrM dimer interfaces comprise two different central patches

The electrostatic properties of the surface of the AvrM-A dimer are significantly different from those of avrM (Figure 3.2 B and 3.3 B). There is a cleft at the midpoint of the AvrM-A dimer interface, but the avrM dimer possesses a shallower interface at its midpoint. The cleft of the AvrM-A dimer is highly negatively charged (acidic), while the shallower

interface on the *avrM* surface is positively charged (basic). Structural analysis shows that the side-chain K253/E316 is located at the central pocket of the dimer interfaces of AvrM-A/*avrM*. A close inspection of the structure reveals that each monomer in the AvrM-A dimer has four charged residues (E237, E309, R313 and E316) exposed in the central cleft, of which three are negatively charged, resulting in the negatively charged pocket (acidic; Figure 3.8 A-B). In contrast, the monomers of *avrM* dimers deploy four charged residues (R170, E246, R250 and K253) in the central surface, of which three are positively charged, generating a shallower surface of positive charge (basic; Figure 3.8 C-D). However, a careful inspection of the structures concedes, perhaps surprisingly, that the K232/R170 polymorphic side-chain is likely to play a critical role in exposing these charged residues in the central cleft in AvrM-A as well as in the shallower surface of *avrM*. Specifically, the R170 side-chains in the *avrM* dimer form hydrogen bonds with the non-polymorphic negatively charged side-chain E175, resulting in E175 being enclosed in the interior region of the *avrM* dimer. But the corresponding counterpart K232 residues in the AvrM-A dimer have a different conformation which does not interact with the corresponding E237 side-chains. That is why the two E237 residues are very close together at the central cleft of the AvrM-A dimer (Figure 3.8), allowing the E237 residues along with the E309 and E316 side-chains to form hydrogen bonds with both of the surface-exposed positively charged R313 residues of the AvrM-A dimer. As a result, the positive charge of the R313 side-chains is neutralized by the hydrogen bonds, inducing an overall negatively charged cleft at the central pocket of the AvrM-A dimer interface (Figure 3.8). In case of *avrM*, the buried conformation of the E175 side-chains favours the central R250 side-chains forming non-hydrogen bonded orientations compared to the counterpart arginine residues (R313) in AvrM-A (Figure 3.8 C & D). In fact, R313/R250 is a positively charged residue, which contributes positive charge to the central surface of the *avrM* dimer, but is neutralized in the central cleft of the AvrM-A dimer. However, mutation analysis of K253/E316, E263/K326 and E270/K333 in *avrM*/AvrM-A, by replacement with each allelic counterpart residue, revealed that these residue mutations did not destabilize the interaction with M, either in plant or in Y2H assays (Catanzariti et al., 2010a). As a result, E237, E309 and R313 residues of AvrM-A are targeted further in this project to demonstrate any role in AvrM/M interaction. Although E237, E309 and R313 residues are non-polymorphic in AvrM-A and *avrM*, all are charged residues located at the α_8 and α_{11} helices that expose them to the

central charged surface of the effector dimers. The polymorphic side-chain R170/R232 is surface exposed and located at the α_8 helix. These R232 residues are oriented outwardly from the central cleft of AvrM-A dimer and do not hamper any negative charge of the cleft, but in *avrM*, the counterpart R170 residues are oriented inwardly, form H-bonds with E175 residues to neutralize the negative charge of the central pocket, favouring an overall positive charge on its surface (Figure 3.7 D).

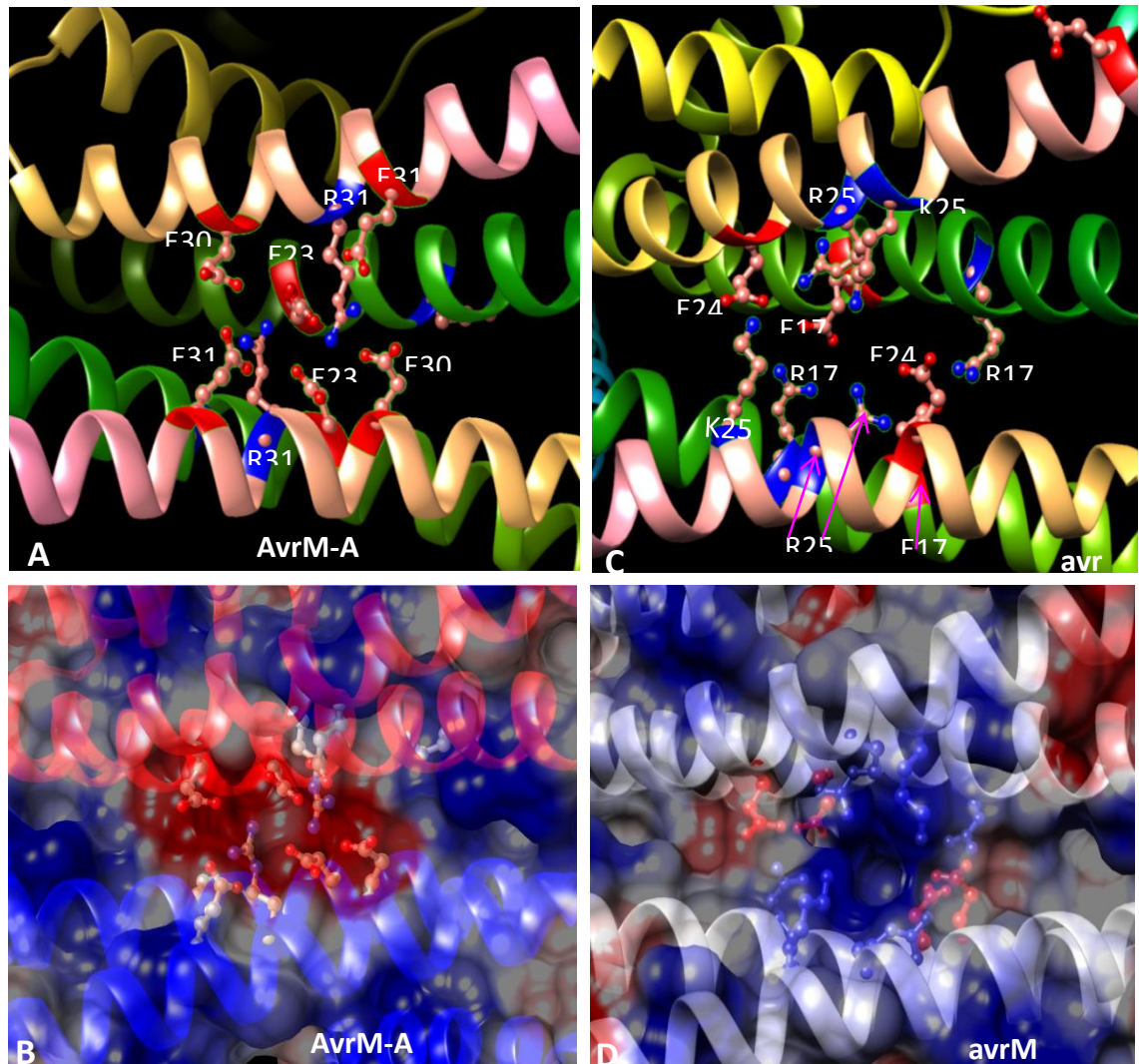


Figure 3.8: Highlighting the central patches of AvrM-A (left) and *avrM* (right) controlling R protein interaction. (A & C) Ribbon structures showing the important residues contributing charge to the central surfaces of the effector dimers. (B & D) Transparent surface representations of the same views as in A & C, respectively.

3.3.3 Selection of critical residue/s involved in M detection

Necrotic cell death is the resistance response by the M flax resistance protein following recognition of AvrM. Of the six variants, only AvrM-A and AvrM-D proteins interact physically with the M protein (Catanzariti et al., 2010a), suggesting that direct interaction is a prerequisite for the recognition specificity of an R protein (Krasileva et al., 2010). Deletion studies manifested that amino acids 206-335 of AvrM-A (the counterparts of amino acids 144-272 in *avrM*) form the minimal region (Figure 3.1) required to induce HR similar to the wild-type and to interact physically with the M protein in Y2H assays (Catanzariti et al., 2010a). The α 7-11 helices of the AvrM-A and *avrM* structures have been implicated as the minimal region differentiating the AvrM alleles, containing 11 of the 13 polymorphic side-chains (Figure 3.1). Structural analysis of AvrM-A/*avrM* dimer surfaces indicates that the 11 polymorphic side-chains (Q164/K226, K232/R170, S179/L241, T186/I248, N197/T259, Δ L218/P1280 and T247/I310, K253/E316, E263/K326 and E270/K333) are surface exposed (Figure 3.2 and 3.3), and facilitators for controlling interaction with the M resistance protein. All these polymorphisms are located in the anti-parallel CC-domains (α ₈ and α ₁₁ helices), including the loops connecting α ₁₀ and α ₁₁ helices (Figure 3.2 and 3.3). Four of the polymorphisms (Q164/K226, K253/E316, E263/K326 and E270/K333) are exposed on the exterior surface of the AvrM dimer, three of them (K232/R170, N197/T259 and Δ L218/P1280) are on the interior surface, while the residual three residues (S179/L241, T186/I248 and T247/I310) are entombed inside the surfaces.

3.3.4 Mutagenesis and *in planta* assay

3.3.4.1 Reciprocal mutation in polymorphisms

Mutagenesis of AvrM-A/*avrM* along with *in planta* assays revealed that single residue substitutions either in polymorphic or non-polymorphic charged residues have no visible effect on the HR intensity compared with their respective progenitors, which suggests that cumulative effects of multiple residues control interaction between AvrM and M. The results of this project clearly demonstrate that more than one residue controls interaction of AvrM effector proteins with the cognate R protein, which is completely inconsistent with a previous study where two individual single substitutions, E92K and D191G in the ATR1-ATR1-Maks9 effector protein, altered the effector into a conformation favourable for

complete recognition by the cognate resistance protein, RPP1-NdA (Krasileva et al., 2010). Another study showed that four single residue mutants in ATR1–Cala2 separately enabled the effector protein to be recognized by the resistance protein, RPP1–WsB (Chou et al., 2011). Specifically, a single mutation N158K in ATR1 gained very mild recognition, V122L and S125T induced intermediate recognition, and Y140D achieved strong recognition by the resistance protein, RPP1–WsB. Furthermore, a mutation study of the AvrL567 effector protein confirmed that three individual residue substitutions each altered the recognition specificity of the corresponding R protein (Wang et al., 2007). From these contrasting results (Krasileva et al., 2010; Wang et al., 2007), it seems that AvrM is a more elusive effector protein than AvrL567 and ATR1 with respect to avoiding R protein detection. Because single residue mutations in AvrM do not alter the recognition specificity by M, it suggests that combined mutations must be tested for altering the pertinent resistance detection. This prediction is consistent with a previous study where a quadruple mutation in the ATR1–Cala2 effector protein (V122L + S125T + Y140D + N158K) gained recognition by the cognate RPP1–WsB protein and the reciprocal quadruple substitution in ATR1–Emoy2 significantly delayed activation by RPP1–WsB (Chou et al., 2011). Of these residues, V122L, S125T and N158K are buried in the surface of the effector protein, but Y140D is partially exposed. In our mutational analyses, neither buried residues nor surface exposed residues in the AvrM protein could alone change the recognition specificity.

3.3.4.2 Alanine substitution of non-polymorphic charged residues

Since the negatively charged surface of the central cleft in AvrM-A is predicted to be required for resistance protein detection (Ve, 2011), two side-chains in AvrM-A, namely E237 and E309 were substituted with neutrally charged alanine residues (E237A and E309) to reduce the negative charge in the central pocket and thereby knockdown interaction with the M protein. Surprisingly, the results conflict with that prediction, as the alanine mutants induced strong HR in tobacco leaves expressing M protein. A similar conflict with a prediction has been described in ATR1 effector proteins, where single residue mutations that reduced the required negative charge (E92K and D191G) established recognition by the cognate R protein (Krasileva et al., 2010). In the same study, even a double mutant, ATR1–Emoy2^{K92E+G191D}, likely to increase the negative charge of the protein surface, completely abolished recognition by the RPP1-NdA protein. The mutation study in ART1-

Emoy2 demonstrated that increasing the negative charge of the protein surface tends to destabilize, and increasing the positive charge tends to strengthen the interaction with the resistance protein RPP1-NdA. Based on structural analysis of the residue positions in AvrM proteins, the alanine mutations are likely to alter the charge of the central pocket, but below the threshold level to knockdown recognition specificity by the M protein. This suggests that multiple charged side-chains control the central pockets of the AvrM effector proteins. Furthermore, a deletion study confirmed that the C-terminal region of the AvrM effector protein controls interaction with the M protein (Catanzariti et al., 2010a), supported by a mutational analysis in AvrL567, where all the residues found to concede resistance specificity are located in the C-terminal region (Wang et al., 2007). In contrast, in the case of ATR1 effector proteins, the critical residues controlling the resistance specificity are scattered over the whole region of the effector proteins (Krasileva et al., 2010; Chou et al., 2011).

Our mutational analysis demonstrates that an evolutionary link between host resistance and pathogen susceptibility leads AvrM and M genes towards diversifying selection, which indicates that flax rust evolved more than one amino acid polymorphism to escape detection by the M flax resistance protein. It has been suggested by evolutionary analyses that many effector genes and their cognate R genes are evolving under diversifying selection in nature (Win et al., 2007; Mondragon-Palomino, 2002).

3.4 Conclusion

The crystal structures of the AvrM-A and avrM proteins affirmed an unusual non-globular homo-dimer consisting of novel L-shaped helical folds. The detailed analyses of the structures hypothesised that the negative charge in the central cleft on the exterior surface of the AvrM-A effector dimer favours interaction with the M protein (Ve, 2011). This chapter attempted to investigate the critical residue/s contributing the charged cleft. The reciprocal mutation analysis of the polymorphic residues along with the *in planta* assays have shown that no single residue mutants can change the recognition specificity of the cognate M protein. Furthermore, alanine substitution of conserved charged residues in AvrM-A has revealed that the central acidic cleft (negatively charged) is controlled by more than one charged residue, as individual alanine substitutions could not knockdown the HR intensity induced by interaction of the recombinant AvrM-A with the M protein. This clearly demonstrates that a single alanine substitution, in either of the three charged side-chains (E237, E309 and R313), does not alter the total charge of the central surface of the AvrM-A effector dimer, and more than one charged residue controls the charge of the central cleft. It suggests that a combination of substitutions of the three charged residues may increase the change in negative charge to a threshold level that destabilizes interaction between AvrM and M proteins.

In conclusion, the polymorphic residues play a major role in structural configuration of the effector proteins. Due to the polymorphisms between AvrM-A and avrM proteins, the different configurations of the allelic effector proteins expose the non-polymorphic side chains in two different ways, resulting in an acidic pocket in AvrM-A while avrM has evolved a basic surface that allows the parasite to avoid detection by the cognate M protein.

In chapter 4, I will now attempt to disrupt and restore M recognition by AvrM-A and avrM, respectively, by generating pairwise double, triple and quadruple mutations of these polymorphic and non-polymorphic residues. I will also explore the bio-physical properties of these proteins in solution, and measure their interaction with M by the Y2H assay.

Chapter Four: Combined residue mutation

(Pages 78 - 121)

I have written this chapter and presented as a draft of a scientific manuscript with a target to submit to 'The Plant Journal'. I will be the sole first author of this work, however, given that this forms part of my PhD thesis for examination, it is yet to be sent to the authors listed on the following page for their suggestion and input. For the SEC-MALS and SEC-SAXS analyses, I generated the mutations in an expression vector (pMCSG7) and then induced and purified the proteins. Finally, Simon Williams, Lachlan Casey and Alan Zhang (University of Queensland, Brisbane) performed the two analyses (Figure 4.8) using my purified proteins. For the Yeast Two-Hybrid (Y2H) analysis, I generated the mutations in the binary vector (pEG201), and then Maud Bernoux (CSIRO Plant Industry, Canberra) cloned the mutant genes from the binary vector to bait (GAL4-BD) and prey (GAL4-AD) constructs and performed the Y2H analysis (Figure 4.9). All other data presented were performed by me, Motiur Rahman.

Dimerization of the fungal effector AvrM is required for recognition by the M resistance protein

Motiur Rahman^a, Simon J. Williams^b, Thomas Ve^b, Lachlan Casey^b, Alan Zhang^b, Maud Bernoux^c, Peter N. Dodds^c, Bostjan Kobe^{b,1} and Peter A. Anderson^{a,1}

Address: ^aSchool of Biological Sciences, Flinders University, Adelaide, SA 5001, Australia; ^bSchool of Chemistry and Molecular Biosciences, Australian Infectious Diseases Research Centre and Institute for Molecular Bioscience, University of Queensland, Brisbane, QLD 4072, Australia; ^cCommonwealth Scientific and Industrial Research Organization Plant Industry, Canberra, ACT 2601, Australia.

4.1 Summary

The *AvrM* effector locus of the flax rust fungus, *Melampsora lini*, encodes six variants designated AvrM A-E and *avrM*. Structural and bio-physical analysis of AvrM-A predicts that the protein exists as a stable homo-dimer, forming a unique negatively charged pocket at the dimer interface, not found in the similar region of *avrM*. Previous research has demonstrated that AvrM-A is recognised by, and interacts with, the M flax rust resistance protein, but that *avrM*'s lack of recognition and interaction is limited to a region containing 13 polymorphic residues between AvrM-A and *avrM*. More detailed analysis shows that no single polymorphic residue controls this recognition event. Here we show that when three polymorphic residues in *avrM* are changed to their AvrM-A counterparts, partial M recognition occurs, and an additional change enables full recognition. Furthermore, when three non-polymorphic charged residues that collectively form a negatively charged pocket at the interface of the AvrM-A dimer are substituted by alanine, the charged pocket is neutralized, preventing interaction and recognition by M. Collectively, these data suggest that the effector molecules must form homo-dimers to be recognised by M, and that the negatively charged pocket at the dimer interface of the AvrM-A protein facilitates interaction with, and activation of, the M protein. Thus, alteration of the quaternary structure of an effector protein represents a way in which a pathogen can avoid recognition by the plant innate immune system.

4.2 Significance

Flax rust is an ideal model system to investigate how effector proteins can manipulate the host resistance mechanism. As part of the cocktail of effector proteins secreted by flax rust, the AvrM effector proteins have become recognizable by the M flax rust resistance protein, and upon binding of AvrM-A, M activates Effector Triggered Immunity (ETI). We unravelled how the AvrM protein escapes M detection, which will guide scientists to understand how each effector molecule is detected by the cognate resistance protein.

4.3 Introduction

Plants provide almost all of the world food supply and are under constant attack by microbial invaders, which poses a tremendous threat to world food security. Of these invaders, rust fungi are obligate biotrophic pathogens that depend solely on haustoria for the acquisition of nutrients from living cells of the hosts (Hahn and Mendgen, 2001; Voegelé and Mendgen, 2003; Catanzariti et al., 2006; Weßling et al., 2012). Haustoria mediate the molecular interface between pathogen and host, and remarkably the translocation of effector molecules into the host cytoplasm by a mechanism that is still unclear (Rafiqi et al., 2012). Collectively, effector molecules subvert the infected host cell by redirecting nutrients and dampening the host innate immune response. Those effector molecules that are recognizable by the host, termed avirulence (Avr) proteins, elicit a powerful and rapid cell death response known as a hypersensitive response (HR). The HR is activated by resistance (R) protein and serves to limit colonisation and disease. Flax rust (*Melampsora lini*), the fungal agent that causes rust disease in flax (*Linum usitatissimum*) and other related species of the *Linum* genus, is ideally suited to study the molecular components of this sophisticated interaction. In flax, 31 different rust resistance genes (*R*) have been identified and mapped to five loci, namely *K*, *L*, *M*, *N* and *P* (Islam and Mayo, 1990). Of these 31 specificities, 20 *R* genes have been cloned from four loci (*K*, *L*, *M*, *N* and *P*), each encoding a protein of the TIR-NBARC-LRR class (Lawrence et al., 1995, 2010b; Anderson et al., 1997; Ellis et al., 1999; Dodds et al., 2001a, 2001b; Catanzariti et al., 2010b). In flax rust, four effector proteins have been identified (Dodds et al., 2004, 2006; Catanzariti et al., 2006; Dodds and Thrall, 2009), in two of which the three-dimensional structure has been determined (Wang et al., 2007; Ve et al., 2013). The degree of structural similarity of flax R proteins contrasts sharply with the diverse structures of the rust effectors. Here we focus on the AvrM effector proteins

from flax rust (Catanzariti et al., 2006), some of which are recognised by the M flax rust resistance protein (Anderson et al., 1997). In the flax rust strain CH5, the *AvrM* locus consists of six different variants constituting a small effector gene family of five avirulence alleles (*AvrM-A*, *AvrM-B*, *AvrM-C*, *AvrM-D* and *AvrM-E*) and a single virulence allele, *avrM* (Catanzariti et al., 2006; Catanzariti et al., 2010a). Expression of *AvrM-A* triggers the strongest M-mediated cell death response, followed by *AvrM-D*, while *AvrM-B* and *AvrM-C* give a significantly weaker HR (Catanzariti et al., 2006; Catanzariti et al., 2010a). Of the six variants, *AvrM-A* has been reported to interact with M, inducing a very strong HR, while the virulent *avrM* does not interact at all (Catanzariti et al., 2006, 2010). Previous analysis has narrowed the region responsible for M recognition to the C-terminus of *AvrM-A*, in particular residues 108-343, which is also sufficient to interact with the M protein in the yeast two-hybrid (Y2H) assay (Catanzariti et al., 2010a). In contrast, *avrM* varies from *AvrM-A* by a large internal deletion coding for 69 aa residues, although this deletion does not cover residues 108-343 of *AvrM-A*. Within the region spanning residues 108-343 of *AvrM-A*, 13 polymorphic residues exist between *AvrM-A* and *avrM* (Catanzariti et al., 2006; Catanzariti et al., 2010a; Ve, 2011). Three of these polymorphic residues, K253/E316, E263/K326 and E270/K333 in *avrM/AvrM-A* respectively, do not alter M recognition either as single or combined mutations (Catanzariti et al., 2010a). Subsequently, mutation studies showed that no single reciprocal mutation in the remaining polymorphic side-chains of the C-terminal region alter recognition by the M protein (This work was presented in chapter 3 of this thesis and published in part in Ve et al., 2013). This suggests that multiple contact points are required for the *AvrM/M* interaction, consistent with reports of two other effector/R protein pairs. In the flax/flax rust pair, L5, L6 and *AvrL567 A, D* (Wang et al., 2007), and the *Arabidopsis/Hyaloperonospora arabidopsidis* interaction involving RPP1 and ATR1 (Krasileva et al., 2010; Chou et al., 2011), although single mutations can alter interaction with, and recognition by, their respective R protein, consistent and reciprocal knock in and knock out mutations can only be achieved by the cumulative effects of multiple amino acids.

As the crystal structure of *AvrM-A* and *avrM* have been reported (Ve et al., 2011) we are in a position to predict those polymorphic residues that control M recognition. Gel filtration analysis predicted that both *AvrM-A* and *avrM* proteins form homo-dimers in solution, with a distinctive charged pocket located at the *AvrM-A* dimer interface, not seen in *avrM* (Ve et

al., 2011; Ve et al., 2013). Ve (2011) predicted that this charged surface in the AvrM-A interface controls the interaction with M. The side of the crystal structure exposing the central charge interface is referred to as the exterior surface, whereas the opposite side is denoted as the interior surface (Ve, 2011). On the basis of the crystal structure, we predict that this pocket is formed by the singular or cumulative effects of the polymorphic side-chains, R170/K232, S179/L241 and T247/I310 in avrM and AvrM-A, respectively. Here we targeted these polymorphisms to engineer pairwise double and triple mutants in the effector proteins to identify the residues involved in the M recognition specificity. Ve (2011) also demonstrated by structural analysis that three non-polymorphic charged residues of AvrM-A, E237, E309 and R313, form a distinctive negatively charged pocket at the central interface of the effector dimer that is not evident in the avrM structure. These charged residues in AvrM-A were also targeted in this mutational analysis, as they seem to be important in generating a structural motif in the central surface of AvrM-A that may be necessary for interaction with M.

In order to test M recognition in plants, we used *Agrobacterium*-mediated transformation expression (AMTE) to deliver the effector genes into a tobacco plant (*Nicotiana tabacum*) already expressing M resistance protein (W38::M). To confirm the expression of each AvrM effector protein in plant tissue, we engineered an N-terminal HA tag onto the effector protein and tested expression in *N. benthamiana* leaves by SDS-PAGE and immunoblot analysis. We have also tested the impact of key mutants of this analysis on the ability, or otherwise, to interact with the M protein in the Y2H assay. Furthermore, we have tested the biophysical properties of the proteins using size-exclusion chromatography (SEC) coupled with multi-angle light scattering (MALS), or small angle X-ray scattering (SAXS) to verify the dimeric state of the proteins in solution. On the basis of the results of this study, we predict that for M recognition, AvrM-A must form a dimer in a particular conformation that facilitates the formation of highly negatively charged pocket at the dimer interface of the flax rust effector protein. We acknowledge, however, that recognition of AvrM by the M protein, and their interaction, is via an *Agrobacterium* delivery system (i.e. an artificial gene delivery system) and furthermore, is done in a heterologous host (*Nicotiana sp.*). Hence, our results may vary from what occurs in nature, and we can only extrapolate to that of the flax/flax rust interaction.

4.4 Results

4.4.1 AvrM construct

With the aim of identifying the residues important for controlling M recognition and taking into consideration all of the data previously reported (Catanzariti et al., 2010a; Ve 2011; Ve et al., 2013), the *AvrM-A* and *avrM* genes were truncated and engineered to encode proteins from residues 108-343 and 46-280, respectively. These genes were placed into the pEarleygate201 vector (Earley et al., 2006) with a CaMV 35S promoter. This construct also engineered a sequence encoding a hemagglutinin (HA) epitope tag or a 6XHis onto the N-termini of the effector proteins. After *Agrobacterium*-mediated transformation, these tags facilitated detection of the gene construct in the leaves of *N. benthamiana* and assisted with purification by nickel affinity chromatography.

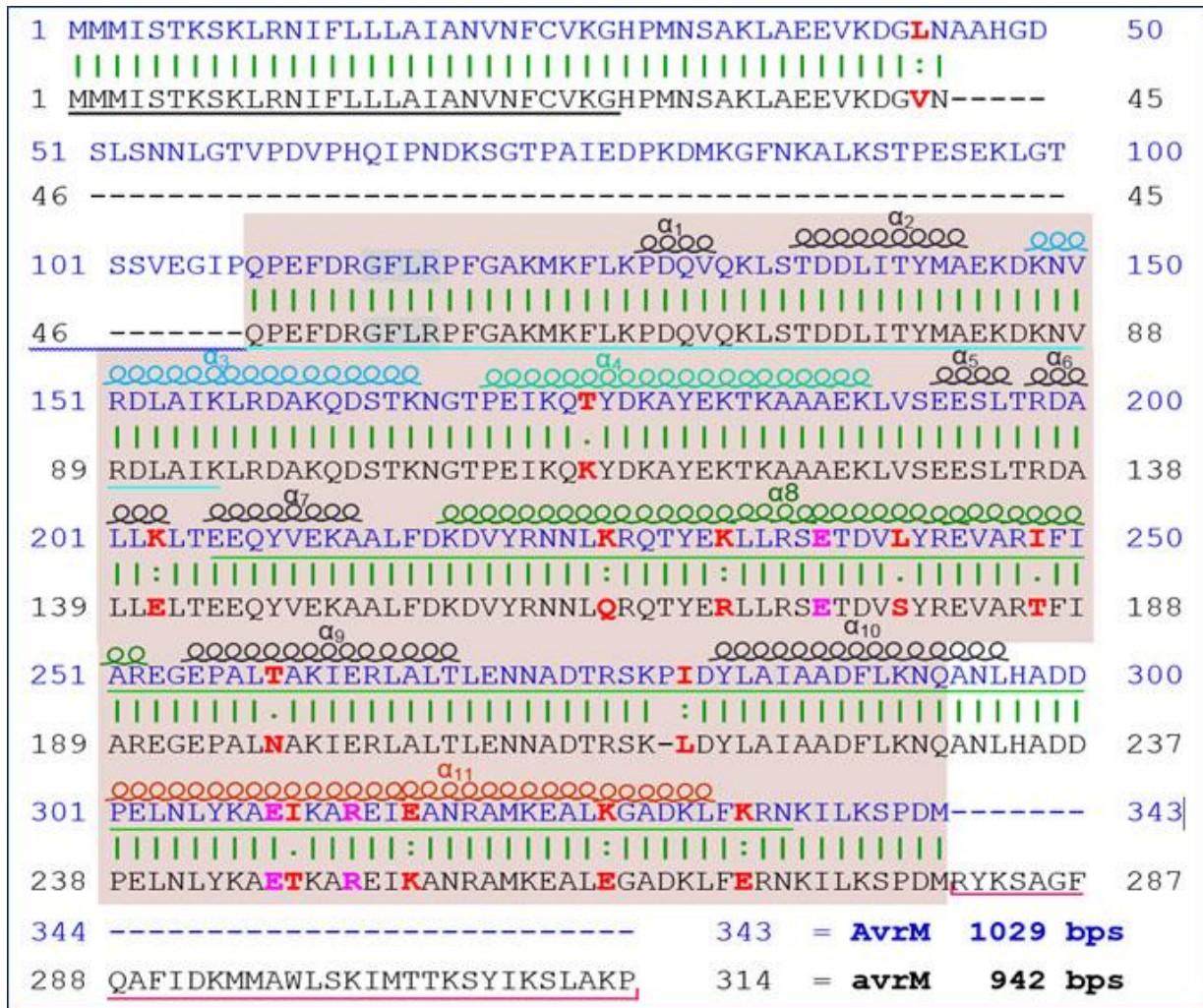
4.4.2 Structures comparison of the coiled-coil regions in AvrM-A and avrM

We previously reported crystal structures for *avrM* and *AvrM-A*, with atomic coordinates and structural factors (Ve 2011; Ve et al., 2013), which we deposited in the Protein Data Bank (PDB ID [4BJM](#) for *avrM* and [4BJN](#) for *AvrM-A*). Insights into the reported molecular structures are the basis of the mutational analysis in this article. The details of the residue locations in *AvrM-A* and *avrM* effector proteins are indicated in Figure 4.1a, b. The exact positions and exposures of the targeted residues of *AvrM-A* and *avrM* in the protein structures have been indicated in Figures 4.2a-b and 4.3a-b.

Superimposition of the *AvrM-A* and *avrM* structures (Ve, 2011) reveals that the α_8 and α_{11} helices at the interface of the *AvrM-A* dimer deviate significantly from those of *avrM*. The structural analysis suggests that these configuration differences are caused by the side-chain exposure of T247/I310 (in the α_{11} helix) together with S279/L241 (in the α_8 helix) that are predominantly buried and influence the positioning of a tyrosine side-chain Y243 in *avrM* and Y306 in *AvrM-A* (Figures 4.2a-b and 4.3a-b). The exposure of Y243/Y306 clearly demonstrates considerable variation in the conformation of the two core helices, α_8 and α_{11} (Video S4.1, 4.2). Combined reciprocal mutation of these two polymorphisms is likely to reposition this tyrosine (Y243/Y306) as well as alter the orientation of other non-polymorphic residues, which in turn may influence the surface properties of the dimer interface. This interpretation of the structures, coupled with the *in planta* assay, suggests that the *avrM* protein is likely to be less stable in solution. The two effector proteins have

been tested by SEC-MALS and -SAXS analyses, confirming that AvrM-A is a stable dimer in solution, but indicating that avrM is not. Nevertheless, for the purpose of elucidating and comparing mutational analyses, avrM will be considered as a dimer in the following sections.

Interestingly, the polymorphisms S179/L241 at α_8 and T247/I310 at α_{11} helices are predicted to induce an almost 180° rotation of the Y306 side-chain in AvrM-A compared to the corresponding side-chain Y243 in avrM. As a result, the Y306 side-chain in AvrM-A juts out from the plane of its coiled-coil (CC)-domain towards the α_8 and α_{11} helices of the counter monomer, which is likely to remodel the configuration of the CC-domains compared to avrM (Figure 4.3a-b and Video S4.1, indicated by magenta colour). In avrM, the same conserved side chain, Y243, is oriented inwards to the monomer and away from the dimer interface (Figure 4.2a-b and Video S4.2, indicated by magenta colour). In AvrM-A, the Y306 side-chain is slightly exposed on top of E244 side-chain (Figure 4.3a-b), while the counter residue Y243, is orientated completely away from the E182 side chain in avrM (Figure 4.2a-b). More exactly, the Y243 side-chain of avrM is entombed within the CC-domain and likely to stabilize the interaction between the α_8 and α_{11} helices of its monomer. As a consequence, the Y306 orientates the side-chain of E244 in AvrM-A, allowing the E244 to form hydrogen bond with K232 of its interacting monomer, and the negative charge of the K232 is neutralised by the hydrogen bonds (Ve, 2011). Furthermore, the K232 side-chains are exposed on the interior surface with an outward orientation from the central pocket (Figure 4.3b), while its polymorphic counterpart, R170, points inwardly to the central pocket (Figure 4.2b), which is likely to contribute a positive charge to the central surface of the avrM protein. Based on these structural differences between avrM and AvrM-A, we predict that R170/K232, S279/L241 and T247/I310 residues are critical in the positioning of the α_8 and α_{11} helices to enable dimerization of the AvrM effector.



a

AvrM-A	avrM	Location
T175	K113	α 4
K203	E141	α 6
K226	Q164	α 8
K232	R170	α 8
L241	S179	α 8
I248	T186	α 8
T259	N197	α 9
P179	Δ 217	Loop between α 9 and α 10
I280	L218	
I310	T247	α 11
E316	K253	α 11
K326	E263	α 11
K333	E270	α 11+2

b

Figure 4.1: Sequence comparison of avrM and AvrM-A. (a) Sequence alignment highlighting the sequence differences between avrM and AvrM-A. Redish background indicates the structured regions of the proteins that were used in this article. Secondary structure elements are highlighted above the sequences, adapted from the deposited structures (PDB code ID: 4BJM and 4BJN, respectively; Ve et al., 2013). Green underlined indicates the anti-parallel

(Figure 4.1 continued) CC-domains and cyan underlined indicates the sequences constituted the hairpin domains. Regions involved in host-trafficking from Q46/Q108 to K94/156K and minimal region for HR induction and interaction in Y2H assay from E144/E206 to 272N/N335. (b) Polymorphic residues with their positions and locations in the secondary structures of the effector proteins.

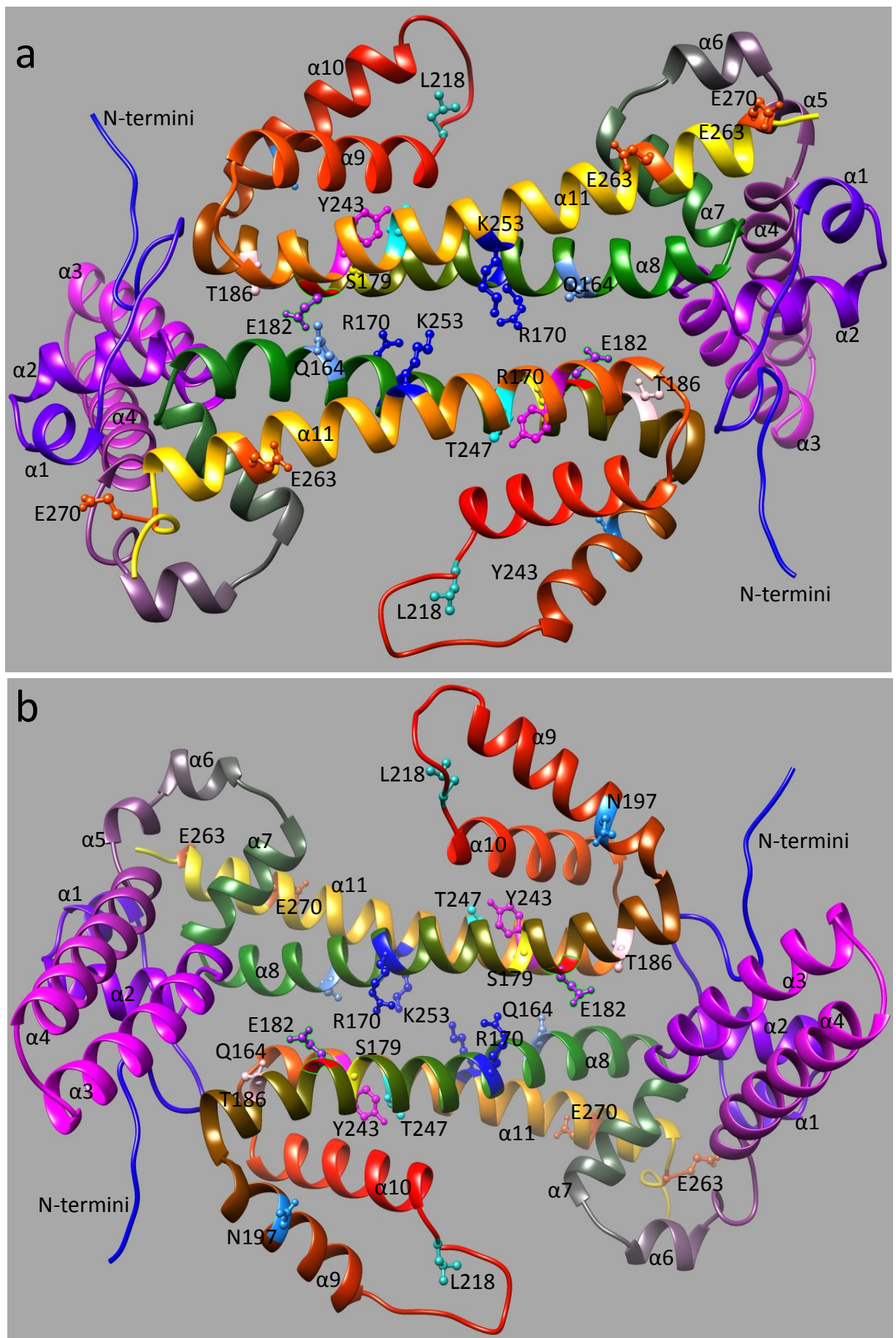


Figure 4.2: Ribbon structures of the avrM effector (dimer) protein highlighting some important residues involved in the virulence function. (a) Exterior view and (b) interior view of avrM showing the variation resulting from the exposure of Y243 (magenta) and E182

(purple) in comparison with the AvrM-A structure (Figure 4.3). Figure 'a' is rotated from left to right by $\sim 180^\circ$ to present the interior side in 'b'.

of the AvrM-A protein showing the variation resulting from the exposure of Y306 (magenta) and E244 (purple) in comparison with the avrM structure (Figure 4.2). Figure 'a' is rotated from left to right by $\sim 180^\circ$ to expose the interior side in 'b'.

4.4.3. Mutations in *avrM* that restore M recognition

To achieve M recognition in *avrM*, we generated pairwise reciprocal mutations, and a combined triple mutation, in the R170/K232, S179/L241 and T247/I310 polymorphic residues in *avrM* (as highlighted in Figure 4.2a-b).

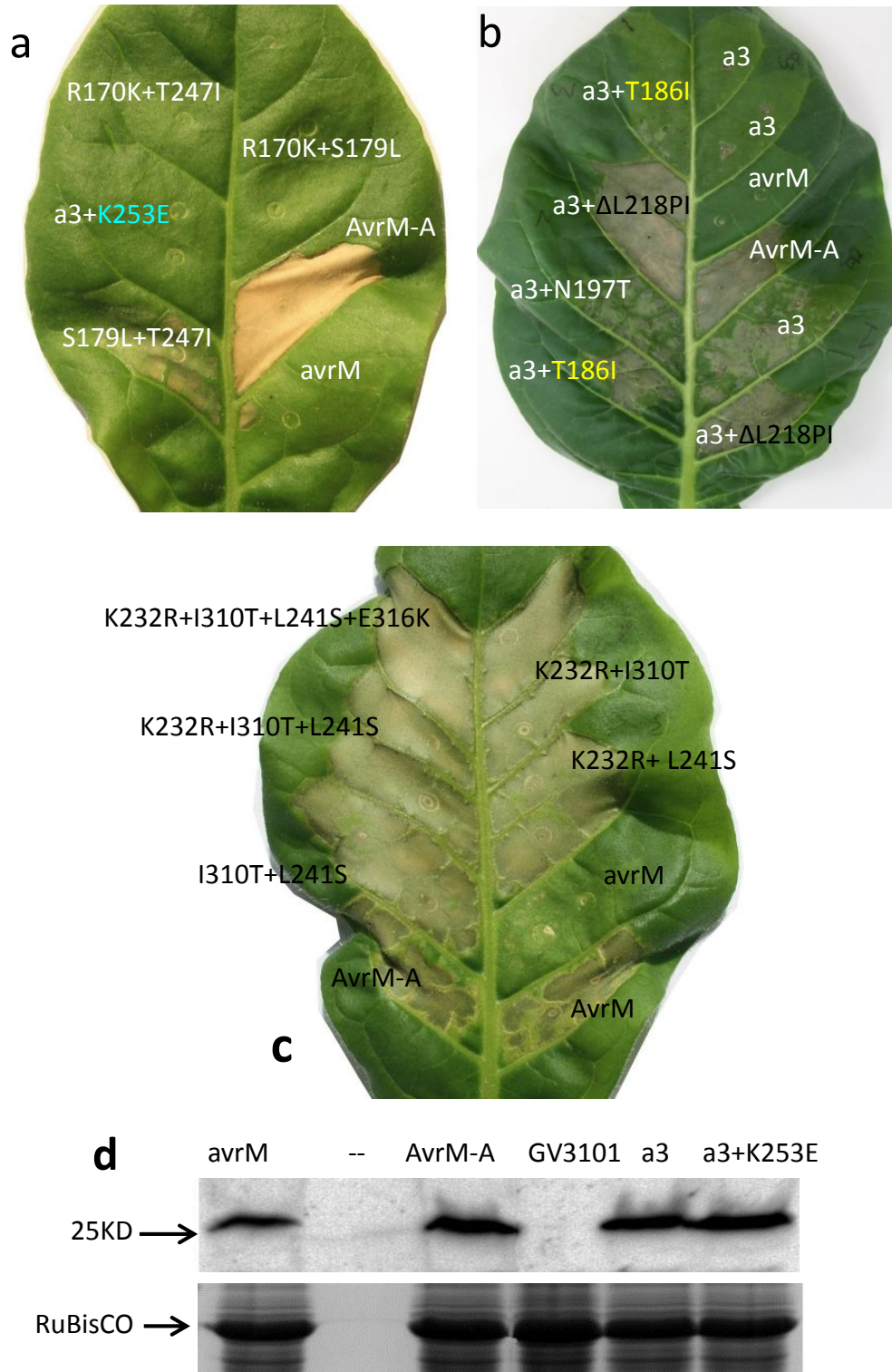


Figure 4.4: *In planta* assay of reciprocal combined mutation in *avrM* (a-b) and *AvrM-A*. (a-b) Polymorphic reciprocal mutations of *avrM*. (c) Combined mutations in *AvrM-A*, that could not alter the recognition specificity. (d) Anti-HA immunoblots showing protein

expression of *avrM* mutants in non-transgenic tobacco leaves (*N. benthamiana*) (upper panel). Coomassie blue staining of RuBisCO indicating equal loading of the extracted protein samples in the SDS-PAGE (lower panel). Here, a3 indicates *avrM*^{R170K+S179L+T247I}.

***avrM*^{R170K+S179L}**

The polymorphisms, R170/K232, S279/L241 and T247/I310 in *avrM*/AvrM-A are located in the α_8 helices of the anti-parallel coiled-coil regions of the hypothesised protein dimer interface. The R170/K232 is positively charged and interiorly exposed (Figure 4.2b, 4.3b), which has a direct influence on the charged interface of the effector dimer and may thus control the interaction with the M protein. The latter S179/L241 is a hydrophobic residue entombed in the protein surface. For a double mutant in *avrM*, R170 was mutated with the AvrM-A counterpart lysine (K), another charged residue, and S179, a polar uncharged residue, substituted with leucine (L), a neutral hydrophobic residue. In the generated *avrM*^{R170K+S179L} double mutant, R170K is likely to contribute positive charge to the dimer interface while S179L presumably reorients the α_8 helices in the dimer. As a result, the combined effect of R170K+S179L is likely to alter the interface surface charge by the R170K and to modify the overall structure by S179L. However, in the agroinfiltration assay, the *avrM*^{R170K+S179L} mutant did not induce a visible HR phenotype (Figure 4.4a, Table 4.1), indicating that the M protein is still unable to detect the *avrM*^{R170K+S179L} mutant protein. So the structural alteration caused by these mutations in the *avrM* effector protein is insufficient to stabilize the interaction with the M protein.

***avrM*^{R170K+T247I}**

In the α_{11} helices, the polymorphism T247 is polar and uncharged in *avrM*, while I310 in AvrM-A is a hydrophobic residue, and both are buried in the protein surface (Figure 4.2 and 4.3). To generate a double mutant, the R170K and T247I mutations were combined together generating *avrM*^{T247I+R170K} mutant and the resultant M recognition was evaluated in tobacco leaves (W38::M). The agroinfiltration assay did not induce HR (Figure 4.4a, Table 4.1), demonstrating that the combined effect of R170K and T247I in *avrM* was insufficient to achieve recognition by the M protein.

***avrM*^{S179L+T247I}**

Unlike the previous two double mutants, S179/L241 and T247/I310 are both uncharged (hydrophobic/polar) residues located in the α_8 and α_{11} helices respectively. In the

quaternary structure of AvrM-A, these residues are entombed inside the surface of the protein dimer (Figure 4.2 and 4.3). When these two side chains were substituted in *avrM* with their counterparts from AvrM-A, the double mutant effector protein resulted in a weak HR phenotype, as tested by the agroinfiltration assay (Figure 4.4b, Table 4.1). This result clearly indicates that the combined effect of the two side-chain mutants enables the *avrM* effector to be partially recognised by the M protein. The HR phenotype induced by *avrM*^{S179L+T247I} indicates that this mutant affects the configuration of the protein structure in a manner likely to favour effector dimerization and thus M recognition. From this result, it can be predicted that these residues require more supports from other polymorphic side-chain/s, and presumably, R170 is one of such critical residues.

***avrM*^{R170K+S179L+T247I}**

To further increase the HR intensity of *avrM*^{S179L+T247I}, a triple mutant was generated by adding the R170K substitution. When the mutant *avrM*^{R170K+S179L+T247I} was tested by agroinfiltration assay in tobacco leaves (W38::M), the HR phenotype induced was increased compared to the double mutant, *avrM*^{S179L+T247I} (Figure 4.4b, Table 4.1). By visual inspection of the infiltrated leaf sectors, this HR intensity is strong and estimated to be ~70% of that generated by AvrM-A. It should be noted, this bioassay was tested many times with the general observation being that it induced a strong response in most of the cases, as shown in Figure 4.4.

***avrM*^{R170K+S179L+T247I+K253E}**

As mentioned earlier, a mutation study reported by Catanzariti et al., (2010) confirmed that three polymorphisms in *avrM* and AvrM-A, namely K253/E316, E263/K326 and E270/K333, in single, double and triple mutations, could not alter M recognition. Of the three side-chains, K253/E316 is located in the central interface of the AvrM effector dimer and is likely to contribute to the charge of the pocket identified in the AvrM-A structure (Figure 4.3a-b). Specifically, E316 is likely to add negative charge to the central surface of the AvrM-A dimer, while K253 is likely to increase the existing positive charge of the central surface of the *avrM* predicted dimer (Figure 4.2a-b). Moreover, the polymorphism K253/E316 also distinguishes two effector variants, AvrM-A and AvrM-D, both of which are recognized by M, from the non-recognizable variants AvrM-B, AvrM-E and *avrM* (Catanzariti et al., 2006). Furthermore,

the structural analysis of AvrM-A and avrM shows that the polymorphism K253/E316 is exposed in the central charged surfaces along with R170/K232, S279/L241 and T247/I310 and R250/R313. So it is predicted that the side-chain K253/E316 should have an additive effect on the triple mutant avrM^{R170K+S179L+T247I}. Therefore, a reciprocal mutation K253E was stacked on the triple mutant backbone generating the avrM^{R170K+S179L+T247I+K253E} mutant with a view to reinforce the HR intensity. This quadruple mutant was tested by agro-infiltration in tobacco leaves (W38::M). Surprisingly, this mutant, instead of reinforcing the HR, completely knocked out the HR gained by the avrM^{R170K+S179L+T247I} triple mutant (Figure 4.4a, Table 4.1). Immunoblot analysis shows that the triple and the quadruple mutant proteins were expressed at a similar level in non-transgenic tobacco leaves (Figures 4.4d). This result, although difficult to interpret from our structural knowledge, indicates that the K253/E316 residue has an important functional role on controlling M protein recognition.

Similarly to the avrM mutants described above, reciprocal polymorphic double, triple and quadruple mutants in AvrM-A were engineered and tested by agroinfiltration assay, but none affected the recognition by the M protein (Figure 4.4c and Table 4.1), indicating that other polymorphic residues between avrM and AvrM-A are still sufficient in AvrM-A to promote M recognition.

Additive effects of I186T, N197T and Δ L218PI in avrM^{R170K+S179L+T247I} recognition specificity

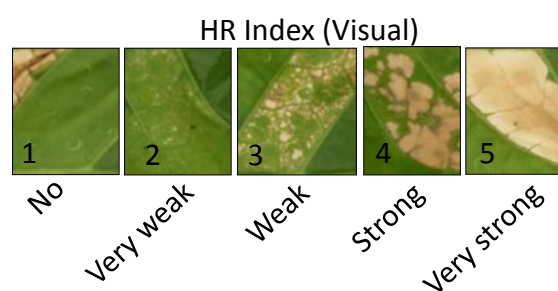
With the intention to achieve full recognition, three polymorphic residues T186, N197 and Δ L218 were targeted to augment further the ability of avrM^{R170K+S179L+T247I} towards full M detection. Accordingly, three separate reciprocal substitutions were made in the avrM^{R170K+S179L+T247I} backbone generating avrM^{R170K+S179L+T247I+T186I}, avrM^{R170K+S179L+T247I+N197T} and avrM^{R170K+S179L+T247I+ Δ L218PI}. In comparison with AvrM-A, the first two mutants produced significantly weaker HR phenotypes than that of avrM^{R170K+S179L+T247I}, while avrM^{R170K+S179L+T247I+ Δ L218PI} induced a very strong HR phenotype, equivalent to that induced by AvrM-A (Figure 4.4b, Table 4.1). This indicates that Δ L218PI supports the avrM^{R170K+S179L+T247I} to complete "knock-in" recognition by the M protein, suggesting that

these four polymorphic contact points of AvrM-A are important in controlling recognition by the M protein.

Table 4.1: Combined reciprocal mutations in *avrM* and AvrM-A, and their recognition specificities by M resistance protein. Red colour represents mutated residues while magenta indicates the non-polymorphic charged residues of the effector proteins. Here, a3 indicates *avrM*^{R170K+S179L+T247I}.

Variants	Mutation	164	170	175	179	186	197	218	246	247	250	251	253	HR induction*
avrM	Wt :	Q	R	E	S	T	N	ΔL	E	T	R	E	K	No
	S179L+T247I:	K	R	E	L	T	N	ΔL	E	I	R	E	K	Weak
	R170K+T247I:	K	K	E	S	T	N	ΔL	E	I	R	E	K	No
	R170K+S179L:	K	K	E	L	T	N	ΔL	E	T	R	E	K	No
a3: R170K+S179L+T247I		K	K	E	L	T	N	ΔL	E	I	R	E	K	Strong
	a3+K253E	K	K	E	L	T	N	ΔL	E	I	R	E	E	No
	a3+T186I	K	K	E	L	I	N	ΔL	E	I	R	E	K	Weak
	a3+N197T	K	K	E	L	T	T	ΔL	E	I	R	E	K	Weak
	a3+ΔL218PI	K	K	E	L	T	N	PI	E	I	R	E	K	Very strong
AvrM-A^P	WT :	Q	R	E	S	T	N	PI	E	T	R	E	K	Very strong
	L241I+I310T :	K	K	E	S	I	T	PI	E	T	R	E	E	Very strong
	K232R +I310T:	K	R	E	S	I	T	PI	E	I	R	E	E	Very strong
	K232R+L241I:	K	R	E	L	I	T	PI	E	T	R	E	E	Very strong
	K232R +L241I+I310T :	K	R	E	S	I	T	PI	E	T	R	E	E	Very strong
	K232R+L241I+I310T+E316K :	K	R	E	S	I	T	PI	E	T	R	E	K	Very strong
AvrM-A	Wt :	K	K	E	L	I	T	PI	E	I	R	E	E	Very strong
Variants	Mutation	226	232	237	241	248	259	280	309	310	313	314	316	HR induction*

^PPositions are shown in the bottom lane. *HR index (adapted from Bernoux et al., 2016)



4.4.4. Mutations that neutralize the non-polymorphic charged residues of AvrM-A abolish recognition

Though the mutations in *avrM* that gained recognition when tested as reciprocal mutations in AvrM-A did not alter its recognition specificity, we targeted three non-polymorphic charged residues, namely E175/E237, E246/E309 and R250/R313, which are located and exposed in the central charged pocket of the AvrM-A dimer (Figure 4.6a-d). These side-chains are likely to generate a negatively charged pocket in the AvrM-A dimer interface. Substitution of alanine for each of these three individual residues did not change the recognition specificity by the M protein (Figure 4.5a-b). However, we tried pairwise combinations of these mutations. The glutamates, E237 and E309, are two negatively charged residues located respectively in the α_8 and α_{11} helices, two core helices of the central interface of the AvrM-A dimer. As negatively charged residues, these two glutamic side-chains are most likely to contribute negative charge to the central dimer interface of the effector protein that is hypothesized to stabilize interaction with the M protein (Ve, 2011). These two residues (E237 and E309) are also reported to neutralize the positive charge of the R313 side-chain by H-bonding (Ve, 2011), which maintains the central pocket in an overall negatively charged condition (Figure 4.6a, c). When E237 and E309 were substituted with alanine (A), AvrM-A^{E237A+E309A} showed a dramatic decrease in the intensity of the HR phenotype, as tested by *in planta* assay in tobacco leaves (W38::M; Figure 4.5a-b, Table 4.2), to less than 10% by visual inspection, indicating that AvrM-A^{E237A+E309A} destabilizes the interaction with the M protein. Structural analysis showed that this alanine double substitution converts the central negatively charged pocket into a positively charged surface (Figure S4.2), which is consistent with the hypothesis (Ve, 2011) that the central negative charged surface favours recognition by the M protein.

Unlike E237 and E309, the arginine R313 is positively charged that is located in the α_{11} helices of the AvrM-A dimer, and is exposed at the central negatively charged surface of AvrM-A. The combined alanine substitutions, AvrM-A^{E237A+R313A} and AvrM-A^{E309A+R313A}, were also generated and tested by agroinfiltration, but there was no change in the HR intensity compared to AvrM-A (Figure 4.5a, Table 4.2). Furthermore, when the three alanine substitutions generated a triple mutant, AvrM-A^{E237A+E309A+R313A}, there was no change to the knockdown HR of AvrM-A^{E237A+E309A} (Figure 4.5a-b, Table 4.2). By immunoblot analysis, we

detected that AvrM-A^{E237A+E309A} and AvrM-A^{E237A+E309A+R313A} proteins were expressed at a similar level in *N. benthamiana* leaves (Figure 4.5e). However, the structural analysis shows that the additive effect of R313A slightly reduced the positive charge of the central pocket in comparison to the dimer interface of AvrM-A^{E237A+E309A} (Figure S4.1).

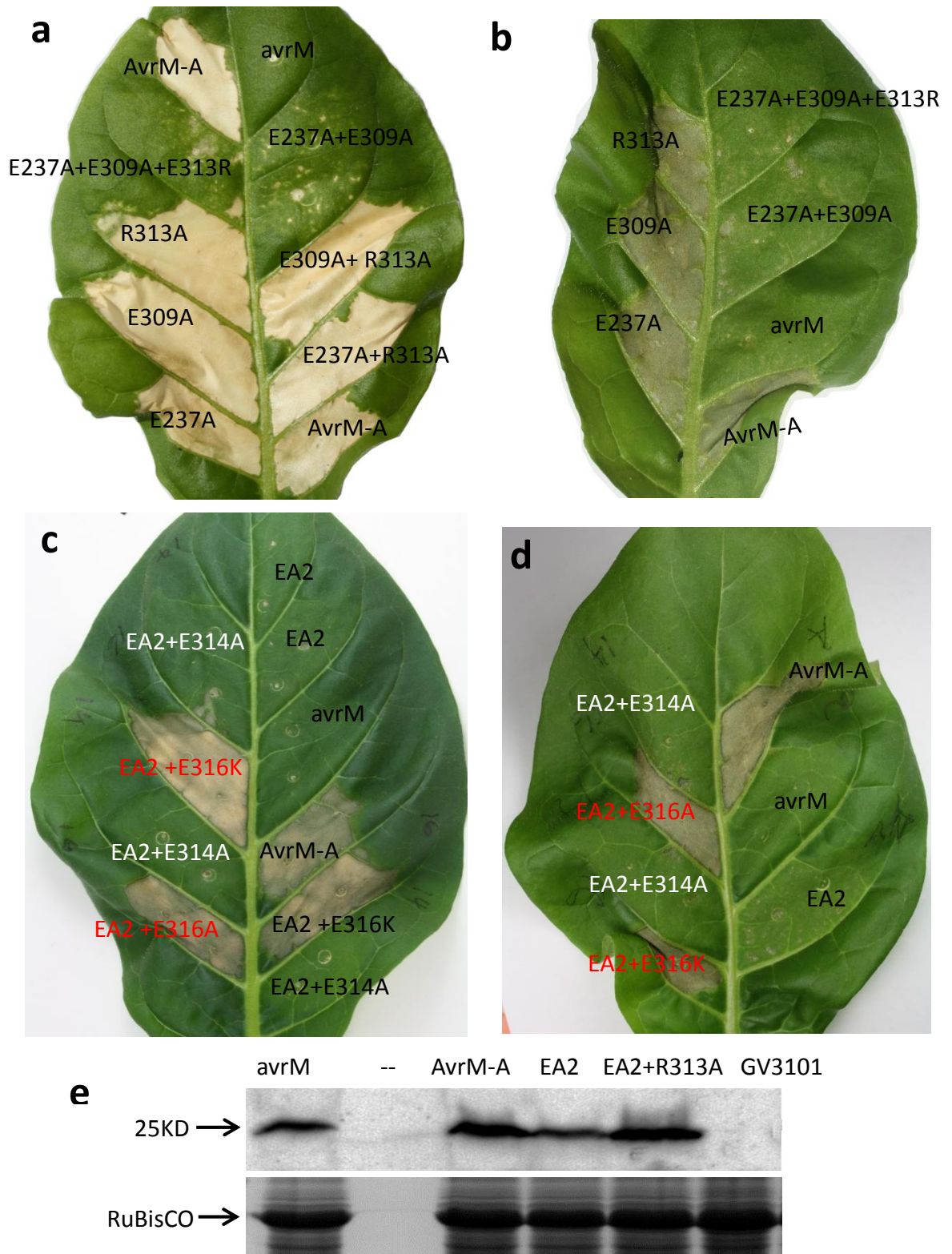


Figure 4.5: *In planta* assay for alanine substitution in AvrM-A. (a-d) *In planta* assay for non-polymorphic (charged) residue mutants. (e) Anti-HA immunoblot detection of the

expressed effector proteins in non-transgenic tobacco leaves (*N. benthamiana*) (upper panel). Coomassie blue staining of RuBisCO indicates equal loading of the extracted protein samples in the SDS-PAGE (lower panel). Here, EA2 is coded for AvrM-A^{E237A+E309A}.

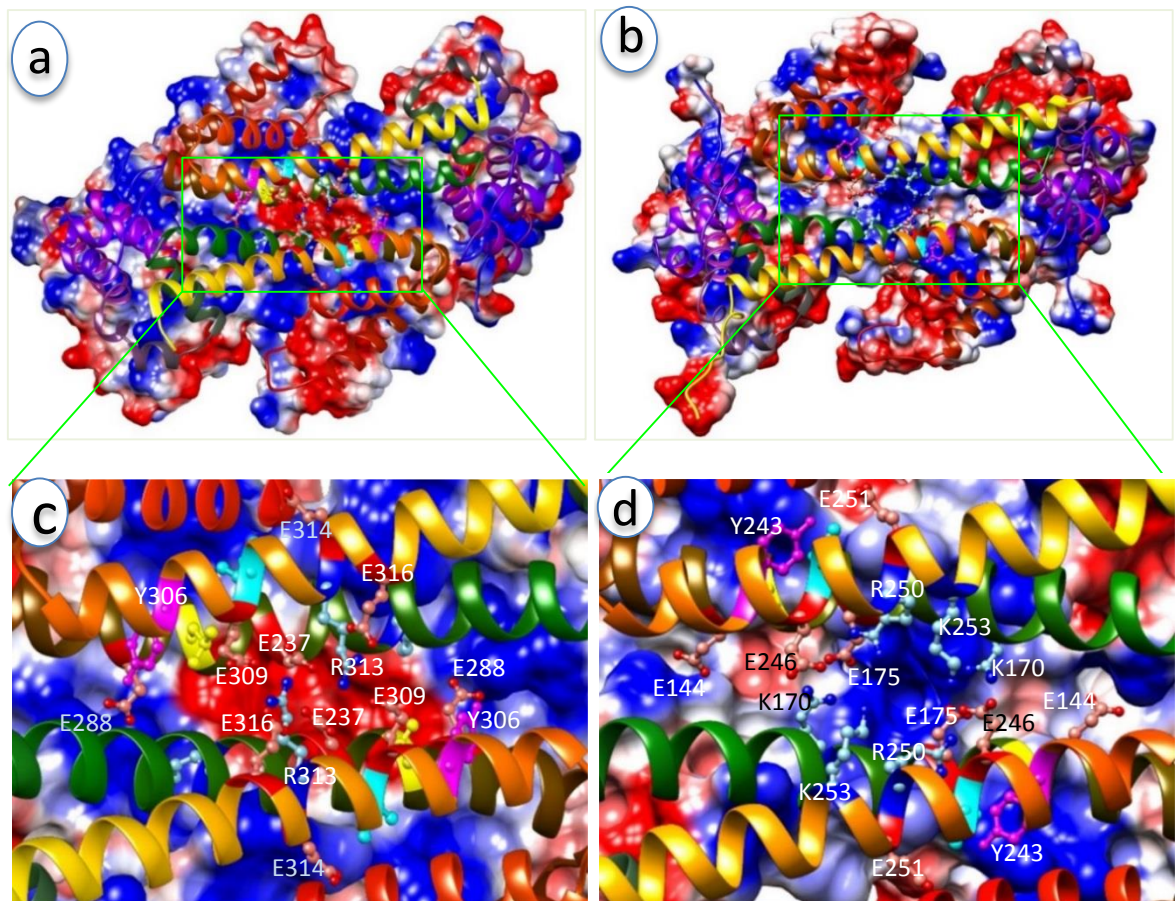


Figure 4.6: Surface representation of AvrM-A (a, c) and avrM (b, d; a predicted dimer) protein dimers, showing the charged differences. Some residues are shown here predicted to involve in dimerization and thereby contribute the charged patched.

AvrM-A^{E237A+E309A+E316A}

A glutamic acid side-chain E316 is also located in the negatively charged pocket of the AvrM-A dimer. Predicting that E316 could have an additive effect on knock down of M recognition in AvrM-A^{E237A+E309A}, an alanine mutant E316A was added to generate a triple mutant AvrM-A^{E237A+E309A+E316A} that was tested by agro-infiltration assay. Surprisingly, although AvrM-A^{E237A+E309A} induced a very weak HR in the agro-infiltration assay, the triple mutant resulted in a very strong HR in the same transgenic tobacco leaves (W38::M) (Figure 4.5c-d, Table 4.2). To further confirm the additive effect of the third residue (E316), it was also substituted

with a lysine (K, the counterpart in AvrM-A), generating AvrM-A^{E237A+E309A+E316K}, but the *in planta* assay resulted in a similarly strong HR to that induced by AvrM-A^{E237A+E309A+E316A} (Figure 4.5c-d, Table 4.2). The surface of the predicted protein structure, AvrM-A^{E237A+E309A+E316A/K} showed no visible alteration to the dimer interface, in comparison to that of AvrM-A^{E237A+E309A}, due to the addition of E316A or E316K (Figure S4.2). Although difficult to interpret from our structural knowledge, this result indicates that the K253/E316 residue has an important functional role in controlling M protein recognition. In both AvrM-A and avrM, combined mutants that were either gaining or reducing M recognition, the combined influence of the mutation in the K253/E316 residue showed unexpected and counterintuitive results. Based on our current structural information, we cannot explain these results, but speculate that this residue has a critical biochemical and/or catalytic role in the effector protein.

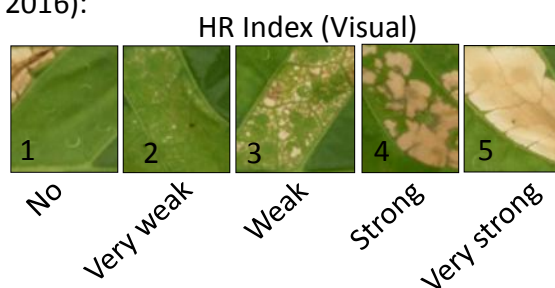
AvrM-A^{E237A+E309A+E314A}

In the AvrM-A protein, there is a glutamic acid side-chain E314 adjacent to R313, which is exposed at the surface 25.56Å from the centre of the charged pocket of the effector dimer. Aiming for complete knockout of AvrM-A^{E237A+E309A} recognition by the M protein, an alanine substitution of E314 was added to the backbone of AvrM-A^{E237A+E309A} to generate triple mutant AvrM-A^{E237A+E309A+E314A} and the effect on M recognition verified by agroinfiltration. The *in planta* assay showed a complete knockdown of HR induction (Figure 4.5c-d, Table 4.2), similar to that of avrM, revealing that the glutamic side-chain at 314 of AvrM-A has a strong additive effect on AvrM-A^{E237A+E309A} in converting the behaviour of the AvrM protein to that of the avrM effector with respect to M detection. In the predicted protein structure, the AvrM-A^{E237A+E309A+E314A} mutant showed no visible alteration in the central charged surface in comparison to that of the AvrM-A^{E237A+E309A} mutant protein (Figure S4.2).

Table 4.2: Combined alanine substitutions in AvrM-A and their effects on recognition specificity by the M resistance protein. Red colour represents mutated residues while magenta indicates the non-polymorphic charged residues in the AvrM-A effector protein.

Variants	Mutation	226	232	237	241	248	259	280	309	310	313	314	316	HR induction*
AvrM-A	Wt :	K	K	E	L	I	T	PI	E	I	R	E	E	Very strong
	E237A+R313A :	K	K	A	L	I	T	PI	E	I	A	E	E	Very strong
	R313+E309A :	K	K	E	L	I	T	PI	A	I	A	E	E	Very strong
	E237A+E309A(EA2) :	K	K	A	L	I	T	PI	A	I	R	E	E	Very weak
	E237A+E309A+R313A:	K	K	A	L	I	T	PI	A	I	A	E	E	Very weak
	E237A+E309A+E316A :	K	K	A	L	I	T	PI	A	I	R	E	A	Very strong
	E237A+E309A+E316K :	K	K	A	L	I	T	PI	A	I	R	E	K	Very strong
	E237A+E309A+E314A :	K	K	A	L	I	T	PI	A	I	R	A	E	No
	avrM WT :	Q	R	E	S	T	N	-L	E	T	R	E	K	No
	Positions in avrM	164	170	175	179	186	197	218	246	247	250	251	253	HR induction

*HR index (adapted from Bernoux et al., 2016):



4.4.5. Solution properties of AvrM-A, avrM and mutants therein

Previously, Ve et al. (2011) reported that AvrM-A and avrM were both dimers in solution as determined by their identical elution profile of gel filtration (GF) i.e., SEC. Following expression and purification, the truncated AvrM-A (108-343) proteins were analyzed by SEC on a combined with in-line MALS with a refractive index (RI) detector (Figure 4.7a). SEC-MALS and SEC-SAXS analyses confirm that AvrM-A is a dimer in solution. To further examine the molecular mass of AvrM-A protein in solution, SEC-SAXS analysis was performed that confirmed that AvrM-A behaves in solution as a dimer (Figure 4.7b, c). However, the SEC-MALS and SEC-SAXS analyses revealed striking differences in the bio-physical properties of avrM and AvrM-A, showing that avrM is not consistent with a dimer in solution, suggesting the protein behaves more like a monomer in solution (Figure 4.7a-d). For AvrM-A protein, the molecular weight obtained by SEC-MALS was 55 kDa, corresponding to the molecular weight (54.4 kDa) for a dimer of the protein, which is consistent with previous analyses of the AvrM-A protein (Catanzariti et al., 2010a; Ve et al., 2011). Using the same SEC-MALS and SEC-SAXS technique, the avrM protein was eluted (by SEC) at a volume level corresponding to ~55kDa, but the molecular weight determined by MALS depending on the readings from the laser light and the RI detectors, was ~35kDa, which is close to the calculated molecular weight (27.18 kDa) for a monomer of AvrM protein. These results reveal that in solution, AvrM-A is a stable dimer, but avrM is a monomer (by MALS) or a very loosely bound dimer *in vitro* (by SEC). Previously it was also predicted that avrM might dimerize weakly in plant and yeast (Catanzariti et al., 2010a).

Similarly, the combined mutants, avrM^{R170K+S179L+T247I}, avrM^{R170K+S179L+T247I+K253E} and avrM^{R170K+S179L+T247I+ΔL218PI} were analysed by SEC-MALS and SEC-SAXS (Figure 4.8a-c). As determined by the RI detector (arbitrary units) during SEC (Superdex 200 10/300 GL), the molecular weights were ~54.4kDa for avrM^{R170K+S179L+T247I} and avrM^{R170K+S179L+T247I+K253E} (Figure 4.8a, c), and ~50.0kDa for the avrM^{R170K+S179L+T247I+ΔL218PI} (Figure 4.8a-c). In these cases, the obtained molecular weights of the recombinant effector proteins, those that gained recognition by the M resistance protein, indicate that they are stable homodimers in solution. These results clearly demonstrate that the progenitor avrM is not a stable dimer, but the combined residue mutants, avrM^{R170K+S179L+T247I}, or with either of an additive effect of K253E or ΔL218PI enabled the each recombinant effector protein to form a stable

homodimer and coincidentally alter recognition specificity by M. The SEC-SAXS curves of avrM and AvrM-A represent two different scattering intensities, indicating their two different molecular masses (Figure 4.8c). These data coupled with SEC-MALS results (Figure 4.7a-b) further confirm that AvrM-A is a stable dimer and avrM is a monomer in solution. The scattering intensities of AvrM-A^{E237A+E309A} (a loss-of-recognition mutant) and AvrM-A^{E237A+E309A+E316A}, suggest they are still stable dimers in solution (Figure 4.8c), and their corresponding molecular weights were very close to 55kDa (Table 4.3). These data clearly demonstrate that the combined alanine substitutions to the non-polymorphic side-chains turned the AvrM-A protein for knockout M resistance recognition without perturbing the stability and dimerization of the protein.

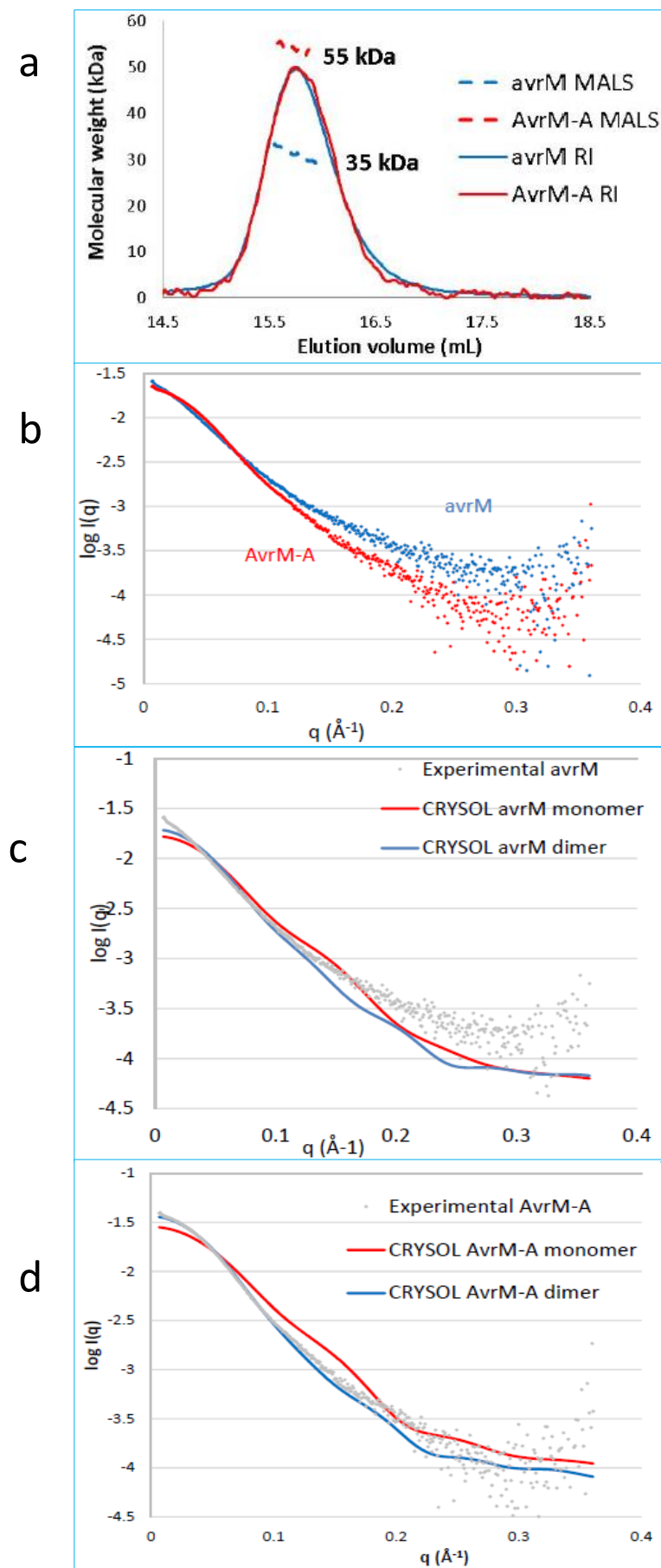


Figure 4.7: Determination of molecular masses of avrM (blue) and AvrM-A (red). (a) MALS calculated molar masses (kDa) for avrM and AvrM-A. The solid lines represent the normalised refractive index (RI) for the proteins eluted from an in-line Superdex 200 10/300 column.

Figure 4.7 (continued): Dotted lines under the peaks correspond to the average molecular weight (MW; y-axis) distributions across the peaks as determined by MALS. (primary axis, dotted line) and the normalised RI (secondary axis, solid line) over size-exclusion elution volume (ml) of avrM (blue) and AvrM-A (red). (b) SAXS curves of avrM (blue) and AvrM-A (red). This is represented as the scattering intensity, $\log I(q)$, as a function of the magnitude of the scattering vector, q (\AA^{-1}). SAXS curves of avrM (c) and AvrM-A (d) overlapped with the CRY SOL calculated theoretical scattering curves derived from their monomer and dimer crystal structures.

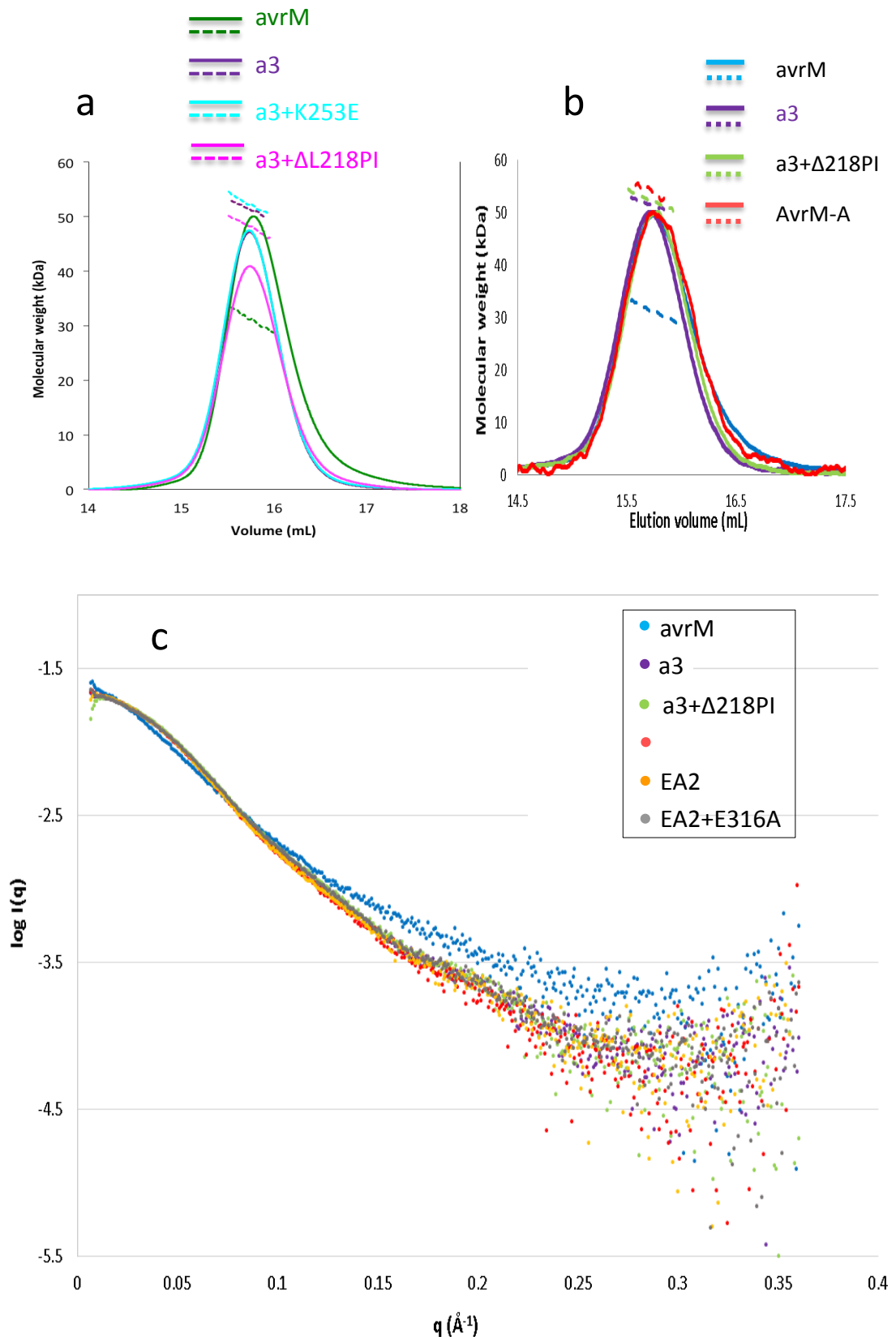


Figure 4.8: Determination of effector molecular mass by SEC-MALS and SEC-SAXS analyses. (a-b) SEC-MALS calculated molar masses (kDa) for avrM, AvrM-A (red), a3 (purple), a3+K253E (cyan) and a3+ΔL218PI. Each item is colour coded with figures. The solid lines represent the normalised refractive index (RI) for proteins eluted from an in-line Superdex from an in-line Superdex 200 10/300 column.

Figure 4.8: (continued) Broken lines under the peak correspond to the averaged molecular weight (MW; y-axis) distributions across the peaks as determined by MALS. Broken lines (equivalent coloring) under the peak correspond to the averaged molecular weight (y-axis) distributions across the peak as determined by MALS. In their x-axis, solid lines indicate the trace from the refractive index (RI) detector (arbitrary units) during SEC (Superdex 200 10/300 GL) for each sample as indicated by different colors. (c) SEC-SAXS curves of avrM and AvrM-A, and their mutants, a3, a3+ Δ L218PI, EA2 and EA2+E316A (each item is indicated by different colours). This is represented as the scattering intensity, $\log I(q)$, as a function of the magnitude of the scattering vector, q (\AA^{-1}). Here, a3 represents avrM^{R170K+S179L+T247I} and EA2 indicates AvrM-A^{E237A+E309A}.

4.4.6 Yeast Two-hybrid Assay

Previous data demonstrated that AvrM-A effector and M resistance proteins interact in a Y2H assay whereas avrM does not (Catanzariti et al., 2010a). Here, a Y2H assay was employed to investigate the interaction of the recombinant AvrM proteins with the M protein (Figure 4.9). This system was used for only those recombinant AvrM proteins that resulted in alteration of recognition specificity with the M resistance protein in tobacco leaves (W38::M). For this assay, bait (GAL4-BD) and prey (GAL4-AD) constructs were prepared expressing each of the avrM^{R170K+S179L+T247I}, avrM^{R170K+S179L+T247I+ Δ L218PI}, AvrM-A^{E237A+E309A}, AvrM-A^{E237A+E309A+E316A}, AvrM-A^{E237A+E309A+E314A} and M proteins fused C-terminal to either of the GAL4 DNA-binding domain (GAL4-BD) or the transcriptional activation domain (GAL4-AD). Our Y2H assay showed an interaction between AvrM-A and M, but no interaction between avrM and M (Figure 4.9a). To verify the interaction, the Y2H assay was carried out in two different orientations, (i) GAL4-BD-AvrM and GAL4-AD-M and (ii) GAL4-AD-AvrM and GAL4-BD-M, to assess the interaction between the AvrM mutant effectors and the M resistance proteins. The results are presented in Figure 4.9a. Yeast transformation was done twice and the same results were obtained. As shown by immunoblot detection (Figure 4.9b), all the proteins were expressed in the yeast system, although avrM and AvrM-A^{E237A+E309A+E316A} seemed to be less stable. AvrM-A^{E237A+E309A+E316A} induced a strong HR in the plant (Figure 4.5c-d), but there was no interaction in the Y2H system, possibly due to lower stability in the yeast system.

Similarly, the *avrM* combined mutants, *avrM*^{R170K+S179L+T247I} and *avrM*^{R170K+S179L+T247I+ΔL218PI} induced a strong HR by AMTE *in planta* but did not show any interaction in the Y2H assay (Figure 4.9a) which is inconsistent with maintaining a correlation between R/Avr protein-protein interaction and the HR in the plant. Though the mutant results in *avrM* are inconsistent between plant and Y2H, a report by Maqbool et al., (2015) showed that the binding affinities between effectors and the cognate R proteins can occasionally be different *in vitro* and *in planta*. However, all of the effector proteins in the Y2H system were detected by immunoblot analysis, except that *avrM* and *AvrM-A*^{E237A+E309A+E316A} showed a lower level of expression (Figure 4.9b) that may contribute to the lack of interaction. This is supported by a previous result that suggested that a higher level expression of effector proteins might increase the level of recognition and interaction by the cognate R proteins (Kanzaki et al., 2012).

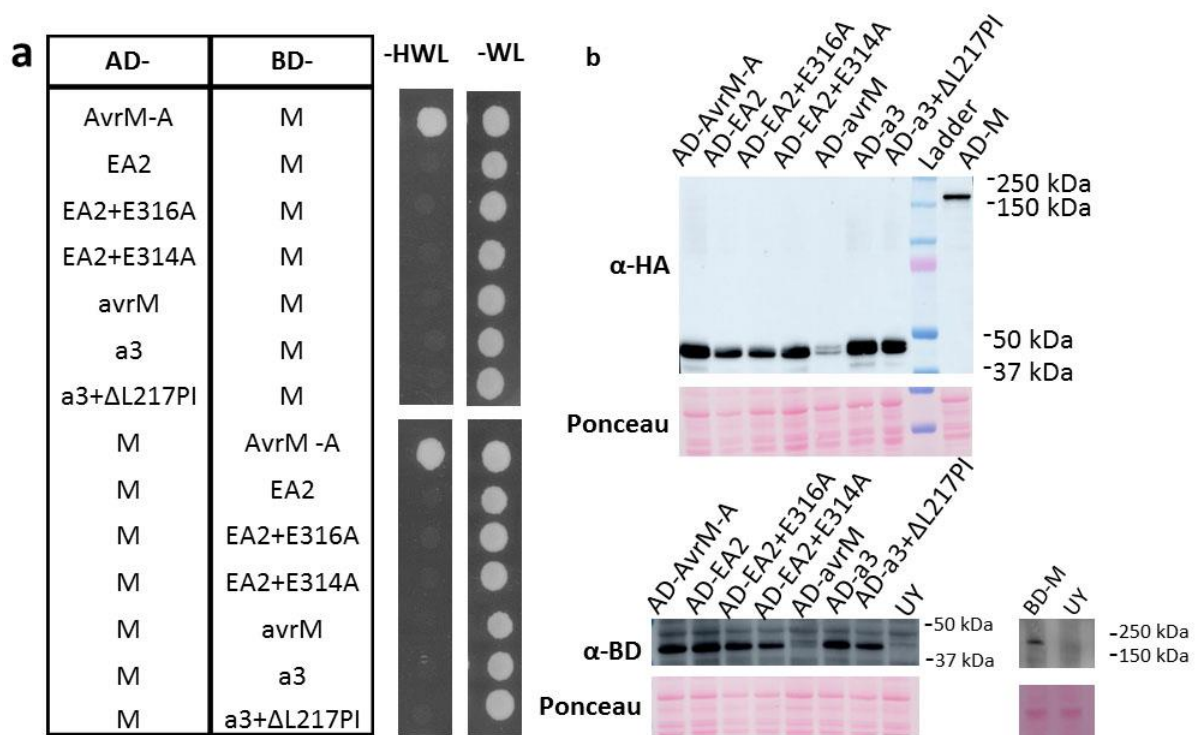


Figure 4.9: Physical interaction of *avrM* and *AvrM-A* mutants with the M protein. (a) Growth of yeast cells co-expressing GAL4-AD fusions of *AvrM-A/avrM* mutants with GAL4-BD fusions of M on non-selective media lacking tryptophan and leucine (-WL) or selective media additionally lacking histidine (-HWL). (b) Immunoblot detection of the recombinant GAL4-AD and GAL4-BD fusion effector proteins. Proteins were detected using anti-HA

(GAL4-AD AvrM-A and *avrM* mutant fusions) and anti-BD (GAL4-BD-M fusion) antibodies. Negative control is indicated by a YU that corresponds to untransformed yeast (UY). Protein loading is indicated by red Ponceau staining. Here, EA2 indicates AvrM-A^{E237A+E309A} and a3 stands for *avrM*^{R170K+S179L+T247I}.

4.5 Discussion

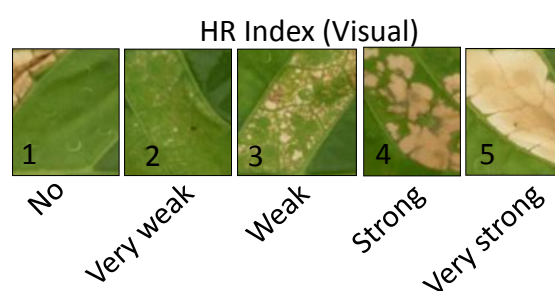
Despite recent advancement in the screening and cloning of many effector genes from diverse pathogens, the molecular basis of recognition specificity, HR activation and virulence functions for almost all of the effector proteins remains a mystery. Under strong positive selection, the evolution of pathogenic effectors has been shown to be more rapid than that of resistance (R) proteins in the host plants. This result in an increasing level of divergence in effector virulence that creates difficulties in predicting recognition specificities and pathogenicity of the newly evolved effector proteins. This circumstance emphasizes careful attention in research of the effector proteins to enable R proteins in defending the host plants from the rapidly evolved pathogens. The crystal structures of the AvrM effector proteins are different from those of other effectors, including AvrB (Lee et al., 2004), ToxA (Sarma et al., 2005), AvrL567 (Wang et al., 2007), AvrPto (Dong et al., 2009), ATR1 (Chou et al., 2011), ATR13 (Leonelli et al., 2011), AvrPiz-t (Zhang et al., 2013), AvrLm4-7 (Blondeau et al., 2015). The unique characteristic feature of AvrM effector proteins is that they form a homo-dimer with a large charged surface in the dimer interface. The monomers of the AvrM protein homo-dimerize folding into a C-terminal anti-parallel coiled-coil region with each monomer composed of eleven α -helices, including an N-terminal hairpin domain with two helices. The hairpin domain is oriented perpendicular to the rest of the protein with the anti-parallel coiled-coil region turning it into a non-globular L-shaped molecule. This distinctive conformation may facilitate the AvrM effector protein to achieve versatile recognition specificity for the cognate R protein. The AvrM proteins seem likely to possess complex recognition sites as multiple contact points are required to alter the recognition specificity, while a single residue controls the specificity in other effector proteins (Wang et al., 2007; Chau et al., 2011). It can also be predicted that the AvrM effector proteins may target different proteins and other immune components inside the host cells to promote pathogenicity. Although the R protein appears to require the effector to be dimerized to trigger resistance responses

(Krasileva et al., 2010; Bernoux et al., 2011a; Maekawa et al., 2011) as well as several other fungal and oomycete effectors work as monomers (Wang et al., 2007; Chou et al., 2011), the flax rust effector protein (AvrM) functions as a dimer *in vivo* and *in vitro*. This indicates that AvrM serves as a dimerization platform for M resistance recognition.

Table 4.3: AvrM mutants summarising the *in planta* HR assays, averaged MW calculated directly from the SEC-MALS and calculated using volume-of-correlation (Vc) method (Rambo and Tainer, 2013) from SEC-SAXS data.

Effector Protein	HR induction	Y2H interaction	SEC-MALS	SEC-SAXS
avrM	No	No*	30.8	35.3
avrM ^{R170K+S179L}	Weak	n/t	n/t	n/t
avrM ^{R170K+S179L+T247I}	Strong	No	51.4	50.7
avrM ^{R170K+S179L+T247I+K253E}	No	No	52.5	n/t
avrM ^{R170K+S179L+T247I+ΔL218PI}	Very strong	No	52.3	51.2
AvrM-A	Very strong	Very strong	55.3	55.8
AvrM-A ^{E237A+E309A}	Very weak	No	n/t	55.9
AvrM-A ^{E237A+E309A+R313A}	Very weak	No	n/t	n/t
AvrM-A ^{E237A+E309A+E316A}	Very strong	No*	n/t	52.5
AvrM-A ^{E237A+E309A+E316K}	Very strong	n/t	n/t	n/t
AvrM-A ^{E237A+E309A+E314A}	No	No	n/t	n/t

Note: n/t indicates not tested. * indicates lower expression in yeast system. HR index (adapted from Bernoux et al., 2016):



4.5.1 AvrM polymorphic residues provide physical support for recognition specificity

The 13 residues polymorphic in *avrM* and *AvrM-A* effector sequences make the proteins slightly different in structure, resulting in major differences in recognition by the M protein. With the aid of *avrM* and *AvrM-A* molecular structure predictions, our mutational analysis

reveals that the polymorphisms R170/K232 and S179/L241 in the $\alpha 8$ helix and T247/I310 in the $\alpha 11$ helix are cumulatively responsible for supporting a particular configuration of each effector protein. These polymorphic side-chains provide additive support to other residues as was evident when the K253E or Δ L218PI mutant was added to $\text{avrM}^{\text{R170K+S179L+T247I}}$. The stepwise polymorphic double, triple and quadruple mutations in both avrM and AvrM-A effector proteins revealed that four residues, R170, S179, T247 and PI218, provide mechanical support to the avrM protein in maintaining a structure capable of virulence specificity, while the four counter residues in AvrM-A enable additive support with other residue/s to generate a structure suitable for avirulence specificity and recognition by M. Mapping the polymorphic residues that alter the recognition specificity onto the structures of avrM and AvrM-A proteins suggests that the anti-parallel CC-domains control direct interaction with the M protein. This is consistent with a deletion study that found that the CC-domain alone is required to interact directly with the M protein (Catanzariti et al., 2010a). Superimposition of avrM and AvrM-A structures revealed significant differences in the two core $\alpha 8$ and $\alpha 11$ helices and in the electrostatic surface potential on the exterior sides of the dimer interfaces. On the basis of structural analysis, the polymorphisms R170/K232, S179/L241, T247/I310 and Δ L218/PI280 are predicted to be involved in these structural differences. Mutational analysis combined with *in planta* assay confirmed the role of these residues in interacting with the M protein. Our mutation study revealed that combined triple mutant requires an additive effect, and accordingly, the quadruple avrM mutant ($\text{avrM}^{\text{R170K+S179L+T247I+\Delta L218PI}}$) enhanced the partial recognition specificity obtained in the triple mutant to that of the AvrM-A protein.

The SEC-MALS and SEC-SAXS analyses show that avrM , which is not recognised by the M protein, is a monomer in solution and that the avrM mutants that gain M recognition are dimers. This result suggests that the AvrM effector protein must form a dimer to be detected by the M protein. The triple mutant $\text{avrM}^{\text{R170K+S179L+T247I}}$ gained a balanced conformation achieving a favorable charged surface that enabled the avrM effector protein to be recognized by the M protein, while subsequent addition of K253E imbalanced the protein conformation and returned it to a state similar to avrM . In contrast, the addition of Δ L218PI to the $\text{avrM}^{\text{R170K+S179L+T247I}}$ mutant fully restored avirulence function in $\text{avrM}^{\text{R170K+S179L+T247I+\Delta L218PI}}$. Consequently, residues mutated to give

the triple mutant (a3) had an additive effect, and a quadruple *avrM* mutant (*avrM*^{R170K+S179L+T247I+ΔL218PI}) resulted in a very strong HR with timing and intensity similar to *AvrM-A* (Table 4.1). This analysis indicates that the polymorphic side-chains render mechanical support to the *AvrM* effector structure to expose the charged residues in a particular fashion that presents the charged surface in the dimer interface of the effector protein to the M protein for recognition and activation.

4.5.2 *AvrM* charged residues contribute chemical support for recognition specificity

Although the quadruple *avrM* mutant behaved similarly to *AvrM-A*, the reciprocal quadruple mutant of *AvrM-A* did not alter the recognition specificity (Figure S4.1), indicating that other polymorphisms still provide suitable structural support for the protein configuration required for avirulence specificity. As shown by the *AvrM-A* crystal structure, the conserved charged residues, E237, E309, R313 and E316, comprise the negatively charged pocket in the interface of *AvrM-A* dimer, predicted to support the recognition specificity of M (Ve, 2011). Thus, these charged residues were substituted with alanine residues to neutralize the negatively charged surface in the *AvrM-A* effector dimer. The *in planta* assay showed that the combined alanine substitution *AvrM-A*^{E237A+E309A} effectively reduced M recognition, inducing a weak HR, which was unchanged by addition of R313A to give *AvrM-A*^{E237A+E309A+R313A} (Table 4.2). The combination of E316A/K with *AvrM-A*^{E237A+E309A} generated the triple mutant *AvrM-A*^{E237A+E309A+E316A/K} that surprisingly fully regained recognition, while the triple mutant *AvrM-A*^{E237A+E309A+E314A}, completely abrogated recognition (Table 4.2). This suggests that more than one charged residue influences the central charged pocket of the *AvrM* effector protein. With respect to the predicted role of the central negatively charged patch in recognition specificity (Ve, 2011), the alanine substitutions are unlikely to provide structural support, but probably change the negatively charged patch to a positive surface, thereby preventing recognition by the M protein. Indeed, the resultant effect of alanine substitutions in the charged residues showed variable yet cumulative recognition levels by the M protein, indicating that the charged residues have chemical supports for the central charged pocket.

The combined alanine substitution in the *AvrM-A*^{E237A+E309A} protein neutralized the negatively charged surface (Figure S1) that was controlling the interaction of *AvrM-A* protein with the M protein in yeast and the activation of the M protein *in planta*.

Surprisingly and unexplainably, the addition of E316A/K generating AvrM-A^{E237A+E309A+E316A/K} protein re-established the recognition, whereas addition of E314A to form AvrM-A^{E237A+E309A+E314A} completely abolished the M detection (Figure 4.5c-d). This result indicates that while the negatively charged surface is required for M interaction and activation, the E316 residue has a more functional role in controlling activation of the M protein. Alternatively the addition of E316A or E316K to AvrM-A^{E237A+E309A} may have restored the negatively charged surface in the dimer interface of AvrM-A^{E237A+E309A+E316A/K} and/or enable the closely position E314 to act in the place of the altered E316, and thus restore M recognition. The latter of these possibilities is supported by the fact that when E314, that further contributes to the negative charge surface, is changed to alanine, the AvrM-A^{E237A+E309A+E314A} protein is fully unrecognizable to the M protein. This result reveals that the non-polymorphic charged residues in the AvrM effector proteins contribute chemical supports to the central charged surface of the AvrM effector dimers. The alanine mutants that gained recognition changed the surface property of the AvrM protein, which abrogated detection by the M protein, suggesting that changes in the tertiary structure of AvrM-A protein altered its recognition specificity. The SEC-MALS and SEC-SAXS data coupled with the *in planta* assay suggest that AvrM proteins needs to form a dimer for M detection. Of the AvrM effector molecules, the charged residues provide chemical supports in inducing the negatively charged pocket in the dimer interface that is critical for M recognition.

4.5.3 Surface properties also influence recognition

Structural analysis revealed that the surface properties of AvrM-A and avrM are different (Figure 4.6). The most notable feature is that the AvrM-A effector dimer possesses a highly negatively charged surface pocket (acidic) in the centre of its dimer interface, while avrM has a highly positively charged patch (basic) in its predicted dimer interface (Figure 4.6a-d). It was predicted that these central charged patches control the recognition specificities of these two effector proteins (Ve, 2011). Manipulation of the negatively charged surface patch in AvrM-A protein prevents recognition specificity by the M protein (Figure 4.5a-d) without affecting the physical properties of the AvrM-A mutant proteins, as analyzed by SEC-SAXS (Figure 4.8c). Therefore this result predicts

that while a stable dimer is required for the M recognition, the surface properties of the effector protein also impact on recognition specificity.

Our mutational analysis of the *avrM* protein showed various alterations in recognition specificity (Figure 4.4a-b), but SEC-MALS and SEC-SAXS confirmed that the mutant effector proteins, either gain-of-recognition mutants (a3, a3+ Δ L218PI) or loss-of-recognition mutant (a3+K253E), are always stable dimers in solution (Figures 4.8a-c). This result indicates that the AvrM effector proteins need to be dimerized to be detected by the M resistance protein. On the other hand, alteration of the central charged pocket by alanine substitutions in AvrM-A protein changed the recognition specificity by the M (Figure 4.5), while SEC-SAXS analysis confirmed that the AvrM-A mutant proteins, either loss-of-recognition (EA2) or restorer-of recognition (EA2+E316A), are still dimers in solution (Figure 4.8c). Moreover, all the mutant proteins of *avrM* and AvrM-A effectors are well expressed *in planta* and in yeast as determined by immunoblot detection (Figures 4.4d, 4.5e and 4.9b). Therefore it is suggested that for *avrM* to be recognised by the M protein, requires to gain quaternary structure, which also needs to have an appropriate conformation for a negatively charged surface in the dimer interface.

4.6 Conclusion

This work demonstrates that the AvrM effector proteins can escape detection by altering their quaternary structures. This is inconsistent with those described previously for AvrL567 and ATR1 effector proteins (Wang et al., 2007; Krasileva et al., 2010, Chou et al., 2011) which reported that multiple contact points of a monomeric effector proteins control recognition with their cognate R protein. The fact that *avrM* still appears to have an association with itself (albeit rather weakened) reveals the idea that it is likely to be able of escaping recognition possibly without compromising function, as the dimerization is most likely to be important in the protein function. Collectively this study also highlights the fact that not only the crystal structures but also the physical properties of the protein in solution can elucidate the complete story of AvrM effectors.

4.7 Experimental procedures

4.7.1 AvrM constructs preparation

On the basis of a deletion study (Catanzariti et al., 2010a), and the crystal structures of AvrM-A and avrM (Ve et al., 2013), the flax rust effector genes, *AvrM-A* and *avrM* (provided by Peter N. Dodds, CSIRO, Canberra) were truncated that can be designated respectively as AvrM-A Δ 107 and avrM Δ 45/CT Δ 34 and cloned in pEG201 vector (Earley et al., 2006) by Gateway cloning system. The constructs were checked by sequencing and stored as a DNA stock for subsequent site-directed mutagenesis (SDM). DNA constructs encoding AvrM-A Δ 107 and avrM Δ 45/CT Δ 34 proteins driven by the *Cauliflower mosaic virus* (CaMV) 35S promoter were engineered in the binary vector, pEG201 with a view to studying the AvrM/M interaction, gene knock-out/knock-in by mutating specific amino acid side-chains and expression *in planta* by Agrobacterium-mediated transient expression (AMTE).

4.7.2 Site-directed mutagenesis and transformation of the recombinant genes

Site-directed mutagenesis PCR was performed to engineer the combined mutations in AvrM-A and avrM genes contained within the pEG201 vector following some previous methods (Catanzariti et al., 2006; Catanzariti et al., 2010a, Williams et al., 2011). Mismatch primers were designed (Appendix 3b) to introduce the desired mutation/s in the effector genes. The mutant genes were prepared and electroporated in bacteria [*E. coli* (DH10B, BL21), *Agrobacterium tumefaciens* (strain GV3101)] following a protocol of Sambrook et al., (1989).

4.7.3 Transient *in planta* expression assays

The Agrobacterium-mediated transient expression (AMTE) bioassay was used to study the interaction of the recombinant effector proteins and the M resistance protein following some previous methods previously used (Catanzariti et al., 2010a, Williams et al., 2011; Krasileva et al., 2010; Chou et al., 2011).

4.7.4 Protein extraction and purification

The expression and extraction of AvrM-A/avrM proteins and mutants thereof in tobacco plant (*Nicotiana benthamiana*) were performed following some previous methods (Catanzariti et al., 2006, 2010; Ve et al., 2013).

4.7.5 Sodium Dodecyl Sulphate Polyacrylamide Gel Electrophoresis (SDS-PAGE)

Polyacrylamide gels (15%) were prepared (Appendix 3) for separating extracted proteins by SDS-PAGE following the procedure previously stated by Laemmli, 1970. For *E. coli* produced protein samples, each protein sample was mixed with 3xSDS-PAGE sample buffer (Appendix 1b) in a ratio of 2:1 and boiled/denatured at 98°C for 5 minutes before loading. Following loading the samples, the gels were electrophoresed in 1X running buffer by running at 170V for 60min or until the dye had run off the gel in a Mini-Protean® Tetra Cell gel electrophoresis unit (Bio-Rad, NSW, Australia). For each gel, a Pre-stained Protein Marker, Broad Range (7-175 kDa) (NEB) was used for enabling the molecular weights of the desired protein. Then the gels were used for either coomassie staining, or western analysis by transferring the proteins onto a nitrocellulose membrane.

4.7.6 Immunoblot analysis

A western immune-blotting technique was adapted from the method described by Towbin et al. (1979). For this analysis, collected protein samples were separated by 15% SDS-PAGE. Following some previous methods (Williams, 2009; Sornaraj, 2013; deCourcy-Ireland, 2014), immunoblot analysis and coomassie staining were carried out to detect the expression of effector protein in tobacco leaf tissue.

4.7.7 AvrM-A/avrM construction for expression

For production and purification of the recombinant effector proteins, the *AvrM-A/avrM* genes were cloned into the pMCSG7 vector (Stols et al., 2002) inframe with a sequence encoding an N-terminal 6×Histidine tag. In these recombinant genes, the target mutations were generated (methods as stated before) for protein production in *E. coli* (BL21). Methods used for effector protein extraction and purification are outlined by Ve et al. (2011).

4.7.8 Size-exclusion chromatography (SEC)-coupled multi-angle light scattering (MALS)

SEC-MALS was performed using an inline Superdex 200 100/300 GL SEC column (GE Healthcare) combined with a Dawn Heleos II 18-angle light-scattering detector coupled with an Optilab TrEX refractive index detector (Wyatt Technology, Santa Barbara, CA, USA). Purified effector proteins (1-0.5mg) were separated at 0.5 ml/min in 10 mM HEPES pH 7.5, 150 mM NaCl at room temperature. Molecular mass calculation was performed using Astra6.1 software (Wyatt Technology). To estimate the molecular mass, the input of the

refractive increment (dn/dc values) was fixed at 0.186 ml/g, with an assumption that dn/dc is invariable for unmodified proteins (Wen et al., 1996). The peak of the eluted protein was used to determine the molecular mass.

4.7.9 Size-exclusion chromatography (SEC)-coupled small-angle X-ray scattering (SAXS)

SEC-SAXS was performed at the SAXS/WAXS beamline of the Australian Synchrotron using a Pilatus 1M detector. For each protein, 50 μ L of sample was injected into an inline 3ml Superdex S200 Increase column (GE Healthcare) at 16°C and flow rate of 0.1 ml/min, in 10 mM HEPES (pH 7.5), 150 mM NaCl buffer with 1.0 mM DTT. Data were collected through a 1mm quartz capillary mounted post-column, in 1 s exposures. The sample-to-detector distance was 2.6 m, and a wavelength of 1.033 Å at 12 keV yielded a range of momentum transfer $0.007 < q < 0.361 \text{ \AA}^{-1}$, where $q = 4\pi \cdot \sin(\theta)/\lambda$. Data reduction and subtraction were performed using SAXS Software, scatterBrain, available in the following link:

<http://www.synchrotron.org.au/index.php/aussyncbeamlines/saxswaxs/software-saxswaxs>.

Unless noted otherwise, subsequent analysis was performed using the tools in version 2.6 of the ATSAS program suite. 100 frames immediately preceding each peak were summed and normalised for exposure time to obtain buffer blanks. These buffers were subtracted from each image individual to generate a series of subtracted frames across the elution peak, from which I and R_g were calculated for each frame using the Guinier approximation as implemented in batch-mode AUTORG. Molecular weights were calculated using the volume of correlation (V_c) method in the range $0 < q < 0.3$.

Frames corresponding to the peak centres were summed and averaged to produce high signal-to-noise datasets for shape analysis. Invariant parameters were calculated in PRIMUS. Distance distributions, P(r), were obtained by indirect transformation in GNOM, informed by AUTOGNOM. Theoretical scattering was derived from atomic models using FoXS. Normalised Kratky plots were calculated manually, incorporating R_g values obtained using PRIMUS.

4.7.10 Yeast Two-Hybrid assay

M (21-1305) was cloned into pGBT9 and pGADT7 vectors (Clontech) as previously described (Catanzariti et al., 2010a). AvrM (109-344), avrM (46-281) and corresponding mutants were cloned into pGBT9 and pGADT7 vectors (Clontech) as *EcoRI*-*BglIII* fragments.

All constructs were verified by sequencing. Yeast (HF7c strain) transformation and growth assays were performed as described in the Yeast Protocols Handbook (Clontech). Yeast protein extraction for immunoblot analysis was performed following a post-alkaline extraction method as described in Kushnirov, 2000. Protein fusion detection was performed using anti HA-hrp (Roche, clone 3F10), and anti GAL4 DNA BD (SIGMA, G3042) antibodies.

For confirming the interaction of the mutated effector proteins with the cognate M resistant protein, Yeast two-hybrid (Y2H) assay was conducted following some previous protocols (Dodds et al., 2006, Catanzariti et al., 2010a). For this assay, M (21-1305) was cloned into pGBT9 and pGADT7 vectors (Clontech) as previously described (Catanzariti et al., 2010a). AvrM-A (107-344), avrM (46-281) and corresponding mutants were cloned into pGBT9 and pGADT7 vectors (Clontech) as *EcoRI-BglII* fragments. All constructs were verified by sequencing. Yeast (HF7c strain) transformation and growth assays were performed as described in the Yeast Protocols Handbook (Clontech). Yeast protein extraction for immunoblot analysis was performed following a post-alkaline extraction method as described by Kushnirov, 2000. Protein fusion detection was performed using anti HA-hrp (Roche, clone 3F10), and anti GAL4 DNA BD (SIGMA, G3042) antibodies.

4.8 References

Please see the Bibliography (page 151-175)

4.9 Supplementary Materials

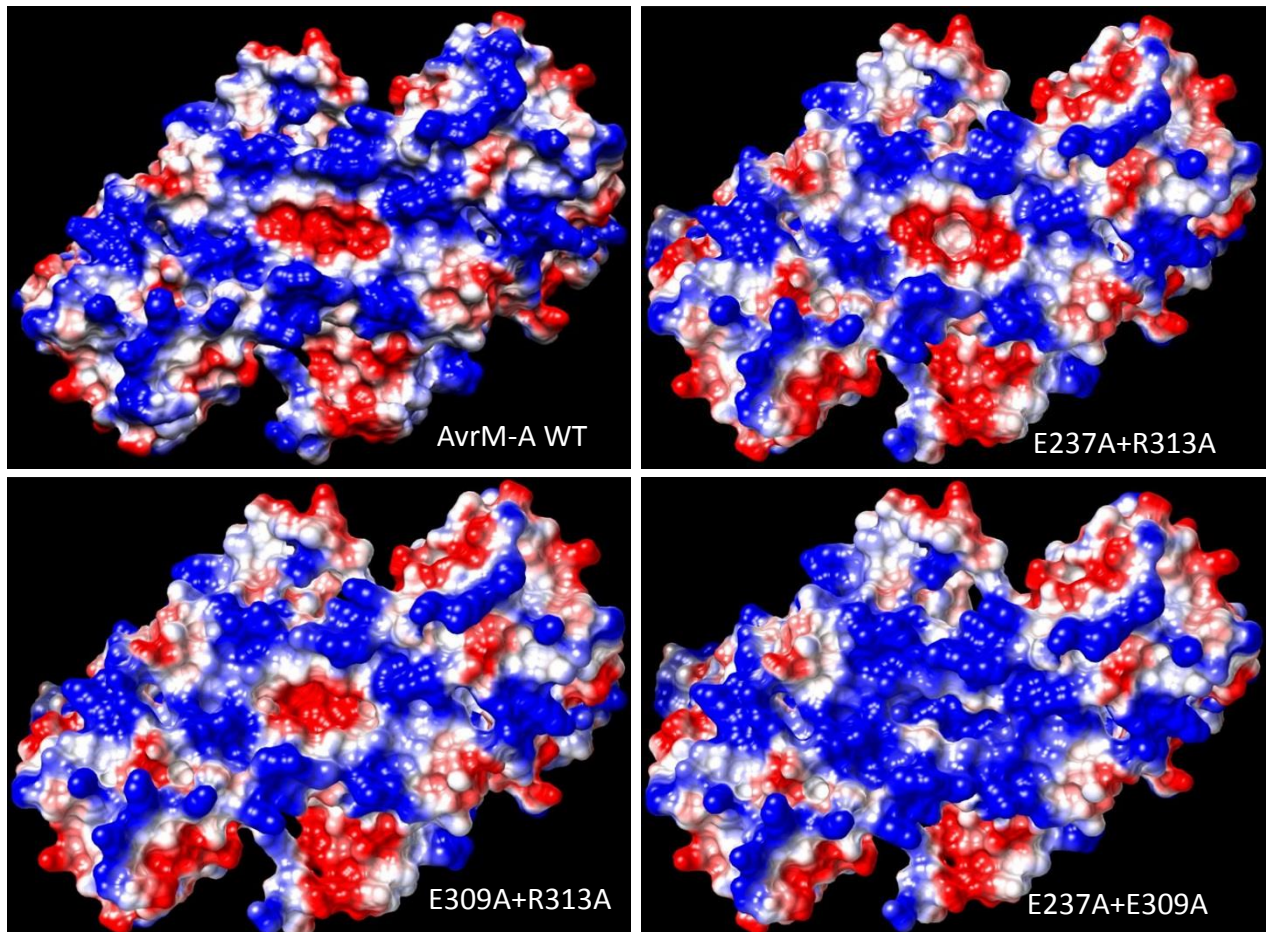


Figure S4.1: Comparative views of surface representation of AvrM-A and its non-polymorphic double mutants. The predicted structures have been generated, using the AvrM-A structure (Ve et al., 2013) as a template, that show an alteration, in comparison of AvrM-A, in the central negatively charged pockets due to the alanine substitutions as indicated in the respective pictures.

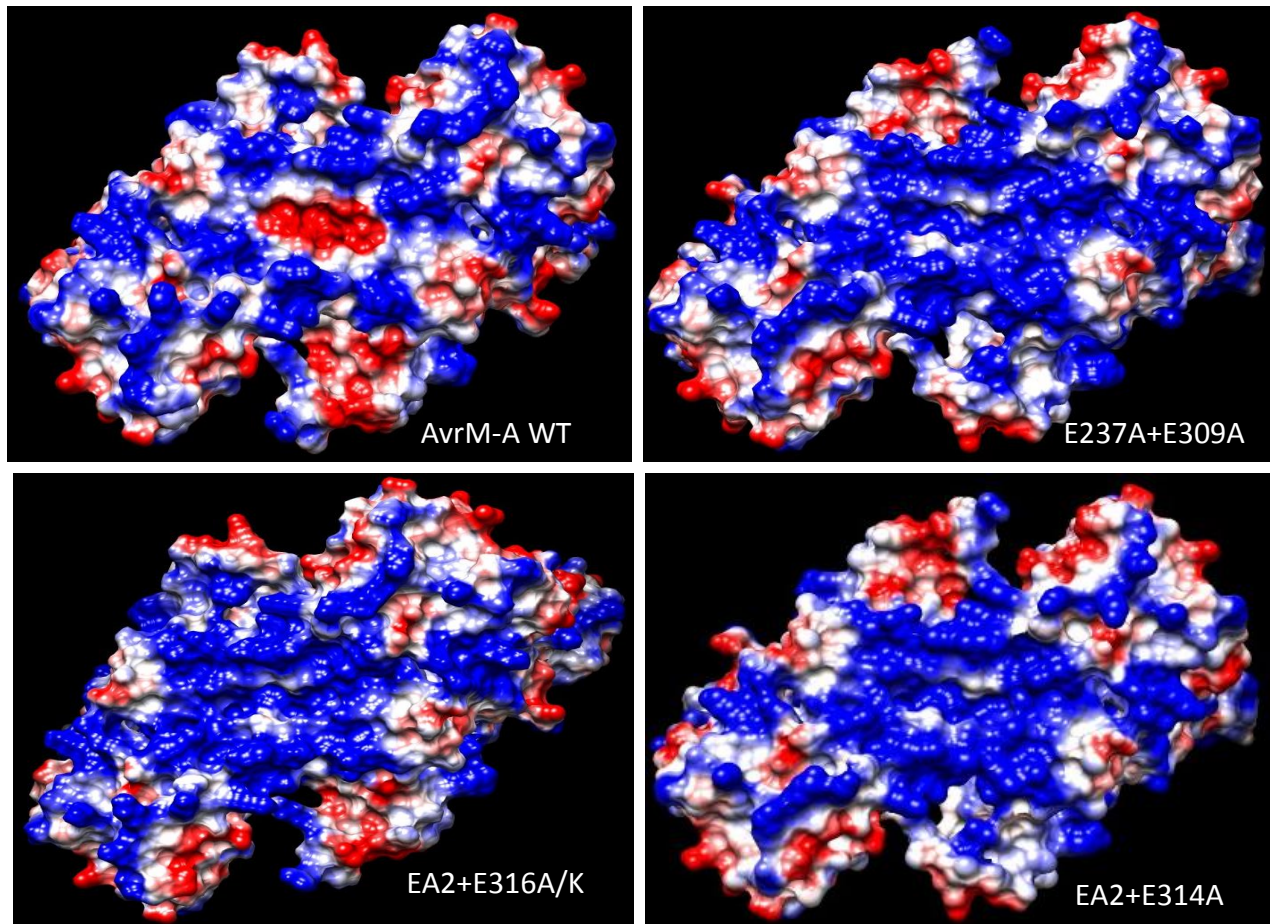


Figure S4.2: Comparative views of surface representation of AvrM-A and its non-polymorphic combined mutants that altered recognition (as shown in Figure 7). The structures have been generated, using the AvrM-A structure (Ve et al., 2013) as a template, that show an alteration in the central negatively charged pockets due to the alanine substitutions as indicated in the respective pictures.

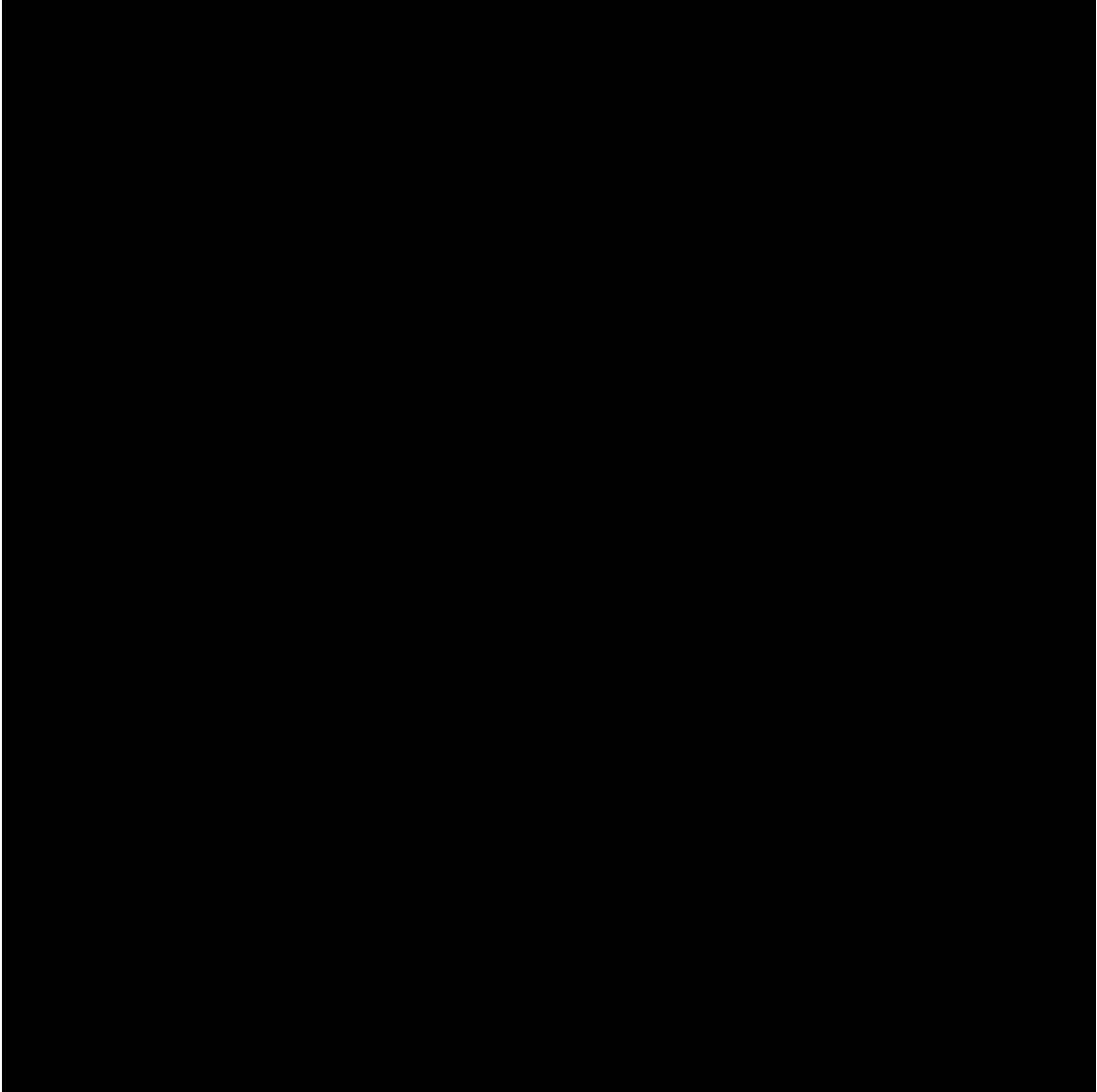
Video S4.1: Ribbon structures of the avrM effector (dimer) protein highlighting some important residues involved in the virulence function.



Web link:

<https://www.youtube-nocookie.com/embed/DI7pDO8Wx5I?rel=0&controls=0&showinfo=0>

Video S4.2: Ribbon structures of the AvrM-A effector protein (dimer) highlighting some important residues involved in the avirulence function.



Web link:

<https://www.youtube-nocookie.com/embed/QRxLGMHyJFY?rel=0&controls=0&showinfo=0>

Chapter Five: Final Discussion

(Pages 123 - 140)

5.1 Discussion

The central goal of this project was to investigate the structures of the flax rust AvrM effector proteins, to obtain clues about the interaction with the M flax rust resistance protein. Structural analysis has provided a platform to elucidate the biological functions of many effector proteins and the recognition specificities of their cognate R proteins (Wang et al., 2007; Chou et al., 2011; Maqbool et al., 2015; Blondeau et al., 2015). The flax rust AvrM-A effector protein has been reported to be recognised by the M flax resistance protein *in planta* as well as interacting directly in the Y2H system (Catanzariti et al., 2010a; Ve et al., 2013). A direct interaction was also reported in the Y2H assay between the variable flax rust effector proteins of AvrL567 and the corresponding flax resistance proteins, L5, L6, and L7 (Dodds et al., 2006). AvrM, another flax rust effector with six allelic variants, was chosen for investigation to unravel the molecular basis of this host-pathogen interaction. By sequence comparison of the six variants of AvrM, 13 polymorphisms were identified to be involved in differential recognition specificity (Catanzariti et al., 2006). Furthermore, a deletion study confirmed that the C-terminal half of the AvrM-A protein controls the interaction with the flax M protein (Catanzariti et al., 2010a). This is consistent with the mutational analysis of AvrL567, where all the residues identified to alter resistance specificity were found to be located in the C-terminal region (Wang et al., 2007; Ravensdale et al., 2012). Additional support is that for Avr3a effectors secreted by *Phytophthora infestans*, where the C-terminal region (75 aa) is sufficient to interact with its cognate resistance protein, R3a of potato plant (Bos et al., 2006). In this regard, a contrasting result has been reported in the case of ATR1 effectors secreted by *H. arabidopsidis*, where the critical residues controlling the resistance specificity are scattered throughout the whole effector structure (Krasileva et al., 2010; Chou et al., 2011). Of the two variants of flax rust AvrM effectors included in this project, AvrM-A is recognized by the M flax resistance protein, resulting in activation of a necrotic cell death response (Catanzariti et al., 2010a; Ve et al., 2013). Although the other variant, avrM, shares 94% sequence identity with AvrM-A in the C-terminal domain (Ve et al., 2011), it is not recognised by M (Catanzariti et al., 2006, 2010). Deletion studies demonstrated that the coiled-coil (CC)-domain of the effector protein is both necessary and sufficient to interact with the M protein (Catanzariti et al., 2010a), and mutation analyses confirmed that no single polymorphic residue mutants of the C-termini alter the M recognition specificity (Catanzariti et al., 2010a; Ve et al., 2013). This suggests that more than one residue act as contact points of the AvrM effector proteins and are thus associated with the virulence or

avirulence function for the effector protein. Consistent with this is a mutational study of AvrL567-C, where multiple contact points (T50, D56 and S96) were found to control recognition specificity to both L5 and L6 resistance proteins (Wang et al., 2007; Ravensdale et al., 2012). Based on the protein structures of AvrM-A and avrM effectors, three polymorphic side-chains (R170/K232, S179/L241 and T247/I310) were targeted (Figures 4.2 and 4.3) to determine the functional role of each in mediating pathogenicity in host plants. To evaluate the role of each of these three residues in mediating interaction with the M protein, pairwise reciprocal doubles and a triple mutant were generated in both effectors, which showed varying degrees of recognition by the M in Agro-infiltration assay in tobacco leaves (W38::M). These mutants were tested for interaction with M using AMTE *in planta* assay for recognition specificity (Figures 4.4, 4.5 and Table 4.1) as well as Y2H assay to determine AvrM/M interaction (Figure 4.9). Extensive dimeric interfaces are visible in the crystal structures, consistent with the finding that AvrM-A exists as a stable dimer in solution (Catanzariti et al., 2010a; Ve et al., 2011; Ve et al., 2013). The effector proteins (avrM and AvrM-A) and the mutants therein (those altered recognition) were tested for their physical properties by SEC-MALS and -SAXS analyses, which confirmed that AvrM-A and the mutants are stable dimers, but avrM (non-mutant) is not (Figures 4.7 and 4.8). These results revealed that mutations in avrM that gained recognition by M also promote dimerization as determined by SEC-MALS and SEC-SAXS analyses. In agreement with AvrM-A dimerization, there are two reports on the size of the AvrM-A effector molecule as determined by gel-filtration (Catanzariti et al., 2010a; Ve et al., 2011). But for the avrM, our analyses reported here contradict the previous result, where the avrM was reported as a dimer in solution (Ve, 2011; Ve et al., 2011).

The data from SEC-MALS and -SAXS suggests the molecular weight (MW) of avrM is ~33kD, which corresponds to that of an AvrM monomer. Though the monomeric and dimeric AvrM effector molecules have different molecular weights (MWs), they both occupy a similar molecular volume, especially when they rotate in solution and migrate through a size exclusion column. In size-exclusion chromatography (SEC or GF), the pores of the gel beads are capable of passing the similar molecular volumes occupied by the rotating avrM monomer and AvrM-A dimer. As a result, both of the proteins can enter easily through the pores of the gel beads of the column to the same extent. Consequently, both protein molecules travel through the resin, eluting from the column at a similar time point. For this reason, the SEC/GF

analysis reported by Ve et al. (2011) gave a misleading result that predicted *avrM* to be a dimer in solution. Though a previous study reported that *avrM* elution volume range was consistent with that of a dimer, the GF profile shows that *avrM* eluted slightly behind the AvrM-A protein (Figure 1a in Ve et al., 2011), indicating that *avrM* is smaller than AvrM-A. Here, we showed that SEC/GF gives an MW of 50kDa for *avrM*, while our MALS and SAXS analyses showed an MW of *avrM* to be at maximum ~31kD, indicating that *avrM* is a monomer in solution. Moreover, in the crystal structures, extensive dimeric interfaces are visible, which are consistent with the fact that AvrM-A exists as a stable dimer in solution (Catanzariti et al., 2010a; Ve et al., 2011; Ve et al., 2013).

To summarise the step-wise change of *avrM* into a form recognisable by M, the triple mutant, *avrM*^{S179L+T247I+R170K}, gained 70% HR to that of *avrM*. Thus, the *in planta* assays of the double, triple and quadruple mutants of the five reciprocal mutants, R170K, S179S, T247I, ΔL218PI and K253E indicate that the recognition specificity of AvrM effector is controlled by the first four contact points, which mainly provide mechanical support enabling the effector in self-association (homo-dimerization). The subtractive effects of T186I, N197T and K253E on resistance recognition are likely to have very subtle effects on AvrM effector structure, enabling recognition by, and activation of, the M protein. As seen in the crystal structure of AvrM-A, three conserved non-polymorphic charged residues E237, E309 and R313 contribute to a charged pocket at the interface of the effector dimer. These were targeted for alanine substitution to abrogate the detection of the effector protein by the M. But the alanine substitution revealed that a single alanine substitution at any of the three charged residues mentioned is insufficient to destabilize interaction with the M protein. In order to complement the recognition specificity study in the AvrM-A effector, three pairwise double mutants and a triple mutant with the three alanine substitutions were engineered and tested by Agro-infiltration. Of the double mutants, only AvrM-A^{E237A+E309A} substantially reduced recognition, inducing only a very weak HR. The triple mutant AvrM-A^{E237A+E309A+R313A} showed no change to the loss-of-recognition compared to the double mutant (Figure 4.5a-d, Table 4.2). However, when an alanine mutant E316A was added to the AvrM-A^{E237A+E309A} loss-of-recognition mutant, this fully restored recognition to the triple mutant AvrM-A^{E237A+E309A+E316A} and induced a very strong HR, which was anticipated to abolish completely the mild recognition by the AvrM-A^{E237A+E309A}. To confirm the role of the E316 side chain, a reciprocal

mutant E316K, in the same position, was also added to the double mutant AvrM-A^{E237A+E309A}, but AvrM-A^{E237A+E309A+E316K} also induced a very strong HR. Conversely, the addition of another alanine mutation E314A to AvrM-A^{E237A+E309A}, giving A^{E237A+E309A+E314A}, did achieve complete destabilization of M recognition. These data indicate that the three conserved residues, E237, E309 and R313, located at the dimer interface of the AvrM-A, render additive effects in strengthening recognition by, and stabilizes the interaction of the effector protein with, the M resistance protein.

The recombinant avrM and AvrM-A proteins were stably expressed *in planta* (Figures 4.4d and 4.5e) and in yeast (Figure 4.9), suggesting differential recognition of the combined mutants by the M protein is most likely due to differences in the surface properties, and not their expression level or stability. The avrM mutants that gained recognition achieved a convenient surface property that stabilized physical interaction with the M resistance protein, while AvrM-A mutants that lost recognition, lost these surface properties and this destabilized the interaction. In the case of AvrM-A^{E237A+E309A} and AvrM-A^{E237A+E309A+E314A} mutants, the results of the *in planta* assay correlated well with that of the Y2H assay, while the mutants AvrM-A^{E237A+E309A+E316A/K} that restored recognition *in planta*, did not show any interaction in the Y2H assay (Figure 4.9). On the other hand, none of the combined mutants in of avrM showed any interaction in Y2H assay. A similar trend was also found in the case of the AvrL567-C effector, where two double mutants restored weak interaction by the L6 resistance protein in yeast, but it did not induce any HR in an *in planta* assay (Ravensdale et al., 2012). This is supported by mutational analyses where binding affinities between effectors and the cognate R proteins occasionally vary between *in vitro* and *in planta* conditions (Maqbool et al., 2015).

5.1.1 Dimerization of AvrM favours M recognition

Data from the crystal structures, site-directed mutagenesis (SDM) and *in planta* assays combined with SEC-MALS and -SAXS analyses indicated that self-association of AvrM effector is a requirement for being detected by the flax resistance M protein. The SEC-MALS and -SAXS analyses clearly revealed that the flax rust AvrM-A effector protein is a homo-dimer in solution, a result that is supported by gel filtration (Catanzariti et al., 2010a; Ve et al., 2011). The avrM protein was previously reported to form a dimer in solution (Ve et al., 2011), but our SEC-MALS and -SAXS data contradicted this and indicated that the avrM protein may form a loose dimer,

but is clearly not a stable dimer in a solution (Figure 4.7a-d). Therefore, this result suggests that dimerization of AvrM proteins is a prerequisite for detection by M protein. Similarly, Boutemy et al. (2011) reported that the oomycete effector PexRD2 from *Phytophthora infestans* dimerizes both *in vivo* and *in vitro*. The AVR3a effector protein of *P. infestans* has also been reported to experience homodimerization (Wawra et al., 2012b) and the Avr2 effector protein secreted by *Fusarium oxysporum* forms a homo-dimer *in vivo* and interacts with the tomato I-2 resistance protein (Ma et al., 2013). Deletion studies revealed that the entire region of the Avr2 protein (except for N-terminal 17 aa) controls dimerization and activation of the cognate R protein (Ma et al., 2013).

As an alternative to dimerization, many other effector proteins deploying diverse function possess repeated regions. For example, the flax rust effector AvrL567 is a monomer, but is a repeated structure of β -sandwich folds dominated by two antiparallel β -sheets, A and B, arranged into an incompletely closed β -barrel (Wang et al., 2007). Similarly, the oomycete effector ATR1 is a monomer of a repeated structure of two repeats, repeat-1 and repeat-2 (Krasileva et al., 2010; Chou et al., 2011). The effector protein AvrPiz-t is also a repeated structure, composed of two antiparallel β -sheets, each consisting of three β -helices (Zhang et al., 2013). Similarly, repeated structures have also been found in Cin1 (Mesarich et al., 2012) and Ecp6 effectors (Sánchez-Vallet et al., 2013). The repeated architectures or structural motifs of several plant-associated pathogenic effectors have been suggested to play diverse roles in effector functions, such as host cell association and trafficking, effector adaptive evolution, blocking resistance response, broadening the protein surface area to accommodate more functional surface patches/epitopes and interaction with diverse host targets (Mesarich et al., 2015). Almost all effector proteins are repeated, or oligomer-structured, and host resistance proteins, in some cases, have this feature. Self-association of the flax rust resistance protein L6 is also a prerequisite for a resistance response, and some individual surface patches engaged in self-association, signalling and negative regulation have been identified (Bernoux et al., 2011b).

Our SEC-MALS and -SAXS analysis revealed that avrM is not a dimer but engineered mutants of avrM that gained recognition do dimerize in solution. Furthermore, alanine-substituted recombinant AvrM-A proteins lost recognition but remained dimeric, suggesting that the mutations altered the negative charge pocket without perturbing the

dimeric structure of effector proteins. The M protein failed to interact with the mutated effector due to the alteration of the central charge pocket by the alanine mutants. Indeed, with this data, it can be predicted that AvrM effector proteins require duplication such as homo-dimerization and/or self-repetition to deploy their proper pathogenicity function. It is predicted, therefore, that loss of dimerization exists as a strategy to avoid M detection and activation of the resistance response. What cannot be determined, however, is whether *avrM* has lost its pathogenicity function.

5.1.2 Central charged pocket of AvrM dimer favours M recognition

Structural analysis revealed that the electrostatic properties of the dimer interface of the AvrM-A protein are significantly different from those of *avrM* (Figure 4.6). The surface structures show that the AvrM-A dimer has a highly negatively charged (acidic) cleft at its midpoint, while the predicted *avrM* dimer possesses a shallower interface and is highly positively charged (basic) at its central surface. This disparity in the dimer interfaces of AvrM-A and *avrM* proteins causes a significant difference in their recognition specificities.

A mutational study of M flax rust resistance protein (an autoactive mutant M^{D555V}) reveals that M protein is independent of AvrM effectors to induce necrotic cell death leading to HR (Williams et al., 2011), indicating that M protein is responsible for the suicide of the infected host cell. Furthermore, the mutational analysis also confirmed that the Rx potato resistance, and flax *L6* resistance, proteins can also circumvent the necessity of effector recognition/interaction (Bendahmane et al., 2002; Howles et al., 2005). On the contrary, many mutations have been tested in both the AvrM-A and *avrM* proteins, but no mutation has been found to be autoactive in inducing HR. This implies, in the case of M/AvrM-A interaction, the effector proteins provide a physical change to the M protein, similar to the autoactive mutants of the M, converting the M into an activator (or perhaps a toxin) that activates killing of the infected host cells for the sake of the whole plant. The acidic pocket of the AvrM-A protein, a feature not found in the *avrM* protein, is most probably responsible for such a physical change for M resistance activation. In the case of the alanine mutants that lost M recognition, the alanine substitutions for the glutamic acids (E237 and E309) or arginine (R313) are very unlikely to alter the gross structures of the mutant proteins, as alanine is a simple, charge neutral and small (MW 89.09 Dalton) residue with a non-polar hydrophobic chemical property. In the AvrM-A effector protein, alanine substitutions of the

charged residues are most likely to neutralize the central negative charge pocket without perturbing the quaternary structures of the mutant proteins. As per the prediction of the central negative charge pocket in controlling resistance detection (Ve, 2011), the loss-of-recognition by AvrM-A^{E237A+E309A} and AvrM-A^{E237A+E309A+E314A} mutants is probably due to neutralization of the acidic pocket, or alteration of a negatively charged to a positively charged surface. Data from the alanine substitution experiments revealed that the loss-of-recognition of the alanine mutants can be attributed just to the alteration in the central acidic surface, but not to structural distortion.

On the other hand, polymorphic mutants of *avrM* that gained recognition achieve a suitable configuration to enable the mutant proteins to form a dimer. This dimerization may expose charged residues in the central patch, generating a negatively charged patch similar to that of the AvrM-A dimer. This speculation could be confirmed by solving crystal structures of the *avrM* mutant proteins. The immunoblot analysis showed that all the proteins that are change-of-recognition mutants in both *avrM* and AvrM-A are well expressed *in planta* (Figures 4.4d & 4.5e), and the data of SEC-MALS and -SAXS analyses confirmed that they are all dimers in solution (Figure 4.8a-c). In conclusion, the data from our mutant analyses support the proposal that the negative charge pocket (acidic) of the AvrM-A dimer interface forms when the effector protein forms a stable dimer in solution, and together these features control the interaction with the M resistance protein, as was predicted by Ve (2011).

5.1.3 AvrM is a highly evolved complex effector

While indirect R/Avr interaction imposes selection against the Avr function of an effector, the way to direct resistance recognition favours pathogens to evolve their effectors by means of sequence diversification, which is assumed to surmount host resistance rather than causing loss of function (Dodds et al., 2006). The AvrM-A effector protein is recognized by the M resistance protein, but the *avrM* is not (Catanzariti et al., 2010a; Ve et al., 2013), and the mutation analysis using single polymorphic and non-polymorphic mutations coupled with an *in planta* assay suggests that the recognition specificity of AvrM effectors is controlled by multiple residue contacts (Chapter 3). Accordingly, combined effects of multiple (3-4 residues) polymorphic residue mutants enabled the *avrM* effector to gain recognition by the M, indicating that a maximum of four polymorphic residues is controlling avirulence specificity. On the contrary, the combined effect of the same polymorphic counter residue mutants could not switch specificity,

revealing that more than four polymorphic sites are likely to control virulence specificity in AvrM effector (Figure 4.4c). However, combined effect of three alanine substitutions, is to alter the central negatively charge pocket, abrogated the recognition by the M. That is why, our mutational analysis suggests that AvrM recognition by the M relies on multiple residue contacts of the effector protein. These residue sites are scattered on the surface structure, suggesting that AvrM proteins have multiple distinct surface epitopes that control virulence and avirulence specificities. Furthermore, this project has confirmed that the C-terminal CC-domain ($\alpha 8$ and $\alpha 11$ helices) controls interaction with M through the resultant effects of multiple residue contacts, whereas single residue contacts of many other effectors control interaction with their cognate R proteins. Consistent with our findings about AvrM, a quadruple mutation in the ATR1-Cala2 effector protein (V122L + S125T + Y140D + N158K) was found to gain recognition by the cognate RPP1-WsB resistance protein, and the reciprocal quadruple substitution in ATR1-Emoy2 significantly delayed activation by RPP1-WsB (Chou et al., 2011).

However, many other effectors are reported to utilise single residue sites for control of specificities. For example, a mutation study in three variants (A, D, C) of AvrL567 effector proteins confirmed that single residues individually control recognition specificities with the corresponding R proteins (Wang et al., 2007; Ravensdale et al., 2012). In AvrL567-A, the residue I50 determines avirulence with respect to both L5 and L6 resistance proteins. In AvrL567-D, T50 and L96 each regulate virulence function to L5, and the latter residue (L96) additionally to L6. For the virulent variant AvrL567-C, a single mutant S96R restores a weak interaction with the resistance protein L6 (Ravensdale et al., 2012). Another mutational test revealed a single residue mutant (cysteine to alanine) at two cysteine residues causes a gain of avirulence function in the AvrPiz-t effector protein (Li et al., 2012). A similar experiment showed that two individual single substitutions, E92K and D191G in ATR1-Maks9 effector protein altered the conformation of the effector so it was completely recognized by the cognate resistance protein, RPP1-NdA (Krasileva et al., 2010). Another study showed that four single-residue mutants in ATR1-Cala2 have individual effects on recognition of the effector protein by the resistance protein, RPP1-WsB (Chou et al., 2011). Specifically, a single mutation N158K gains very mild recognition, V122L and S125T induce intermediate recognition, and Y140D strong recognition by the resistance protein, RPP1-WsB. Furthermore, the *Brassica napus* pathogen *Leptosphaeria maculans* secretes the AvrLm4-7 effector protein, which confers a dual recognition specificity

by two resistance proteins, Rlm4 and Rlm7 (Parlange et al., 2009). Mutation analysis in the AvrLm4-7 protein confirmed that only a reciprocal substitution G120R resulted in loss-of-recognition by the Rlm4 resistance protein without perturbing *AvrLm7* specificity (Parlange et al., 2009). A further study showed that either of the polymorphic mutants, R100P, F102S or S112R destabilized the interaction with Rlm7 protein (Daverdin et al., 2012).

Furthermore, in the case of the AvrM, not only the specificity but also the host cell translocation is different from other effector proteins. Like the oomycete effector proteins, AvrM-A has three putative RXLR motifs. However, a mutation study showed that none of the motifs can alone prevent uptake of AvrM into the plant cell, suggesting that AvrM utilizes a different translocation mechanism (Rafiqi et al., 2010). So, AvrM translocation is completely contrasting with the proposed hypothesis of host-cell entry by other oomycete and fungal effectors (Kale et al., 2010; Kale and Tyler, 2011). By functional analysis, it has been confirmed that a conserved hydrophobic surface patch in the AvrM effectors is required for plant cell internalization (Ve et al., 2013).

As revealed by the sequence polymorphisms coupled with structural and mutational analyses, AvrM is a highly evolved complex effector protein having 13 polymorphisms with repeat-containing motifs. Unlike many other effectors, AvrM also forms a complex dimeric architecture, which is possibly a potential step in its evolution to strengthen pathogenicity and manipulate a diverse range of host targets. The published data, combined with that presented in this study, suggest that AvrM is a protein with structural repeats that facilitate dimerization, thus achieving a larger molecular surface to broaden host specificity and pathogenicity.

5.1.4 Multiple contacts provide dynamic rather than cumulative support

Mutation analysis of the *avrM* effector protein coupled with *in planta* assays indicate the resultant effect of the three reciprocal mutants (R170K, S179L and T247I) to influence the quaternary structure of the *avrM* protein, possibly to expose the charged residues (E175, E249, R250 and K253) in a particular fashion that converts the central positive charge patch to a negatively charged surface thus allowing M recognition. Subsequently, the addition of K253E mutant in the *avrM*^{R170K+S179L+T247I+K253E} mutant, instead of augmenting recognition, results in complete loss-of-recognition. This nullification in gain-of-recognition may imply that the K253E mutant reorients the quaternary structure of the triple mutant to one similar to the progenitor

avrM, or perhaps disturbs the central charged surface gained by the mutant, avrM^{R170K+S179L+T247I}. Further addition of either I186T or N197T to the triple mutant avrM^{R170K+S179L+T247I} has a subtractive effect, weakening the gain-of-recognition in each corresponding quadruple mutant (Table 4.1). However, subsequent stacking of Δ L218P to the same triple mutant backbone gained an additively stronger recognition than that of the triple mutant. In contrast, similar reciprocal triple and quadruple mutants in AvrM-A could not destabilise interaction with M, indicating that other residues still have enough support to stabilise the interaction. This data of avrM effector revealed that the resultant effect of combined polymorphic mutations follows a dynamic rather than a cumulative process in stabilizing interaction with the M resistance protein.

As revealed by the crystal structure and polymorphic mutation analysis coupled with *in planta* assays, recognition specificity of the AvrM effector is controlled by some of the charged residues, which have mechanical support from the polymorphic residues. Similar to mutation analysis of avrM, data of the combined alanine substitutions in AvrM-A indicates that the resultant effect of the three alanine substitutions, E237A, E309A and R313A, results in neutralization of the central negatively charged patch of the AvrM-A molecule, most likely by converting the central patch from a negative to a positive charge, thus destabilizing M detection. Subsequent addition of E316A/K mutants to the AvrM-A^{E237A+E309A} mutant, instead of abrogating recognition, reinstated the complete gain-of-recognition. The reinstatement of the gain-of-recognition could happen through the subtractive effects of the E316A/K mutant that reoriented the quaternary structure of the AvrM-A^{E237A+E309A} mutant to a similar as, or slightly different to, the progenitor AvrM-A, which reinstated the central acidic surface in the dimer interface of the AvrM-A^{E237A+E309A+E316A/K} mutant protein. However, the addition of E314A mutant to the AvrM-A^{E237A+E309A} mutant showed an additive effect, abolishing complete recognition of the triple mutant (Table 4.2). This data revealed that the resultant effect of the alanine substitutions, similar to the combined reciprocal mutants in avrM, works in a dynamic process, rather than cumulative, in destabilizing the interaction with the M resistance protein. In both avrM and AvrM-A, the results of the combined mutants, which altered the recognition specificities by the M flax resistance protein, revealed that the multiple contact points provide supports in a dynamic way rather than cumulative.

5.1.5 Polymorphism K253/E316 has extra support to overcome effector targets

Pathogenic avirulence proteins are recognized by the cognate R proteins either by indirectly detecting any change in the host targets, or through directly interacting with the cognate Avr protein. A polymorphic position, K253/E316 in *avrM*/*AvrM-A*, negates the effects of both combined mutants, *avrM*^{S179S+T247I+R170K} and *AvrM-A*^{E237A+E309A}, as has been shown in Figure 4.4a-b, 4.5a-d, Table 4.1 and 4.2 in Chapter 4). In this case, the role of the polymorphism K253/E316 indicates that this residue may be responsible for evading any effector targeting decoy, or it may be an extra result of evolution to retain its pathogenic/virulence function that tackles any adverse circumstance imposed by the host's immunity. Substitution of glutamic acid (E) to K253 in the central patch of the *avrM*^{S179S+T247I+R170K} mutant protein, designated as *avrM*^{S179S+T247I+R170K+K253E}, abolished gain-of-recognition function of the triple mutant. This indicates that a positively charged residue (like K) is required in the central patch to balance the negatively charged surface in the dimer interface of the triple mutant for retention of the gain-of-recognition (avirulence) function of the M resistance protein. Indeed, this has been found in several other phytopathogen effectors. Structure-function experiments of *Avr3a* effector proteins demonstrated that polymorphisms K80E and I103M contribute to effector specificity as well to the perception by cognate resistance protein, R3a, confirming that these two polymorphisms contribute to its effector functions as well as the perception by the R3a. This study revealed that K80 has a critical effect on the avirulence function, while M103 attributes to the virulence function (Bos et al., 2006). Although *avrM*^{S179S+T247I+R170K} is a gain-of-recognition mutant, the addition of K253E reductively blocked the recognition, returning the effector to virulence. In contrast, *AvrM-A*^{E237A+E309A} is a loss-of-recognition mutant and the addition of E316A/K mutants enabled the protein to return to avirulence function. It is notable that these two critical residues (K253 and E316 of *avrM* and *AvrM-A*) are polymorphic in similar locations of the two variants.

It can also be hypothesized that the role of the K253/E316 evolution is that a step of the evolution of *AvrM-A* to virulence specificity imbalanced a surface property (most probably the surface charge) that was subsequently balanced by a mutation that replaced the lysine (K) with a glutamic acid (E) in residue 316. Similarly, the addition of K253E to the *avrM*^{S179S+T247I+R170K} gain-of-recognition mutant may have a disproportionate effect on the surface property (charge), obliterating the recognition that was gained in the triple mutant

of the resistance protein. So the polymorphic residue K253 (a counter position of E316 in AvrM-A) appears to have evolved as a side-chain for extra support to deal with the assorted repertoires of host immune components.

The critical role of this polymorphism may be attributed to indirect recognition and interaction with the host targets. As described as the arms race dynamics (Woolhouse et al., 2002), this extra evolved residue may be involved in the diverse role of effector function, or possibly contribute to the adaptive evolution of the effector, which is yet to be explored. Since both K253 and E316 showed similar negating effects in regards to avirulence and virulence functions of avrM and AvrM-A, respectively, this polymorphism may have evolved to compete with the diverse range of host targets as a means of escalating pathogenicity in the host plants. As the charge pocket is critical for R protein interaction, a particular side chain, a lysine (K) at 253 of avrM and a glutamic acid (E) at 316 of AvrM-A, is probably required for activating M-mediated HR.

5.1.6 AvrM quaternary structure has an important role in M recognition

As the structures of AvrM have no direct clues about function, mutational analysis and *in planta* assays were used to unravel the molecular functions of the AvrM effectors. Each structure of avrM and AvrM-A has a novel elongated alpha helical fold resembling a circular dichroism structure (Ve, 2011). The most prominent features of the proteins are an N-terminal hairpin domain and a C-terminal anti-parallel CC-domain, which are oriented perpendicular to each other, establishing an overall non-globular L-shaped architecture. Several of the residues involved in stabilising the overall fold of the AvrM structures are conserved in the eight homologs of *M. larici* (Mlp) (Ve, 2011; Ve et al., 2013), suggesting that the L-shaped repeats are important characteristic features for the pathogenic functions of the effector molecules. In the crystal structure of AvrM-A, an extensive dimeric interface is visible, which is consistent with the fact that AvrM-A exists as stable dimers in solution (Catanzariti et al., 2010a; Ve et al., 2011). As shown by the structures, two anti-parallel CC-domains interact forming an anti-parallel four-helical bundle in the dimer, and the dimeric structures have an overall non-globular arc-shape (Ve et al., 2013). However, although the data presented here (SEC-MALS and SEC-SAXS analyses) confirms that AvrM-A forms a stable dimer *in vitro*, it was shown that avrM is monomeric. As shown by the mutation analysis in avrM, the polymorphic triple mutant, avrM^{S179S+T247I+R170K}, designed to structural alteration,

enabled partial M recognition, and a subsequent addition of Δ L218PI mutant resulted in complete avirulence specificity, similar as AvrM-A.

In this case, the avrM mutant proteins and the progenitor avrM protein are equally stable in plant and yeast cells (Figures 4.4d, 4.5e and 4.9b in Chapter 4). Moreover, the SEC-MALS and SEC-SAXS analyses demonstrate that although the alanine mutants of AvrM-A, those of lost recognition by M, are still stable dimers in solution. Surprisingly, the combined polymorphic avrM-mutants that gained recognition by M, become stable dimers in solution, as demonstrated by SEC-MALS and -SAXS analyses (Figure 4.8a-c). This result reveals that the gain-of-recognition specificity in the avrM-mutants can be attributed to the alteration in quaternary structure retained by the combined polymorphic substitution. In fact, the resultant effect of the multiple polymorphic mutants in avrM, that caused gain-of-recognition, restored the dimeric quaternary structure similar as the AvrM-A, and in doing so, it also reinstated recognition *in planta*.

5.2 Future direction

5.2.1 A proposed model for the AvrM-M interaction

The main hypothetical models for interaction between effector and resistance proteins are direct physical interaction and indirect interaction, or the guard hypothesis (Ravensdale et al., 2011). Following the direct interaction, a model for AvrM specificity has been presented (Figure 5.1) based only on the functional evidence and biochemical properties obtained in this study. The decisive fragments of evidence in formulating this model are as follows:

- The C-terminal domain of AvrM is sufficient to establish a physical interaction with the cognate resistance M protein (Catanzariti et al., 2010a; Ve et al., 2013).
- To interact with M, AvrM needs to dimerize by self-association (homo-dimerization), achieving a negative charge pocket (acidic) in the central patch of the dimer interface. The data from this project confirm that AvrM-A dimerizes and is recognized by M, and that avrM neither dimerizes nor is recognized by M. Consistent with this, our data demonstrate that the avrM mutants that gained recognition also gained the ability to dimerize in solution.
- In AvrM-A, the polymorphic amino acid side-chains provide mechanical supports for homo-dimerization, achieving an appropriate orientation that enables the non-polymorphic

charged residues (E237, E309 and E314) in transmuting the central charged pocket that is crucial to interact with the M. Indeed, the polymorphic residues physically expose the non-polymorphic charged residues in a fashion that enables them to chemically induce the acidic pocket in the dimer surface.

- The activated M protein alone causes necrotic cell death following recognition and interaction with the AvrM-A effector protein. M is also independent of the effector in inducing HR, which was demonstrated by an autoactive mutant, M^{D555V} (Williams et al., 2011). It appears that interaction with AvrM-A results in a chemical alteration in M, possibly to a form similar to that of the M^{D555V} autoactive mutant, becoming an activator that causes host cell death (HR). It is also evident that the interaction between a recognisable AvrM-A and an inactive M^{K286L} mutant cannot induce HR (Table 5.1).

Table 5.1: M is independent of AvrM for signalling HR (Williams et al., 2011).

R protein	Effector protein	Signalling HR
M	AvrM-A	++++
	no	----
M ^{D555V}	AvrM-A	++++
	no	++++
M ^{K286L}	AvrM-A	----
	no	----
M ^{K286L+D555V}	AvrM-A	----
	no	----

Note: ++++ implies and ---- for no HR. Here M and AvrM-A is active proteins

- Dimeric AvrM influences the M protein to activate defence signalling, which can be deduced by the evidence of the autoactive M mutant, M^{D555V}, which has a higher rate of ATP hydrolysis than the non-mutant M protein (Sornaraj, 2013, Williams *et al.*, 2011). This rate is likely to be increased by interaction with AvrM, and even the autoactive mutant induces a more intense HR when co-infiltrated with AvrM-A (Sornaraj, 2013).

As found in previous studies (Catanzariti et al., 2010a, Ve et al., 2013), data presented here confirms that the C-terminus of AvrM (consisting of R170/K232, S179/L241, T247/I310 and ΔL217/PI279 polymorphisms) controls the interaction with the M resistance protein.

However, the LRR domain of the M protein is likely to be the site that binds to AvrM, as this domain seems to be a major determinant of recognition specificity in most other plant R proteins (Ellis et al., 1999; Jia et al., 2000; Dodds et al., 2001b; Shen et al., 2003; Rairdan and Moffett, 2006; Tameling et al., 2006; Padmanabhan et al., 2009). As a result, it is predicted that the LRR domain of the M protein binds to the C-terminus of the AvrM protein to induce defence signalling. To probe more deeply into the basis of AvrM-M interaction and the possible virulence-associated functions of the AvrM effectors, it would be desirable to investigate the structure of the AvrM-M complex. Nonetheless, in agreement with the ideas mentioned above, this study proposes a model for AvrM-M interaction and the subsequent resistance signalling. In this model, the acidic pocket constituted by the C-terminal region of AvrM interacts with the LRR domain of M, which chemically alters the M protein possibly by modifying the negative charge of the acidic patch. The resultant alteration changes M into an activator that signals the resistance response and induces HR. Thus, the effector appears to be a stimulator and M an activator in signalling the defence response in the host plant. With assumptions mentioned above, this model will be relevant for only effector-resistance, AvrM-M, interaction in the flax and flax rust model system.

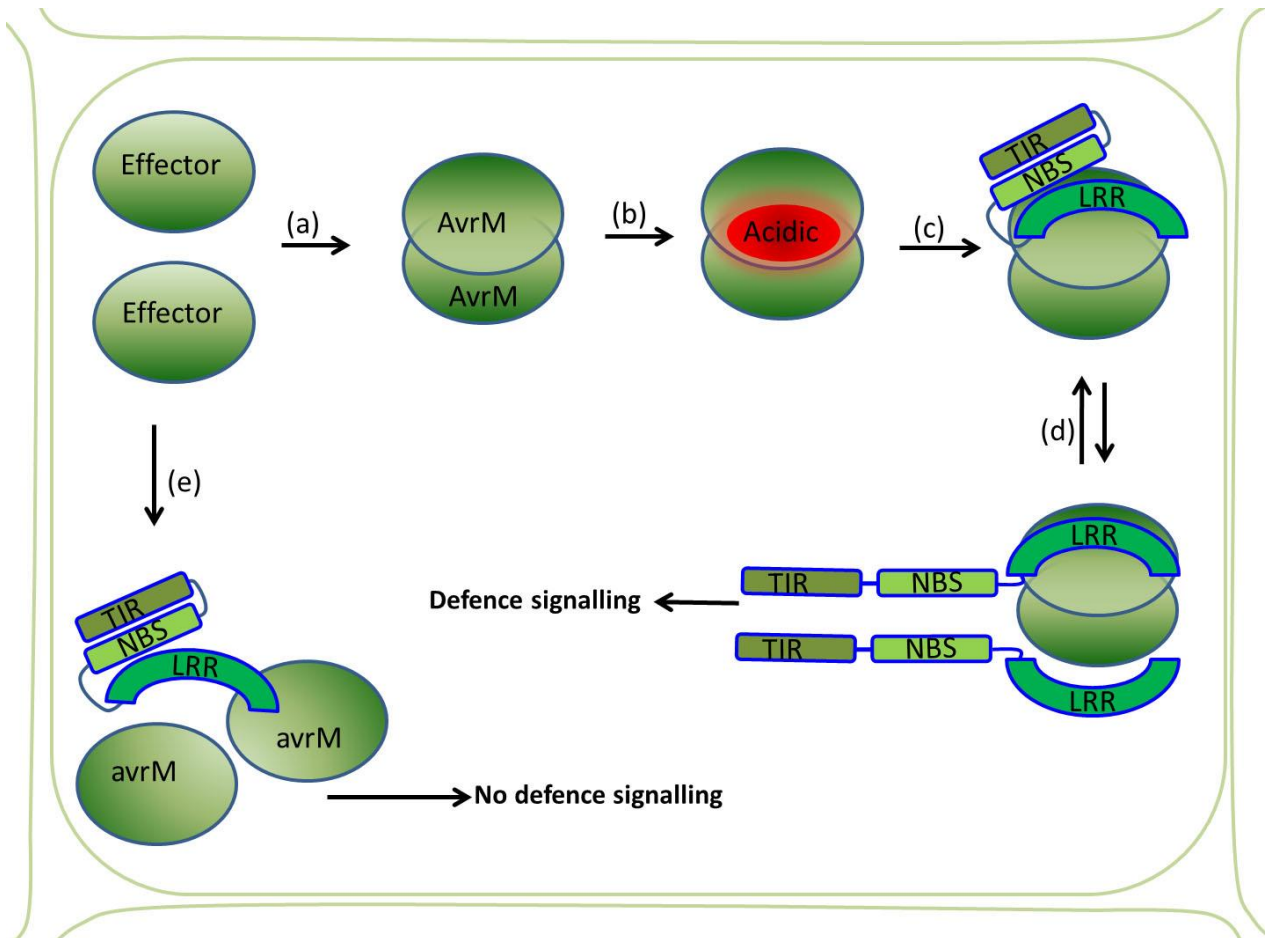


Figure 5.1: A proposed model for interaction between flax rust AvrM effector and flax M resistance protein. (a-b) The AvrM-A effector dimerizes, achieving a negatively charged (acidic) pocket (shown in red) in the dimer interface. (c) The LRR domain of the M resistance protein binds and interacts with the acidic pocket. (d) Then M protein becomes an activator that initiates defence signalling and induces HR. (e) The avrM effector does not form a dimer, and thus, the M cannot bind to it. So there is no interaction between M and avrM, and no signalling.

5.2.2 AvrM/M complex structure - a future direction

The 'gene-for-gene' hypothesis of host-pathogen interactions proposed by Harold Henry Flor (1955, 1971) provided the initial direction for research of plant-pathogen interaction. Subsequently, the crystal structure of the AvrPto-Pto protein complex in the tomato pathogen, *P. syringae* (Xing et al., 2007) offered substantial insights into the interface of host-pathogen interaction. Though flax M resistance and flax rust AvrM effector proteins provide an excellent model system for studying host-pathogen interaction, structural models of the M protein, or of an interacting complex with an effector have not yet been

achieved. There is, however, a structural model for the LRR domain of flax rust L5 resistance protein and of the L5/AvrL567 interacting complex (Wang et al., 2007; Ravensdale et al., 2011), which has stimulated research into the molecular mechanism of the interaction and several crucial residues in both R and Avr proteins determining recognition specificity have been identified (Ravensdale et al., 2012). Recently, the structural complex for direct interaction of the rice blast (*M. oryzae*) effector, AVR-PikD with a rice resistance protein, Pikp-HMA has been described, which clarified the protein-protein interaction in the rice-rice blast pathosystem (Maqbool et al., 2015). The structural and mutation analyses of flax rust AvrM presented here have so far provided many clues to the interaction of effector-resistance protein. However, to fully understand the interaction between AvrM and M, structural information on an AvrM-M complex is required. Hence, this project advises that the most important future direction to investigate the molecular basis of the protein-protein interaction in this effector-resistance model system is to solve the structure of the AvrM-M interacting complex.

Moreover, self-association of the AvrM protein, and its interaction with the M flax resistance protein can be further elucidated by analysing both of purified proteins on SPR (Surface Plasmon Resonance) using the Biacore instrument. This analysis is under way in our laboratory. Furthermore, determination of the crystal structure of the recombinant effector proteins, those identified in this study that altered recognition specificity, may also complete the full story of functional specificity of AvrM effector proteins. Hence, this task is highly recommended as a future goal.

5.3 Conclusion

Effector proteins are acute components of plant pathogens, required for host colonization, redirection of host physiology, and ultimately, disease onset. Though plants have developed a sophisticated resistance mechanism, they are in constant battle with the rapid genome evolution of diverse pathogenic components. As a control measure, we require a precise understanding of the function of effector proteins at the molecular level. The research presented here, on the flax/flax rust pathosystem, constitutes a model for many other (more economically important) host-pathogen interactions. The overall goal of this thesis was to dissect the molecular structure of the AvrM effector protein and elucidate the molecular basis of recognition by the M flax rust resistance protein. It is hoped that this work will motivate and steer biochemical analyses to further explain the mechanisms that effector proteins use to manipulate host resistance mechanisms and thereby colonize the host plant. Furthermore, a deeper understanding of the molecular machinery that controls pathogenicity may lead to novel techniques of disease control in the future.

Appendices

(Page 142-149)

Appendix 1 (a, b and c)

Appendix 1 (a): Culture media with its chemical components. Medium was sterilized by autoclaving at 121°C for 20 minutes.

Medium	Composition
Luria-Bertani (LB)	Tryptone 10 gL ⁻¹ , yeast extract 5 gL ⁻¹ , NaCl 10 gL ⁻¹ (Ph 7)
LB-agar	Luria-Bertani (LB) plus bacto-agar 15gL ⁻¹
MS media	MS salt (4.3 gL ⁻¹ +sucrose 30gL ⁻¹ +Spectanimycin 50mgL ⁻¹ + agar 8 mgL ⁻¹ (Ph 5.8)

Appendix 1 (b): Solutions and buffers.

Solution/Buffer	Constituents
SDS-PAGE gels, Coomassie staining and Western analyses	
SDS-PAGE buffer stock (3x) (3x Laemmli Buffer)	0.24M Tris-Cl pH 6.8, 6 % SDS (w/v), 30% glycerol (w/v), 0.006% bromophenol blue, 16% β-mercaptoethanol, 5M urea
5x SDS-PAGE running buffer	125 mM Tris(pH 8.3), 960 mM glycine, 0.5 % SDS (w/v)
1xTransfer buffer (western blot)	25 mM Tris, 152 mM glycine (pH should be 8.3, no need to adjust)
TBS-T buffer	20 mM Tris pH 7.4, 0.1 % tween (v/v), 150 mM NaCl
Blocking buffer	5 % (w/v) skim milk powder in TBS-T buffer
Coomassie staining solutions	
Fixer	Acetic acid 10 % (v/v), ethanol 40 % (v/v)
Coomassie staining	Fixing solution + coomassie brilliant blue R-250 0.1% (w/v)
De-staining	Acetic acid 10 % (v/v), ethanol 10 % (v/v)
AvrM-A, avrM and therein mutant proteins purification buffers	
Cell wash buffer (1X)	50 mM Tris (pH 7.5), 150 mM NaCl
Lysis buffer (1X)	50 mM HEPES (pH 8.0) and 500 mM NaCl
Elution buffer (1X)	Lysis buffer + 500mM imidazole
NiA buffer A	0.1 NiSO ₄
EDTA Buffer	0.1M EDTA pH 8
GF buffer	20 mM Tris pH 7.5, 150 mM NaCl, 10% glycerol, 10 mM magnesium acetate, 1 mM DTT

Appendix 1 (c): Chemical composition for 1 litre 10 X TE (Tris-EDTA) Buffer.

Ingredient	Amount (ml)	Concentration in 1X
1 M Tris-HCl pH 7.5	100	100mM
500 mM EDTA pH 8.0	20	10mM
Ultrapure water	880	

NB: Working concentration is 1

Appendix 2 (a): Oligonucleotide sequences (5'- 3') to engineer AvrM-A and avrM genes.

AvrMattBF (5'-3')55bp	GGGGACAAGTTTGTACAAAAAAGCAGGCTTCCAACCAGAATTTGACAGAGGATTC
AvrMattBR (5'-3') 58bp	GGGGACCACTTTGTACAAGAAAGCTGGGTCTCACATGTCTGGAGATTTCAATATCTTG
AvrM_Fw :	CCAGAATTTGACAGAGGATTC
AvrM_Rv:	GTCTGGAGATTTCAATATCTTGTTGC

Appendix 2 (b): Oligonucleotide sequences (-5' - 3') used to engineer point mutation in avrM and AvrM-A. Reverse complementary sequences were used for the reverse primers of the same forward primers. Blue colour indicates the codon for the incoming mutant residue in which the changed nucleotide/s are underlined.

Mutation	Name of Primers	AvrM/avrM Sequencing Primers
AvrM-A primers		
AvrM ^{K226Q}	AvrM_K226Q_FW	GTATCGAAACAATCTC <u>CAG</u> AGGCAAACCTTATG
	AvrM_K226Q_RV	CATAAGTTTGCCT <u>CTG</u> GAGATTGTTTCGATAC
AvrM ^{K232R}	AvrM_K232R_FW	AGGCAAACCTTATGAA <u>CGT</u> CTTCTACGTTCC
	AvrM_K232R_RV	GGAACGTAGAAG <u>ACG</u> TTCATAAGTTTGCCT
AvrM ^{E237A}	AvrM_E237A_FW	CTTCTACGTTCC <u>GCT</u> ACGGATGTTTTG
	AvrM_E237A_RV	CAAACATCCGT <u>AGC</u> GGAACGTAGAAG
AvrM ^{L241S}	AvrM_L241S_FW	CCGAGACGGATGTT <u>TCG</u> TATAGGGAGGT
	AvrM_L241S_RV	ACCTCCCTATA <u>CGA</u> AACATCCGTCTCGG
AvrM ^{N259T}	AvrM ^{T259N} _FW	GAACCGGCGTTA <u>AAT</u> GCGAAGATCGAAC
	AvrM ^{T259N} _RV	GTTTCGATCTTCGC <u>ATT</u> TAACGCCGGTTC
AvrM _{PI280ΔL}	AvrM ^{PI280ΔL} _Fw	CACCCGAAGCAAAC <u>TT</u> * GATTACCTTGC {*ATT deleted}
	AvrM ^{PI280ΔL} _Rv	GCAAGGTAATC* <u>AA</u> GTTTGCTTCGGGTG {*AAT deleted}
AvrM ^{E309A}	AvrM_E309A_FW	GTATAAGGCT <u>GCT</u> ATCAAGGCGCG
	AvrM_E309A_RV	CGCGCCTTGAT <u>AGC</u> AGCCTTATAC
AvrM ^{I310T}	AvrM_I310T_FW	GTATAAGGCTGAG <u>ACC</u> AAGGCGC
	AvrM_I310T_RV	GCGCCTT <u>GGT</u> TCTCAGCCTTATAC
AvrM ^{R313A}	AvrM R313A _Fw	GAGATCAAGGCG <u>GCT</u> GAAATTGAAG
	AvrM R313A _Rv	CTTCAATTT <u>AGC</u> CGCCTTGATCTC
QuadAvrM	AvrM R313A _FwQuad	AGACCAAGGCG <u>GCT</u> GAAATTGAAGC
	AvrM R313A _RvQuad	GCTTCAATTT <u>AGC</u> CGCCTTGGTCT

(Table continued)

(Table continued)

AvrM ^{E316K}	AvrM ^{E316K} _Fw	GGCGCGTGAAATT <u>AAAGCCAACAGAGCT</u>
	AvrM ^{E316K} _Rv	AGCTCTGTTGGCTTTAATTTACGCGCC
AvrM ^{E309A} (Double)	AvrM_E309A_Fw(Dble)	GTATAAGGCTGCTATCAAGGCG <u>GCTG</u>
	AvrM_E309A_Rv(Dble)	<u>CAGC</u> CGCCTTGAT <u>AGC</u> AGCCTTATAC
EA3 (Triple)	AvrM-A ^{EA2+E316A} _Fw	GCGCGTGAAATT <u>GCT</u> GCCAACAGAGC
	AvrM-A ^{EA2+E316A} _Rv	GCTCTGTTGGC <u>AGC</u> AATTTACGCGC
avrM Primers		
avrM ^{K164Q}	avrM ^{K164Q} _FW	GTGTATCGAAACAATCTC <u>AAG</u> AGGCAAACCT
	avrM ^{K164Q} _RV	TTCATAAGTTTGCCT <u>CTI</u> GAGATTGTTTCG
avrM ^{R232K}	avrM_R232K_FW	GGCAAACCTATGAA <u>AAG</u> CTTCTACGTTCC
	avrM_R232K_RV	GGAACGTAGAAG <u>CTT</u> TTTCATAAGTTTGCC
avrM ^{S241L}	avrM_S241L_FW	CCGAGACGGATGTTT <u>IG</u> TATAGGGAGGT
	avrM_S241L_RV	ACCTCCCTATAC <u>CA</u> AAACATCCGTCTCGG
avrM ^{T248I}	avrM_T248I_FW	GAGGTTGCTAGAA <u>ATT</u> TCATCGCCAGG
	avrM_T248I_RV	CCTGGCGATGAA <u>AAT</u> TCTAGCAACCTC
avrM ^{N197T}	avrM ^{N197T} _FW	CCGGCGTTA <u>ACT</u> GCGAAGATCG
	avrM ^{N197T} _Rv	CGATCTTCGC <u>AGI</u> TAACGCCGG
avrM ^{ΔL217PI}	avrM ^{ΔL217PI} _Fw	GACACCCGAAGCAAAC <u>CCTATT</u> GATTACCTTGCTATCGC
	avrM ^{ΔL217PI} _Rv	GCGATAGCAAGGTAATC <u>AATAGG</u> TTTGCTTCGGGTGTC
avrM ^{T310I}	avrM ^{T310I} _Fw	GTATAAGGCTGAG <u>ATT</u> AAGGCGCGTGA
	avrM ^{T310I} _Rv	TCACGCGCCTT <u>AAT</u> TCTCAGCCTTATAC
avrM ^{K243E}	avrM ^{K243E} _Fw	GCGCGTGAAATT <u>GA</u> AGCCAACAGAG
	avrM ^{K243E} _Rv	CTCTGTTGGCTT <u>CA</u> AATTTACGCGC

Appendix 3: Sodium dodecyl sulphate polyacrylamide gel preparation

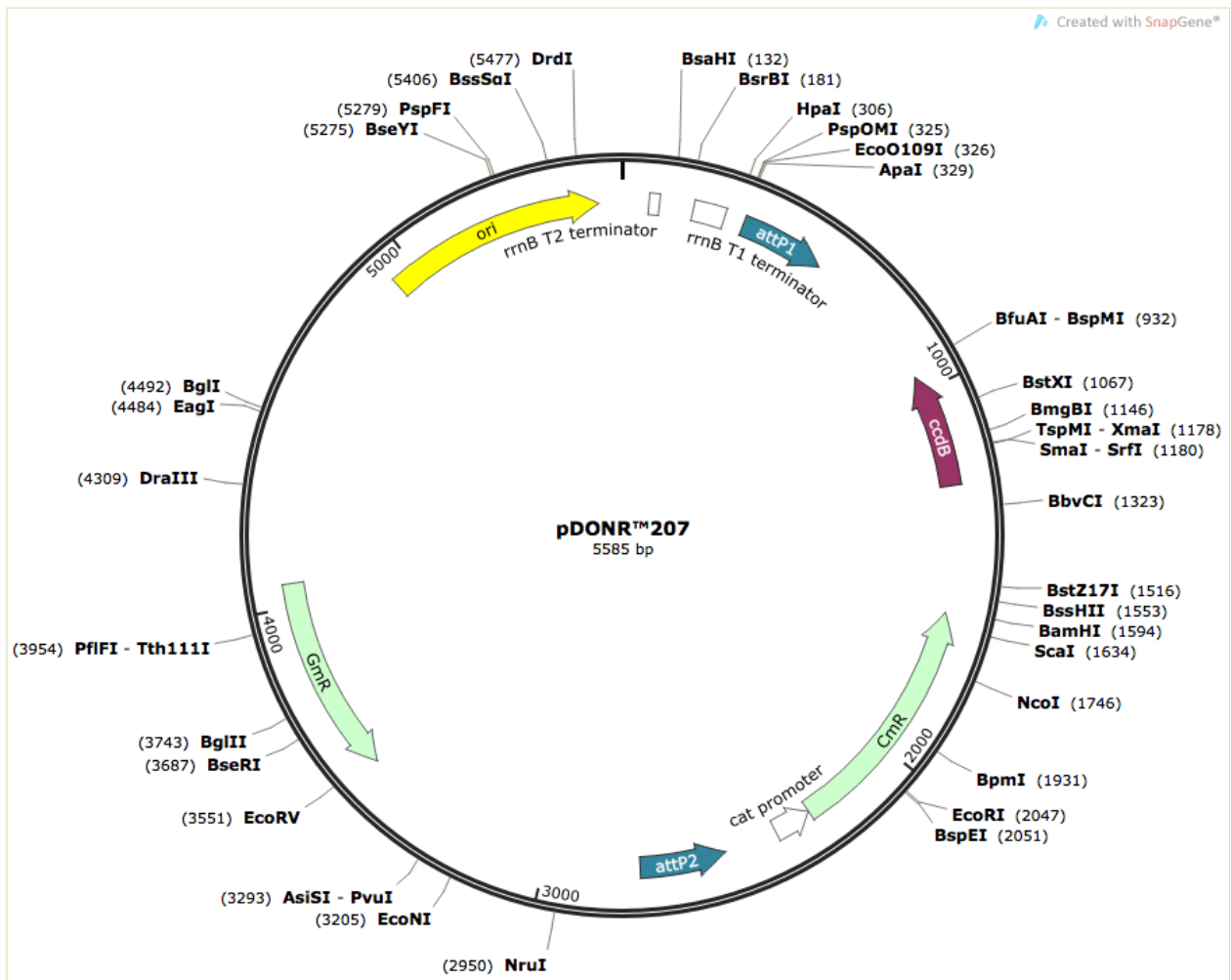
← Required amounts as per the numbers of gels →

15% Resolving gel									
No. of gel	1	2	3	4	5	6	7	8	9
Acrylamide (40%)	1.875	3.750	5.625	7.500	9.375	11.250	13.125	15.000	16.875
Mili-Q H ₂ O	1.798	3.595	5.393	7.190	8.988	10.785	12.583	14.380	16.178
1.5M Tris HCl pH 8.8	1.250	2.500	3.750	5.000	6.250	7.500	8.750	10.000	11.250
10% SDS	0.050	0.100	0.150	0.200	0.250	0.300	0.350	0.400	0.450
APS	0.025	0.050	0.075	0.100	0.125	0.150	0.175	0.200	0.225
TEMED	0.003	0.005	0.008	0.010	0.013	0.015	0.018	0.020	0.023

← Required amounts as per the numbers of gels →

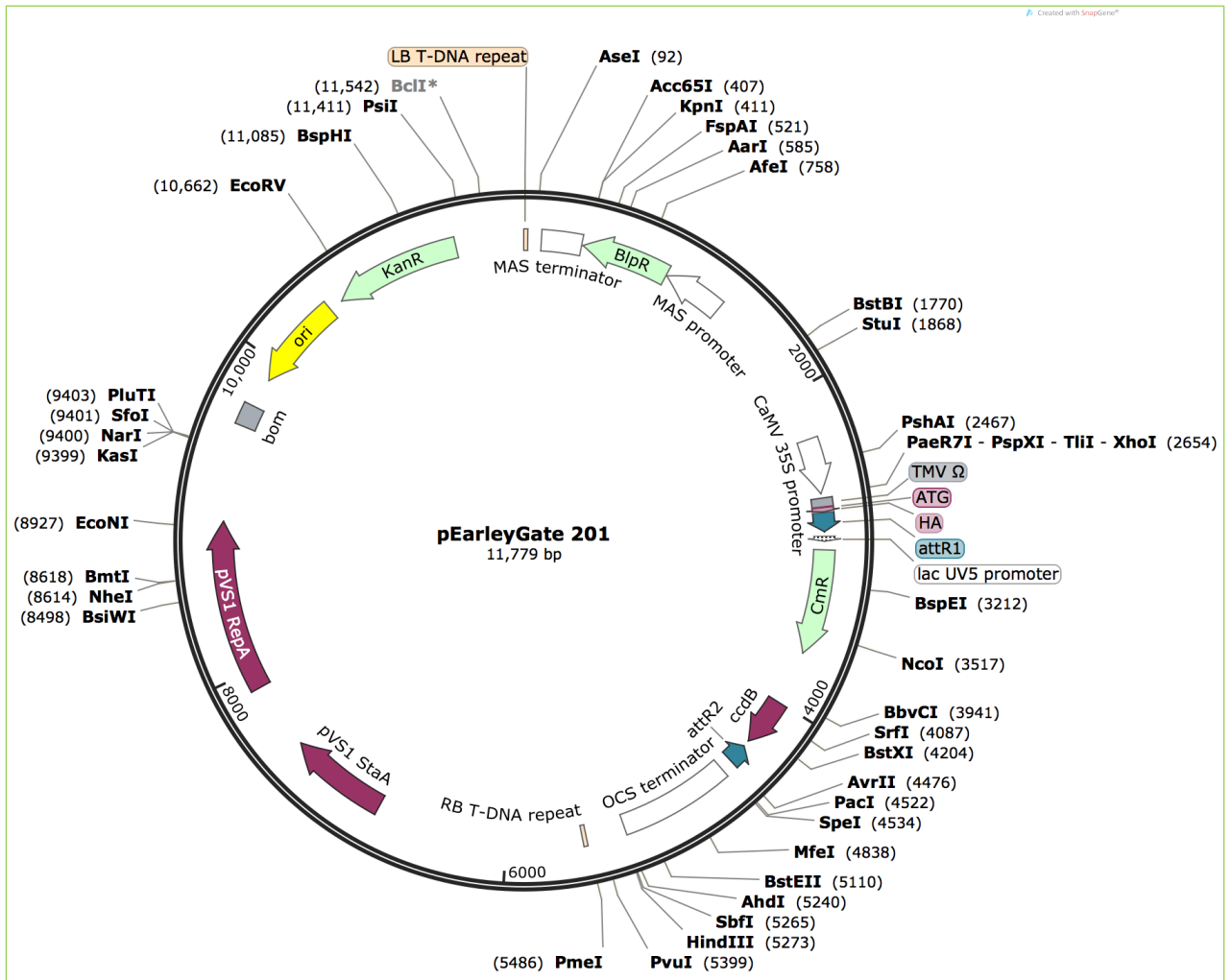
Stacking Gel									
No. of gel	1	2	3	4	5	6	7	8	9
Acrylamide	0.2500	0.500	0.750	1.000	1.250	1.500	1.750	2.000	2.250
DH₂O	1.585	3.170	4.755	6.340	7.925	9.510	11.095	12.68	14.265
0.5M Tris HCl pH 6.8	0.625	1.250	1.875	2.500	3.125	3.750	4.375	5.000	5.625
10% SDS	0.025	0.050	0.075	0.100	0.125	0.150	0.175	0.200	0.225
APS	0.0125	0.025	0.0375	0.050	0.063	0.075	0.088	0.100	0.113
TEMED	0.0025	0.005	0.0075	0.01	0.013	0.015	0.018	0.020	0.023

Appendix 4: Map and Sequence of pDONR 207 vector.



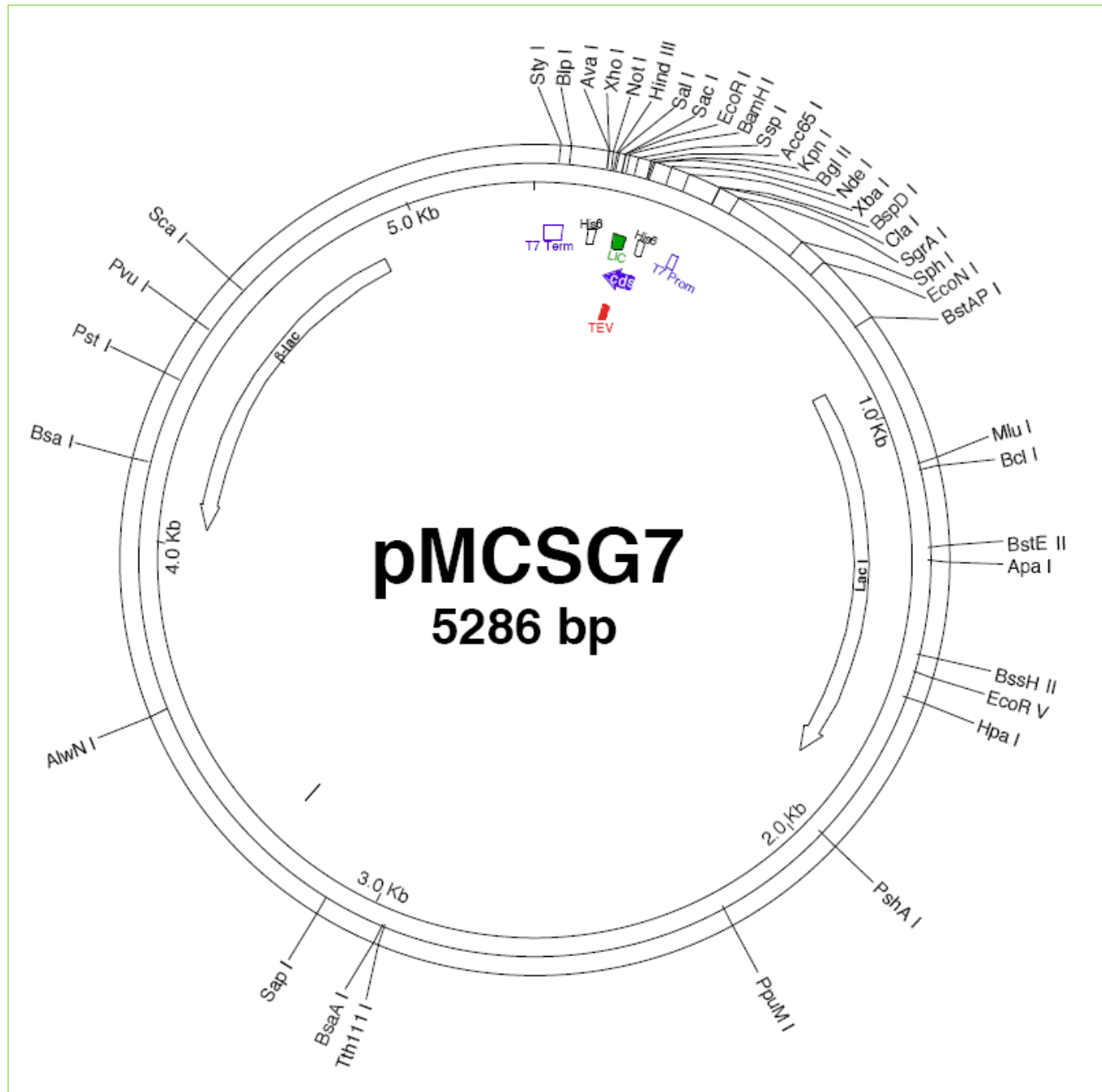
http://www.snapgene.com/resources/plasmid_files/gateway_cloning_vectors/pDONR207/

Appendix 5: Map and Sequence of pEarleyGate 201 vector.



http://www.snapgene.com/resources/plasmid_files/plant_vectors/pEarleyGate_201/

Appendix 6: Map and Sequence of pEarleyGate 201 vector.



MCSG Technologies: <http://bioinformatics.anl.gov/mcsg/technologies/vectors.html>

Bibliography

(Page 151-175)

Bibliography

- Allen, R. L., Bittner-Eddy, P. D., Grenville-Briggs, L. J., Meitz, J. C., Rehmany, A. P., Rose, L. E., and Beynon, J. L. (2004). Host-parasite coevolutionary conflict between *Arabidopsis* and downy mildew. *Science*, *306*(5703), 1957-1960.
- Anderson, P. A., Lawrence, G. J., Morrish, B. C., Ayliffe, M. A., Finnegan, E. J., and Ellis, J. G. (1997). Inactivation of the flax rust resistance gene M associated with loss of a repeated unit within the leucine-rich repeat coding region. *The Plant Cell Online*, *9*(4), 641-651.
- Armstrong, M. R., Whisson, S. C., Pritchard, L., Bos, J. I., Venter, E., Avrova, A. O., Rehmany, A. P., Böhme, U., Brooks, K. and Cherevach, I. (2005). An ancestral oomycete locus contains late blight avirulence gene *Avr3a*, encoding a protein that is recognized in the host cytoplasm. *Proceedings of the National Academy of Sciences of the United States of America*, *102*(21), 7766-7771.
- Bailey, K., Çevik, V., Holton, N., Byrne-Richardson, J., Sohn, K. H., Coates, M., Woods-Tör, A., Aksoy, H. M., Hughes, L., Baxter, L., Jones, J. D. G., Beynon, J., Holub E. B. and Tör M.(2011). Molecular cloning of ATR5Emoy2 from *Hyaloperonospora arabidopsidis*, an avirulence determinant that triggers RPP5-mediated defense in *Arabidopsis*. *Molecular Plant-Microbe Interactions*, *24*(7), 827-838.
- Baker, C., Chitrakar, R., Obulareddy, N., Panchal, S., Williams, P., and Melotto, M. (2010). Molecular battles between plant and pathogenic bacteria in the phyllosphere. *Brazilian Journal of Medical and Biological Research*, *43*(8), 698-704.
- Baker, N. A., Sept, D., Joseph, S., Holst, M. J., and McCammon, J. A. (2001). Electrostatics of nanosystems: application to microtubules and the ribosome. *Proceedings of the National Academy of Sciences*, *98*(18), 10037-10041.
- Baldauf, S. L., Roger, A., Wenk-Siefert, I., and Doolittle, W. F. (2000). A kingdom-level phylogeny of eukaryotes based on combined protein data. *Science*, *290*(5493), 972-977.
- Balesdent, M. H., Attard, A., Kuhn, M. L. and Rouxel, T. (2002). New avirulence genes in the phytopathogenic fungus *Leptosphaeria maculans*. *Phytopathology*, *92*, 1122-1133.
- Bendahmane, A., Farnham, G., Moffett, P., and Baulcombe, D. C. (2002). Constitutive gain-of-function mutants in a nucleotide binding site-leucine rich repeat protein encoded at the Rx locus of potato. *The Plant Journal*, *32*(2), 195-204.

- Bent, A. F., and Mackey, D. (2007). Elicitors, effectors, and *R* genes: the new paradigm and a lifetime supply of questions. *Annu. Rev. Phytopathol.*, 45, 399-436.
- Bernoux, M., Burdett, H., Williams, S. J., Zhang, X. Chen, C., Newell, K., Lawrence, G. J., Kobe, B., Ellis, J. G., Anderson, P. A. and Dodds, P. N. (2016). Comparative analysis of the flax immune receptors L6 and L7 suggests an equilibrium-based switch activation model. *The Plant Cell*, TPC2015-00303-RA.
- Bernoux, M., Ellis, J. G., and Dodds, P. N. (2011b). New insights in plant immunity signaling activation. *Current Opinion in Plant Biology*, 14(5), 512-518.
- Bernoux, M., Ve, T., Williams, S., Warren, C., Hatters, D., Valkov, E., Zhang, X., Ellis, J. G., Kobe, B. and Dodds, P. N. (2011a). Structural and functional analysis of a plant resistance protein TIR domain reveals interfaces for self-association, signaling, and autoregulation. *Cell Host and Microbe*, 9(3), 200-211.
- Birch, P. R., Boevink, P. C., Gilroy, E. M., Hein, I., Pritchard, L., and Whisson, S. C. (2008). Oomycete RXLR effectors: delivery, functional redundancy and durable disease resistance. *Current Opinion in Plant Biology*, 11(4), 373-379.
- Bittner-Eddy, P. D., Crute, I. R., Holub, E. B., and Beynon, J. L. (2000). RPP13 is a simple locus in *Arabidopsis thaliana* for alleles that specify downy mildew resistance to different avirulence determinants in *Peronospora parasitica*. *The Plant Journal*, 21(2), 177-188.
- Block, A., Li, G., Fu, Z. Q., and Alfano, J. R. (2008). Phytopathogen type III effector weaponry and their plant targets. *Current Opinion in Plant Biology*, 11(4), 396-403.
- Blondeau, K., Blaise, F., Graille, M., Kale, S. D., Linglin, J., Ollivier, B., Labarde, A., Lazar, N., Daverdin, G. and Balesdent, M. H. (2015). Crystal structure of the effector AvrLm4-7 of *Leptosphaeria maculans* reveals insights into its translocation into plant cells and recognition by resistance proteins. *The Plant Journal*, 83(4), 610-624.
- Bohnert, H. U., Fudal, I., Dioh, W., Tharreau, D., Notteghem, J. L. and Lebrun, M. H. (2004). A putative polyketide synthase/peptide synthetase from *Magnaporthe grisea* signals pathogen attack to resistant rice. *Plant Cell*, 16, 2499-2513.
- Boller, T., and He, S. Y. (2009). Innate immunity in plants: an arms race between pattern recognition receptors in plants and effectors in microbial pathogens. *Science (New York, NY)*, 324(5928), 742.
- Bonas, U., and Ackerveken, G. (1997). Recognition of bacterial avirulence proteins occurs inside the plant cell: a general phenomenon in resistance to bacterial diseases? *The Plant Journal*, 12(1), 1-7.

- Bonman, J., Khush, G., and Nelson, R. (1992). Breeding rice for resistance to pests. *Annual Review of Phytopathology*, 30(1), 507-528.
- Bos, J. I., Chaparro-Garcia, A., Quesada-Ocampo, L. M., Gardener, B. B. M., and Kamoun, S. (2009). Distinct amino acids of the *Phytophthora infestans* effector AVR3a condition activation of R3a hypersensitivity and suppression of cell death. *Molecular Plant-Microbe Interactions*, 22(3), 269-281.
- Bos, J. I., Kanneganti, T. D., Young, C., Cakir, C., Huitema, E., Win, J., Miles R. Armstrong, M. R., Birch P. R. J. Kamoun, S. (2006). The C-terminal half of *Phytophthora infestans* RXLR effector AVR3a is sufficient to trigger R3a-mediated hypersensitivity and suppress INF1-induced cell death in *Nicotiana benthamiana*. *The Plant Journal*, 48(2), 165-176.
- Boutemy, L. S., King, S. R., Win, J., Hughes, R. K., Clarke, T. A., Blumenschein, T. M., Kamoun, S. and Banfield, M. J. (2011). Structures of *Phytophthora* RXLR effector proteins a conserved but adaptable fold underpins functional diversity. *Journal of Biological Chemistry*, 286(41), 35834-35842.
- Bozkurt, T. O., Schornack, S., Win, J., Shindo, T., Ilyas, M., Oliva, R., Cano, L. M., Jones, A. M. E., Huitema, E. and van der Hoorn, R. A. (2011). *Phytophthora infestans* effector AVRblb2 prevents secretion of a plant immune protease at the haustorial interface. *Proceedings of the National Academy of Sciences*, 108(51), 20832-20837.
- Bradford, M. M. (1976). A rapid and sensitive method for the quantitation of microgram quantities of protein utilizing the principle of protein-dye binding. *Analytical biochemistry*, 72(1), 248-254.
- Buell, C. R., Joardar, V., Lindeberg, M., Selengut, J., Paulsen, I. T., Gwinn, M. L., Dodson, R. J., Deboy, R. T., Durkin, A. S. and Kolonay, J. F. (2003). The complete genome sequence of the Arabidopsis and tomato pathogen *Pseudomonas syringae* pv. tomato DC3000. *Proceedings of the National Academy of Sciences*, 100(18), 10181-10186.
- Catanzariti, A. M., Dodds, P. N., and Ellis, J. G. (2007). Avirulence proteins from haustoria-forming pathogens. *FEMS Microbiology Letters*, 269(2), 181-188.
- Catanzariti, A. M., Lim, G. T., and Jones, D. A. (2015). The tomato *I-3* gene: a novel gene for resistance to Fusarium wilt disease. *New Phytologist* (2015) 207: 106–118.
- Catanzariti, A.-M., Dodds, P. N., Lawrence, G. J., Ayliffe, M. A. and Ellis, J. G. (2006). Haustorially expressed secreted proteins from flax rust are highly enriched for avirulence elicitors. *The Plant Cell Online*, 18(1), 243-256.

- Catanzariti, A.-M., Dodds, P. N., Ve, T., Kobe, B., Ellis, J. G. and Staskawicz, B. J. (2010a). The AvrM effector from flax rust has a structured C-terminal domain and interacts directly with the M resistance protein. *Molecular Plant-Microbe Interactions*, 23(1), 49-57.
- Catanzariti, A.-M., Dodds, P., Ellis, J. and Staskawicz, B. (2010b). The interaction of avirulence and resistance gene products in flax rust disease-providing advances in rust research†. *Canadian Journal of Plant Pathology*, 32(1), 11-19.
- Cheng, W., Munkvold, K. R., Gao, H., Mathieu, J., Schwizer, S., Wang, S., Sha Y., Yong-bin W., Jinjing M., Gregory, B. and Chai, J. (2011). Structural analysis of *Pseudomonas syringae* AvrPtoB bound to host BAK1 reveals two similar kinase-interacting domains in a type III Effector. *Cell Host and Microbe*, 10(6), 616-626.
- Chisholm, S. T., Coaker, G., Day, B. and Staskawicz, B. J. (2006). Host-microbe interactions: shaping the evolution of the plant immune response. *Cell*, 124(4), 803-814. doi:10.1016/j.cell.2006.02.008
- Chou, S., Krasileva, K. V., Holton, J. M., Steinbrenner, A. D., Alber, T. and Staskawicz, B. J. (2011). Hyaloperonospora arabidopsidis ATR1 effector is a repeat protein with distributed recognition surfaces. *Proceedings of the National Academy of Sciences*, 108(32), 13323-13328.
- Coates, M. E. and Beynon, J. L. (2010). *Hyaloperonospora arabidopsidis* as a pathogen model. *Annual Review of Phytopathology*, 48, 329-345.
- Collemare, J., Pianfetti, M., Houle, A. E., Morin, D., Camborde, L., Gagey, M. J., Barbisan, C., Fudal, I., Lebrun, M. H. and Bo?hnert, H. U. (2008). *Magnaporthe grisea* avirulence gene *ACE1* belongs to an infection-specific gene cluster involved in secondary metabolism. *New Phytol.* 179, 196-208.
- Collier, S. M. and Moffett, P. (2009). NB-LRRs work a “bait and switch” on pathogens. *Trends in Plant Science*, 14(10), 521-529.
- Collins, N., Drake, J., Ayliffe, M., Sun, Q., Ellis, J., Hulbert, S. and Pryor, T. (1999). Molecular characterization of the maize Rp1-D rust resistance haplotype and its mutants. *The Plant Cell*, 11(7), 1365-1376.
- Collmer, A. (1998). Determinants of pathogenicity and avirulence in plant pathogenic bacteria. *Current Opinion in Plant Biology*, 1(4), 329-335.
- Cui, H., Xiang, T. and Zhou, J. M. (2009). Plant immunity: a lesson from pathogenic bacterial effector proteins. *Cellular Microbiology*, 11(10), 1453-1461.

- Dangl, J. L. and Jones, J. D. (2001). Plant pathogens and integrated defence responses to infection. *Nature*, *411*(6839), 826-833.
- Dangl, J. L., Horvath, D. M. and Staskawicz, B. J. (2013). Pivoting the plant immune system from dissection to deployment. *Science*, *341*(6147), 746-751.
- Daverdin, G., Rouxel, T., Gout, L., Aubertot, J.-N., Fudal, I., Meyer, M., Parlange, F., Carpezat, J. and Balesdent, M.-H. (2012). Genome structure and reproductive behaviour influence the evolutionary potential of a fungal phytopathogen. *PLoS Pathog*, *8*(11), e1003020. doi:1003010.1001371/journal.ppat.100 3020.
- de las Mercedes Dana, M., Pintor-Toro, J. A., and Cubero, B. (2006). Transgenic tobacco plants overexpressing chitinases of fungal origin show enhanced resistance to biotic and abiotic stress agents. *Plant Physiology*, *142*(2), 722-730.
- De Wit, P. J. G. M., Lauge, R., Honee, G., Joosten, M. H. A. J., Vossen, P., Kooman-Gersmann, M., Vogelsang, R. and Vervoort, J. J. M. (1997). Molecular and biochemical basis of the interaction between tomato and its fungal pathogen *Cladosporium fulvum*. *Antonie Van Leeuwenhoek*, *71*, 137-141.
- Dean, R., Van Kan, J. A., Pretorius, Z. A., Hammond-Kosack, K. E., Di Pietro, A., Spanu, P. D., Rudd, J. J., Dickman, M., Kahmann, R. and Ellis, J. (2012). The Top 10 fungal pathogens in molecular plant pathology. *Molecular Plant Pathology*, *13*(4), 414-430.
- deCourcy-Ireland, E. (2014). Refining the Model of Plant Disease Resistance Protein Activation *PhD Thesis, Flinders University, Australia*.
- Dodds, P. and Thrall, P. (2009). Goldacre paper: Recognition events and host-pathogen co-evolution in gene-for-gene resistance to flax rust. *Functional Plant Biology*, *36*(5), 395-408.
- Dodds, P. N., and Rathjen, J. P. (2010). Plant immunity: towards an integrated view of plant-pathogen interactions. *Nature Reviews Genetics*, *11*(8), 539-548.
- Dodds, P. N., Catanzariti, A.-M., Lawrence, G. J., and Ellis, J. G. (2007). Avirulence proteins of rust fungi: penetrating the host-haustorium barrier. *Crop and Pasture Science*, *58*(6), 512-517.
- Dodds, P. N., Lawrence, G. J., and Ellis, J. G. (2001a). Contrasting modes of evolution acting on the complex N locus for rust resistance in flax. *The Plant Journal*, *27*(5), 439-453.
- Dodds, P. N., Lawrence, G. J., and Ellis, J. G. (2001b). Six amino acid changes confined to the leucine-rich repeat β -strand/ β -turn motif determine the difference

- between the P and P2 rust resistance specificities in flax. *The Plant Cell*, *13*(1), 163-178.
- Dodds, P. N., Lawrence, G. J., Catanzariti, A.-M., Teh, T., Wang, C.-I., Ayliffe, M. A., Kobe, B. and Ellis, J. G. (2006). Direct protein interaction underlies gene-for-gene specificity and coevolution of the flax resistance genes and flax rust avirulence genes. *Proceedings of the National Academy of Sciences*, *103*(23), 8888-8893.
- Dodds, P. N., Rafiqi, M., Gan, P. H., Hardham, A. R., Jones, D. A., and Ellis, J. G. (2009a). Effectors of biotrophic fungi and oomycetes: pathogenicity factors and triggers of host resistance. *New Phytologist*, *183*(4), 993-1000.
- Dong, J., Xiao, F., Fan, F., Gu, L., Cang, H., Martin, G. B. and Chai, J. (2009). Crystal structure of the complex between Pseudomonas effector AvrPtoB and the tomato Pto kinase reveals both a shared and a unique interface compared with AvrPto-Pto. *The Plant Cell*, *21*(6), 1846-1859.
- Dou, D., Kale, S. D., Wang, X., Chen, Y., Wang, Q., Wang, X., Jiang, R. H., Arredondo, F. D., Anderson, R. G. and Thakur, P. B. (2008). Conserved C-terminal motifs required for avirulence and suppression of cell death by *Phytophthora sojae* effector Avr1b. *The Plant Cell Online*, *20*(4), 1118-1133.
- Earley, K. W., Haag, J. R., Pontes, O., Opper, K., Juehne, T., Song, K., and Pikaard, C. S. (2006). Gateway-compatible vectors for plant functional genomics and proteomics. *The Plant Journal*, *45*(4), 616-629.
- Eckardt, N. A. (2006). Identification of rust fungi avirulence elicitors. *The Plant Cell Online*, *18*(1), 1-3.
- Ellingboe, A. (1992). Segregation of avirulence/virulence on three rice cultivars in 16 crosses of *Magnaporthe grisea*. *Phytopathology*, *82*(5), 597-601.
- Ellis, J. G., Lawrence, G. J., Luck, J. E. and Dodds, P. N. (1999). Identification of regions in alleles of the flax rust resistance gene L that determine differences in gene-for-gene specificity. *The Plant Cell Online*, *11*(3), 495-506.
- Ellis, J. G., Mago, R., Kota, R., Dodds, P. N., McFadden, H., Lawrence, G., Spielmeier, W. and Lagudah, E. (2007a). Wheat rust resistance research at CSIRO. *Crop and Pasture Science*, *58*(6), 507-511.
- Ellis, J. G., Rafiqi, M., Gan, P., Chakrabarti, A., and Dodds, P. N. (2009). Recent progress in discovery and functional analysis of effector proteins of fungal and oomycete plant pathogens. *Current Opinion in Plant Biology*, *12*(4), 399-405.

- Ellis, J., Catanzariti, A.-M., and Dodds, P. (2006). The problem of how fungal and oomycete avirulence proteins enter plant cells. *Trends in Plant Science*, 11(2), 61-63.
- Ellis, J., Lawrence, G., Ayliffe, M., Anderson, P., Collins, N., Finnegan, J., Frost, D., Luck, J. and Pryor, T. (1997). Advances in the molecular genetic analysis of the flax-flax rust interaction. *Annu. Rev. Phyto-pathol.* 35, 271-291.
- Flor, H. H. (1955). Host-parasite interaction in flax rust-its genetics and other implications. *Phytopathology*, 45(12), 680-685.
- Flor, H. H. (1956). The complementary genic systems in flax and flax rust. *Adv. Genetics*, 8, 29-54.
- Flor, H. H. (1971). Current status of the gene-for-gene concept. *Annual review of phytopathology*, 9(1), 275-296.
- Freeman, B. C., and Beattie, G. A. (2008). An overview of plant defenses against pathogens and herbivores. *The Plant Health Instructor*, <http://www.apsnet.org/edcenter/intropp/topics/Pages/OverviewOfPlantDiseases.aspx>.
- Galán, J. E., and Collmer, A. (1999). Type III secretion machines: bacterial devices for protein delivery into host cells. *Science*, 284(5418), 1322-1328.
- Gallagher, S., and Chakavarti, D. (2008). Immunoblot Analysis. *J. Vis. Exp.* (16), e759, doi:10.3791/759. <http://www.jove.com/video/759/immunoblot-analysis>
- Gan, P. H., Rafiqi, M., Hardham, A. R., and Dodds, P. N. (2010). Effectors of biotrophic fungal plant pathogens. *Functional Plant Biology*, 37(10), 913-918.
- Gimenez-Ibanez, S., Hann, D. R., Ntoukakis, V., Petutschnig, E., Lipka, V., and Rathjen, J. P. (2009). AvrPtoB targets the LysM receptor kinase CERK1 to promote bacterial virulence on plants. *Current Biology*, 19(5), 423-429.
- Göhre, V., and Robatzek, S. (2008). Breaking the barriers: microbial effector molecules subvert plant immunity. *Annu. Rev. Phytopathol.*, 46, 189-215.
- Göhre, V., Spallek, T., Häweker, H., Mersmann, S., Mentzel, T., Boller, T., de Torres, M., Mansfield, J. W. and Robatzek, S. (2008). Plant pattern-recognition receptor FLS2 is directed for degradation by the bacterial ubiquitin ligase AvrPtoB. *Current Biology*, 18(23), 1824-1832.

- Gómez-Gómez, L., and Boller, T. (2000). FLS2: an LRR receptor-like kinase involved in the perception of the bacterial elicitor flagellin in *Arabidopsis*. *Molecular Cell*, 5(6), 1003-1011.
- Goss, E. M., Tabima, J. F., Cooke, D. E., Restrepo, S., Fry, W. E., Forbes, G. A., Fieland, V. J., Cardenas, M. and Grünwald, N. J. (2014). The irish potato famine pathogen *phytophthora infestans* originated in central mexico rather than the andes. *Proceedings of the National Academy of Sciences*, 111(24), 8791-8796.
- Greenberg, J. T. (1997). Programmed cell death in plant-pathogen interactions. *Annual Review of Plant Biology*, 48(1), 525-545.
- Gu, K., Yang, B., Tian, D., Wu, L., Wang, D., Sreekala, C., Yang, F., Chu, Z., Wang, G-L. and White, F. F. (2005). *R* gene expression induced by a type-III effector triggers disease resistance in rice. *Nature*, 435(7045), 1122-1125.
- Gunderson, J. H., Elwood, H., Ingold, A., Kindle, K., and Sogin, M. L. (1987). Phylogenetic relationships between chlorophytes, chrysophytes, and oomycetes. *Proceedings of the National Academy of Sciences*, 84(16), 5823-5827.
- Gururani, M. A., Venkatesh, J., Upadhyaya, C. P., Nookaraju, A., Pandey, S. K., and Park, S. W. (2012). Plant disease resistance genes: current status and future directions. *Physiological and Molecular Plant Pathology*, 78, 51-65.
- Haas, B. J., Kamoun, S., Zody, M. C., Jiang, R. H., Handsaker, R. E., Cano, L. M., Grabherr, M., Kodira, C. D., Raffaele, S., Torto-Alalibo, T., Bozkurt, T. O., Ah-Fong, A. M., Alvarado, L., Anderson, V. L., Armstrong, M. R., Avrova, A., Baxter, L., Beynon, J., Boevink, P. C., Bollmann, S. R., Bos, J. I., Bulone, V., Cai, G., Cakir, C., Carrington, J.C., Chawner, M., Conti, L., Costanzo, S., Ewan, R., Fahlgren, N., Fischbach, M. A., Fugelstad, J., Gilroy, E. M., Gnerre, S., Green, P. J., Grenville-Briggs, L. J., Griffith, J., Grunwald, N. J., Horn, K., Horner, N. R., Hu, C. H., Huitema, E., Jeong, D. H., Jones, A. M., Jones, J. D., Jones, R. W., Karlsson, E. K., Kunjeti, S. G., Lamour, K., Liu, Z., Ma, L., Maclean, D., Chibucos, M. C., McDonald, H., McWalters, J., Meijer, H. J., Morgan, W., Morris, P. F., Munro, C. A., O'Neill, K., Ospina-Giraldo, M., Pinzon, A., Pritchard, L., Ramsahoye, B., Ren, Q., Restrepo, S., Roy, S., Sadanandom, A., Savidor, A., Schornack, S., Schwartz, D. C., Schumann, U. D., Schwessinger, B., Seyer, L., Sharpe, T., Silvar, C., Song, J., Studholme, D. J., Sykes, S., Thines, M., van de Vondervoort, P. J., Phuntumart, V., Wawra, S., Weide, R., Win, J., Young, C., Zhou, S., Fry, W., Meyers, B. C., van West, P., Ristaino, J., Govers, F., Birch, P. R., Whisson, S. C., Judelson, H. S., and Nusbaum, C. 2009. Genome sequence and analysis of the Irish potato famine pathogen *Phytophthora infestans*. *Nature*, 461:393-398.

- Hahn, M., and Mendgen, K. (2001). Signal and nutrient exchange at biotrophic plant-fungus interfaces. *Current Opinion in Plant Biology*, 4(4), 322-327.
- Hahn, M., Jungling, S. and Knogge, W. (1993). Cultivar-specific elicitation of barley defense reactions by the phytotoxic peptide NIP1 from *Rhynchosporium secalis*. *Mol. Plant-Microbe Interact.* 6, 745-754.
- Haldane, J. (1992). Disease and evolution. *Current Science*, 63(9), 599-604. {often recited, e.g., in Dronamraju, K. (Editor), 1990, Selected Genetic Papers of J.B.S. Haldane, Garland Publishing, New York/London}.
- Han, S.-W., Sriariyanun, M., Lee, S.-W., Sharma, M., Bahar, O., Bower, Z., and Ronald, P. C. (2011). Small protein-mediated quorum sensing in a Gram-negative bacterium. *PLoS One*, 6(12), e29192-e29192.
- Hardham, A. R., and Cahill, D. M. (2010). The role of oomycete effectors in plant-pathogen interactions. *Functional Plant Biology*, 37(10), 919-925.
- Harris, C. J., Sloopweg, E. J., Govere, A., and Baulcombe, D. C. (2013). Stepwise artificial evolution of a plant disease resistance gene. *Proceedings of the National Academy of Sciences*, 110(52), 21189-21194.
- Haverkort, A., Boonekamp, P., Hutten, R., Jacobsen, E., Lotz, L., Kessel, G., Visser, R. and Van der Vossen, E. (2008). Societal costs of late blight in potato and prospects of durable resistance through cisgenic modification. *Potato Research*, 51(1), 47-57.
- He, Y.-W., Wu, J. e., Cha, J.-S., and Zhang, L.-H. (2010). Rice bacterial blight pathogen *Xanthomonas oryzae* pv. *oryzae* produces multiple DSF-family signals in regulation of virulence factor production. *BMC Microbiology*, 10(1), 187.
- Heath, M. C. (1997). Signalling between pathogenic rust fungi and resistant or susceptible host plants. *Annals of Botany*, 80(6), 713-720.
- Hoch, H. C., Staples, R. C., Whitehead, B., Comeau, J., and Wolf, E. D. (1987). Signaling for growth orientation and cell differentiation by surface topography in *Uromyces*. *Science*, 235(4796), 1659-1662.
- Holub, E. B. (2008). Natural history of *Arabidopsis thaliana* and oomycete symbioses *The Downy Mildews-Genetics, Molecular Biology and Control* (pp. 91-109): Springer.
- Holub, E., and Beynon, J. (1997). Symbiology of mouse-ear cress (*Arabidopsis thaliana*) and oomycetes. *Advances in Botanical Research*, 24, 228-275.

- Howles, P., Lawrence, G., Finnegan, J., McFadden, H., Ayliffe, M., Dodds, P., and Ellis, J. (2005). Autoactive alleles of the flax L6 rust resistance gene induce non-race-specific rust resistance associated with the hypersensitive response. *Molecular Plant-Microbe Interactions*, 18(6), 570-582.
- Huang, C. C. and Lindhout, P. (1997). Screening for resistance in wild *Lycopersicon* species to *Fusarium oxysporum* f. sp. *lycopersici* race 1 and race 2. *Euphytica*, 93, 145-153.
- Hückelhoven, R. (2007). Cell wall-associated mechanisms of disease resistance and susceptibility. *Annu. Rev. Phytopathol.*, 45, 101-127.
- Hueck, C. J. (1998). Type III protein secretion systems in bacterial pathogens of animals and plants. *Microbiology and Molecular Biology Reviews*, 62(2), 379-433.
- Islam, M., and Mayo, G. (1990). A compendium on host genes in flax conferring resistance to flax rust. *Plant Breeding*, 104(2), 89-100.
- Jeong, K. S., Lee, S. E., Han, J. W., Yang, S. U., Lee, B. M., Noh, T. H., and Cha, J.-S. (2008). Virulence reduction and differing regulation of virulence genes in *rpf* mutants of *Xanthomonas oryzae* pv. *oryzae*. *Plant Pathol J*, 24(2), 143-151.
- Jia, Y., McAdams, S. A., Bryan, G. T., Hershey, H. P., and Valent, B. (2000). Direct interaction of resistance gene and avirulence gene products confers rice blast resistance. *The EMBO Journal*, 19(15), 4004-4014.
- Joardar, V., Lindeberg, M., Jackson, R. W., Selengut, J., Dodson, R., Brinkac, L. M., Daugherty, S. C., DeBoy, R., Durkin, A. S. and Giglio, M. G. (2005). Whole-genome sequence analysis of *Pseudomonas syringae* pv. *phaseolicola* 1448A reveals divergence among pathovars in genes involved in virulence and transposition. *Journal of Bacteriology*, 187(18), 6488-6498.
- Jones, J. D., and Dangl, J. L. (2006). The plant immune system. *Nature*, 444(7117), 323-329.
- Jones, J. T., Haegeman, A., Danchin, E. G., Gaur, H. S., Helder, J., Jones, M. G., Kikuchi, T., Manzanilla-López, R., Palomares-Rius, J. E. and Wesemael, W. M. (2013). Top 10 plant-parasitic nematodes in molecular plant pathology. *Molecular Plant Pathology*, 14(9), 946-961.
- Joosten, M. H. A. J. and De Wit, P. J. G. M. (1999). The tomato-*Cladosporium fulvum* interaction: a versatile experimental system to study plant-pathogen interactions. *Annu. Rev. Phytopathol.* 37, 335-367.
- Judelson, H. S., and Blanco, F. A. (2005). The spores of *Phytophthora*: weapons of the plant destroyer. *Nature Reviews Microbiology*, 3(1), 47-58.

- Kale, S. D., and Tyler, B. M. (2011). Entry of oomycete and fungal effectors into plant and animal host cells. *Cellular Microbiology*, 13(12), 1839-1848.
- Kale, S. D., Gu, B., Capelluto, D. G., Dou, D., Feldman, E., Rumore, A., Arredondo, F. D., Hanlon, R., Fudal, I. and Rouxel, T. (2010). External lipid PI3P mediates entry of eukaryotic pathogen effectors into plant and animal host cells. *Cell*, 142(2), 284-295.
- Kamoun, S. (2003). Molecular genetics of pathogenic oomycetes. *Eukaryotic Cell*, 2(2), 191-199.
- Kamoun, S. (2006). A catalogue of the effector secretome of plant pathogenic oomycetes. *Annu. Rev. Phytopathol.*, 44, 41-60.
- Kamoun, S., Furzer, O., Jones, J. D., Judelson, H. S., Ali, G. S., Dalio, R. J., Roy, S. G., Schena, L., Zambounis, A. and Panabières, F. (2015). The Top 10 oomycete pathogens in molecular plant pathology. *Molecular Plant Pathology*, 16(4), 413-434.
- Kamoun, S., van West, P., Vleeshouwers, V. G., de Groot, K. E., and Govers, F. (1998). Resistance of *Nicotiana benthamiana* to *Phytophthora infestans* is mediated by the recognition of the elicitor protein INF1. *The Plant Cell*, 10(9), 1413-1425.
- Kang, S., Sweigard, J. A. and Valent, B. (1995) The *PWL* host specificity gene family in the blast fungus *Magnaporthe grisea*. *Mol. Plant-Microbe Interact.* 8, 939-948.
- Kanzaki, H., Yoshida, K., Saitoh, H., Fujisaki, K., Hirabuchi, A., Alaux, L., Fournier, E., Tharreau, D. and Terauchi, R. (2012). Arms race co-evolution of *Magnaporthe oryzae AVR-Pik* and rice *Pik* genes driven by their physical interactions. *The Plant Journal*, 72(6), 894-907.
- Kaschani, F., Shabab, M., Bozkurt, T., Shindo, T., Schornack, S., Gu, C., Ilyas, M., Win, J., Kamoun, S. and van der Hoorn, R. A. (2010). An effector-targeted protease contributes to defense against *Phytophthora infestans* and is under diversifying selection in natural hosts. *Plant Physiology*, 154(4), 1794-1804.
- Kay, S., Hahn, S., Marois, E., Hause, G., and Bonas, U. (2007). A bacterial effector acts as a plant transcription factor and induces a cell size regulator. *Science*, 318(5850), 648-651.
- Kemen, E., Kemen, A. C., Rafiqi, M., Hempel, U., Mendgen, K., Hahn, M. and Voegelé, R. T. (2005). Identification of a protein from rust fungi transferred from haustoria into infected plant cells. *Molecular Plant-Microbe Interactions*, 18(11), 1130-1139.

- Kemen, E., Kemen, A., Ehlers, A., Voegelé, R., and Mendgen, K. (2013). A novel structural effector from rust fungi is capable of fibril formation. *The Plant Journal*, 75(5), 767-780.
- Khan, M., Subramaniam, R., and Desveaux, D. (2016). Of guards, decoys, baits and traps: pathogen perception in plants by type III effector sensors. *Current Opinion in Microbiology*, 29, 49-55.
- Kobayashi, I., Kobayashi, Y., and Hardham, A. R. (1994). Dynamic reorganization of microtubules and microfilaments in flax cells during the resistance response to flax rust infection. *Planta*, 195(2), 237-247.
- Krasileva, K. V., Dahlbeck, D., and Staskawicz, B. J. (2010). Activation of an *Arabidopsis* resistance protein is specified by the in planta association of its leucine-rich repeat domain with the cognate oomycete effector. *The Plant Cell Online*, 22(7), 2444-2458.
- Kushnirov, V. V. (2000). Rapid and reliable protein extraction from yeast. *Yeast*, 16(9), 857-860.
- Laemmli, U. K. (1970). Cleavage of structural proteins during the assembly of the head of bacteriophage T4. *Nature*, 227(5259), 680-685.
- Latijnhouwers, M., de Wit, P. J., and Govers, F. (2003). Oomycetes and fungi: similar weaponry to attack plants. *Trends in Microbiology*, 11(10), 462-469.
- Laugé, R., and De Wit, P. J. (1998). Fungal avirulence genes: structure and possible functions. *Fungal Genetics and Biology*, 24(3), 285-297.
- Lawrence, G. J., Anderson, P. A., Dodds, P. N., and Ellis, J. G. (2010b). Relationships between rust resistance genes at the M locus in flax. *Molecular Plant Pathology*, 11(1), 19-32.
- Lawrence, G. J., Dodds, P. N., and Ellis, J. G. (2007). Rust of flax and linseed caused by *Melampsora lini*. *Molecular Plant Pathology*, 8(4), 349-364.
- Lawrence, G. J., Dodds, P. N., and Ellis, J. G. (2010a). Technical advance: transformation of the flax rust fungus, *Melampsora lini*: selection via silencing of an avirulence gene. *The Plant Journal*, 61(2), 364-369.
- Lawrence, G. J., Finnegan, E. J., Ayliffe, M. A., and Ellis, J. G. (1995). The L6 gene for flax rust resistance is related to the *Arabidopsis* bacterial resistance gene *RPS2* and the tobacco viral resistance gene *N*. *The Plant Cell Online*, 7(8), 1195-1206.

- Lee, C. C., Wood, M. D., Ng, K., Andersen, C. B., Liu, Y., Luginbühl, P., Spraggon, G. and Katagiri, F. (2004). Crystal structure of the type III effector AvrB from *Pseudomonas Syringae*. *Structure*, 12(3), 487-494.
- Lee, S.-K., Song, M.-Y., Seo, Y.-S., Kim, H.-K., Ko, S., Cao, P.-J., Yi, G., Roh, J-H. and Lee, S. (2009). Rice Pi5-mediated resistance to *Magnaporthe oryzae* requires the presence of two coiled-coil-nucleotide-binding-leucine-rich repeat genes. *Genetics*, 181(4), 1627-1638.
- Lee, S.-W., Han, S.-W., Bartley, L. E., and Ronald, P. C. (2006). Unique characteristics of *Xanthomonas oryzae* pv. *oryzae* AvrXa21 and implications for plant innate immunity. *Proceedings of the National Academy of Sciences*, 103(49), 18395-18400.
- Leonelli, L., Pelton, J., Schoeffler, A., Dahlbeck, D., Berger, J., Wemmer, D. E., and Staskawicz, B. (2011). Structural elucidation and functional characterization of the *Hyaloperonospora arabidopsidis* effector protein ATR13. *PLoS Pathogens*, 7(12), e1002428.
- Leung, H., Borromeo, E. S., Bernardo, M. A., and Notteghem, J. L. (1988). Genetic analysis of virulence in the rice blast fungus *Magnaporthe grisea*. *Phytopathology*, 78(9), 1227-1233.
- Lévesque, C. A., Brouwer, H., Cano, L., Hamilton, J. P., Holt, C., Huitema, E., Raffaele, S., Robideau, G. P., Thines, M. and Win, J. (2010). Genome sequence of the necrotrophic plant pathogen *Pythium ultimum* reveals original pathogenicity mechanisms and effector repertoire. *Genome Biology*, 11(7), R73.
- LI Ping, D. B., ZHOU Heng etc. (2012). Functional analysis of cysteine residues of the *Magnaporthe oryzae* avirulence protein AvrPiz-t. *Acta Phytopathologica Sinica*, 42(5), 474–479.
- Li, W., Wang, B., Wu, J., Lu, G., Hu, Y., Zhang, X., Zhang, Z., Zhao, Q., Feng, Q. and Zhang, H. (2009). The *Magnaporthe oryzae* avirulence gene AvrPiz-t encodes a predicted secreted protein that triggers the immunity in rice mediated by the blast resistance gene Piz-t. *Molecular Plant-Microbe Interactions*, 22(4), 411-420.
- Lindeberg, M., Cunnac, S., and Collmer, A. (2012). *Pseudomonas syringae* type III effector repertoires: last words in endless arguments. *Trends in Microbiology*, 20(4), 199-208.
- Lindeberg, M., Myers, C. R., Collmer, A., and Schneider, D. J. (2008). Roadmap to new virulence determinants in *Pseudomonas syringae*: insights from comparative genomics and genome organization. *Molecular Plant-Microbe Interactions*, 21(6), 685-700.

- Lo Presti, L., Lanver, D., Schweizer, G., Tanaka, S., Liang, L., Tollot, M., Zuccaro, A., Reissmann, S. and Kahmann, R. (2015). Fungal effectors and plant susceptibility. *Annual Review of Plant Biology*, 66, 513-545.
- Lucas, J., Hayter, J., and Crute, I. (1995). The downy mildews: Host specificity and pathogenesis. *Pathogenesis and Host Specificity in Plant Diseases*, 2, 217-238.
- Luderer, R., and Joosten, M. H. (2001). Avirulence proteins of plant pathogens: determinants of victory and defeat. *Molecular Plant Pathology*, 2(6), 355-364.
- Ma, L., Cornelissen, B. J., and Takken, F. L. (2013). A nuclear localization for Avr2 from *Fusarium oxysporum* is required to activate the tomato resistance protein I-2. *Frontiers in Plant Science*, 4.
- Ma, L., Lukasik, E., Gawehns, F., and Takken, F. L. (2012). The use of agroinfiltration for transient expression of plant resistance and fungal effector proteins in *Nicotiana benthamiana* leaves *Plant Fungal Pathogens* (pp. 61-74): Springer.
- Maekawa, T., Cheng, W., Spiridon, L. N., Töller, A., Lukasik, E., Saijo, Y., Liu, P., Shen, Q-H., Micluta, M. A. and Somssich, I. E. (2011). Coiled-coil domain-dependent homodimerization of intracellular barley immune receptors defines a minimal functional module for triggering cell death. *Cell Host and Microbe*, 9(3), 187-199.
- Mansfield, J., Genin, S., Magori, S., Citovsky, V., Sriariyanum, M., Ronald, P., Dow, M., Verdier, V., Beer, S. V. and Machado, M. A. (2012). Top 10 plant pathogenic bacteria in molecular plant pathology. *Molecular Plant Pathology*, 13(6), 614-629.
- Maqbool, A., Saitoh, H., Franceschetti, M., Stevenson, C., Uemura, A., Kanzaki, H., Kamoun, S., Terauchi, R. and Banfield, M. (2015). Structural basis of pathogen recognition by an integrated HMA domain in a plant NLR immune receptor. *Elife*, 4, e08709.
- Marois, E., Van den Ackerveken, G., and Bonas, U. (2002). The *Xanthomonas* type III effector protein AvrBs3 modulates plant gene expression and induces cell hypertrophy in the susceptible host. *Molecular Plant-Microbe Interactions*, 15(7), 637-646.
- Martin, G. B. (1999). Functional analysis of plant disease resistance genes and their downstream effectors. *Current Opinion in Plant Biology*, 2(4), 273-279.
- Martin, G. B., Bogdanove, A. J., and Sessa, G. (2003). Understanding the functions of plant disease resistance proteins. *Annual Review of Plant Biology*, 54(1), 23-61:

- McDowell, J. M. (2013). Genomic and transcriptomic insights into lifestyle transitions of a hemi-biotrophic fungal pathogen. *New Phytologist*, 197(4), 1032-1034.
- McDowell, J. M., Dhandaydham, M., Long, T. A., Aarts, M. G., Goff, S., Holub, E. B., and Dangl, J. L. (1998). Intragenic recombination and diversifying selection contribute to the evolution of downy mildew resistance at the RPP8 locus of *Arabidopsis*. *The Plant Cell*, 10(11), 1861-1874.
- Mesarich, C. H., Bowen, J. K., Hamiaux, C., and Templeton, M. D. (2015). Repeat-containing protein effectors of plant-associated organisms. *Frontiers in Plant Science*, 6(872):1-19. doi:10.3389/fpls.2015.00872
- Mesarich, C. H., Schmitz, M., Tremouilhac, P., McGillivray, D. J., Templeton, M. D., and Dingley, A. J. (2012). Structure, dynamics and domain organization of the repeat protein Cin1 from the apple scab fungus. *Biochimica et Biophysica Acta (BBA)-Proteins and Proteomics*, 1824(10), 1118-1128.
- Mishra, B., Solovyeva, I., Schmuker, A., and Thines, M. (2015). Modelling of structures of ATR1-homologs from sister species of *Hyaloperonospora arabidopsidis* suggests different patterns for target-mediated and R-protein-mediated selection. *Mycological Progress*, 14(9), 1-8.
- Mole, B. M., Baltrus, D. A., Dangl, J. L., and Grant, S. R. (2007). Global virulence regulation networks in phytopathogenic bacteria. *Trends in Microbiology*, 15(8), 363-371.
- Mondragón-Palomino, M., Meyers, B. C., Michelmore, R. W., and Gaut, B. S. (2002). Patterns of positive selection in the complete NBS-LRR gene family of *Arabidopsis thaliana*. *Genome Research*, 12(9), 1305-1315.
- Morel, J.-B., and Dangl, J. L. (1997). The hypersensitive response and the induction of cell death in plants. *Cell Death and Differentiation*, 4(8), 671-683.
- Murashige, T., and Skoog, F. (1962). A revised medium for rapid growth and bio assays with tobacco tissue cultures. *Physiologia Plantarum*, 15(3), 473-497.
- Murray, G. M., and Brennan, J. P. (2009). Estimating disease losses to the Australian wheat industry. *Australasian Plant Pathology*, 38(6), 558-570.
- Nürnbergger, T., Brunner, F., Kemmerling, B., and Piater, L. (2004). Innate immunity in plants and animals: striking similarities and obvious differences. *Immunological Reviews*, 198(1), 249-266.

- O'Connell, R. J., Thon, M. R., Hacquard, S., Amyotte, S. G., Kleemann, J., Torres, M. F., Damm, U., Buiate, E. A., Epstein, L. and Alkan, N. (2012). Lifestyle transitions in plant pathogenic *Colletotrichum* fungi deciphered by genome and transcriptome analyses. *Nature Genetics*, 44(9), 1060-1065.
- Oerke, E.-C., and Dehne, H.-W. (2004). Safeguarding production-losses in major crops and the role of crop protection. *Crop Protection*, 23(4), 275-285.
- Oh, S.-K., Young, C., Lee, M., Oliva, R., Bozkurt, T. O., Cano, L. M., Win, J., Bos, J. I., Liu, H.-Y. and van Damme, M. (2009). *In planta* expression screens of *Phytophthora infestans* RXLR effectors reveal diverse phenotypes, including activation of the *Solanum bulbocastanum* disease resistance protein Rpi-blb2. *The Plant Cell*, 21(9), 2928-2947.
- Ohm, R. A., Feau, N., Henrissat, B., Schoch, C. L., Horwitz, B. A., Barry, K. W., Condon, B. J., Copeland, A. C., Dhillon, B. and Glaser, F. (2012). Diverse lifestyles and strategies of plant pathogenesis encoded in the genomes of eighteen Dothideomycetes fungi. *PLoS Pathog*, 8(12), e1003037.
- Orbach, M. J., Farrall, L., Sweigard, J. A., Chumley, F. G. and Valent, B. (2000) A telomeric avirulence gene determines efficacy for the rice blast resistance gene *Pi-ta*. *Plant Cell*, 12, 2019-2032.
- Padmanabhan, M., Cournoyer, P., and Dinesh-Kumar, S. (2009). The leucine-rich repeat domain in plant innate immunity: a wealth of possibilities. *Cellular Microbiology*, 11(2), 191-198.
- Panstruga, R., and Dodds, P. N. (2009). Terrific protein traffic: the mystery of effector protein delivery by filamentous plant pathogens. *Science (New York, NY)*, 324(5928), 748.
- Parker, J. E., Coleman, M. J., Szabò, V., Frost, L. N., Schmidt, R., van der Biezen, E. A., Moores, T., Dean, C., Daniels, M. J. and Jones, J. (1997). The Arabidopsis downy mildew resistance gene RPP5 shares similarity to the toll and interleukin-1 receptors with N and L6. *The Plant Cell*, 9(6), 879-894.
- Parker, J. E., Holub, E. B., Frost, L. N., Falk, A., Gunn, N. D., and Daniels, M. J. (1996). Characterization of eds1, a mutation in Arabidopsis suppressing resistance to *Peronospora parasitica* specified by several different RPP genes. *The Plant Cell*, 8(11), 2033-2046.
- Parkinson, N., Aritua, V., Heeney, J., Cowie, C., Bew, J., and Stead, D. (2007). Phylogenetic analysis of *Xanthomonas* species by comparison of partial gyrase B gene sequences. *International Journal of Systematic and Evolutionary Microbiology*, 57(12), 2881-2887.

- Parlange, F., Daverdin, G., Fudal, I., Kuhn, M. L., Balesdent, M. H., Blaise, F., Grezes-Besset, B. and Rouxel, T. (2009). Leptosphaeria maculans avirulence gene AvrLm4-7 confers a dual recognition specificity by the *Rlm4* and *Rlm7* resistance genes of oilseed rape, and circumvents Rlm4-mediated recognition through a single amino acid change. *Molecular Microbiology*, 71(4), 851-863.
- Petre, B., and Kamoun, S. (2014). How do filamentous pathogens deliver effector proteins into plant cells? *PLoS Biology*, 12(2), e1001801.
- Petre, B., Joly, D. L., and Duplessis, S. (2014). Effector proteins of rust fungi. *Plant-Microbe Interaction*, 5, 416.
- Pretsch, K., Kemen, A., Kemen, E., Geiger, M., Mendgen, K., and Voegelé, R. (2013). The rust transferred proteins—a new family of effector proteins exhibiting protease inhibitor function. *Molecular Plant Pathology*, 14(1), 96-107.
- Rafiqi, M., Ellis, J. G., Ludowici, V. A., Hardham, A. R., and Dodds, P. N. (2012). Challenges and progress towards understanding the role of effectors in plant–fungal interactions. *Current Opinion in Plant Biology*, 15(4), 477-482.
- Rafiqi, M., Gan, P. H., Ravensdale, M., Lawrence, G. J., Ellis, J. G., Jones, D. A., Hardham, A. R. and Dodds, P. N. (2010). Internalization of flax rust avirulence proteins into flax and tobacco cells can occur in the absence of the pathogen. *The Plant Cell Online*, 22(6), 2017-2032.
- Rairdan, G. J., and Moffett, P. (2006). Distinct domains in the ARC region of the potato resistance protein Rx mediate LRR binding and inhibition of activation. *The Plant Cell*, 18(8), 2082-2093.
- Rambo, R. P., and Tainer, J. A. (2013). Accurate assessment of mass, models and resolution by small-angle scattering. *Nature*, 496(7446), 477-481.
- Ravensdale, M., Bernoux, M., Ve, T., Kobe, B., Thrall, P. H., Ellis, J. G., and Dodds, P. N. (2012). Intramolecular interaction influences binding of the flax L5 and L6 resistance proteins to their AvrL567 ligands. *PLoS Pathogens*, 8(11), e1003004.
- Ravensdale, M., Nemri, A., Thrall, P. H., Ellis, J. G., and Dodds, P. N. (2011). Co-evolutionary interactions between host resistance and pathogen effector genes in flax rust disease. *Molecular Plant Pathology*, 12(1), 93-102.
- Rehmany, A. P., Gordon, A., Rose, L. E., Allen, R. L., Armstrong, M. R., Whisson, S. C., Kamoun, S., Tyler, B. M., Birch, P. R. and Beynon, J. L. (2005). Differential recognition of highly divergent downy mildew avirulence gene alleles by RPP1 resistance genes from two *Arabidopsis* lines. *The Plant Cell*, 17(6), 1839-1850.

- Rep, M., van der Does, H. C., Meijer, M., van Wijk, R., Houterman, P. M., Dekker, H. L., De Koster, C. G. and Cornelissen, B. J. C. (2004). A small, cysteine-rich protein secreted by *Fusarium oxysporum* during colonization of xylem vessels is required for I-3-mediated resistance in tomato. *Mol. Microbiol.* 53, 1373-1383.
- Ribot, C., Césari, S., Abidi, I., Chalvon, V., Bournaud, C., Vallet, J., Lebrun, M. H., Morel, J. B. and Kroj, T. (2013). The *Magnaporthe oryzae* effector AVR1-CO39 is translocated into rice cells independently of a fungal-derived machinery. *The Plant Journal*.
- Römer, P., Hahn, S., Jordan, T., Strauß, T., Bonas, U., and Lahaye, T. (2007). Plant pathogen recognition mediated by promoter activation of the pepper *Bs3* resistance gene. *Science*, 318(5850), 645-648.
- Rose, M. S., Yun, S.-H., Asvarak, T., Lu, S.-W., Yoder, O., and Turgeon, B. G. (2002). A decarboxylase encoded at the *Cochliobolus heterostrophus* translocation-associated Tox1B locus is required for polyketide (T-toxin) biosynthesis and high virulence on T-cytoplasm maize. *Molecular Plant-Microbe Interactions*, 15(9), 883-893.
- Ryan, R. P., Vorhölter, F.-J., Potnis, N., Jones, J. B., Van Sluys, M.-A., Bogdanove, A. J., and Dow, J. M. (2011). Pathogenomics of *Xanthomonas*: understanding bacterium-plant interactions. *Nature Reviews Microbiology*, 9(5), 344-355.
- Sambrook J., F. E. a. M. T. (1989). *Molecular cloning: a laboratory manual*: Cold Spring Harbour Laboratory Press, New York.
- Sánchez-Vallet, A., Saleem-Batcha, R., Kombrink, A., Hansen, G., Valkenburg, D.-J., Thomma, B. P., and Mesters, J. R. (2013). Fungal effector Ecp6 outcompetes host immune receptor for chitin binding through intrachain LysM dimerization. *Elife*, 2, e00790.
- Sanger, F., and Coulson, A. R. (1975). A rapid method for determining sequences in DNA by primed synthesis with DNA polymerase. *Journal of Molecular Biology*, 94(3), 441-448.
- Sarma, G. N., Manning, V. A., Ciuffetti, L. M., and Karplus, P. A. (2005). Structure of Ptr ToxA: An RGD-containing host-selective toxin from *Pyrenophora tritici-repentis*. *The Plant Cell*, 17(11), 3190-3202.
- Schmidt, S. A., Williams, S. J., Wang, C. I. A., Sornaraj, P., James, B., Kobe, B., Dodds, P. N., Ellis, J. G. and Anderson, P. A. (2007a). Purification of the M flax-rust resistance protein expressed in *Pichia pastoris*. *The Plant Journal*, 50(6), 1107-1117.

- Scholthof, K. B. G., Adkins, S., Czosnek, H., Palukaitis, P., Jacquot, E., Hohn, T., Hohn, B., Saunders, K., Candresse, T. and Ahlquist, P. (2011). Top 10 plant viruses in molecular plant pathology. *Molecular Plant Pathology*, 12(9), 938-954.
- Schornack, S., Ballvora, A., Gürlebeck, D., Peart, J., Ganal, M., Baker, B., Bonas, U. and Lahaye, T. (2004). The tomato resistance protein Bs4 is a predicted non-nuclear TIR-NB-LRR protein that mediates defense responses to severely truncated derivatives of AvrBs4 and overexpressed AvrBs3. *The Plant Journal*, 37(1), 46-60.
- Schornack, S., Huitema, E., Cano, L. M., Bozkurt, T. O., Oliva, R., van Damme, M., Schwizer, S., Raffaele, S., CHAPARRO-GARCIA, A. and Farrer, R. (2009). Ten things to know about oomycete effectors. *Molecular Plant Pathology*, 10(6), 795-803.
- Schornack, S., van Damme, M., Bozkurt, T. O., Cano, L. M., Smoker, M., Thines, M., Gaulin, E., Kamoun, S. and Huitema, E. (2010). Ancient class of translocated oomycete effectors targets the host nucleus. *Proceedings of the National Academy of Sciences*, 107(40), 17421-17426.
- Schraidt, O., and Marlovits, T. C. (2011). Three-dimensional model of Salmonella's needle complex at subnanometer resolution. *Science*, 331(6021), 1192-1195.
- Segretin, M. E., Pais, M., Franceschetti, M., Chaparro-Garcia, A., Bos, J. I., Banfield, M. J., and Kamoun, S. (2014). Single amino acid mutations in the potato immune receptor R3a expand response to *Phytophthora* effectors. *Molecular Plant-Microbe Interactions*, 27(7), 624-637.
- Shen, Q.-H., Zhou, F., Bieri, S., Haizel, T., Shirasu, K., and Schulze-Lefert, P. (2003). Recognition specificity and RAR1/SGT1 dependence in barley *Mla* disease resistance genes to the powdery mildew fungus. *The Plant Cell*, 15(3), 732-744.
- Smith, A.F. 2012. Potato: A global history, Reaktion Books, pp 102-109.
- Smith, J., and Leong, S. (1994). Mapping of a Magnaporthe grisea locus affecting rice (*Oryza sativa*) cultivar specificity. *Theoretical and Applied Genetics*, 88(8), 901-908.
- Sogin, M. L., and Silberman, J. D. (1998). Evolution of the protists and protistan parasites from the perspective of molecular systematics. *International Journal For Parasitology*, 28(1), 11-20.
- Sohn, K. H., Lei, R., Nemri, A., and Jones, J. D. (2007). The downy mildew effector proteins ATR1 and ATR13 promote disease susceptibility in *Arabidopsis thaliana*. *The Plant Cell Online*, 19(12), 4077-4090.

- Sohn, K. H., Zhang, Y., and Jones, J. D. (2009). The *Pseudomonas syringae* effector protein, AvrRPS4, requires in planta processing and the KRVY domain to function. *The Plant Journal*, 57(6), 1079-1091.
- Song, J., Win, J., Tian, M., Schornack, S., Kaschani, F., Ilyas, M., van der Hoorn, R. A. and Kamoun, S. (2009). Apoplastic effectors secreted by two unrelated eukaryotic plant pathogens target the tomato defense protease Rcr3. *Proceedings of the National Academy of Sciences*, 106(5), 1654-1659.
- Sornaraj, P. (2013). Activation of the M flax-rust resistance protein. *PhD Thesis, Flinders University, Australia*.
- Staskawicz, B. J., Ausubel, F.M., Baker, B.J., Ellis, J.G., and Jones, J.D. (1995). Molecular genetics of plant disease resistance. *Science*, 268, 661-667.
- Staskawicz, B. J., Mudgett, M. B., Dangl, J. L., and Galan, J. E. (2001). Common and contrasting themes of plant and animal diseases. *Science*, 292(5525), 2285-2289.
- Stassen, J. H., and Van den Ackerveken, G. (2011). How do oomycete effectors interfere with plant life? *Current Opinion in Plant Biology*, 14(4), 407-414.
- Stergiopoulos, I., and de Wit, P. J. (2009). Fungal effector proteins. *Annual Review of Phytopathology*, 47, 233-263.
- Stergiopoulos, I., Collemare, J., Mehrabi, R., and De Wit, P. J. (2013). Phytotoxic secondary metabolites and peptides produced by plant pathogenic Dothideomycete fungi. *FEMS Microbiology Reviews*, 37(1), 67-93.
- Stols, L., Gu, M., Dieckman, L., Raffin, R., Collart, F. R., and Donnelly, M. I. (2002). A new vector for high-throughput, ligation-independent cloning encoding a tobacco etch virus protease cleavage site. *Protein Expression and Purification*, 25(1), 8-15.
- Studholme, D. J., Ibanez, S. G., MacLean, D., Dangl, J. L., Chang, J. H., and Rathjen, J. P. (2009). A draft genome sequence and functional screen reveals the repertoire of type III secreted proteins of *Pseudomonas syringae* pathovar tabaci 11528. *BMC Genomics*, 10(1), 395.
- Sweigard, J. A., Carroll, A. M., Kang, S., Farrall, L., Chumley, F. G. and Valent, B. (1995). Identification, cloning, and characterization of *PWL2*, a gene for host species specificity in the rice blast fungus. *Plant Cell*, 7, 1221-1233.
- Takemoto, D., Rafiqi, M., Hurley, U., Lawrence, G. J., Bernoux, M., Hardham, A. R., Ellis, J. G., Dodds, P. N. and Jones, D. A. (2012). N-terminal motifs in some plant

- disease resistance proteins function in membrane attachment and contribute to disease resistance. *Molecular Plant-Microbe Interactions*, 25(3), 379-392.
- Tameling, W. I., Vossen, J. H., Albrecht, M., Lengauer, T., Berden, J. A., Haring, M. A., Cornelissen, B. J. and Takken, F. L. (2006). Mutations in the NB-ARC domain of *I-2* that impair ATP hydrolysis cause autoactivation. *Plant Physiology*, 140(4), 1233-1245.
- Thines, M. (2014). Phylogeny and evolution of plant pathogenic oomycetes—a global overview. *European Journal of Plant Pathology*, 138(3), 431-447.
- Thines, M., and Kamoun, S. (2010). Oomycete-plant coevolution: recent advances and future prospects. *Current Opinion in Plant Biology*, 13(4), 427-433.
- Thomma, B. P. H., Van Esse, H. P., Crous, P. W. and De Wit, P. J. G. M. (2005). *Cladosporium fulvum* (syn. *Passalora fulva*), a highly specialized plant pathogen as a model for functional studies on plant pathogenic Mycosphaerellaceae. *Mol. Plant Pathol.* 6, 379-393.
- Tian, M., Win, J., Song, J., van der Hoorn, R., van der Knaap, E., and Kamoun, S. (2007). A *Phytophthora infestans* cystatin-like protein targets a novel tomato papain-like apoplastic protease. *Plant Physiology*, 143(1), 364-377.
- Torto, T. A., Li, S., Styer, A., Huitema, E., Testa, A., Gow, N. A., van West, P. and Kamoun, S. (2003). EST mining and functional expression assays identify extracellular effector proteins from the plant pathogen *Phytophthora*. *Genome Research*, 13(7), 1675-1685.
- Towbin, H., Staehelin, T., and Gordon, J. (1979). Electrophoretic transfer of proteins from polyacrylamide gels to nitrocellulose sheets: procedure and some applications. *Proceedings of the National Academy of Sciences*, 76(9), 4350-4354.
- Tyler, B. M. (2009). Entering and breaking: virulence effector proteins of oomycete plant pathogens. *Cellular Microbiology*, 11(1), 13-20.
- Tyler, B. M., Tripathy, S., Zhang, X., Dehal, P., Jiang, R. H., Aerts, A., Arredondo, F. D., Baxter, L., Bensasson, D. and Beynon, J. L. (2006). *Phytophthora* genome sequences uncover evolutionary origins and mechanisms of pathogenesis. *Science*, 313(5791), 1261-1266.
- Upadhyaya, N. M., Mago, R., Staskawicz, B. J., Ayliffe, M. A., Ellis, J. G., and Dodds, P. N. (2014). A bacterial type III secretion assay for delivery of fungal effector proteins into wheat. *Molecular Plant-Microbe Interactions*, 27(3), 255-264.
- Valent, B., Farrall, L. and Chumley, F. G. (1991). *Magnaporthe grisea* genes for

- pathogenicity and virulence identified through a series of backcrosses. *Genetics*, 127, 87-101.
- Valent, B., Farrall, L., and Chumley, F. G. (1991). Magnaporthe grisea genes for pathogenicity and virulence identified through a series of backcrosses. *Genetics*, 127(1), 87-101.
- Van Der Biezen, E. A., and Jones, J. D. (1998). Plant disease-resistance proteins and the gene-for-gene concept. *Trends in Biochemical Sciences*, 23(12), 454-456.
- van der Hoorn, R. A., and Kamoun, S. (2008). From guard to decoy: a new model for perception of plant pathogen effectors. *The Plant Cell Online*, 20(8), 2009-2017.
- Ve, T. (2011). Structural basis of disease resistance in flax against flax rust. *PhD Thesis, The University of Queensland, Australia*.
- Ve, T., Williams, S. J., Catanzariti, A.-M., Rafiqi, M., Rahman, M., Ellis, J. G., Hardham, A. R., Jones, D. A., Anderson, P. A. and Dodds, P. N. (2013). Structures of the flax-rust effector AvrM reveal insights into the molecular basis of plant-cell entry and effector-triggered immunity. *Proceedings of the National Academy of Sciences*, 110(43), 17594-17599.
- Ve, T., Williams, S., Bernoux, M., Catanzariti, A.-M., Rahman, M., Jones, D., Ellis, J. G., Anderson, P. Dodds, P. N., and Kobe, B. (2011). Structural basis of disease resistance in flax against flax rust. *Solving Nanoscale Structures Using Focussed Electron Beams*, p 59.
- Vleeshouwers, V. G., and Oliver, R. P. (2014). Effectors as tools in disease resistance breeding against biotrophic, hemibiotrophic, and necrotrophic plant pathogens. *Molecular Plant-Microbe Interactions*, 27(3), 196-206.
- Vleeshouwers, V., Rietman, H., Krenek, P., Champouret, N., Young, C., Oh, S.-K., Wang, M., Bouwmeester, K., Vosman, B. and Visser, R. G. (2008). Effector genomics accelerates discovery and functional profiling of potato disease resistance and *Phytophthora infestans* avirulence genes. *PLoS One*, 3(8), e2875.
- Voegelé, R. T., and Mendgen, K. (2003). Rust haustoria: nutrient uptake and beyond. *New Phytologist*, 159(1), 93-100.
- Wang, C.-I. A., Gunčar, G., Forwood, J. K., Teh, T., Catanzariti, A.-M., Lawrence, G. J., and Anderson, P. A. (2007). Crystal structures of flax rust avirulence proteins AvrL567-A and-D reveal details of the structural basis for flax disease resistance specificity. *The Plant Cell Online*, 19(9), 2898-2912.

- Wawra, S., Agacan, M., Boddey, J. A., Davidson, I., Gachon, C. M., Zanda, M., and Porter, A. J. (2012b). Avirulence protein 3a (AVR3a) from the potato pathogen *Phytophthora infestans* forms homodimers through its predicted translocation region and does not specifically bind phospholipids. *Journal of Biological Chemistry*, 287(45), 38101-38109.
- Wawra, S., Belmonte, R., Löbach, L., Saraiva, M., Willems, A., and van West, P. (2012a). Secretion, delivery and function of oomycete effector proteins. *Current Opinion in Microbiology*.
- Wen, J., Arakawa, T., and Philo, J. S. (1996). Size-exclusion chromatography with on-line light-scattering, absorbance, and refractive index detectors for studying proteins and their interactions. *Analytical Biochemistry*, 240(2), 155-166.
- Weßling, R., Schmidt, S. M., Micali, C. O., Knaust, F., Reinhardt, R., Neumann, U., and Panstruga, R. (2012). Transcriptome analysis of enriched *Golovinomyces orontii* haustoria by deep 454 pyrosequencing. *Fungal Genetics and Biology*, 49(6), 470-482.
- Whisson, S. C., Boevink, P. C., Moleleki, L., Avrova, A. O., Morales, J. G., Gilroy, E. M., and Chapman, S. (2007). A translocation signal for delivery of oomycete effector proteins into host plant cells. *Nature*, 450(7166), 115-118.
- White, F. F., Yang, B., and Johnson, L. B. (2000). Prospects for understanding avirulence gene function. *Current Opinion in Plant Biology*, 3(4), 291-298.
- Wichmann, G., and Bergelson, J. (2004). Effector genes of *Xanthomonas axonopodis* pv. *vesicatoria* promote transmission and enhance other fitness traits in the field. *Genetics*, 166(2), 693-706.
- Williams, S. J. (2009). Biochemical Characterisation of the M and L6 Flax-Rust Disease Resistance Proteins. *PhD Thesis, Flinders University, Australia*.
- Williams, S. J., Sornaraj, P., deCourcy-Ireland, E., Menz, R. I., Kobe, B., Ellis, J. G., Dodds, P. N. and Anderson, P. A. (2011). An autoactive mutant of the M flax rust resistance protein has a preference for binding ATP, whereas wild-type M protein binds ADP. *Molecular Plant-Microbe Interactions*, 24(8), 897-906.
- Win, J., Chaparro-Garcia, A., Belhaj, K., Saunders, D., Yoshida, K., Dong, S., and Hogenhout, S. (2012). *Effector biology of plant-associated organisms: concepts and perspectives*. Paper presented at the 'Cold Spring Harbor' symposia on Quantitative Biology.

- Win, J., Morgan, W., Bos, J., Krasileva, K. V., Cano, L. M., Chaparro-Garcia, A., and Kamoun, S. (2007). Adaptive evolution has targeted the C-terminal domain of the RXLR effectors of plant pathogenic oomycetes. *The Plant Cell*, *19*(8), 2349-2369.
- Woolhouse, M. E., Webster, J. P., Domingo, E., Charlesworth, B., and Levin, B. R. (2002). Biological and biomedical implications of the co-evolution of pathogens and their hosts. *Nature Genetics*, *32*(4), 569-577.
- Xiang, T., Zong, N., Zou, Y., Wu, Y., Zhang, J., Xing, W., Li, Y., Tang, X., Zhu, L. and Chai, J. (2008). *Pseudomonas syringae* effector AvrPto blocks innate immunity by targeting receptor kinases. *Current Biology*, *18*(1), 74-80.
- Xing, W., Zou, Y., Liu, Q., Liu, J., Luo, X., Huang, Q., Chen, S, Zhu, L, Bi, R and Hao, Q. (2007). The structural basis for activation of plant immunity by bacterial effector protein AvrPto. *Nature*, *449*(7159), 243-247.
- Yeast Protocols Handbook (July, 2009), Protocol No. PT3024-1, Version No. PR973283, *Clontech Laboratories, Inc.*
- Yi, M., and Valent, B. (2013). Communication between filamentous pathogens and plants at the biotrophic interface. *Annual Review of Phytopathology*, *51*, 587-611.
- Yin, C., and Hulbert, S. (2011). Prospects for functional analysis of effectors from cereal rust fungi. *Euphytica*, *179*(1), 57-67.
- Yin, C., Jurgenson, J. E., and Hulbert, S. H. (2011). Development of a host-induced RNAi system in the wheat stripe rust fungus *Puccinia striiformis* f. sp. *tritici*. *Molecular Plant-Microbe Interactions*, *24*(5), 554-561.
- York, W. S., Qin, Q., and Rose, J. K. (2004). Proteinaceous inhibitors of endo- β -glucanases. *Biochimica et Biophysica Acta (BBA)-Proteins and Proteomics*, *1696*(2), 223-233.
- Yoshida, K., Schuenemann, V. J., Cano, L. M., Pais, M., Mishra, B., Sharma, R., Lanz, C., Martin, F. N., Kamoun, S. and Krause, J. (2013). The rise and fall of the *Phytophthora infestans* lineage that triggered the Irish potato famine. *Elife*, *2*, e00731.
- Zhang, Z.-M., Zhang, X., Zhou, Z.-R., Hu, H.-Y., Liu, M., Zhou, B., and Zhou, J. (2013). Solution structure of the *Magnaporthe oryzae* avirulence protein AvrPiz-t. *Journal of Biomolecular NMR*, *55*(2), 219-223.

- Zhou, B., Qu, S., Liu, G., Dolan, M., Sakai, H., Lu, G., Bellizzi, M. and Wang, G.-L. (2006). The eight amino-acid differences within three leucine-rich repeats between Pi2 and Piz-t resistance proteins determine the resistance specificity to *Magnaporthe grisea*. *Molecular Plant-Microbe Interactions*, 19(11), 1216-1228.
- Zipfel, C., and Felix, G. (2005). Plants and animals: a different taste for microbes? *Current Opinion in Plant Biology*, 8(4), 353-360.